SHELL-SIDE TRANSFER IN SHELL-AND-TUBE HEAT EXCHANGERS

A thesis submitted to the Board of the Faculty of Engineering, University of Aston in Birmingham, for the degree of

DOCTOR OF PHILOSOPHY

by

SUKHVINDER PAL SINGH NIBBER

Dept. of Chemical Engineering,
University of Aston in
Birmingham,
Birmingham,
B4 7ET.

S.P.S. Nibber.

October, 1981.

SUMMARY

Local mass transfer coefficients were determined by using the electrochemical technique. A simple model of a heat exchanger with segmental nickel tube joined to p.v.c. rods replaced the exchanger tubes. Measurements were made for both no-leakage, semi-leakage and total leakage configurations. Baffle-spacings of 47 .6 mm, 66.6 mm, 97 mm and 149.2 mm were studied. Also studied were the overall exchanger pressure drops for each configuration.

The comparison of the heat transfer data with this work showed good agreement at high flow rates for the no-leakage case, but the agreement became poor for lower flow rates and leakage configurations. This disagreement was explained by non-analogous driving forces existing in the two systems.

The no-leakage data showed length-wise variation of transfer coefficients along the exchnager length. The end compartments showing transfer coefficients inferior by up to 26% compared to the internal compartments, depending on Reynolds number. With the introduction of leakage streams this variation however became smaller than the experimental accuracy. A model is outlined to show the characteristic behaviour of individual electrode segments within the compartment. This was able to discriminate between cross and window zonesfor the no-leakage case, but no such distinction could be made for the leakage case.

A flow area was found which, when incorporated in the Reynolds number, enabled the correlation of baffle-cut and baffle-spacing parameters for the no-leakage case. This area is the free flow area determined at the baffle edge. Addition of the leakage area to this flow area resulted in correlation of all commercial leakage geometrical parameters.

The procedures used to correlate the pressure drop data from a total of eighteen different configurations on a single curve are also outlined.

KEYWORDS: LENGTH-WISE, TRANSFER COEFFICIENTS, CORRELATIONS, SHELL-AND-TUBE, ELECTROCHEMICAL.

Acknowledgement

The author wishes to express his gratitude to:

The Science Research Council for sponsoring the work, The Heat Transfer and Fluid Flow Service AEA Harwell and National Engineering Laboratory for providing the Case Award.

Dr. B. Gay and Dr. J. D. Jenkins for their supervision. Professor G. V. Jeffreys for provision of research facilities in the Department of Chemical Engineering, University of Aston in Birmingham.

Dr. G. Polley for his guidance during the industrial period at N.E.L., East Kilbride.

Supporting Publications

S.P.S. Nibber, J.D. Jenkins and B. Gay, Length-Wise variation of heat transfer coefficients in shell-and-tube heat exchangers, HTFS Research Symposium, St. Catherine College, Oxford University (1979).

S.P.S. Nibber, J.D. Jenkins and B. Gay, Heat Transfer coefficients for a complete shell-and-tube exchanger with leakage, HTFS Research Symposium, St. Catherine College, Oxford University (1980).

G.T. Polley and S.P.S. Nibber, Optimisation of process design parameters relating to heat exchangers, ibid (1980).

CONTENTS

List of Tables

List of Figures

INTRODUCTION

The United States market for heat exchanger units, at £380M in 1978, is expected to increase steeply to £700M 1988, according to a report entitled 'The Heat Exchanger Market' (1). Similar proportional increases would also be expected in Europe and the United Kingdom.

The Report mentioned that shell-and-tube exchanger units accounted for more than 90% of all units sold, and for two-thirds of the market value. Also mentioned is the fact that computer design services are being widely used. The Heat Transfer Fluid-flow Service (National Engineering Laboratory and Harwell) have also developed such a design service, and requires additional experimental data to improve its design programs.

Most of the previous experimental studies have been devoted to measuring bundle-average heat transfer coefficients. In the past this was adequate for the purpose of predicting shell-side performances with the methods that were available at the time. However, the advent of precise design procedures for predicting shell-side heat transfer performance requires localised transfer coefficient data for various bundle arrangements.

Much work has been directed towards establishing a reliable experimental technique for obtaining these local measurements. The use of diffusion-controlled mass transfer techniques and the Chilton-Colburn analogy (2) has been successfully employed to obtain accurate local transfer coefficient data. One of these techniques was developed by Mackley (3) to study the transfer co-efficients of individual tubes in an internal compartment having various bundle geometries. Prowse (4) later adapted the equipment to study the end compartment.

In this third stage of these shell-side investigations the same technique is used to obtain local transfer coefficient data for internal, end and intermediate compartments, therefore providing an effective length-wise study of the shell-side.

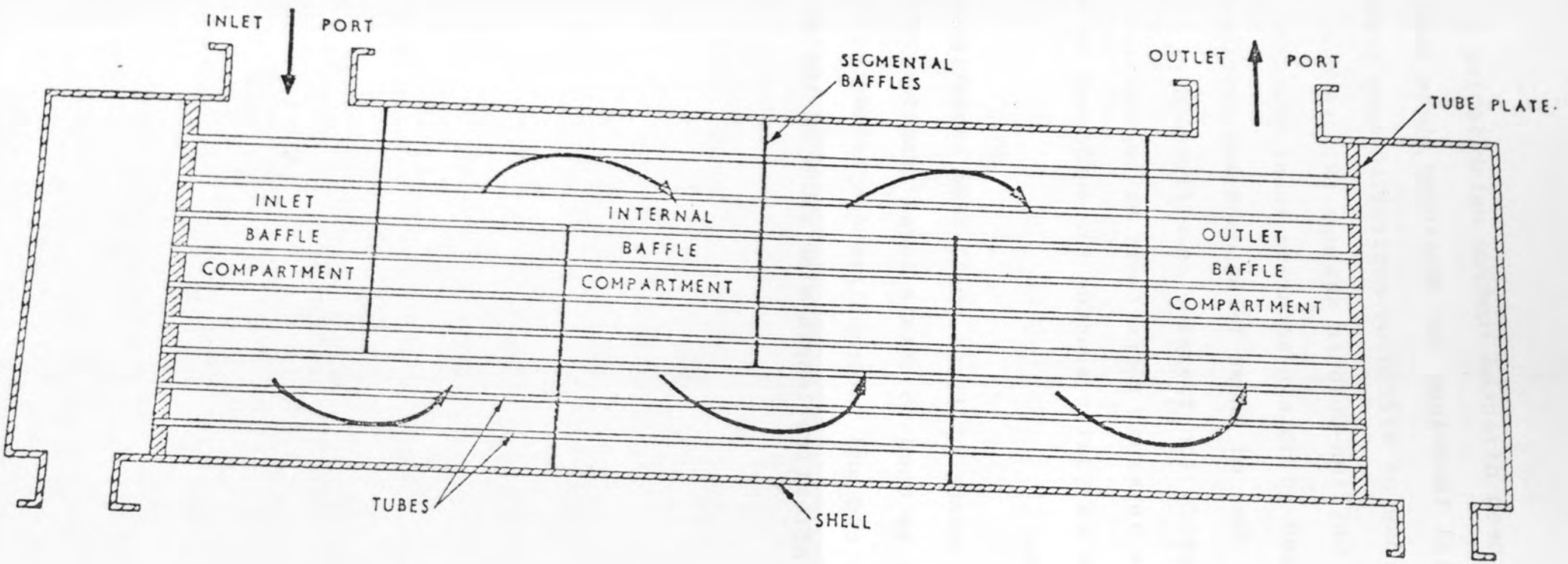

Figure II.1 T.E.M.A. E Type Shell - taken from Mackley

CHAPTER II

II.O Literature Review

II.1 Introduction

The simplest form of shell-and-tube heat exchanger used in industry is the T.E.M.A. 'E'-type shell (5) fitted with segmental baffles as illustrated in Figure II.1 . Its design requires a detailed understanding of the 'clean' surface transfer coefficient for both inside and ouside the tubes, the mean temperature driving-force, and the pressure drop, again for both sides. The present study is confined to the investigation of the single phase shell-side clean transfer coefficients, and the overall shell-side pressure drop.

In fact both transfer coefficient and pressure drop are influenced by the behaviour of the boundary layer established over the surface, the thickness of which is directly dependent on the fluid flow and the physical properties of the fluid. The shape, size and arrangement of the characteristic surface relative to the fluid also greatly effects the boundary layer. The complex geometry on the shell-side with the introduction of baffles and baffle clearances produces many different elements of flow; such as longitudinal, crossflow, eddy, stagnant etc. all influencing the boundary layer in a complicated manner.

The numerous bundle geometrical parameters such as;

baffle spacing,	tube pitch,
baffle cutdown,	tube length,
baffle thickness,	tube diameter,
tube/baffle clearances,	tube arrangement,
baffle/shell clearances,	shell diameter,

will affect each of the flow elements in a different way, hence improving one performance index at the expense of the other. A simple illustrative example is that increasing the baffle spacing would reduce the pressure drop at the expense of reduced heat transfer coefficients. In the past designers have changed the shell-side geometry to improve one of the performance indices without fully understanding the effects of such changes on the others.

In spite of the complex flow arrangement, the heat transfer coefficient and pressure drop in the past were obtained from dimensionless empirical charts of the performance indices against flowrate expressed as Reynolds number. The following section reviews the presently available prediction methods for shell-side heat transfer in segmentally-baffled shell-and-tube heat exchangers. The experimental investigations on which the prediction methods were established are also examined in order to throw light on the causes behind shell-side flow phenomena and particularly to identify inadequacies in previous analyses.

Before considering the flow behaviour in tube bundles a simple example of flow over tubes reveals the relationship

between transfer coefficients and flowrate.

II.2 Flow through an Ideal Rectangular Tube Bank

As the tube bundle in a shell-and-tube exchanger consists of rows of cylinders, investigation of fluid flow over an ideal rectangular tube bank can serve as a starting point from which the more complex shell-side flow can be pieced together.

In tube banks the interaction due to the surrounding tubes causes a marked deviation from flow around a single cylinder (6-8). Pierson (9) in 1937, Kays and London (10) in 1954, Shilham, Schomer and Dwyer (11) in 1954 and others have shown that transfer coefficients varied down the bundle. McAdams (12) in 1954 reported that in staggered tube bundles arrangements the coefficients in the first row were found to be approximately 0.63 times the mean coefficient of an infinite number of rows, and a ten-row tube bank had a mean coefficient equal to 0.93 times the mean coefficient of an infinite tube bank. The higher coefficients at the rear rows of tube banks were attributed to increased turbulence caused by the presence of the tubes in front of them. In banks of tubes it is important to consider whether the rows are staggered or in line. In the former case, the fluid tends to take a more torturous path than in the in-line arrangement. Therefore, the tube pitch and flow length are important parameters in analysing heat transfer coefficient data in these arrangements.

Colburn (13) published in 1933 a correlation of existing data for flows of gases normal to rectangular staggered tube banks, where ($Nu/Pr^{1/3}$) dimensionless group were plotted against Reynolds number. The characteristic area used in determining the velocity was determined by the minimum free flow area. Between Reynolds numbers of 2 000 to 30000 the curve was well represented by the equation

$$Nu = 0.3\ Re_c^{0.6}\ Pr^{0.33} \qquad (II.1)$$

For the in-line arrangement, Colburn (13) derived a similar equation but with a lower coefficient equal to 0.26 in the Reynolds number, showing inferior coefficients compared with the staggered arrangement.

Sieder and Tate (14) in 1936 modified equation II.1 to include changes in fluid viscosity between the bulk of the fluid and the tube surface. They multiplied the right hand side of equation II.1 by the ratio $(\mu/\mu_w)^{0.14}$. Experimental evidence shows that the Colburn curve equation II.1 can not be extrapolated beyond a Reynolds number of 70 000. Sheehan, Schomer and Dwyer (11) extended the Reynolds number range from 70 000 to 10^6 by using

$$Nu = 0.033\ Re_c^{0.8}\ Pr^{1/3}\ (\mu/\mu_w)^{0.14} \qquad (II.2)$$

The Engineering Science Data Unit (15) in 1973 presented a similar correlation for the flow of a constant property fluid in the Reynolds number range of 10 to 10^6, it is

$$Nu = a\ Re_c^{\ m}\ Pr^{1/3}\ F_N \qquad (II.3)$$

The values of a and m are shown in Table II.1 for staggered and in-line tube arrangements for corresponding Reynolds number ranges.

Table II.1 The Equation Constant and Exponent Values of Correlation Described by (15).

Range of Re_c	In-Line		Staggered	
	a	m	a	m
10 to 300	.742	.431	1.309	.36
300 to $2x10^5$	.211	.651	.273	.635
$2x10^5$ to $2x10^6$	.166	.7	.124	.7

The factor F_N corrects for the number of tube rows crossed and is used to account for turbulence generated due to the fluid flow through the bundle. This factor was determined from experimental data. The E.S.D.U. report in 1973 also includes further information on correction factors for fluid property variation and flow at an angle to the tubes. To account for the latter, the normal crossflow Nussult number was modified by multiplying it by $(\sin \theta)^{0.6}$, where θ is the angle between the fluid and surface.

The use of a 1/3 exponent on the Prandtl number in the above heat transfer correlations was confirmed by Zukauskas et al (16,17), Bergelin et al (18,25) and, through the use of the heat and mass transfer analogy, by Jenkins

et al (26).

When the tube bank is contained within a cylindrical shell as is the case in shell-and-tube exchangers, the resultant arrangement is not the ideal bundle. The free flow area used in calculating the cross flow Reynolds number varies from one tube row to the next. The previously defined area for ideal bundles becomes inappopriate in this case. A mean effective area is needed which would be representative of all the tube rows. Instead of adopting the arithmetic mean area, Emerson (27) in 1962 suggested that the effective free flow be defined by

$$A_{eff} = \left[\frac{N}{\Sigma(1/A_r)^{.6}}\right]^{1.67} \qquad (II.4)$$

where A_r is the flow area at r'th row of N rows.

Further more, in commercial exchangers a by-pass stream between the tube bank and the shell is inevitable, the presence of this flow causes further deviation from the ideal tube bank behaviour.

II.3 Shell-Side Heat Transfer Prediction Methods

The baffled exchanger has an extremely complex geometry and hence many non-idealities. The boundary layer is affected by many more geometric parameters, such as baffle spacing, baffle cut and the leakage areas associated with shell and baffle and tube and baffle. It is apparent that a complex three-dimensional flow exists on the shell-side and any analysis of experimental data would require the use of correlating parameters to account for all of these

complexities. The simplest method is discussed first.

II.3.1 Integral Correlations

Earlier correlations for baffled exchangers neglected local effects and produced a simple aggregate correlation over the whole exchanger. The design of the shell-side in cross-baffled exchangers in the 1950's was achieved by the integral methods of Kern (28) and Donohue (29).

Kern, correlating "industrial data with acceptable internal clearances" and a 25 per cent window cut, employed the hydraulic mean diameter D_{ek} of the shell for flow parallel to the tubes as the characteristic dimension in both Nusselt and Reynolds numbers. The mass velocity was calculated from a nominal free flow area computed at the centre of the shell, defined as

$$A_K = D_T(P-d_o)L_s \qquad (II.5)$$

He presented a correlation for the Reynolds number range of 2 000 to 10^6 and suggested an accuracy of 0 to 20%. The correlation is

$$\frac{h.D_{ek}}{k} = 0.36 \left(\frac{G_K D_{ek}}{\mu}\right)^{.55} \left(\frac{C_\mu}{K}\right)^{1/3} \left(\frac{\mu}{\mu_w}\right)^{.14} \qquad (II.6)$$

This correlation, however, takes no account of variations in baffle cut, baffle spacing and leakage areas. For example, Tinker (31) had estimated that the flow through the tube bank varied between 12 and 60% of the total shell-side flow, and was very sensitive to changes in leakage or by-pass streams. Kern's correlation gives no

help in predicting the results of such changes.

Donahue (29), using the data of Short (32), Heinrich (33), Bowman (34), Gardner (35) and Tinker (31), was able to achieve some success in correlating the baffle-cut (when the window area was greater than 15% of the total baffle area) in bundles of different spacing. He obtained the following equation,

$$\frac{hd}{k} = c' \left(\frac{G_Z d}{\mu}\right)^{0.6} \left(\frac{c\mu}{k}\right)^{.33} \left(\frac{\mu}{\mu_W}\right)^{.14} \qquad \text{(II.7)}$$

where G_Z was based on the geometrical mean of crossflow and window flow areas and is given by

$$G_Z = \sqrt{G_C G_W} \qquad \text{(II.8)}$$

Unfortunately, Donohue's coefficient c' in equation II.7 is a function of hydraulic mean crossflow diameter. Another similar correlation prepared by the British Shipbuilders Research Association (36) gave c' as a function of clearance ratio and tube-arrangement factor when Reynolds number was redefined by using Short's average velocity,

$$V_{Av} = 1/3 \left(\frac{W}{A_m} + \frac{W}{A_I} + \frac{W}{A_W}\right) \qquad \text{(II.9)}$$

It is clearly evident from this that c' is very much related to the geometry and influenced by the definition of the fluid velocity.

The above integral methods were commonly used in design offices sometimes to the exclusion of all other methods

for calculation of the shell-side transfer coefficient. Whilst they have the merits of simplicity they take no account of the effects caused by changing bundle geometry. Therefore improved methods are needed which would account for different flow distribution and behaviour in the baffled exchanger.

II.3.2 Flow Stream Correlations

Correlations of this type group all the effects of individual flow streams that exist within the exchanger to yield a representative coefficient.

Bell (37) in 1963 following the recommendations made from the Deleware University research programme (18-25) (discussed further in Section II.4) adopted a semi-analytical approach to analysing the data in exchangers of different bundle geometry. He tried to modify the ideal crossflow correlation to account for the inadequacies which arise in baffled commercial exchangers, viz.

$$h = h_i . F_B . F_L . F_W \qquad (II.10)$$

where h and h_i are overall transfer coefficients of commercial (non-ideal) and ideal tube arrangements respectively. The parameters F_B, F_L and F_W are correction factors for bypass, leakage and window zones respectively. These individual factors are independent of each other and were derived semi-empirically. By using graphical simplifications the method can become simple to use. However in determining these factors a detailed account of the bundle geometry is needed beforehand.

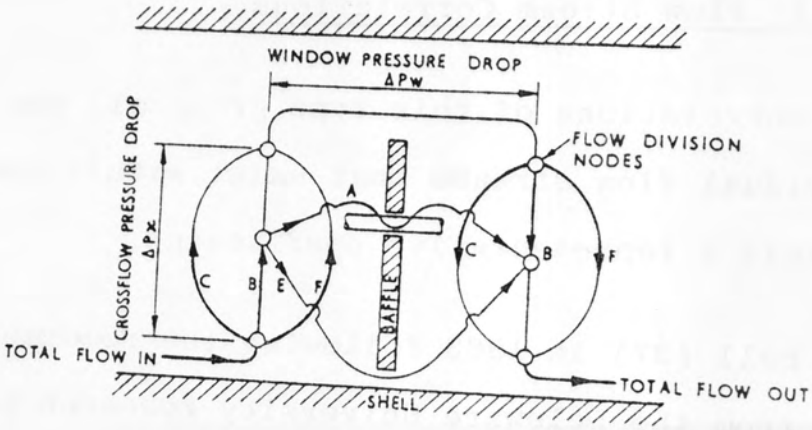

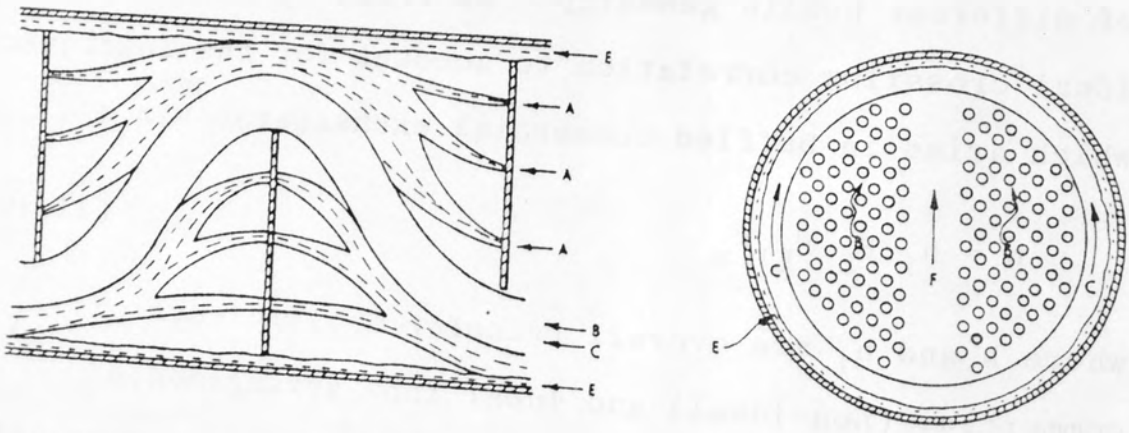

Figure II.2 Flow Stream Model

Tinker (30,31), in 1947, developed a more fundamental stream analysis approach. He divided the shell-side flow into a number of streams giving each an effectiveness factor. The different streams are shown in Figure II.2 By defining an overall 'effective' mass velocity, the bundle heat transfer coefficient can be predicted from existing correlations for ideal tube banks.

Palen and Taborek (38) in 1968 defined the following individual streams, (illustrated in Figure II.2), in decreasing order of effectiveness.

(1) B-stream: the true cross-flow stream, fully effective for heat transfer and pressure drop.

(2) A-stream: the streams passing through the clearance holes, fully effective for heat transfer, reducing pressure drop.

(3) C-stream: the bundle by-pass stream, only partially effective for heat transfer, passing around the outer halves of the outside ring of tubes.

(4) E-stream: passing through the shell-to-baffle clearance, it distorts the temperature profile, and is not effective for heat transfer.

The flow through the window is considered to consist of varying proportions of the the above streams.

A net effective flowrate can then be defined for use in existing ideal cross-flow correlations by

$$Q_{eff} = \alpha_i Q_B + \alpha_Z Q_A + \alpha_3 B_c + \alpha_4 Q_F \qquad (II.11)$$

The effectiveness factors α'S for each stream can be found from data fits, and the flowrate values can be found analytically, as in Palen and Taborek (38), Parker and Mok (39), and Devore (40).

Emerson (27) in 1962, concluded that while the semi-analytical methods are relatively simple to use and superior to integral methods, the total stream analysis methods are however fundamentally more sound and capable of improvement with the availability of better data.

The Heat Transfer and Fluid-Flow Service (HTFS) (of Harwell and the National Engineering Laboratory), are developing a stream analysis method (41). The development requires knowledge of local heat transfer coefficients and pressure drops data. Such data would enable a stringent testing of any computer programme embodying the method and also highlight and identify any weaknesses.

The following section reviews previous experimental investigation arrived at acquiring such data.

II.4 Experimental Shell-Side Studies

The work on stream analysis highlighted the need for more detailed data for the shell-side. Investigations over individual tubes and selections of tube bundles could provide such detailed data. The experimental studies to obtain pressure drop, heat and mass transfer data are now reviewed.

II.4.1 Pressure Drop

There exists a large volume of data in the literature reporting pressure drop in isothermal flow normal to experimental tube banks.

However, the agreement between corresponding data sets has been poor. This has been discussed further by Boucher and Lapple (42).

The most complete and precise pressure drop study in baffle shell-and-tube heat exchangers was by workers at Deleware University (18-25). The configuration tested included four different baffle spacings and three different baffle cuts for the no-leakage case, and single baffle spacing and baffle cut for semi leakage and total leakage cases. The data were represented in the form of Fanning friction factors (f) versus Reynolds numbers plots . The velocity used in both f and Reynolds number was based on the minimum flow area at the centre row of the bundle (A_M). These data are further discussed in Chapters III.3 , V.5.2 and VI.6 .

IV.4.2 Heat Transfer

The local heat transfer experimental studies are discussed below.

Gunter et al (43) in 1947 and Gupta and Katz (44) in 1957 used flow-visualisation studies to investigate the characteristic flow patterns in baffled exchangers. The main observations were that eddy currents created behind

baffles were reduced by increasing the number of baffles (43), and the identification of three characteristic zones; longitudinal flow, cross-flow and eddy-flow (44).

Ambrose and Knudsen (45) in 1958 and Gurushankaria and Knudsen (46) in 1959 made detailed measurements of local heat transfer coefficients in heat exchangers. They found, using an electrically heated test element, the following:

(i) The tubes passing through the baffle tube clearance exhibited 100 to 200% higher coefficients than the pure cross-flow zone.

(ii) Local coefficients of tubes in the window plane were higher than at any point on the same tube in that compartment.

(iii) Eddy zones in the lee of the baffle exhibited higher coefficients than in the pure cross-flow zone. This was explained by the high velocity jets issuing through the tube-baffle clearance as Stachiewicz and Short (47) in 1961 had shown that, for no-leakage bundles, eddy zones exhibited lower coefficients than the cross-flow zone.

Stachiewicz and Short (47) had also observed in their no-leakage baffled rectangular exchanger that the highest coefficients occurred around the baffle tips.

The use of heated test elements for measurements of local shell-side transfer coefficients necessitates large diameter tubes and bulky instrumentation. Moreover,

great difficulty is experienced in making accurate local temperature measurements. The insertion of thermocouples into the tube bundle could disturb the fluid flow causing erroneous readings. Therefore, a better technique which could quickly and comprehensively investigate transfer coefficients without disturbing the flow can be done by using mass transfer modelling techniques.

II.4.3 Mass Transfer Methods

The absence of local shell-side transfer coefficient data for exchanger geometries representative of commercial units, warranted a new series of experiemtnal investigation into thisfield using mass transfer techniques.

II.4.3.1 The Mercury Evaporation Technique

The first relevant study of local transfer coefficients using a mass transfer technique was by Williams (48,49) in 1962. A mercury evaporation technique was utilised giving the corresponding heat transfer data through the Chilton-Colburn heat and mass transfer analogy (see Section IV.2.2). Individual tube coefficients when averaged over the central compartment showed good agreement with the overall bundle average heat transfer coefficients, obtained by Bergelin et al (18-25) using nearly identical exchangers. Investigations were made for three baffle cuts namely 18.4, 31.0 and 43.7 per cent of the shell diameter, but at only a single baffle spacing.

Detailed analysis of William's individual tube data highlighted the earlier remarks (32,50) and (18,25) that baffle geometry as well as shell-side flow rate affects the distribution of transfer coefficients.

Roberts (51,52) in 1969 utilised the local transfer coefficient data of Williams in order to determine the distribution of local velocities within the bundle. From comparison of proportionality constants and the Reynolds number exponents obtained in the correlation of individual tube j-factors he derived velocity ratio terms. In this way the apparent velocity for any tube was related to that of tubes in the middle of the bundle which were considered to possess ideal cross-flow characteristics. Such an approach however assumed that the variation of the tube transfer coefficients were due to changes only in the local fluid flow rate and not for example due to variations on the direction of fluid flow. Of course, this assumption holds less validity in the window zones.

The resulting velocity distribution pattern gave further evidence of flow distribution being affected mainly by bundle by-passing. For the extreme values of baffle cut (18.4 and 43.7%) regions in the bundle were produced where the velocity ratio term changed with flow rate. However, for the intermediate baffle cut (31%), there were fewer tubes of this type and the flow distribution was more uniform. In general, the lowest coefficients were found in the outlet window zone.

Although the investigation of Williams went a considerable way towards modelling a typical commercial heat exchanger, they were, however, restricted to the case of no-leakage. Furthermore, the Reynolds number range covered (50 to 1625) represented the lower end of those encountered in industrial heat exchangers. Inspite of this, Williams proved the viability of mass transfer modelling techniques for local shell-side heat transfer studies. But the mercury evaporation technique had certain disadvantages. The technique is unsuited for rapid data acquisition, and it has certain inherent inaccuracies associated with fluid sampling and mercury deposition, points discussed in detail by Mackley.

After an extensive literature survey by Mackley (3) in 1973, a diffusion-controlled electro-chemical mass transfer technique was shown to have none of these disadvantages. The development of this technique is reported below.

II.4.3.2 The Electrochemical Technique

Mackley (3) found that a Redox system, e.g. potassium ferri-ferrocyanide couple, had numerous advantages over other electrochemical systems, particularly those involving deposition or dissolution processes. These advantages are briefly discussed in Section IV.2.3 .

For the development work Mackley used a similar model

exchanger to those of Williams (48,49) and Bergelin et al (21-25). This model's (model A) characteristic dimensions are given in Table II.2 . Therefore he was able to compare the compartment data with similar data of Williams and the bundle average data obtained from direct heat transfer by Bergelin et al.

The data for the 43.7% baffle cut were in good agreement with those of Bergelin, although there was a slight discrepancy at the lower Reynolds number, this however, was well within experimental error. William's data fell below Mackley's for both baffle cuts, the discrepancies being about 15% for the 31% baffle cut case, and between 5% at Reynolds number of 1000 to 25% at Reynolds number of 50 for the larger baffle cut. Unfortunately, no comparison was possible with Bergelin (20-25) for the 31% baffle cut.

Mackley explained the difference between his and William's data by William's no-leakage arrangement being less effective especially in reducing the shell-to-baffle leakage stream. Mackley further suggested that the mercury evaporation technique had inherent inaccuracies in determining the transfer coefficients from mercury coated sections of the tubes, as allowance for mercury blown off the tubes and deposited was necessary. This greatly distorted the distribution of transfer coefficients and lowered the compartment average coefficients.

Mackley was fully satisfied that the electrochemical method provided a suitable means of obtaining local heat transfer coefficients. In conjunction with HTFS Mackley (3) further utilised this method to study the effect of different geometrics on transfer coefficients. This is discussed in more detail in the following section II.6 as well as the more recent uses of the techniques in this field.

II.5 The Effect of Geometric Parameters on Local Shell-Side Heat Transfer Coefficient

In the development work Mackley tested an idealised exchanger with no-leakage and Reynolds numbers of less than 1500. In a further study he used a similar model (detailed in Table II.2 as model B) to investigate a much wider Reynolds number range and a more commercial type of exchanger with internal leakages. The work can be sub-divided into three sections, single segmental baffles without leakage, single segmental baffles with leakage and double segmental baffles with leakage. The complete study was carried out over only one internal compartment.

II.5.1 Internal Compartment without Leakage

Mackley compared his internal compartment average j-factors against overall bundle average j-factors obtained by Bergelin et al. from direct heat transfer studies. The data for 18.4% baffle cut and 48.5 mm

baffle spacing agreed within 3% of each other for Reynolds numbers higher than 1000. At the lower Reynolds numbers the two sets of data gradually separted to a maximum deviation of 12%, with the direct heat transfer data having the lower values. Mackley attributed the difference at low Reynolds numbers to the fact that internal compartment data were being compared with overall bundle average data. He argued that unlike the internal compartment which exhibits all three zones (inlet window, cross-flow and the outlet window), the end compartments have only two effective zones (a window zone and a cross-flow zone). These end compartments, (inlet and exit), would exhibit different transfer characteristics to the internal compartment and this difference would persist longer through the bundle at lower Reynolds numbers.

Mackley compared his 18.4% baffle cut and 97 mm baffle spacing data with those of Williams. Again good agreement resulted at Reynolds numbers higher than 200, but the discrepancy increased to 15% at a Reynolds number of 100. Mackley suggested that this might be due to shell-to-baffle leakage existing in Williams no-leakage bundle, thus becoming significant at low Reynolds numbers. In spite of this, the good agreement, particularly at higher Reynolds numbers, caused Mackley to believe that his results succesfully predicted the heat transfer coefficients, and this in turn supported the correctness of using the analogy.

Table II.2 Characteristic Dimensions of Exchanger Models used by Mackley

	MODEL A	MODEL B
Baffle Spacing	97 mm	97, 48.5 mm
Baffle Thickness	1.69 mm	1.59, 3.10 mm
Number of Tubes	80	80
Tube Diameter	9.5	9.5
Tube Arrangement	Staggered Square	Staggered Square
P/do	1.25	1.25
Baffle Cutdown	43.7, 31%	37.5, 35, 18.4%
Shell i.d.	133 mm	134 mm
t/B Clearance	0	0, 0.33, .33
s/B Clearance	0	0, 2.66, 1.4
Reynolds Number Range	24 - 1500	300 - 24,000
Baffle Type	Segmental	Segmental, Double Segmental

Examining individual tubes, Mackley found that symmetry existed across the vertical axis of the baffle, as the average coefficients for each half of the compartment differed only by 2%, and the individual symmetrical tube coefficients agreed to within 5%

Further comparison of these individual tubes showed that for constant Reynolds number, the ratio of cross-flow area to window area (A_m/A_w) played an important part in determining flow characteristics. This was done by normalising each individual tube j-factor against the compartment average j-factor and grouping together those which showed the same characterisation. It was also noticed that significant jetting occured at high ratios (A_m/A_w) and for lower or unit ratios this effect was negligible. Jetting produced inlet window coefficients comparable to cross-flow zonal coefficients, while at lower (A_m/A_w) ratios both window zones showed inferior j-factors compared to the cross-flow zone. The latter was clearly observed in the case of 37.5% baffle cut and 97 mm baffle spacing, and the jetting effect was demonstrated at 18.4% baffle cut and 97 mm spacing.

The characteristics of five selected tubes in different zones of the compartment showed remarkable similarity in the gradient of the j-factor versus Reynolds number curve. Also none of the tubes examined in the window and cross-flow zones showed signs of approaching either pure longitudinal or ideal cross-flow respectively. This was explained by the presence of eddy regions and variations in the distribution of velocities through

the bundles distorting the cross-flow and longitudinal flow characteristics. Therefore the velocity based solely on cross-flow area (V_m) could not effectively correlate the data from all the configurations studied.

In an attempt to correlate the effects of baffle geometry, Mackley tried to analyse his compartment data using three different velocity definitions:

(i) Velocity based on minimum cross-sectional area based on centre line of the bundle (A_m),

(ii) Velocity based on geometric mean of cross-flow and window flow areas (see equation II.8), and

(iii) Velocity based on arithmetic mean of maximum, minimum cross-flow and window flow areas (A_{AV}), see equation II.9.

The first failed to produce a suitable correlation of effects caused by baffle geometry. The geometric mean velocity (ii) and arithmetic mean (iii) both correlated the effect of baffle cut to with 10%. However, both failed to account satisfactorily for the baffle spacing.

After failing to correlate overall compartment coefficients, Mackley reverted to correlating individual zones. Moderate success was obtained when correlating the cross-flow zone, by using the minimum cross-flow velocity V_m. The baffle geometries were correlated to within 5% when the ratio of baffle overlap zone to the baffle spacing (L_c/L_s) was was less than unity. In

order to improve this correlation Mackley redefined cross-flow velocity by:

$$V_y = (V_m^2 . V_w)^{1/3} \qquad \text{(II.12)}$$

Only variations in baffle cut were correlated to ± 10%, at the longer spacing and ± 5% at the shorter spacing . The effect of the baffle spacing was again not adequately correlated. None of the aforementioned velocities were able to correlate adequately the effects caused by baffle geometry in either cross-flow or window-flow zones.

Jenkins et al (53) in 1977 developed a rapid computer technique of testing correlations using Mackley's data. In numerous attempts using many different definitions of velocity, no correlation was able to predict the affects caused by baffle geometry. Jenkins echoed Mackley's conclusions that no simple characteristic velocity was known which could adequately correlate effects caused by baffle geometry, represented in this case by baffle-cut and -spacing.

II.5.2 Internal Compartment with Leakage

The incorporation of leakage streams in 18.4% baffle cut and 48.5 mm baffle spacing resulted in a substantial reduction in the baffle compartment average j-factor (as high as 60%) compared with the no-leakage case. Mackley attributed the inferior coefficients with leakage to general redistribution of flow resulting in

greater proportions of longitudinal flow. This was in spite of the same 'Z' values (where 'Z' is related to the ratio of baffle plate thickness to radial clearance) for the thicker and thinner baffles. The former showed lower coefficients than the latter. Mackley pointed out that it was the baffle thickness, different for the two baffles, which was important and not the T.E.M.A. defined Z-factors as previously believed. The effects of leakage is shown to be greater at higher Reynolds numbers, contrary to the observations made by Bergelin et al who showed the effect of leakage on bundle average coefficients to be greater at low Reynolds numbers. For the same baffle cut, spacing and baffle-to-tube clearance. Bergelin's data were 30% inferior at low Reynolds numbers. At higher Reynolds numbers the Mackley data fell around 15% above those of Bergelin. Mackley partly attributed this difference to different shell-to-baffle clearances. In order to explain the different slope of the j-factor against Reynolds number curve, Mackley argued that with leakage, the characteristics of an internal compartment differed widely from those of the overall bundle. He pointed out that in the inlet compartment the tube sheet provides no upstream leakage, similarly there is no downstream leakage in the exit compartment. Mackley, unable to predict the end compartment coefficients demonstrated the need for experi mental measurements of mass transfer coefficients in these compartments.

The distribution of the tube coefficients was

shown to be far more uniform than that from the no-leakage investigations. Few tubes had coefficients different by more than 10% from the compartment average value. This greater uniformity was attributed to the dispersal of the eddy flow and the reduction of fluid jetting.

In commercial exchangers, the baffles are normally arranged such that the shell-side fluid weaves from side-to-side through the bundle. This effect was investigated by Mackley. The difference between side-to-side and up-and-down flow was insignificant, being within the experimental accuracy. The structural advantages of the vertical baffle cut arrangement are not off-set by an inferior transfer performance.

The effect of variation in baffle cut was examined by investigating three different baffle cuts. It was noticed that baffle cut did not have a noticeable effect. The 18.4% and 25% baffle cut data were correlated by a single curve, and the correlation curve for 37.5% baffle cut differed by less than 20% from the above cases. The corresponding value for the no-leakage data was 34%. The effects of baffle cut and leakage area were to oppose and to some extent cancel, each other. This was attributed to a reduction in window area being to some extent offset by an increase in the baffle leakage area, hence affecting the distribution of flow to a lesser extent than would have been the case. Mackley also showed

for all the baffle cuts examined, how leakage coefficients deviated further with increasing Reynolds numbers. This was done by plotting the ratio of leakage to no-leakage j-factors against Reynolds number. The ratio decreased with increasing Reynolds number.

Any correlation of the effect of leakage areas would have required a knowledge of the relative magnitude of the individual flow streams, that is the stream analysis approach. A simpler approach adopted by Mackley from Bell (54) in 1960 was to correlate the effects of leakage on the heat transfer data with leakage flow area. This was studied for thicker baffles when the baffle cut was the only geometrical variable. The variable baffle geometry was described by the ratio (A_L/A_W) representing the additional Longitudinal area produced by leakage clearances to that available in the absence of leakage. The relationship between the effects of shell-and-baffle and tube-and-baffle leakages were assumed by Mackley to be the same as proposed by Bell (54). The equation suggested was

$$\left(1-\frac{j_L}{j_{NL}}\right)_{\substack{\text{combined}\\ \text{exchanger}}} = \left(1-\frac{J_L}{J_{NL}}\right)_O \left[\frac{A_{TB} + 2A_{SB}}{A_L}\right] \qquad \text{(II.13)}$$

From a given value of A_L/A_W, the combined leakage j-factor term was obtained. This was then used in equation (II.13) to obtain the weighted j factor ratio term $(1- j_L/j_{NL})_O$.

Mackley also reported internal compartment pressure drop. Leakage was shown to reduce the pressure drop across a compartment by up to a factor of six compared to the no-leakage case. The onset of fully turbulent flow in the leakage case occurred at a Reynolds number of 16000, compared with 5000 for no-leakage. This late transition to turbulent flow indicated by the leakage data could be attributed to the increased longitudinal flow component. Mackley pointed out that baffle leakage had far greater effect on pressure drop than on the mass transfer coefficients.

II.5.3 Double Segmental Baffle with Leakage

Mackley reported some experimental work using a double segmentally baffled design which demonstrated the general performance characteristics of this baffle arrangement. No previous data were available hence no direct comparisons with previous work was possible. With this baffle type, geometric symmetry exists about the centre plane parallel to the baffle cut, and so the shell-side flow was assumed to be distributed equally between these two halves of the bundle. The flow in each bundle half is similar to flow in a single segmental baffled exchanger. Therefore, a double segmentally baffled unit could be analysed as two equal single segmentally baffled units separated by a fluid-fluid interface.

A comparison of 18.4% baffle cut and 48.5 mm baffle spacing data from the two half bundles showed no difference between averaged j-factors for each half. It

was thus shown that the assumption of symmetry was justified. The shell-side flow converges and diverges in adjacent compartments, and a comparison was made between the two sets of data which showed complete agreement. The zonal averages were also compared, with no significant difference. It was concluded that the double segmental baffle produces extremely uniform flow distribution.

As it was thought that the double segmentally baffled exchanger was equivalent to two equal parallel single segmentally baffled exchangers some tests of this were obviously needed. However, Mackley was unable to provide an exact comparison between the double segmental data and corresponding data from two equal single segmental exchangers in parallel with a total cross-sectional area equal to that of the double segmental exchanger. Hence no true comparison could be made since no common basis existed for comparison. A comparison of the j-factors on a total shell-side flow basis of the 18.4% baffle cut double segmental exchanger with a 37.5% baffle cut single segmental exchanger showed some agreement. The comparison of the pressure drop over the two exchangers also gave good agreement. Hence it was thought that the overall performance of a double segmental arrangement could be matched by that of a single segmental exchanger with twice the baffle cut. However, the double segmental exchanger showed more uniform j-factor distributions than the single segmental exchanger with larger baffle cuts.

II.5.4 End Compartment without Leakage

It was suspected, from Mackley's internal compartment study that the end compartment may behave differently from the internal compartment. Mackley explained the difference between the direct heat transfer data and the no-leakage data, at low Reynolds numbers by the end compartment exhibiting different characteristics to the internal compartment (see Section II.4.1 above). The same explanation was offered for the leakage situation (see Section II.4.2). Bergelin et al (21-25) also assumed the end compartment to be untypical, leading them to use rectanguar type ports rather than the commercial circular ports, in order to reduce the end compartment effects.

Prowse (4) in 1977 investigated the mass transfer characteristics of the end compartment in a similar exchanger model and used the same measuring technique as Mackley. A no-leakage bundle only was investigated with both baffle spacing and baffle cuts fixed at 47.6 mm and 18.4% respectively. Both end compartments, inlet and outlet, were studied. Prowse (4) only used fifteen cathodes in one half of the bundle for these studies, as symmetry was known to exist across the vertical axis. He compared the corresponding fifteen tube average of Mackley's data against an overall average of 78 tubes, and found a difference of less than 2%, therefore justifying the use of 15 tubes to represent the compartment average.

Prowse then compared the inlet compartment average j-factor values against the internal compartment average j-factors obtained by Mackley for both leakage and no-leakage cases. The inlet compartment data fell considerably below both leakage and no-leakage data of Mackley. The difference between the two no-leakage investigations was approximately 125%. Prowse suggested that although small amounts of leakage may have been present in his bundle, in no way could this correspond with the deliberate leakage case of Mackley. Failing to explain the difference, Prowse considered that the inlet compartment possessed considerably inferior mass transfer characteristics compared with the internal compartment.

The inlet and outlet compartments with both horizontal and vertical baffle cut were also examined by Prowse. The outlet compartment average j-factors were shown to be 11% lower than those for the inlet compartment for a horizontal baffle cut. There was no appreciable difference between the inlet and outlet compartments with the vertical baffle cut. This difference was, however, considerably smaller than between end and internal compartments. Further examination of the normalised individual tube j-factor distribution for inlet and outlet compartments showed an identical distribution. Therefore, Prowse concluded that the inlet and outlet compartments showed similar flow characteristics.

Prowse also investigated the effects of baffle orientation by examining the comparative effect of horizontal and vertical baffle cuts. All his end compartments showed that the vertical baffle cut data fell below horizontal baffle cut, although the difference was very slight and all the data could be represented by the same curve. For all end compartment studies, the horizontal baffle cut produced a fairly even j-factor distribution, whilst the vertical orientation gave very uneven distribution. The latter case showed the j-factor values to be considerably higher in both port and window zones relative to the average value. The lowest values were found in the regions furthest away from the above zones. This was explained by flow taking the shortest path through the end compartment causing stagnant zones away from the port and window zones. High j-factor values in port and window zones compensated for the other regions, generating similar overall j-factor values for both orientations. Therefore the compartment average j-factor was found to be independent of baffle orientation.

The large rectangular ports were used by Bergelin et al (21-25) and Mackley (3) in order to reduce the effects of the end compartments persisting through the bundle. Therefore, Prowse (4) studied the effect of this idealised port against a circular port, a type which would be used in industry. The data for the two end compartments and both baffle orientations show the commercial ports to be marginally inferior by 10% to the rectangular ports. This difference was insignificantly

greater than his expected experimental error.

In industry, impingement baffles are sometimes used in the inlet compartments to overcome erosion problems with the tubes nearest to the inlet ports. Prowse investigated the effect of a thin rectangular plate acting as an impingement baffle in the inlet compartment. The data show no significant improvement in the compartment average j-factor for the horizontal baffle cut, and the distribution of j-factor in the inlet compartment was adversely affected. It was concluded that this particular impingement baffle design would only be useful where erosion was the prime concern. For the vertical baffle cut however, the compartment average j-factors were improved by up to 25% at Reynolds number of 10000, with the distribution of the j-factors becoming more uniform.

Unfortunately, Prowse made no attempt to measure the effect of impingement baffles on pressure drop. But Macbeth (55) in 1976 in an extended study of the effects of inlet nozzles on pressure drop in shell and tube heat exchangers found that the presence of impingement greatly increased the pressure drop in the exchanger.

It was therefore concluded that the inclusion of an impingement baffle on the inlet compartment would noticeably improve both the compartment average and the distribution of j-factor. This would, however, result in an even greater increase in pressure drop (55). Hence in cases where the heat transfer performance and flow

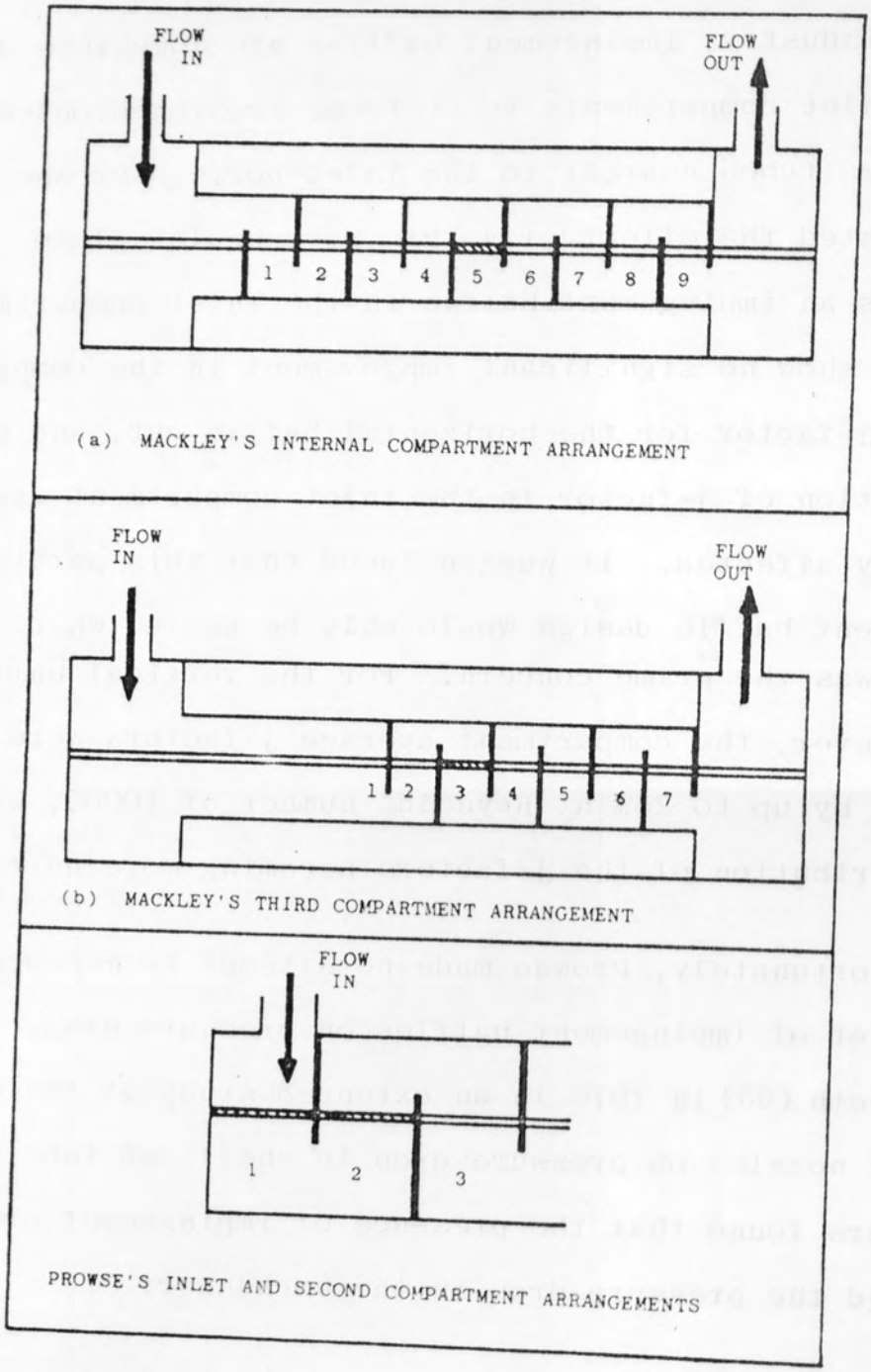

Figure II.3 Positioning of electrodes in Mackley's and Prowse's exchangers

distribution are of major concern, then the inclusion of an impringement baffle may be justified, even when the erosion problem was not a serious one, but at the penalty of a proportionally higher pressure drop.

II.5.5 Length-Wise Variation of Transfer Coefficient

Both Mackley (3) and Prowse (4) suspecting length-wise variation of transfer coefficient along the exchanger extended their investigations to compartments other than the compartments of specific interest to them. Because of restrictions imposed by their equipment their studies were very limited and provided only a tentative investigation.

Mackley (3) studied the third compartment for 37.5% baffle cut and 48.5 mm baffle spacing. This was for a no-leakage bundle and was done by removing the first three upstream baffles while the electrodes remained in the same position. This was illustrated in Figure II.3. When comparing the results with the internal compartment (fifth), the compartment near the the inlet showed itself to be inferior by about 10%. The experimental accuracy of Mackley's data ($\pm$8.6%) made this difference barely significant. Mackley attributed the slight difference to the third compartment still possessing some entrance characteristics.

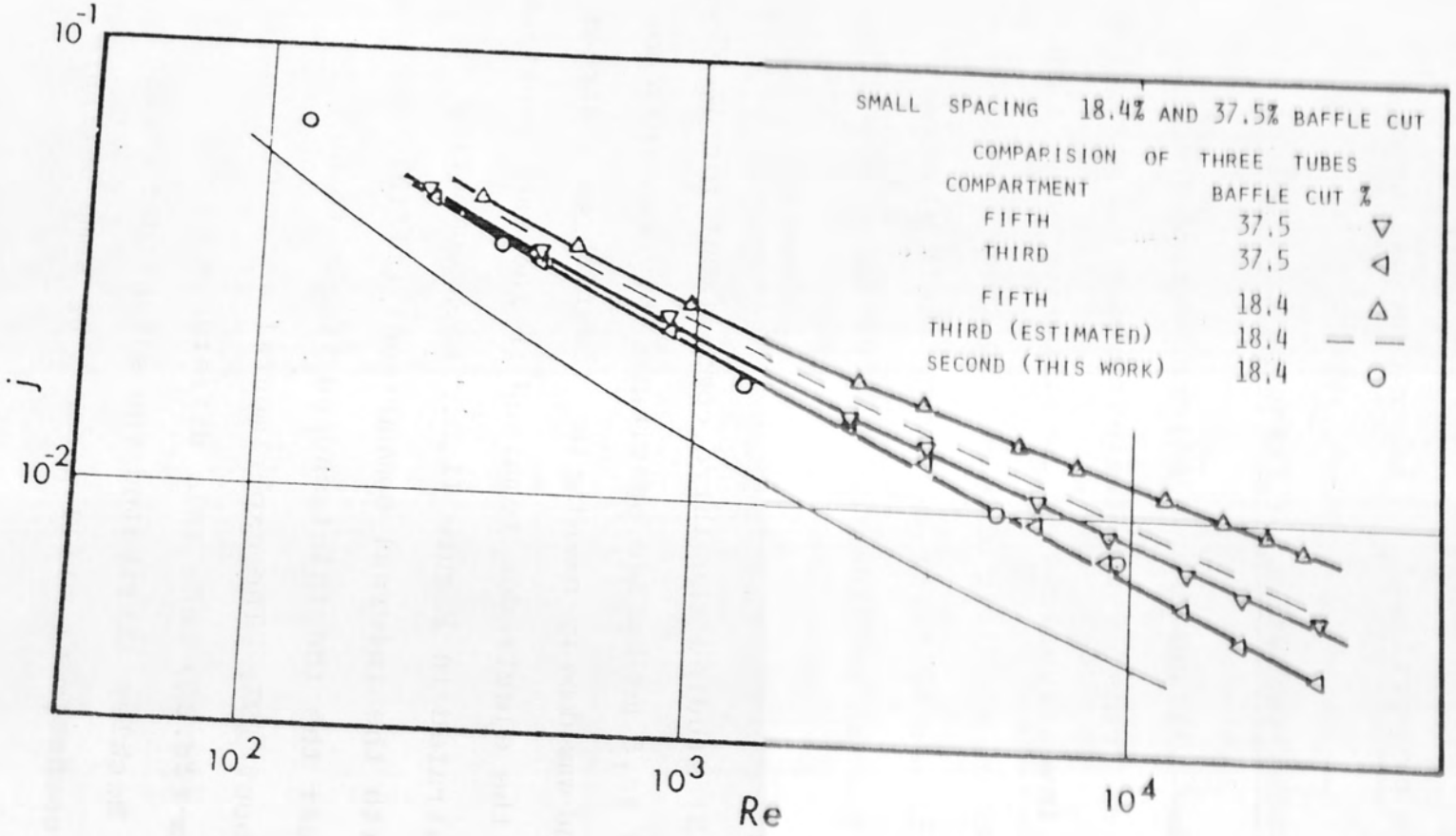

Figure II.4 The suspected length-wise variation of transfer coefficient (4)

Prowse also made a very limited investigation of the second compartment. Three cathodes were deployed in the cross-flow region of the second compartment of an 18.4 baffle cut and 47.6 mm baffle spacing no-leakage bundle. Prowse compared this second compartment cross-flow data against his inlet compartment, and Mackley's internal and third compartments. Prowse recalculated Mackley's data for the cross-flow average j-factors over the corresponding three electrodes in the internal compartment for 18.4% baffle cut and 48.5 mm baffle spacing no-leakage bundle. In order to evaluate the third compartment three tube cross-flow average j-factor for a similar baffle cut of 18.4%, Prowse used the baffle cut correlation achieved by using equation II.8 in defining the the velocity term to transform the existing third compartment 37.5% baffle cut data. This estimate, together with the three tube cross-flow average for the internal and second compartments and overall inlet compartment average j-factors were plotted on a single graph, depicted in Figure II.4.

It could be seen that there was a compartment-wise variation from the inlet to the internal compartment with increasing transfer coefficients from the former to the latter. The second and third compartment correlations lie between inlet and fifth compartments with the third compartment closer to the fifth compartment than its adjacent second compartment.

Prowse argued that the difference was due to Mackley's third compartment data (37.5% baffle cut) being obtained from an abnormal design of the downstream compartments. As can be seen from Figure II.3, Mackley's shell had an unusual inlet compartment, in that it lay downstream of the inlet port. Also, Mackley's third compartment data were obtained by removing the first three baffles leaving the dummy tubes in precisely the same position as for the fifth compartment investigations. The effect of these abnormalities of design could have led to unusually smooth flow characteristics in the third compartment downstream. For this reason, it was suspected that the third compartment data of Mackley showed higher transfer characteristics than for the same compartment in a normal shell. Prowse further postulated that if Mackley's data had been obtained from a shell similar to his, then the third compartment would have fallen closer to the second compartment data.

This limited study suggested that the j-factors increased from the inlet to the central compartments. However,the outlet compartment had similar magnitude j-factors as the inlet compartment. Therefore a gradual fall of compartment average j-factor might be expected to occur from the internal compartments to the outlet. This is a very tentative conclusion and detailed experimental data are required for the intermediate compartments, before concrete conslusions can be drawn about the variation of transfer coefficient along the exchanger length.

The scope of experimental work (see Sections V.1 and VI.1) to be carried out in this study is intended to provide such data which would, among other things, elucidate how the transfer coefficient behaves along the exchanger length.

CHAPTER III

Correlation of a Shell-Side Data

III.1 Introduction

The design of shell-and-tube heat exchangers requires a knowledge of the shell-side transfer coefficient and pressure drop with respect to the fluid-flow rate. It was shown in the previous chapter that such a knowledge was obtained by plotting a dimensionless transfer coefficient and pressure drop factors against Reynolds numbers. However, this picture was complicated by the distribution of fluid-flow caused by the geometry of the cylindrical tube bundles. In Section II.1 it was shown that there were numerous geometrical parameters which could affect the distrbution of flow by changing the bundle geometry. In general, for any given tube arrangement, tube and shell diameters, tube pitch and baffle type the performance of the exchanger is mainly controlled by the baffle geometry. The four geometrical variables which specifically highlighted the influence of baffle geometry are baffle-cut, baffle-spacing, shell-to-baffle clearance and a tube-to-baffle clearance. The baffle thickness also influences the distribution of flow (Section II.5.2), but this

could be associated with the leakage flow path resistance and therefore incorporated into the shell-to-baffle and tube-to-baffle leakage areas. Varying any one of these four parameters produced a different correlation for what is otherwise the same bundle. The difficulty in the past discussed in Chapter II, had been to obtain a correlation independent of baffle geometry, yielding a single correlation which represented all the baffle arrangements. Such a correlation would be most useful in design offices, where the effects of baffle geometry could be quickly and easily determined, and accounted for, in the overall performance of heat exchangers.

To understand the effects caused by each of these geometrical cases, Bergelin et al, Williams and Mackley segregated the baffle-cut and -spacing from the leakage variables by investigating a no-leakage bundle. Later the leakage clearances were incorporated in the same bundle to examine a more commercial type of exchanger. The experimental no-leakage investigation produced much needed information on the influence of baffle-cut and -spacing. However, attempts to correlate these data from all baffle geometries on a single curve failed. The general conclusion was that no suitable flow area was known which, when used to determine the velocity, would correlate the data for both baffle-cut and baffle-spacing.

This chapter attempts to find a characteristic flow area which would effectively account for all baffle geometries.

The next section discusses the transfer coefficient data obtained from both leakage and no-leakage bundles.

III.2 Correlation of Transfer Coefficient Data

III.2.1 No-Leakage Cases

This section attempts to correlate the data from a "simplified" no-leakage bundle, with variations in baffle-cut and baffle-spacing. The data of Bergelin et al (20-25) and Mackley (3) are used. Earlier attempts to correlate the overall bundle and compartment average transfer coefficients are listed in Table III.1. This Table shows the characteristic length and flow area used in each correlation, and the extent of correlation with such an arrangement. The baffle compartment could be subdivided into crossflow and window flow zones, as discussed in Section II.5. The previous attempts to correlate these zonal average transfer coefficients are also listed in the Table.

The correlations given above show that the transfer coefficient is made dimensionless by using either $Nu/PR^{1/3}$ or the Chilton-Colburn j-factor. The transfer coefficients in the direct heat transfer work at Delaware University and mass transfer work by Mackley, Williams and Prowse were all expressed mainly in terms of the j-factor. This dimensionless group is proportional to the transfer coefficient and inversely proportional to velocity. The velocity is

Table III.1 Previous Correlations of Transfer Coefficient Data

REFERENCE	CORRELATION	CHARACTERISTIC		REMARKS
		LENGTH	FLOW AREA	
Colburn (13) Section II.2	$(Nu/Pr^{1/3})=Re_c^b . a$	d	A_c	For x-flow ideal tube banks the constant is a function of tube arrangement.
Emerson (27) Section II.2	$(Nu/Pr^{1/3})=a\ Re^b_{EFF}$	d	A_{EFF}	Crossflow in cylindrical tube banks. Never used in correlations.
Kern (28) Section II.2	$(\frac{Nu_{ek}}{Pr^{1/3}})=a\ Re_{ek}^b$	d_{ek}	A_K	For cross baffled cylindrical exchangers. Empirical data. No account taken for the geometrical parameters.
Donohue (29) Section II.3	$(Nu/Pr^{1/3})=a'Re_Z^b$	d	A_Z	Moderately correlates BC, no correlations of BS, or clearances. a' is a function of hydraulic diameter.
Short (32) Section II.3	$(\frac{Nu}{Pr^{1/3}})=a'Re_{AV}^b$	d	A_{AV}	Baffle cut correlation but a' is a function of tube geometry and no correlation of baffle spacing.
Mackley (3) Section II.5	$j=a\ Rem^{-b}+ pRem^{-q}$	d	A_M	For compartment average. No correlation of geometrical parameters.
Mackley (3) Section II.5	$j_c=a\ Rem^{-b} + pRem^{-q}$	d	A_M	For crossflow zone. Correlation of both BS & BC if ratio LC/LS < 1. Otherwise no correlation.

Continued . . .

Table III.1 (Continued)

REFERENCE	CORRELATION	CHARACTERISTIC		REMARKS
		LENGTH	FLOW AREA	
Mackley (3) Section II.5	$jy=a\ Rey^{-b}+pRey^{-q}$	d	$Ay=(A_m^2A_w)^{1/3}$	For Crossflow Zone. Baffle cut correlated but not baffle spacing.
Jenkins (53) Section II.5	$j_w=a\ Re_w^{-b}+pRe_w^{-q}$	d	A_w	For window zone. No correlation of either baffle cut or spacing.
Jenkins (53)	$j=a\ Re_{H2}^{-b}+pRe_{H2}^{-q}$	d	$A_{H2}=(A_m^2+(FA_w)^2)^{\frac{1}{2}}$ where $O\leq F\leq 1$	For crossflow and overall bundle. Similar to Donohue (29).
Jenkins (53)	$j=a\ Re_{H3}^{-b}+pRe_{H3}^{-q}$	d	$A_{H3}=((FA_m)^2+A_w^2)^{\frac{1}{2}}$ $O\leq F\leq 1$	For window flow. No correlation of geometrical parameters.

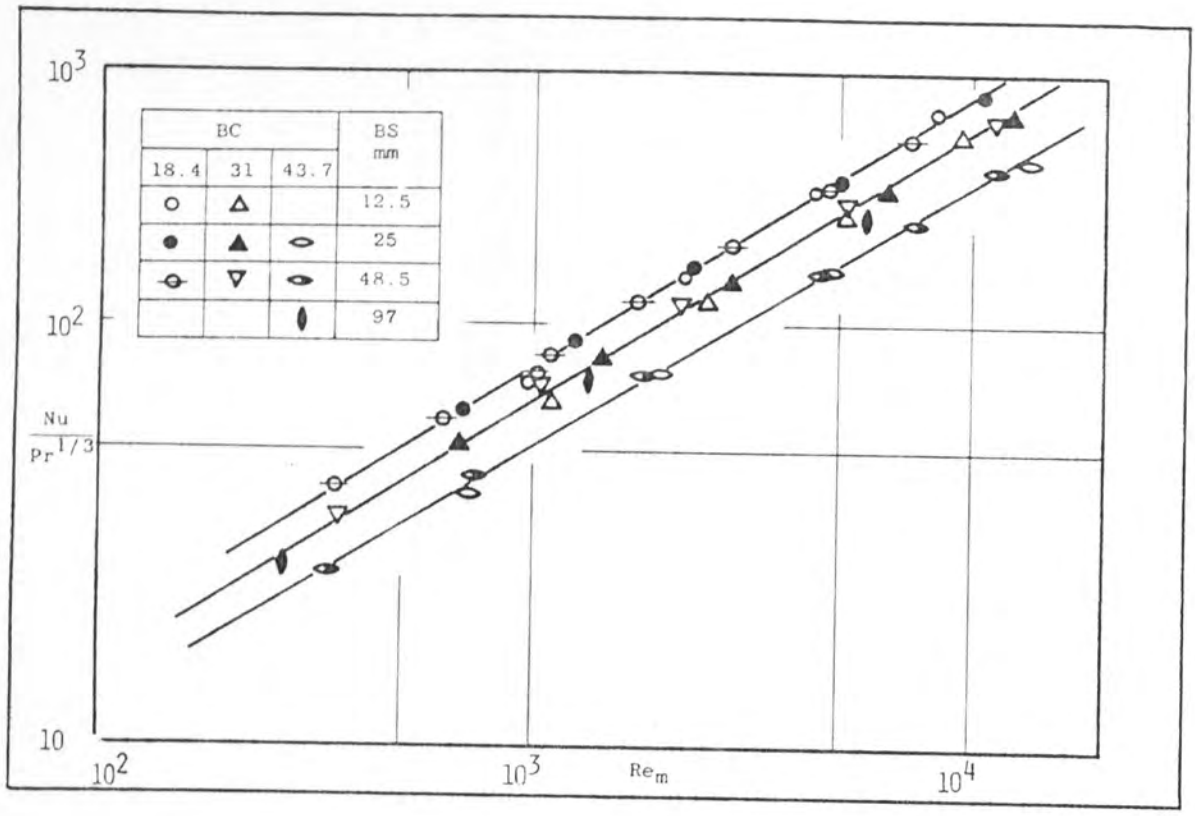

Figure III.1 Correlation of Brown's (23) data by using characteristic velocity V_m

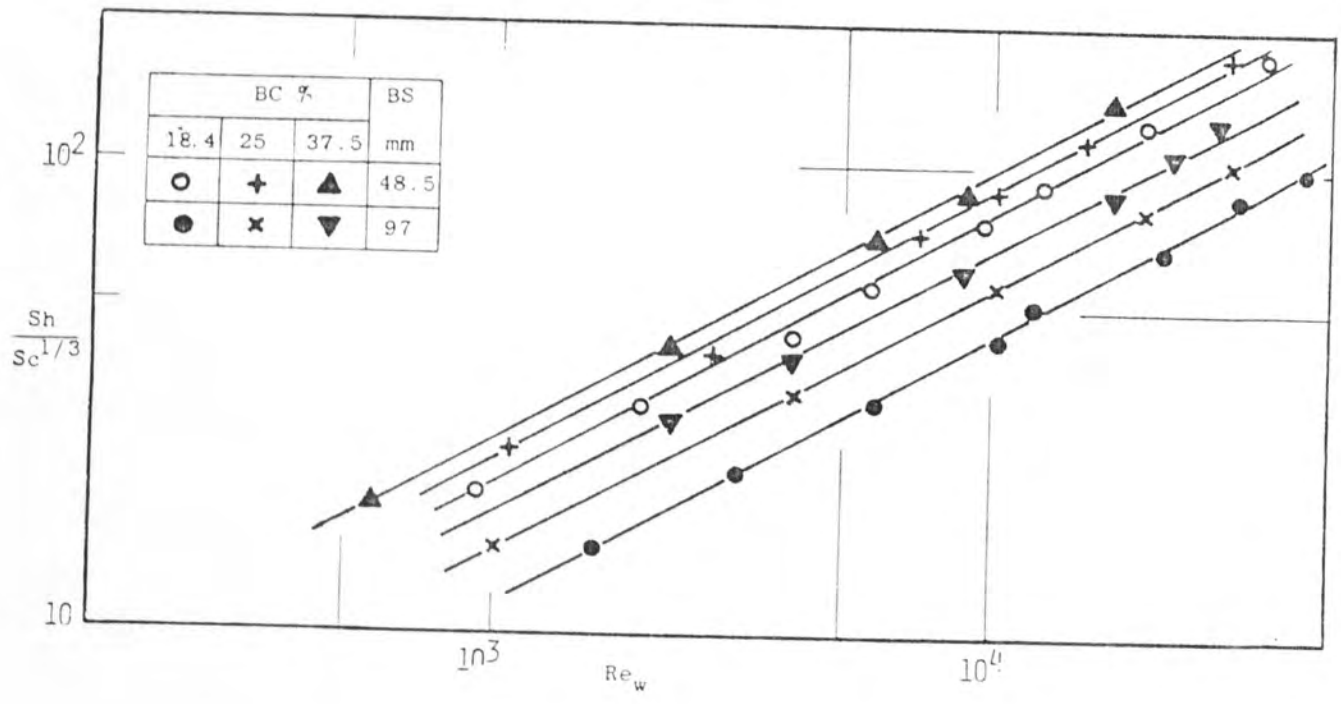

Figure III.2 Correlation of Mackley's (3) data by using characteristic velocity V_w

geometrically dependent and any correction to account for geometry would require both Reynolds number and the j-factor to be corrected. But, if the ordinate were independent of velocity then only the Reynolds number would need changing. This would be the case if $(Nu/Pr^{1/3})$ for heat transfer and the analogous $(Sh/Sc^{1/3})$ for mass transfer replaced the j-factor as the ordinate. The relationship between these two dimensionless groups is simple allowing the j-factor data to be converted by equation III.1

$$\left(\frac{Sh}{Sc^{1/3}}\right) \text{ or } \left(\frac{Nu}{Pr^{1/3}}\right) = j\ Re \qquad \text{(III.1)}$$

where j-factor and Reynolds number are based on the same velocity. Replotting the no-leakage data of Brown (23) in this way with a Reynolds number based on A_M as the flow area results in a correlation of baffle-spacing but not baffle cut as illustrated in Figure III.1. The only exception to this is the 43.7% baffle-cut and 98 mm baffle-spacing case. Analysing the free-flow area A_m it is evident that no account is being taken of the baffle-cut in defining this characteristic area. If the window free-flow area replaced A_m in the Reynolds number, then it is apparent that baffle-cut and -spacing are both not correlated, (see Figure III.2).

However, the influence of baffle-cut is reversed with respect to Figure III.1. The larger baffle-cuts show higher heat transfer coefficients than the smaller baffle-cuts at the same Reynolds number. This is to be

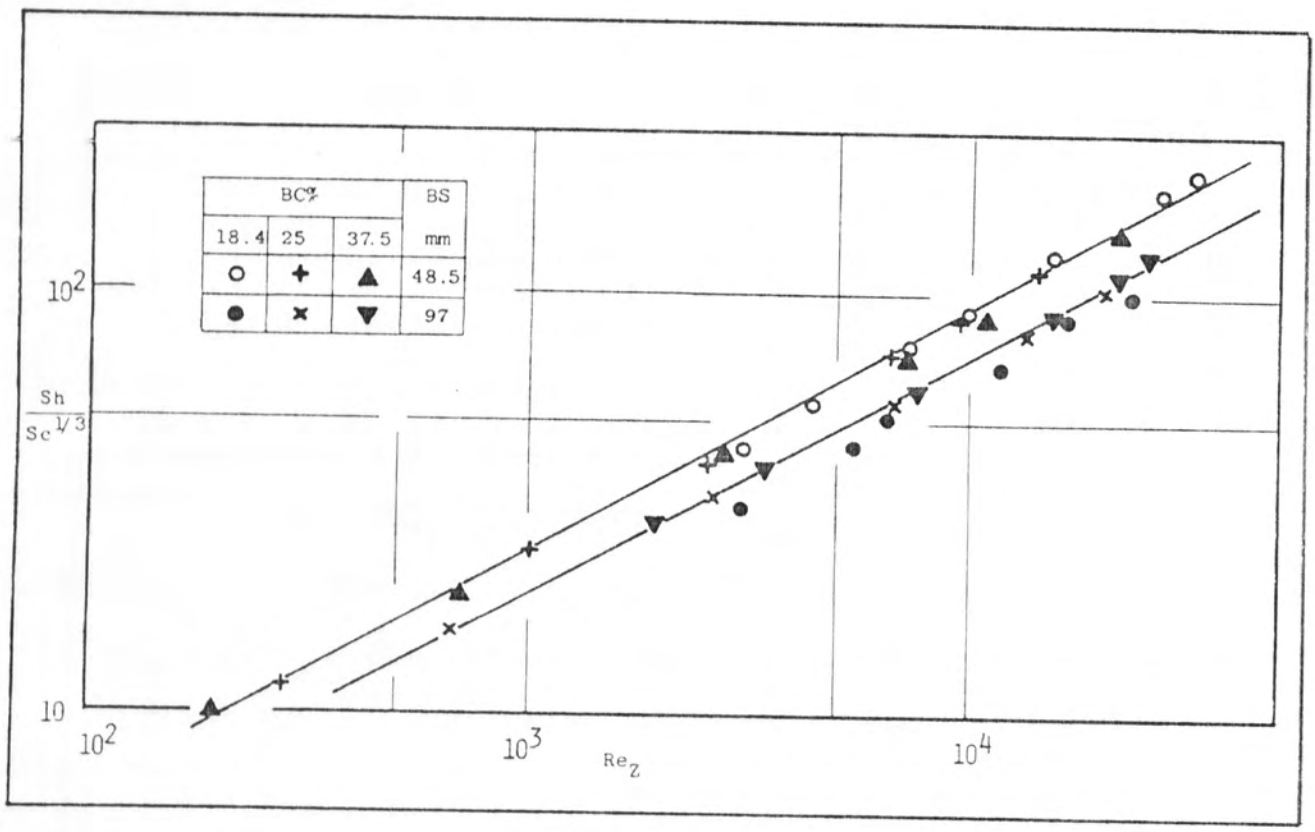

Figure III.3 Correlation of Mackley's data by using characteristic velocity V_Z

expected as, at the same Reynolds number the large baffle-cuts require higher flow rates, thus offsetting the lower coefficient due to greater longitudinal window flow.

Previous correlations combine the window free-flow area A_w with the minimum free-flow area at the centre of the tube bundle A_m. This was done in an attempt to remove the effects of baffle-cut from the baffle-spacing correlation, obtained when using the latter flow area alone. Mackley's data have been replotted with Donohue's (32) geometric mean velocity, (see Figure III.3). This shows a correlation of baffle-cuts at the expense of baffle-spacings. Various combinations of A_w and A_m have been tested by Jenkins (53) without much success. The resulting conslusion was that some other flow area was needed to account for the baffle geometry.

It was noted above that A_w correlated niether baffle-spacing nor baffle-cut, whereas A_m successfully correlated baffle-spacings. Hence, an area similar to A_m is needed which also accounts for the window flow. Consideration of the complexity of the baffle compartment indicates the distribution of the fluid-flow is complicated and only a few tubes are able to experience the same flow regime throughout their length, whether they are in the cross-flow of eddy-flow zone. Therefore, some arbitrary but realistic flow area should be found which would correlate data from most of the geometries investigated. In the past

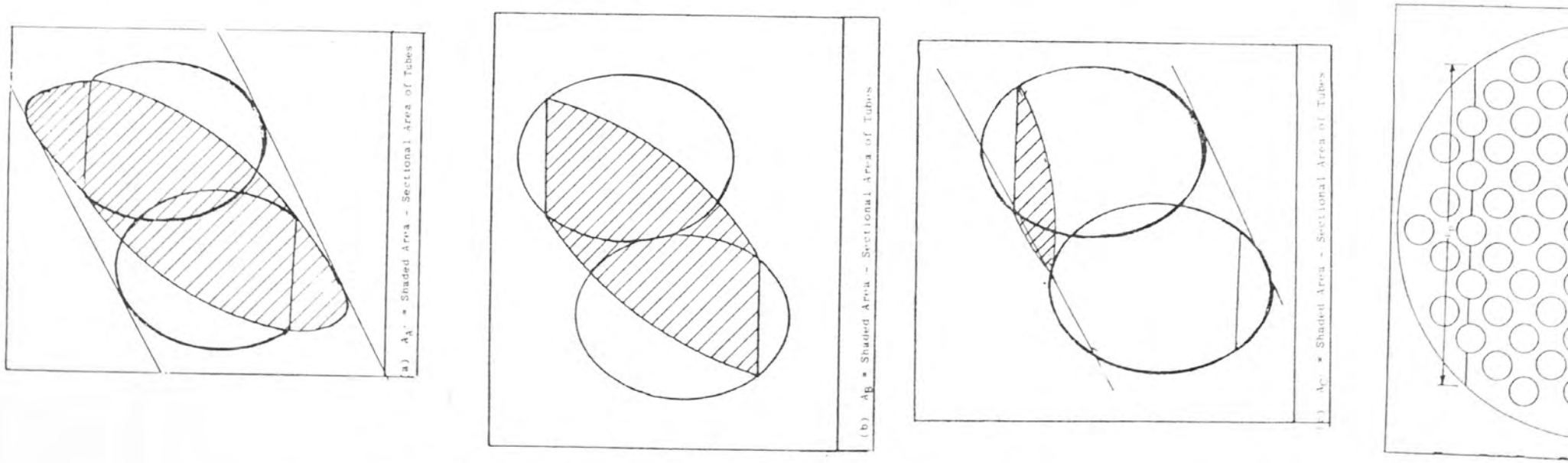

Figure III.4 Arbitrarily defined flow areas related to baffle cut.

baffled exchangers were looked upon as a logical construction of flow past an ideal rectangular bundle, as shown in Section II.2. Therefore, use of the cross-flow area A_m was extended to represent the data for cylindrical baffled exchangers. All the previous attempts to account for the baffle cut had failed when A_w was used with or without A_m.

Numerous arbitrary flow areas could be defined which are functions of both the baffle-cut and -spacing. Some of these possibilities are illustrated in Figure III.4. Mackley's data are replotted using these flow areas in the Reynolds number in Figures III.5 to III.8.

Examination of these figures shows that only Figure III.8 showing correlation of the data with a reasonable degree of success. The Reynolds number here is based on flow area A_I: this is calculated in a similar fashion to A_m but accounts for the baffle cut by defining the flow path at the baffle edge, as illustrated in Figure III.4d. The baffle-cut affects the flow path in two ways; firstly the chord length and secondly the number of tubes at the baffle edge. The maximum spread of Mackley's data is 20%. This spread is reduced to less than 10% if the 18.4% baffle-cut and 48.5 mm baffle-spacing case is omitted. This latter geometrical case could be represented on a different curve.

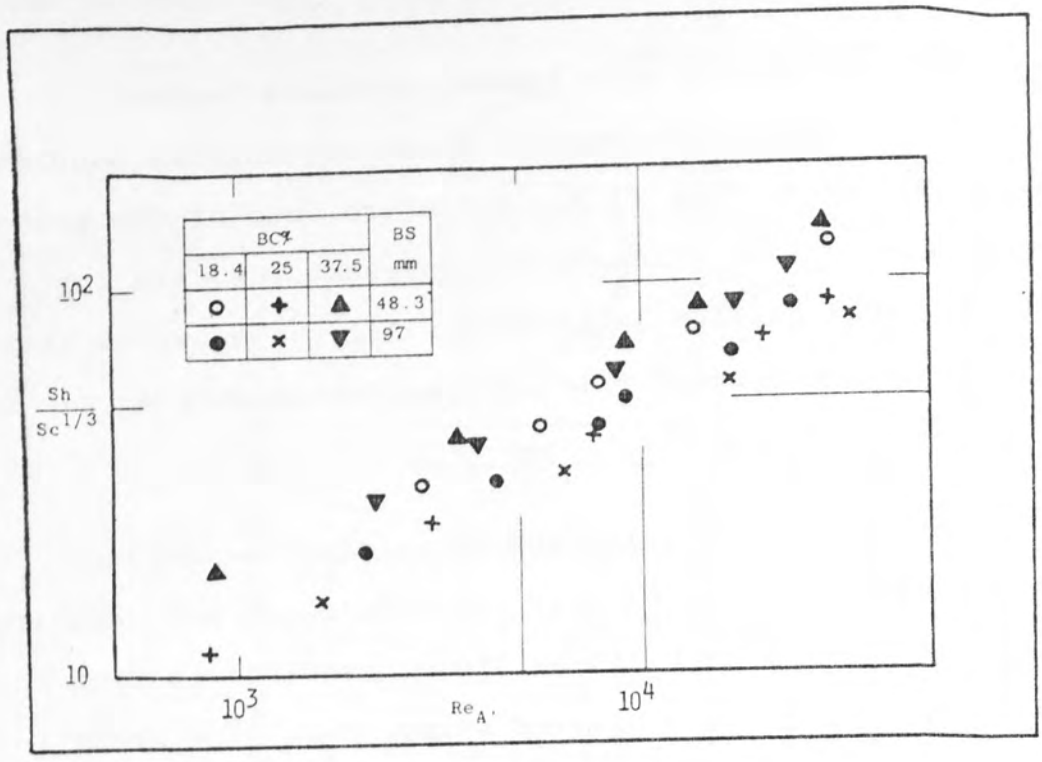

Figure III.5 Correlation of Mackley's data by using characteristic flow area defined in Figure III.4a.

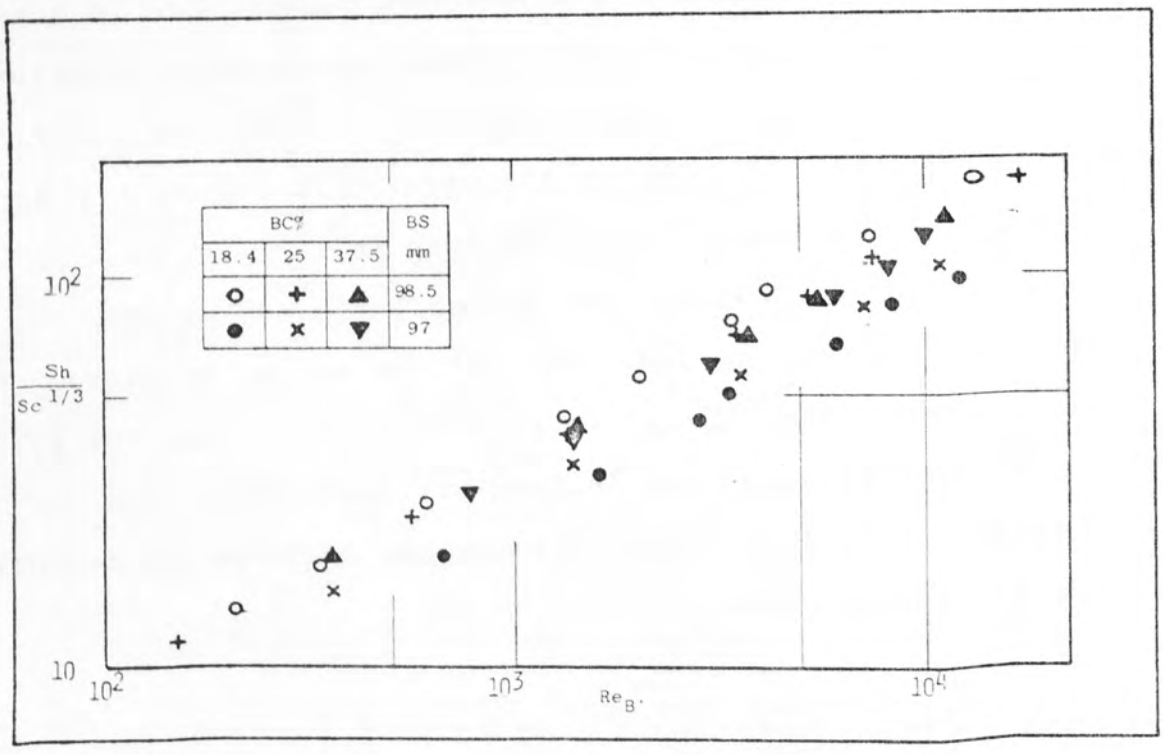

Figure III.6 Correlation of Mackley's data by using characteristic flow area defined in Figure III.4b.

In order to substantiate the correlation further, the data of Brown are replotted using A_I as the characteristic flow area in the velocity. Figure III.9 reveals that all the experimental data lie on three curves. When the data of Mackley and Brown are compared (compare Figures III.8 and III.9) above a Reynolds number of 1500, the upper curve in Figure III.8, representing the 18.4% baffle-cut and 48.5 mm baffle-spacing is coincidental with curve (I) in Figure III.9. The remaining configurations studied by Mackley are coincident with curve (II) in Figure III.9. The third curve in Figure III.9 represents smaller baffle-spacings at a larger (43.7%) baffle-cut.

Below a Reynolds number of 1500 Mackley and Brown's data deviates with decreasing Reynolds number. The difference at lower Reynolds numbers was explained by Mackley to be due to leakage in Brown's exchanger or, limitation on the analogy due to natural convection effects, and other effects discussed further in Chapter IV. The resulting conclusion was that baffle-spacings smaller than 50 mm and with extreme baffle cuts were not correlated by an otherwise geometrically independent correlation obtained for the remaining cases shown in Table III.2.

The remaining geometric configurations not correlated represent exchanger configurations not likely to be used comercially. The configurations with 18.4% baffle-cut and baffle-spacings less than 50 mm produce higher coefficients

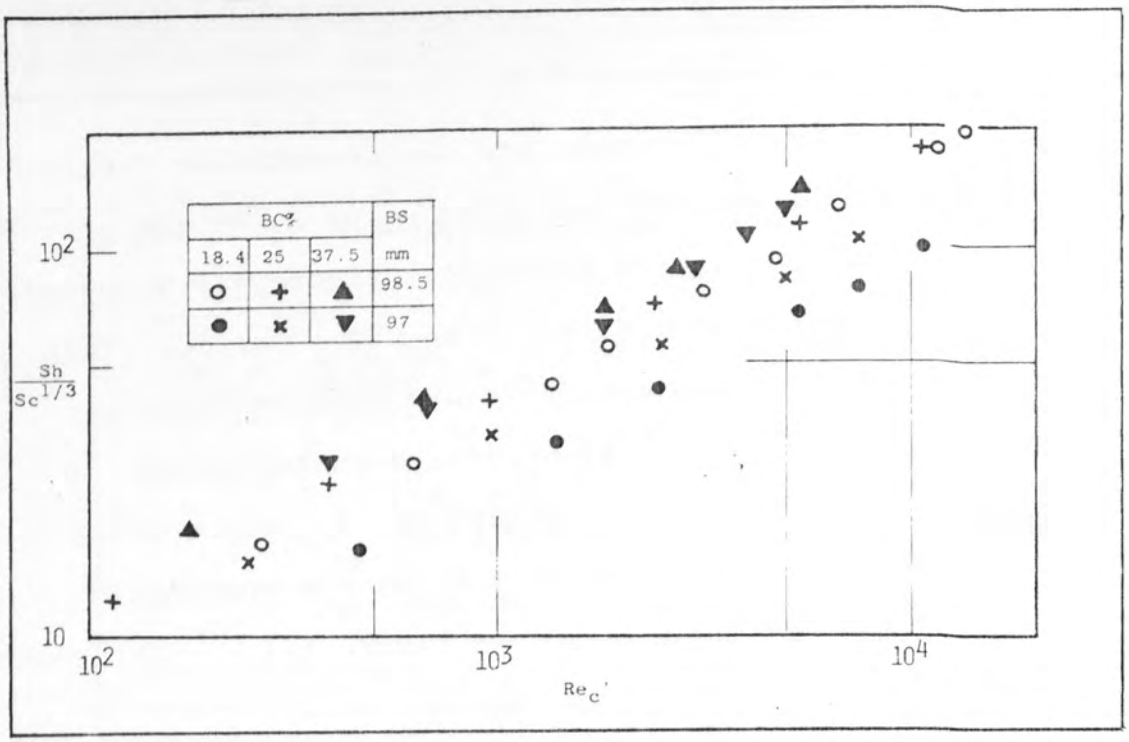

Figure III.7 Correlation of Mackley's data by using characteristic flow area defined in Figure III.4c.

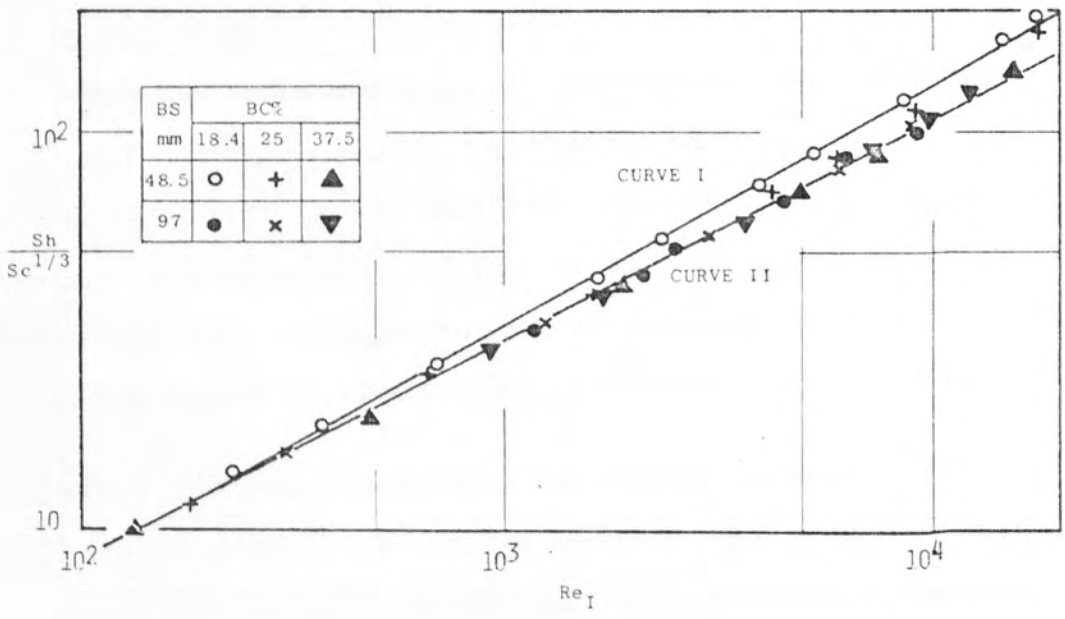

Figure III.8 Correlation of Mackley's data by using characteristic flow area A_I.

Table III.2 Configurations Correlated by Flow Area A_I - Geometrical Independent Correlation

DATA SOURCE	CONFIGURATION	
	BAFFLE-CUT %	BAFFLE-SPACING mm
MACKLEY	18.4 25 37.5	98 48.5, 98 48.5, 98
BROWN	31 43.7	12.5, 25, 48.5 98

by removing eddy currents created behind baffles as noticed by Gunter et al (43), (see Section II.4.2). This would also result in producing extremely high pressure drops making the exchanger ineffective as a commercial process unit. In the case of 43.7% baffle-cut and baffle-spacings less than 50 mm, however, lower coefficients are produced than the geometrically independent correlation predicts This is perhaps because the main fluid stream penetrates through a part of the bundle resulting in large stagnant zones away from the baffle overlap region.

The geometrically independent correlation accounts for all the nine remaining geometrical configurations, (see Table III.2). Both the 18.4% and 43.7% baffle-cut

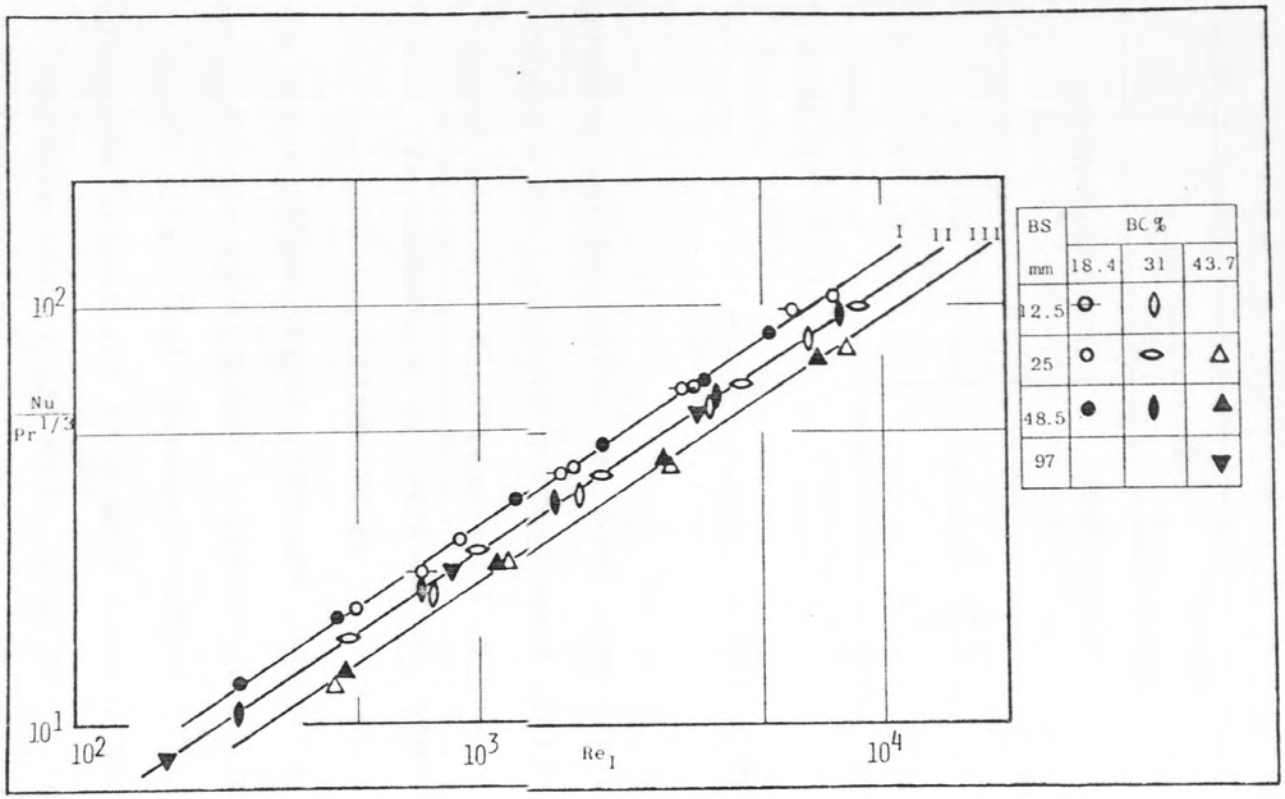

Figure III.9 Correlation of Brown's Data by using characteristic flow area A_I.

at large spacings (97 mm) are correlated by this curve, as well as, all spacings examined for 25%, 31% and 37.5% baffle-cuts. These geometries include most of the conceivable commercial configurations. Therefore, the no-leakage data produced from this work will be correlated using A_I as the flow area in the Reynolds number.

As the effects caused by baffle-cut and baffle-spacing have been correlated, correlation of the leakage data could now be attempted.

III.2.2 The Leakage Case

This section attempts to correlate the leakage transfer coefficient data, with variations in baffle-spacing, baffle-cut and shell-to-baffle and tube-to-baffle clearances.

The previous attempts failed because the effects of baffle-cut and baffle-spacing were not correlated. In order to characterise the leakage transfer coefficients both Bell (37) and Mackley (3) used area ratio terms (A_L/A_m) and (A_L/A_w) respectively. These ratio terms represented the additional longitudinal flow area available due to the leakage clearances against the no-leakage cross and longitudinal window flow areas respectively.

However, it is shown above that neither of the flow areas A_m or A_w are able to correlate the data obtained

for the various no-leakage geometries. Therefore use of these areas to analyse leakage data would complicate the issue by confusing the effects of baffle-cut and -spacing with those of the leakage clearances.

It was shown in the previous section (III.2) that a correlation independent of baffle-cut and -spacing is obtained when the Reynolds number is based on the flow area A_I. The leakage and no-leakage data obtained by Mackley are plotted using this Reynolds number in Figure III.10. The result is that the leakage data lie on two different baffle spacing curves. This is entirely attributable to the presence of leakage, as a similar effect is not observed in the no-leakage situation.

The other notable feature is that the small baffle-spacing (48.5 mm) configuration shows lower transfer coefficients than the large spacing (97 mm) cases, and this difference increases with increasing Reynolds number. The large baffle-spacing correlation further shows consistently lower transfer coefficients, by about 16%, compared to the geometrically independent no-leakage correlation shown in Figure III.8.

The unexpected difference between large and small baffle-spacing curves requires an explanation.

The large spacing correlation curve has a similar gradient to the no-leakage curve. Therefore, it would also have similar effective flow distribution.

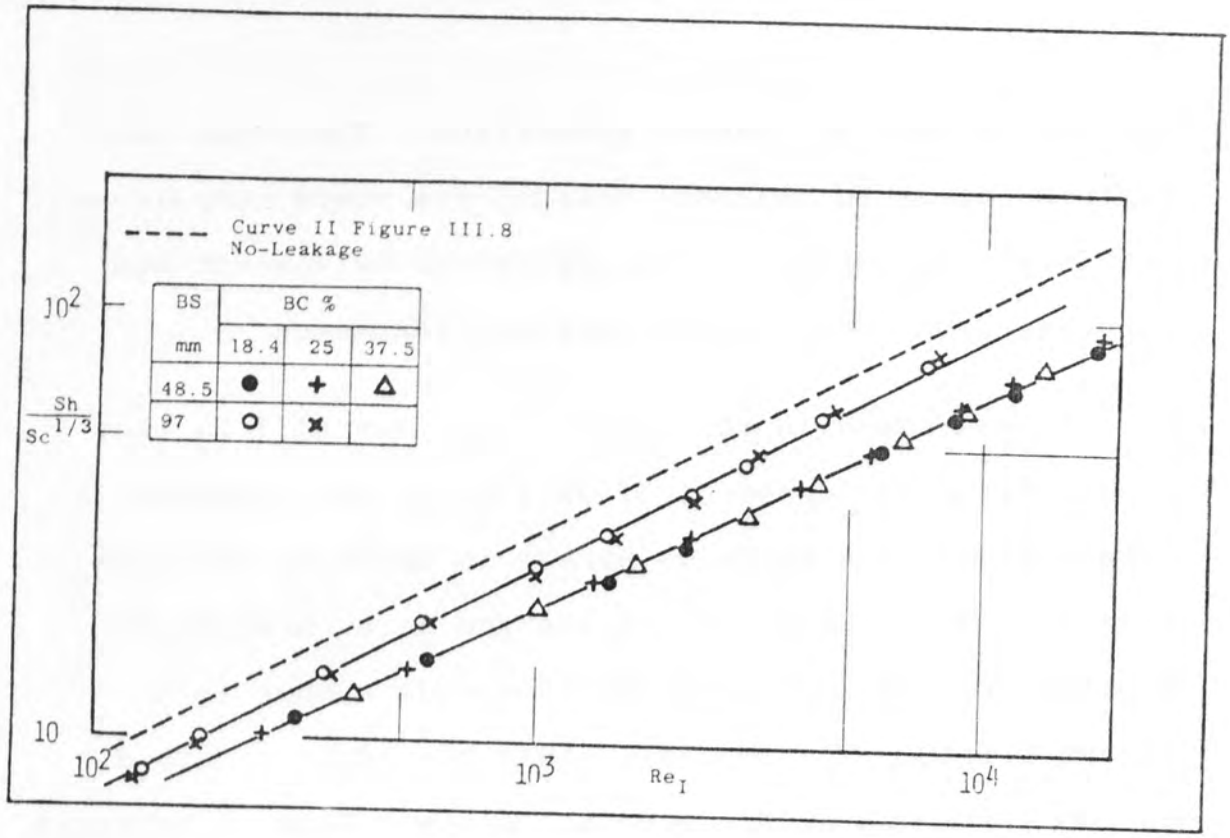

Figure III.10 Correlation of Mackley's leakage data by using characteristic velocity V_I.

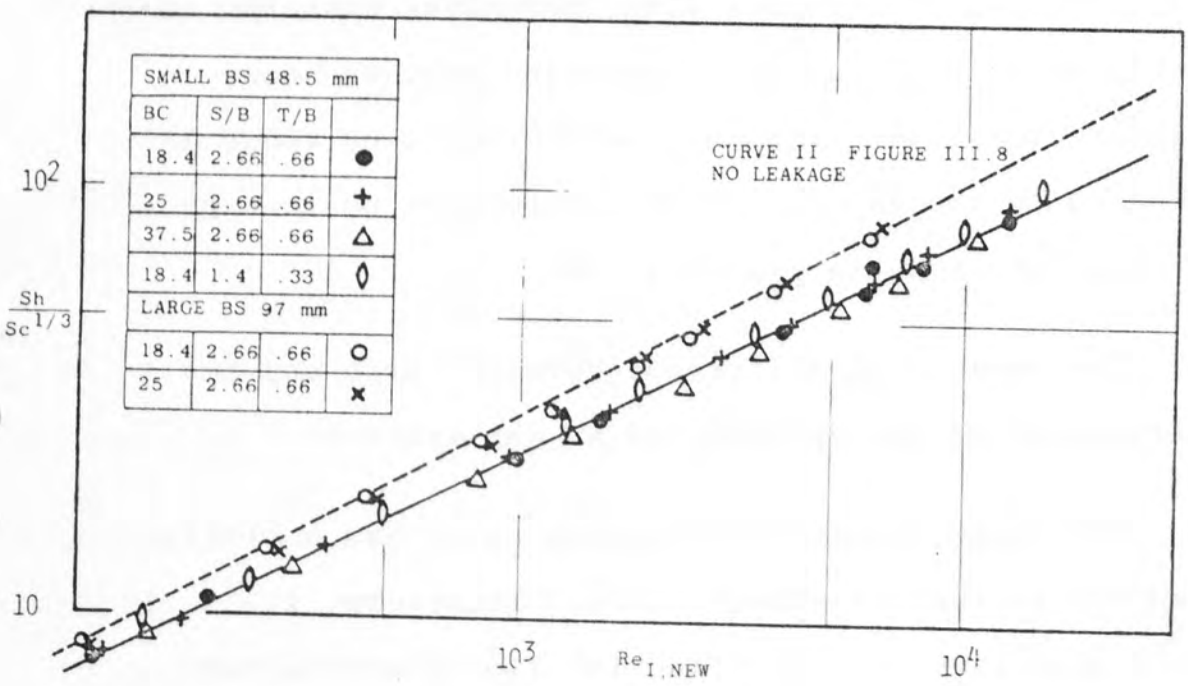

Figure III.11 Correlation of Mackley's leakage data by using characteristic velocity V_I.

In order for this to happen the effect of leakage must be limited, thus causing very little flow re-distribution. As the leakage area (A_L) is much smaller than flow area A_I, only small amounts of fluid could pass through the clearances to alter the no-leakage flow patterns. The net effect of leakage is to divert fluid away from area A_I without completely destroying the original flow patterns. This results in lowering the transfer coefficient with the no-leakage case, but without changing the gradient of the curve.

In the case of the smaller baffle-spacing correlation curve, the gradient is lower than the no-leakage configurations. The effect of leakage in this case greatly influences the distribution of flow. With a relatively smaller A_I, the leakage area becomes significant. Consequently the leakage flow increases, and shell-to-baffle and tube-to-baffle leakage streams become important. As the flow rate increases the latter stream increases further, resulting in distortion of the flow-patterns and departure away from the no-leakage cases.

The effect of baffle-cut in Figure III.10 is correlated to within ± 5% for both spacings. This was expected as Mackley showed in Section II.5.2, that leakage reduced flow through the window zone, hence lowering the effect of baffle-cut.

The remaining problem is to account for the leakage streams. This could now be attempted. With leakage a proportion of the flow is lost through the leakage clearances, thus reducing the net flow passing through flow area, resulting in lower coefficients. By adding the leakage area to the flow area, A_I, the leakage flow could be accounted for. The leakage data for both baffle-spacings are replotted by correcting the Reynolds number by using the flow area defined by equation III.2 below.

$$A_{I,NEW} = A_I + A_L \qquad \text{(III.2)}$$

This is given in Figure III.11, which also shows the no-leakage geometrically independent curve. It is clear that the large baffle-spacing is correlated to within 5% of the no-leakage value by using a Reynolds number based on equation III.2. However, the small baffle-spacing data lie on a separate curve, varying from 14% to 24% at Reynolds number of 200 to 10^4 respectively. This configuration was not satisfactorily correlated as expected, since equation III.2 takes no account of any flow re-distribution.

The 48.5 mm baffle-spacing curve correlated three different leakage areas for as many baffle cuts. Therefore, the difference illustrated in Figure III.11 is purely due to leakage flow disturbing the no-leakage flow pattern and is independent of leakage area. To account for this more leakage data with different shell-to-baffle and tube-to-baffle clearances are required. However, in Figure III.11

Figure III.12 Correlation of Brown's no-leakage pressure drop data

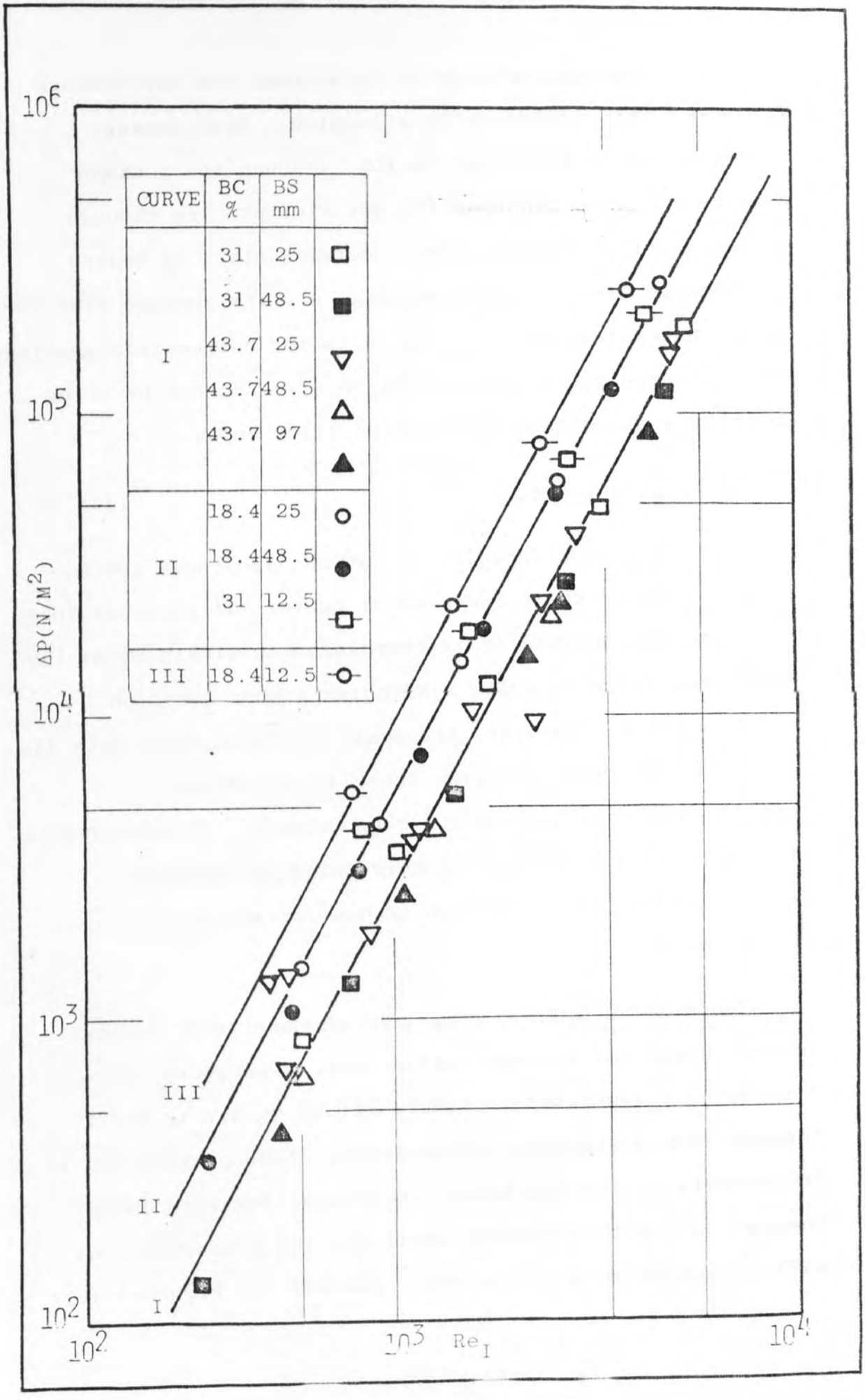

data for the smallest baffle-cut and -spacing with shell-to-baffle and tube-to-baffle clearances of 1.4 mm and 0.33 mm respectively are also plotted. These data coincide with all the configurations correlated by the 48.5 mm baffle-spacing correlation curve. Hence no parameter is known which could account for the effects due to small baffle-spacings. The larger spacing, perhaps more important for commercial exchangers, was satisfactorily correlated.

III.3 Correlation of Pressure Drop Data

The overall bundle pressure drop data of Bergelin et al (24,25) were used to obtain a correlation independent of geometrical parameter, using methods described previously in this chapter for the correlation of transfer-coefficient data.

III.3.1 No-Leakage Case

The no-leakage overall bundle pressure drop data of Brown (23) were plotted using a Reynolds number based on area A_m. However, no correlation of geometrical parameters was obtained. The pressure drop was not dimensionalised as data from similar sized exchangers were being studied. Then the Reynolds number based on flow area A_I was used in an attempt to correlate these data independent of baffle-spacing and baffle-cut. This attempt is depicted in Figure III.12 and shows a relatively successful correlation. The lowest pressure drop

contributing geometries, shown by curve (I) in Figure III.12 are all baffle-spacings larger than 25 mm for 43.7% and 31% baffle-cuts. The spread of the data is reduced with increasing Reynolds numbers. The configurations with a baffle-spacing of 25 mm for both baffle-cuts rapidly deviate away from the above correlation as the Reynolds number decreases from 1500. At a Reynolds number of 500 this difference is 33% with the smaller baffle-spacings showing a higher pressure drop. The other multi-geometrical correlation obtained is for baffle-cuts of 18.4% and 31% with baffle-spacings of 25 mm and 48.5 mm for the former baffle-cut and 12.5 mm for the latter baffle-cut. This is shown by curve II in Figure III.12. This correlation has a similar gradient to the above correlation, but with higher pressure drops by 58%. The highest pressure-drop geometry was for 18.4% baffle-cut and 12.5 mm baffle-spacing, curve III in Figure III.12.

Comparing this figure with the analogous transfer coefficient correlation shown in Figure III.9, it can be seen that the pressure drop and transfer coefficient geometrically independent correlations are not composed of the same geometries. One such example is the case of 18.4% baffle-cut and 12.5 mm baffle-spacing. In the case of the transfer coefficient this configuration is correlated with other configurations having a baffle-cut of 18.4%, but for the pressure drop case the above configuration is correlated separately on

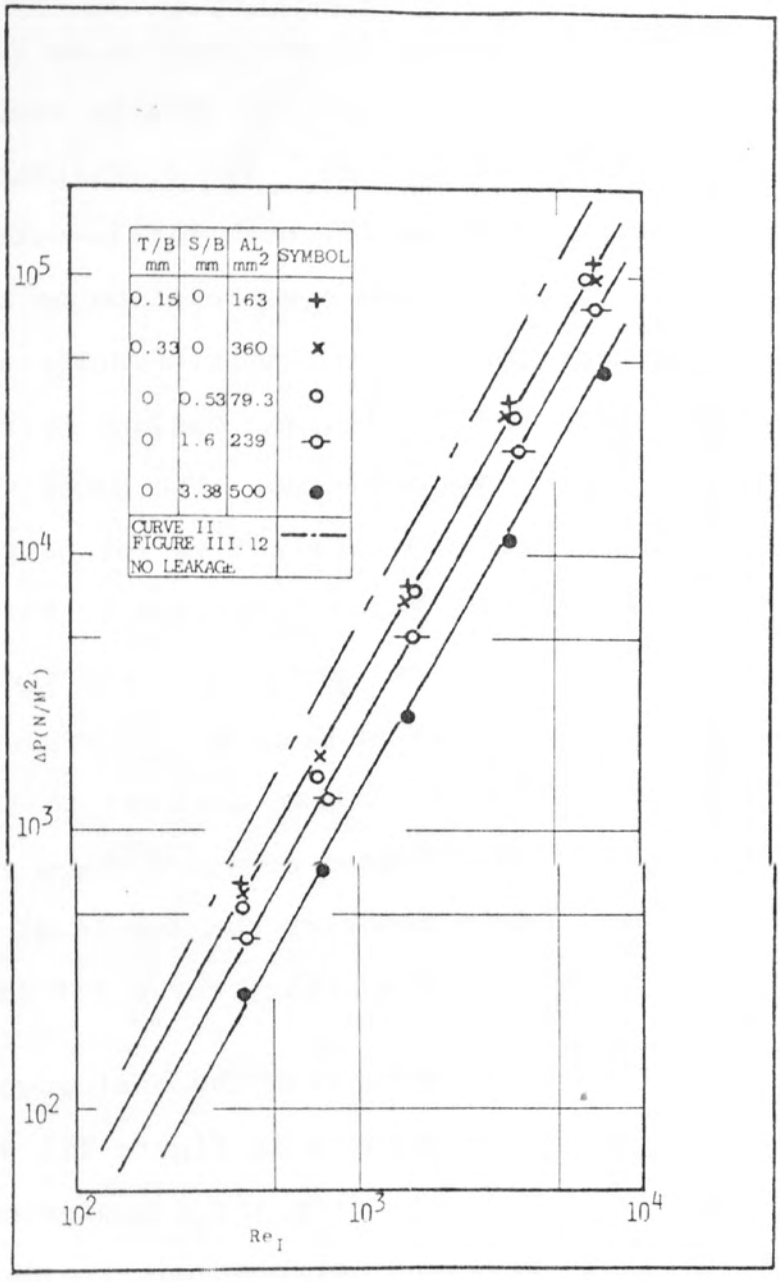

Figure III.13 Correlation of semi-leakage pressure drop data

Curve (III) in Figure III.12. The resultant conclusion is that no particular curve fully correlates the effects of baffle-spacing of -cut, but a correlation is obtained for commercially interesting geometries. The disagreement at lower Reynolds numbers may be primarily attributable to innacuracy existing in pressure drop measuring equipment. The accuracy of Brown's pressure drop data was likely to be ±20%.

It is shown during the correlation of transfer coefficient data that leakage distorts some of the no-leakage correlations. Therefore, an accurate correlation of no-leakage data would not be wholely necessary.

III.3.2 The Leakage Case

This section attempts to correlate the leakage pressure-drop data, available from the work at Delaware University, particularly by Bell et al (37) and Holzman (25).

Bell and Fusco (37,25) segregated the leakage streams into two parts; shell-to-baffle and tube-to-baffle. This was done by using neoprene gaskets. Therefore, their separate effects could be investigated. The data were only for one baffle-cut and -spacing namely 18.4% baffle-cut and 48.5 mm baffle-spacing, and are illustrated in Figure III.13, with a Reynolds number based on flow area A_I. The no-leakage correlation of small baffle-cut and small baffle-spacings, curve (II) in Figure III.12, is

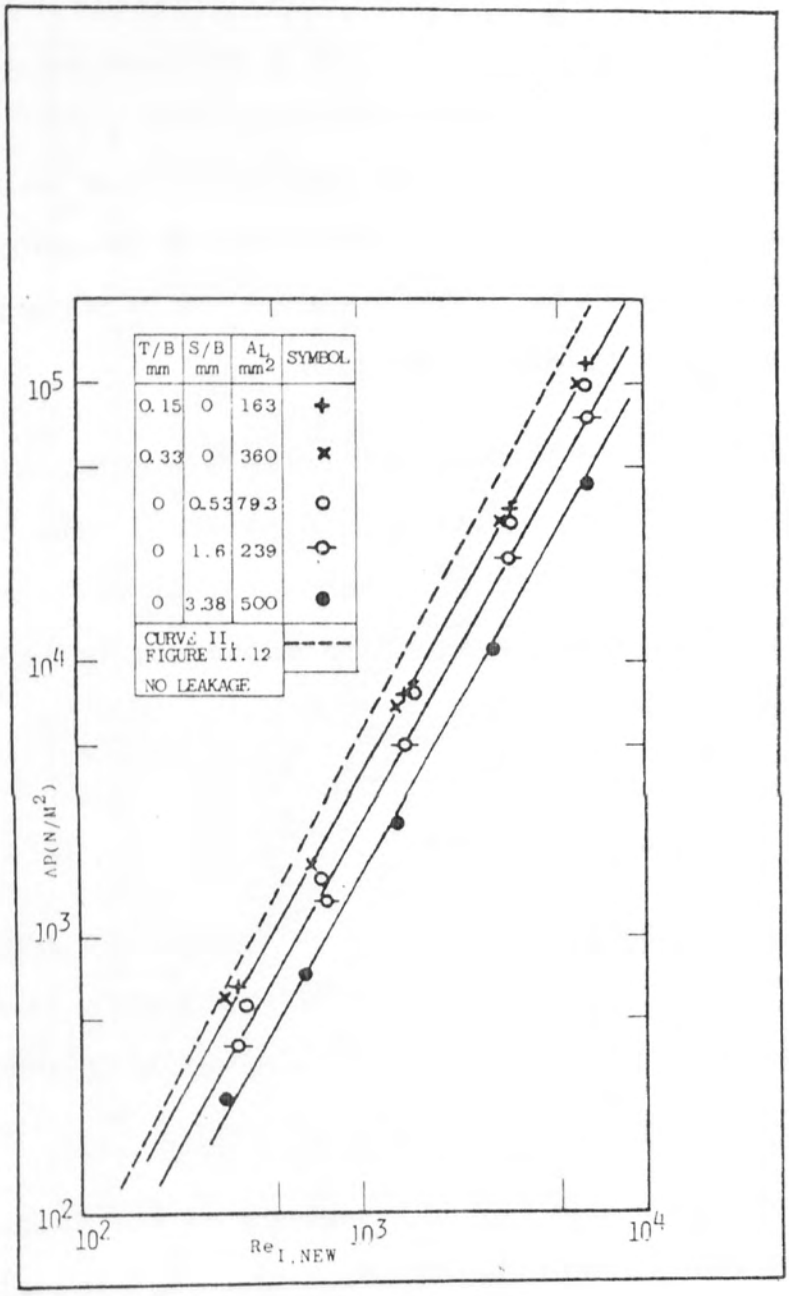

Figure III.14 Correlation of semi-leakage pressure drop data by using characteristic velocity $V_{I,NEW}$.

also shown for comparison. The analagous transfer coefficient comparison is shown in Figure III.10. Since no-leakage data existed for different baffle-cuts and -spacings, a similar conclusion to that derived from Figure III.10 for correlation of baffle-cut and -spacing could not be reached for the correlation of pressure drop data. Thus, uncertainty exists in whether baffle-cut and -spacing could be correlated in the case of pressure drop, when the Reynolds number is based on flow area A_I. Therefore, more data are required with different baffle-spacings and -cuts before a definite conclusion could be made about their effects.

In the case of transfer coefficient data, an attempt is made above to account for leakage by redefining the flow area by equation III.2. This same procedure is adopted in an attempt to correlate the pressure drop data, and is illustrated in Figure III.14. However, only marginal improvement results over the use of a flow area based on A_I. The different size clearances are not correlated, especially in the case of shell-to-baffle leakage. This is unlike the transfer coefficient case, where data for both 2.66 mm and 1.6 mm shell-to-baffle clearances and 0.66 mm and 0.33 mm tube-to-baffle clearances respectively are correlated on a single curve when using a flow area described by equation III.2. Therefore another procedure is necessary to correlate the effect of pressure drop by these leakage streams.

The above pressure drop investigation, however, highlighted two important features:

(i) the effect of leakage increases with Reynolds number echoing the same conclusion as in Section II.5 and Section III.2.2, and,

(ii) the no-leakage pressure drop is directly proportional to Reynolds number squared, and leakage causes the gradient to decrease.

Any attempt to account for the leakage streams is now described. The three distinctly different cases of shell-to-baffle leakages will be analysed firstly and later adapted for the tube-to-baffle case, as well as for the combined leakage situation.

The effect of different shell-to-baffle leakage areas was to reduce the pressure drop as compared with the no-leakage pressure drop, and also to lower the gradient of the pressure drop against Reynolds number curve. In the no-leakage case, pressure drop was directly proportional to the square of fluid velocity over the range of flow rates investigated. It was previously shown in Section III.2 how Mackley and Bell used the ratios A_L/A_w and A_L/A_m respectively to account for leakage when correlating their transfer coefficient data. In this case, the flow area ratio of interest would be A_{SB}/A_I. To determine the influence of this ratio on leakage pressure drop, the square root of the ratio between no-leakage and leakage pressure drops is plotted against this flow area ratio,

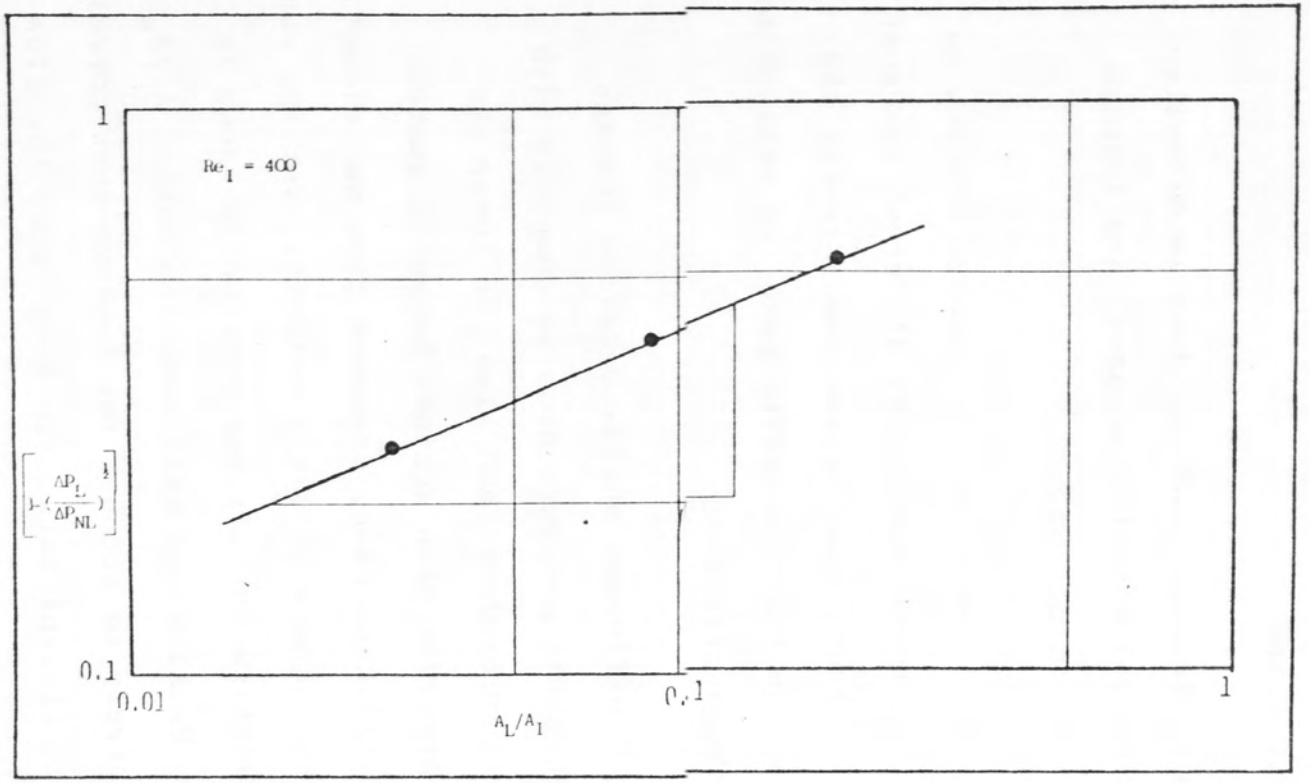

Figure III.15 Model to account for the pressure drop in semi-leakage cases.

as described by equation III.3 and the result is shown in Figure III.15.

$$\left[1-\left(\frac{\Delta P_L}{\Delta P_{L,CORR}}\right)^{\frac{1}{2}}\right] = \left(\frac{A_{SB}}{A_I}\right)^n \qquad \text{(III.3)}$$

The gradient determined from Figure III.15 is equal to 0.4. Therefore to correct for leakage, equation III.4 could be used.

$$\Delta P_{L,CORR} = \left[\frac{\Delta P_L}{1-\left(\frac{A_{SB}}{A_I}\right)^{.4}}\right]^2 \qquad \text{(III.4)}$$

The data of Bell (25,37) are re-plotted with a correlation made for leakage and this is also extended to tube-to-baffle clearances as illustrated in Figure III.16. All the shell-to-baffle clearance cases are well correlated to within 18% of the no-leakage configuration. However, the tube-to-baffle clearances are not represented by this curve (when the flow area A_{SB} is replaced by A_{TB} in equation III.4.) More experimental information about the tube-to-baffle leakage stream would be needed before its effects can be accounted for.

Also shown in Figure III.16 are the combined leakage data of Holzman(25). The flow area used to account for the total leakage is only the shell-to-baffle leakage area. The tube-to-baffle leakage area is not used. In spite of this, the agreement is reasonable and within the experimental accuracy of ± 20%.

The successful correlation of Holzman's pressure

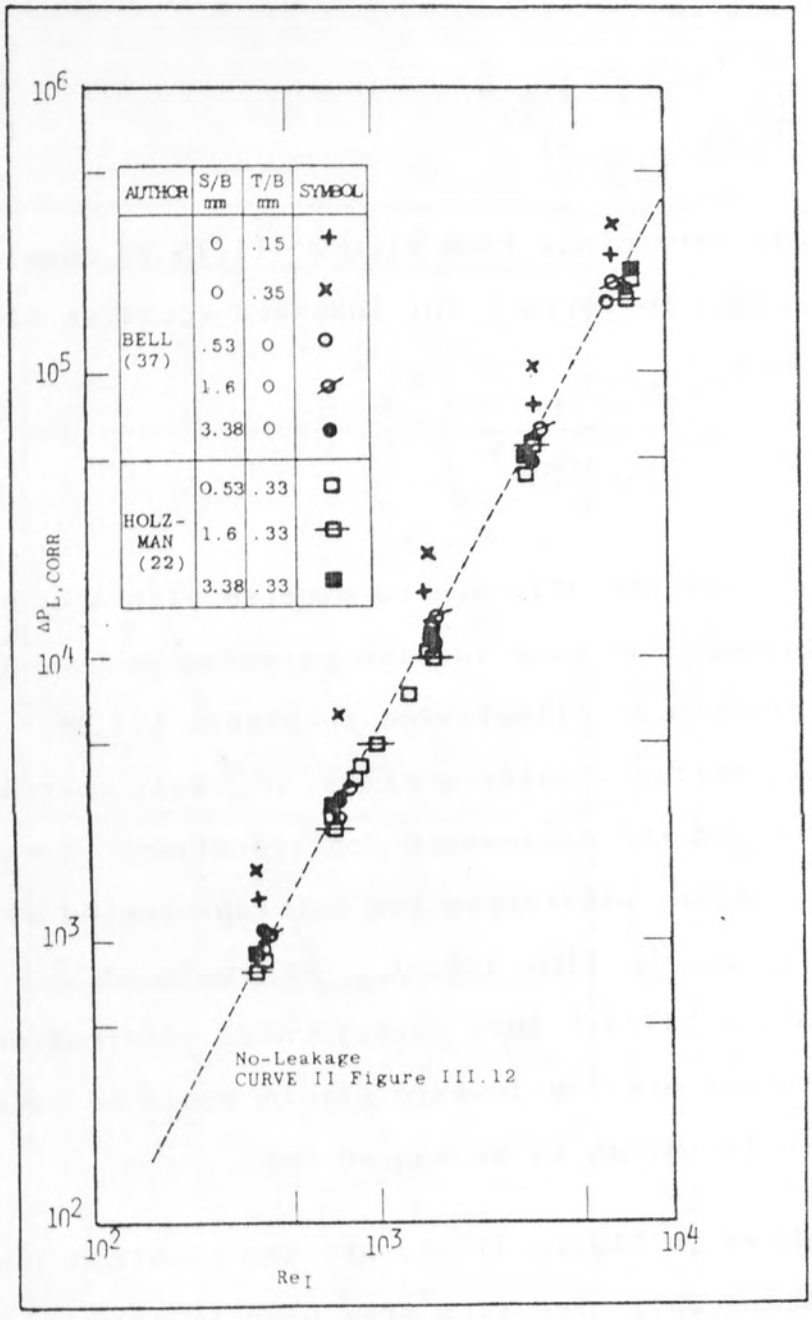

Figure III.16 Correlation of semi and total leakage pressure drop data.

drop data suggests that the tube-to-baffle leakage stream is relatively less effective than the shell-to-baffle leakage system. This is highlighted in Figure III.13 which shows a very small change in pressure drop when the tube-to-baffle clearance is doubled. This is further discussed in Section V.6 and VI.6.

III.4 Conclusions

The following correlation procedures will be adopted to correlate the data of the present work:

(i) the no-leakage transfer coefficient data will be correlated by plotting $(Sh/Sc^{1/3})$ as the ordinate against Reynolds number based on flow area A_I, as detailed in Section III.2.1 and III.3.

(ii) the leakage transfer coefficient data will be correlated using equation III.2.

(iii) the leakage pressure drop data will be correlated using equation III.3.

CHAPTER IV.

IV.O Experimental Method and Apparatus.

IV.1 Introduction.

The electrochemical technique has been widely used and reported in the open literature for the study of transport phenomena problems.

A detailed discussion of the electrochemical technique and experimental procedures employing the Chilton-Colburn analogy to determine the shell-side transfer coefficients had previously been undertaken by Mackley (3). The experimental equipment used in this work was basically similar to that of Prowse (4).

A brief outline of experimental procedures, equipment, electrochemical technique and the analogy employed are given below. Recent modifications to the equipment, together with the operating procedure, are also included.

As with previous investigators of the shell-side transfer coefficients using the mass transfer technique, such as Prowse, Mackley and Williams (48, 49), the tube bundle used was geometrically similar to the small cylindrical unit (model number 9) used by Delaware University workers (21, 25). Therefore this enabled direct comparison between

experimental data to be made.

IV.2 The Electrochemical Systems.

IV.2.1 The Redox System.

In this electrochemical mass transfer system, ions under an electric potential are transferred. The electrolyte used comprises an aqueous solution of sodium hydroxide together with stoichiometric quantities of potassium ferrocyanide and pottasium ferricyanide. The electrolyte flowed past the nickel surface under investigation, which was connected to the negative pole of a direct current power supply and hence became the cathode. Another nickel electrode connected to the positive terminal of the power supply was installed in the flow circuit. The precise shape and location of the anode were not important, as long as its surface area was bigger than that of the cathode.* When an electric potential is applied between the anode and the cathode, the ferricyanide ions transferred to the cathode are reduced to ferrocyanide ions. Thus, the following reaction occurs at the cathode:

$$Fe(CN)_6^{3-} + e = Fe(CN)_6^{4-} \qquad (IV.1)$$

and the reverse reaction at the anode. Therefore, the current passing between the anode and cathode through the medium does not change the overall concentrations of the solution.

*Experiments were carried out with different sizes of cathodes and anodes to varify this.

The rate of the electrochemical reaction in equation IV.1 is a function of concentration gradient (ΔC), surface area of electrode (S) and the mass transfer coefficient (K_m), given by:

$$N_A = K_m S \Delta C \qquad (IV.2)$$

The current (i) measured in the circuit can be converted to the rate of transfer of ferricyanide ions by:

$$N_A = i/Fn \qquad (IV.3)$$

where F and n are Faraday's constant (equal to 96000 coulombs/mol) and the reaction valency respectively. Hence the corresponding mass transfer coefficient over the cathode surface in terms of current is:

$$K_m = \frac{(i/nF)}{S\Delta C} \qquad (IV.4)$$

To ensure that the electrochemical reaction was the characteristic of the cathode, the anode surface area was simply made larger than the sum of all the cathode areas active in the circuit.*

The movement of the ions, and hence flow of the current to the cathode, was brought about in three ways; migration due to the potential field, diffusion due to the concentration gradient and forced convection by fluid flow. With the addition of large excess of indifferent electrolyte, such as sodium hydroxide (whose decomposition

* See footnote on page 61.

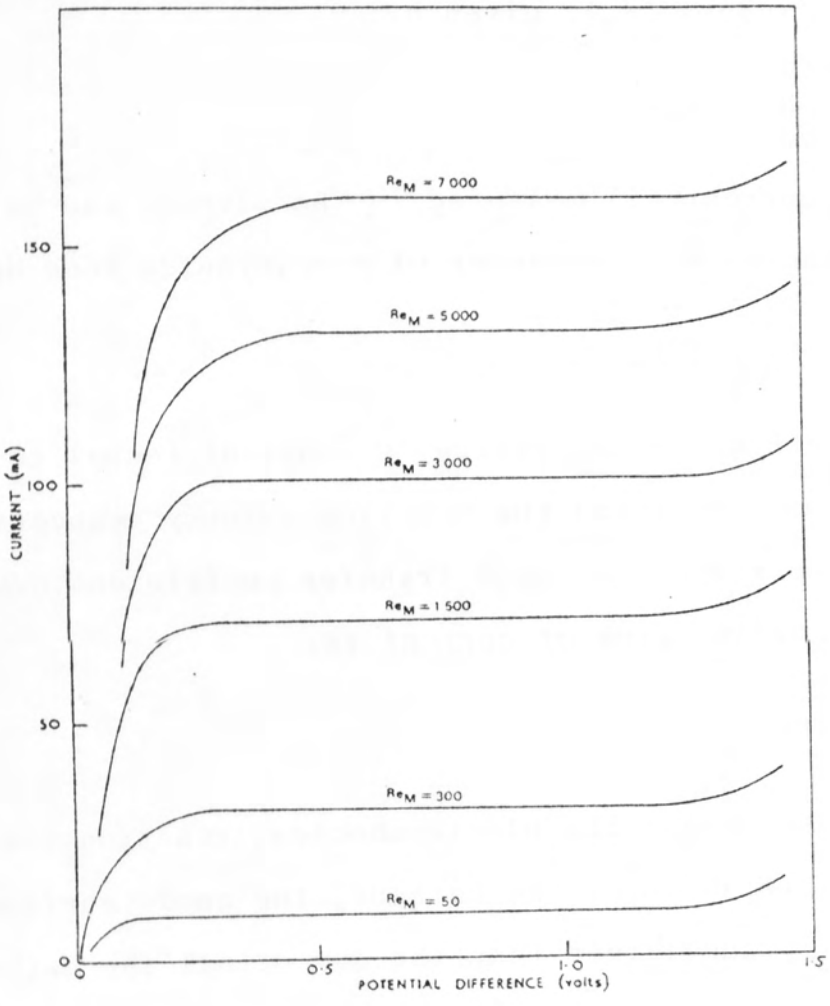

Figure IV.1 Current-potential behaviour for various flow rates.

potential is above that of the Redox reaction) to the solution , the effect of migration due to the potential field could then be neglected (56). These indifferent ions also help in transferring the current by reducing the electrical potential required to operate the system. The migration effect for the present system was found to be less than 0.5% by Sutey and Knudsen (56, 57). Apart from this the indifferent electrolyte played no part in the reaction. Only the latter two methods of transport were present in the system.

A simple test was needed prior to any experiment to check that the electro-chemical reaction was diffusion controlled (concentration polarization) and not reaction controlled (chemical polarization), that is, the ferricyanide ion concentration at the cathode surface was practically zero. In fact it was shown by Lucas et al (58), and Eisenberg et al (59) that the concentration of ferricyanide ions at the cathode surface was less than 10^{-5} kg/m^3 for former case. This could be detected by plotting a curve of current against applied potential with the flow rate of the electrolyte constant, and hence with an established boundary layer. An example of such a plot is depicted in Figure IV.1 . Initially the current increases with increasing potential until the surface concentration of ferricyanide ions becomes negligibly small. Increasing the potential further causes the current to remain unchanged, signifying the electrolyte reaction to be diffusion controlled and hence very nearly zero surface concentration of the ferri-

cyanide ions. Further rise in the potential causes electrolysis of water, hence showing a dramatic increase in the current. The limiting current (i_L) is reached when the surface concentration of ferricyanide ions is very nearly zero. Thus simplifying equation IV.4 gives:

$$K_m = \frac{i_L/nF}{SC_B} \qquad (IV.5)$$

where C_B is the bulk concentration of ferricyanide ions.

To relate the mass transfer coefficient (K_m) to the heat transfer coefficient, an analogy between heat and mass transfer is required.

IV.2.2 The Analogy between Heat and Mass Transfer

Similarity in the differential equations describing the transfer across the boundary layer for heat, mass and momentum allows analogies between each to be derived, provided the boundary conditions are equivalent.

The differential equations governing convective heat, mass and momentum transfer during steady flow in simplified form are;

for heat transfer $C_p \rho V \cdot \nabla T = \kappa \nabla^2 T$ (IV.6)

for mass transfer $V \cdot \nabla C = D_v \nabla^2 C$ (IV.7)

and for momentum transfer $\nabla \cdot V = \frac{\mu}{\rho} \nabla^2 V$ (IV.8)

The solution of these equations under dynamically similar conditions has given rise to various transport

analogies. A complete analytical solution is generally impossible, hence the resultant analogies are semi-empirical in nature.

For turbulent flow in pipes, Colburn (13) found that heat transfer data, correlated in terms of j_H factor, showed approximately the same characteristics as the friction factor (f) correlations. Colburn defined j_H-factors and correlated the heat and momentum relationship by the equation:

$$j_H = StPr^{2/3} = \frac{\tau}{\rho V^2} = 0.023\ Re^{-0.2} \qquad (IV.9)$$

Later, Chilton and Colburn (2) extended the above principle to the analogy between heat and mass transfer by defining a mass transfer j_m-factor as

$$j_m = \frac{Km}{V}.Sc^{2/3} \equiv j_H \qquad (IV.10)$$

They showed from experimental data that this empirical analogy was applicable for not only turbulent flow in pipes, but also flow across tubes and across plane surfaces. In recent years, this analogy has been successfully applied to flow across gauzes (61), across tube banks (3), over plane vertical surfaces (62) and in furnace ducts (58,60).

The exponent on the property number in equations IV,9 and IV.10 has been verified by Jenkins et al (26) to be 0.67 for an adequate description of mass and

heat transfer processes.*

The analogies between heat, mass and momentum have all been derived for turbulent flow conditions. At low Reynolds numbers these simple analogies may be inapplicable, should the thermal gradients distort the boundary layer, i.e. onset of natural convection. A similar effect is not so noticeable in mass transfer systems. The extent to which the natural convection affects the heat transfer boundary layer is characterised by the Grashoff number.

Many workers (61, 66) have however employed their mass transfer systems at low flow rates and successfully converted their results using this analogy. This was for simple geometrics where distortion by thermal gradients were relatively less important.

IV.2.3 Advantages and Disadvantages of Ferri/Ferrocyanide System

The advantages of redox system over other electrochemical systems particularly those involving deposition or dissolution processes are numerous, but there also exist a few disadvantages.

Unlike other systems the electrolyte physical properties remain unaltered during the chemical reaction due to the complementary reactions occuring at the anode

* Systems with significantly different property numbers Pr and Sc may not be compared directly due to different velocity gradients existing in significantly different thickness of mass and heat transfer boundary layers.

and the cathode. This fact enables the bulk concentration and electrolyte physical properties to remain constant. The electrolyte surface also suffers no distortion and remains unchanged. The electrochemical reactions involving electron transfer are very rapid, therefore, the steady state potential is attained in a much shorter time than in deposition reactions. This reduces the measurement time appreciably, especially when there are many cathodes requiring measurement. This also means that the surface concentration of the ferricyanide ions would be negligible even at the higher mass transfer rates, enabling greater flow rates to be examined. In fact, the present work is limited by the capacity of the pump and equipment rather than by the redox system.

The main disadvantage with this system is the sensitivity of the electrolyte to effects of sunlight, oxygen and excessively high temperatures. In order to avoid the decomposition of the electrolyte and prevent competing electrochemical reactions, suitable precautions are necessary, such as, deoxygenating the water by purging nitrogen into the solution and maintaining a nitrogen atmosphere blanket above the solutions, enclosing all pipe work and storage tanks with silver foil to reduce decomposition of solution by sun light and installing cooling coils to maintain constant temperature when operating the pump.

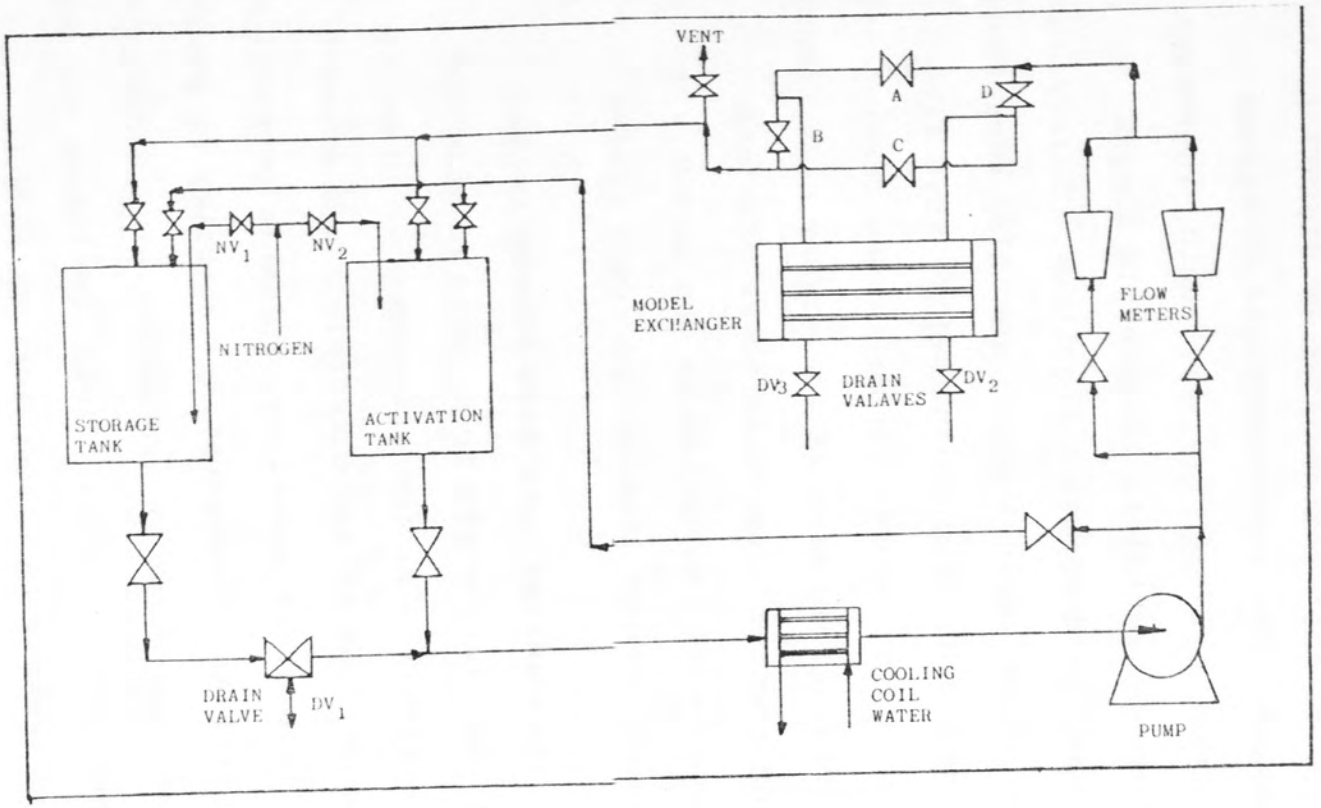

Figure IV.2 Flow diagram of equipment

IV.3 The Experimental Equipment

IV.3.1 The Electrolyte Flow Circuit

A modified version of Mackley's development rig (3) was constructed by Prowse (4) and has been used in this work. This is diagrammatically represented in Figure IV.2 . The exchanger model depicted in Figure IV.2 was constructed from perspex, whereas QVF glass-ware was used in the construction of the flow circuit itself. The QVF pipes of 38 mm ($1\frac{1}{2}$") nominal bore were used to feed the electrolyte storage tank (200 l capacity) and an activation tank (50 l). The solution return from the exchanger model, by pass lines and nitrogen purge lines all entered the two storage vessels through a 16 mm thick perspex lid. The electrolyte storage tank also contained a 6 mm diameter stainless steel pipe 300 mm above the tank outlet. This was connected to a nitrogen supply and was used to purge nitrogen into the electrolyte. The nitrogen atmosphere above the electrolyte and activation solutions was maintained by keeping the pressure in the vessels equal to 125 mm water gauge. This was done by the use of a water-lute relief valve.

The rig was modified to enable reversal of the direction of fluid-flow through the model. This was achieved by appropriately opening and closing valves in

the loop ABCD, illustrated in Figure IV.2 . The flow provided by the QVF pump (GPR/9 - 3hp) was controlled by a 25.4 mm stainless steel ball valve. The flow rate was measured by two variable area flow meters of sizes 18 and 65 equipped with stainless steel floats. These flowmeters were calibrated in situ by using both analytical and experimental methods, as shown in Appendix A1.

Two stainless steel cooling coils, one in the electrolyte storage tank and the other on the suction side of the pump, were used to control the temperature of the solutions. A mercury thermometer located in the thermometer well near the nozzle of the exchanger indicated the temperature of the solutions.

IV.3.2 The Shell and Tube Exchanger Model

The exchanger model employed in the present work was based upon models previously used by Williams, Mackley and Prowse. It was also geometrically similar to an heat transfer study model used by Bergelin et al (25). The shell was a 610 mm perspex pipe with an internal diameter of 133 mm for the no-leakage runs. This internal diameter was later increased to 134 mm for the leakage runs. Two rectangular ports of internal dimensions 47.6 mm by 76.2 mm were mounted in line on the shell. The distance between these port centres allowed for the inside surface of the tube sheets to coincide exactly

with the extreme edges of the ports. The tube bundle was held in position by two thin rigid perspex sheets placed at each end between the tube sheet and the shell end plate. The shell end plates were bolted to the shell flange via a gasket. Each insulated electrical conductor from the electrodes pierced a 10 mm thick rubber sheet. This sheet was held in place by a perspex plate supported by three stainless steel bolts. One 3 mm internal diameter hole was drilled for a pressure tapping through each port, as discussed in section IV.3.5 . Another two 13 mm internal diameter holes were drilled into the shell wall immediately within each end compartment. An adaptor connected to the flexible p.v.c. tubing was permanently cemented into these holes. During the experimental runs these lines were closed by Hoffman clips and opened for draining and washing the exchanger.

The tube bundle* incorporates 3.18 mm thick p.v.c. baffles with eighty 9.5 mm diameter reamed holes together with the associated dummy tubes, and tie rods. The holes were arranged on a rotated square pattern with a pitch to diameter ratio of 1.25. Eight 4 BA stainless steel threaded tie rods and nuts were used to secure the baffles at any designated baffle pitch. The total distance between the tube sheets was 406 mm (16"). The dummy consisted of 500 mm long and 9.5 mm (3/8") outside diameter p.v.c. rods. Twenty rods,

* Tube numbering diagram is shown inside back cover.

spanning half the length of the bundle, i.e. 203 mm, were replaced by composite electrodes to give the total length (see Section IV.3.3 for further details).

As symmetry existed across the vertical axis at least for horizontal baffle cut arrangement (see Section II.5.1), only one half of the compartment needed to be studied. By placing all the twenty electrodes in one half of the bundle with none being a reflection of the other across the horizontal axis of the bundle, this gave adequate information on the behaviour of the whole bundle. The flow direction could be reversed to enable the whole of the exchanger length to be studied. Averaging the j-factor data of Mackley for the corresponding twenty electrodes and comparing the resulting mean to his overall compartment average j-factors for different flowrates showed only small differences, as illustrated in Table IV.1 .

Table (IV.1) - Comparison of Average j-factors between Compartment Average and 20 Tube Average

RE_m	$j_{AV,C}$	$j_{AV,20}$	% Difference
5552	0.01362	0.01369	0.50%
11850	0.01053	0.01054	0.06%

For no-leakage flow condition a 0.5 mm thick p.v.c. sleeving acting as a seal was cemented around the outside

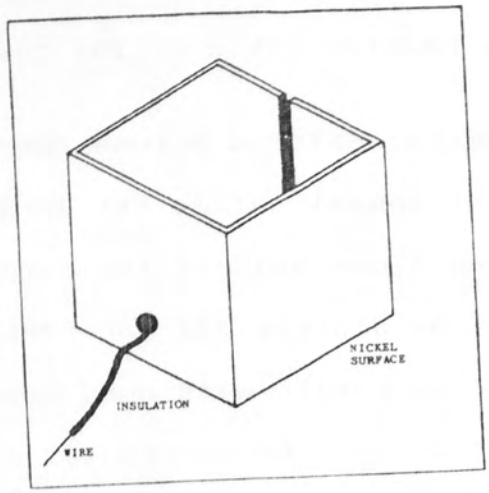

Figure IV.3 Diagram of the anode

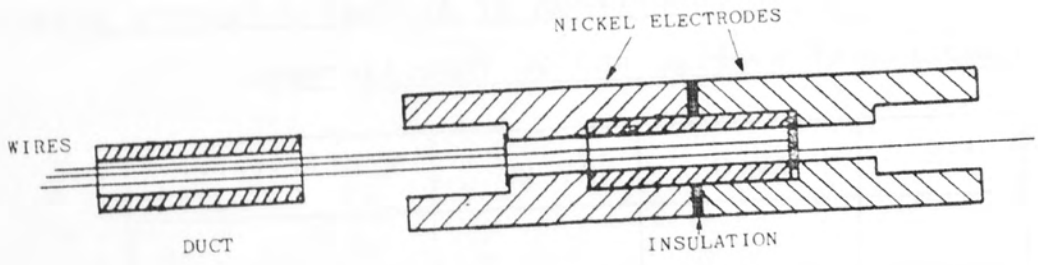

Figure IV.4 Diagram showing construction of multi-electrodes

edge of the baffle using p.v.c. cement.

IV.3.3 Construction of Electrodes

Anodes

To accommodate the large anode surface area it was decided to use two anodes, one in each nozzle of the exchanger. This brought all the cathodes to a common limiting voltage range enabling a specific voltage to be used where all the electrodes possess their limiting current values. The limiting current values were not affected by using either single or two anodes.

Each anode was a box shaped nickel sheet, 80 mm by 50 mm, providing a net surface area of 0.064 m^2 for each anode. A copper-tin wire was bolted to the nickel sheet and sealed to prevent it being attacked by the sodium hydroxide solutions. This is illustrated in Figure IV.3 Thus, the ratio of total anode to the net active cathode area at any time was about four to one.

Cathodes

The cathodes had the same outside diameter as the p.v.c. rods (9.5 mm), but were constructed from nickel. These twenty composite nickel electrodes span across half the length of the exchanger. Each composite electrode comprised six nickel elements; four were 25.4 mm long and two 50.8 mm long. Each element was

insulated from its neighbour and connected by a separate wire (see Figure IV.4) to the external circuits.

The wire was clamped against the electrode by a dreldim tube and cemented in place by using Loctite 648 industrial adhesive. A thin layer of the same adhesive was applied to the electrolyte ends to act as the insulation between its adjacent elements. A universal A.V.O. meter was used to check the effectiveness of the insulation and the wire connection. The outside diameter of the coated wire was 1mm. A copper-tin alloy wire coated with p.v.c. was used in the no-leakage runs and nickel alloy wire was used in the leakage runs. This was because the former was attacked by the caustic solution, hence shortening the life of the composite electrode.

Once the composite electrodes had been fabricated the ends were sealed with liquid Araldite to stop caustic solution penetrating inside and being electrolised on the inside area.

Each connection to the six electrode elements was colour coded as follows: white, blue, green, yellow, red and brown. The remaining four elements were 25.4 mm long, while the initial two were 50.8 mm long. The white coded element was always the last electrode placed in the end compartments, while the Brown-coded element was always the most internal cathode. The

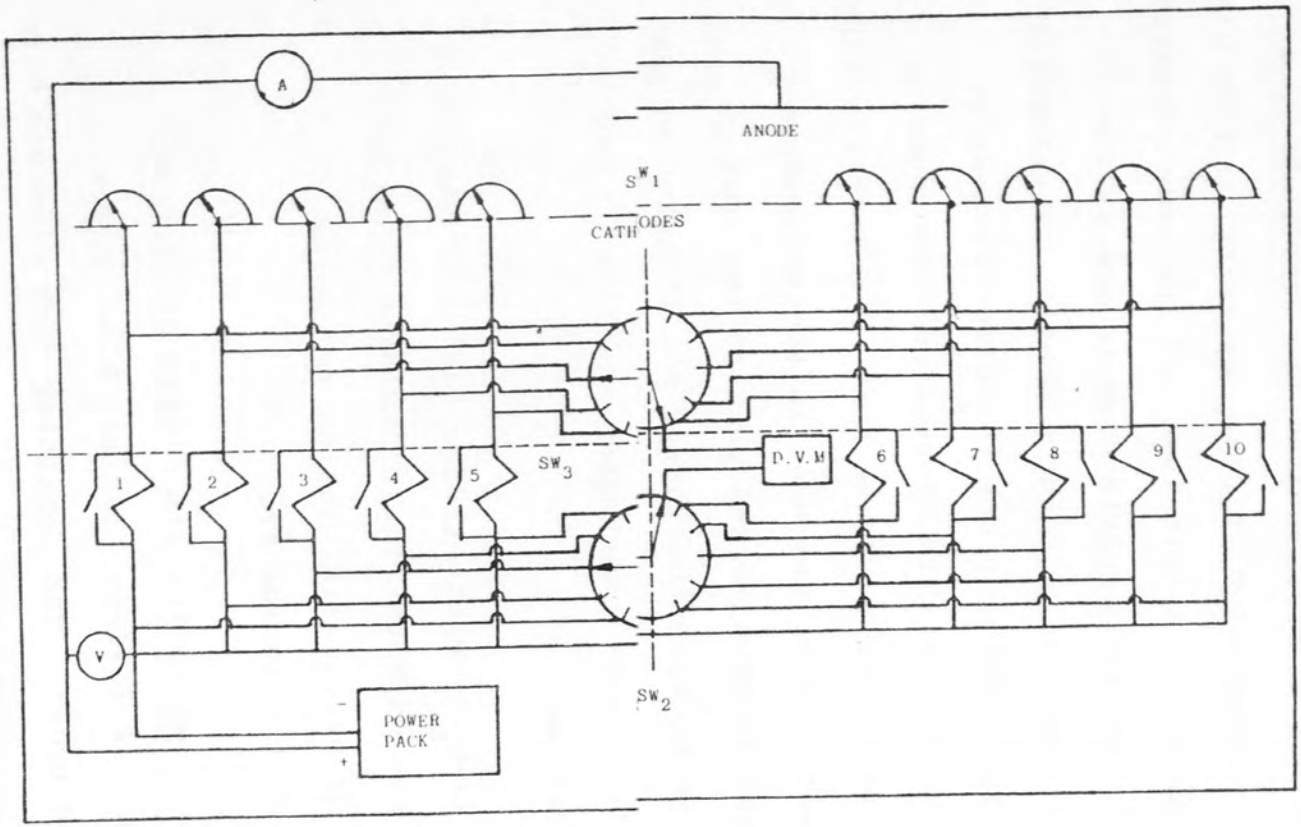

Figure IV.5 Electrical instrumentation layout

composite electrodes allowed investigation of the following nominal baffle spacings: 50 mm, 66.2 mm, 97 mm and even 149.2 mm.

The wires which were passed through the rubber sheet were connected to the switch blocks in the electrical circuit.

IV.3.4 Electrical Instrumentation

The chemical instrumentation circuit is depicted in Figure IV.5 . A direct current voltage supply was obtained from a Farrell L30B power pack. The positive terminals of this unit was connected to the anodes, while the negative terminal was connected to a common lead, consisting of ten 10Ω precision resistors with ± 0.1% tolerance. The other ends of the resistors were separately connected to the ten 12 pole, 1 way wafers on switch SW1. The wires from these wafers were then connected to switch blocks in such a way that when switch SW1 was at position 1, only the first ten white electrode elements were in circuit. For position 2 to 6 on swith SW1, the remaining blue to brown elements of the first ten composite electrodes were separately switched on. When switch SW1 was changed from position 7 to 12, the individual elements starting from whites to the browns were switched on for the remaining ten composite electrodes. Therefore, each wafer on switch SW1 accommodated two composite electrodes on its twelve poles.

Another switch SW2 comprising of two wafers, each

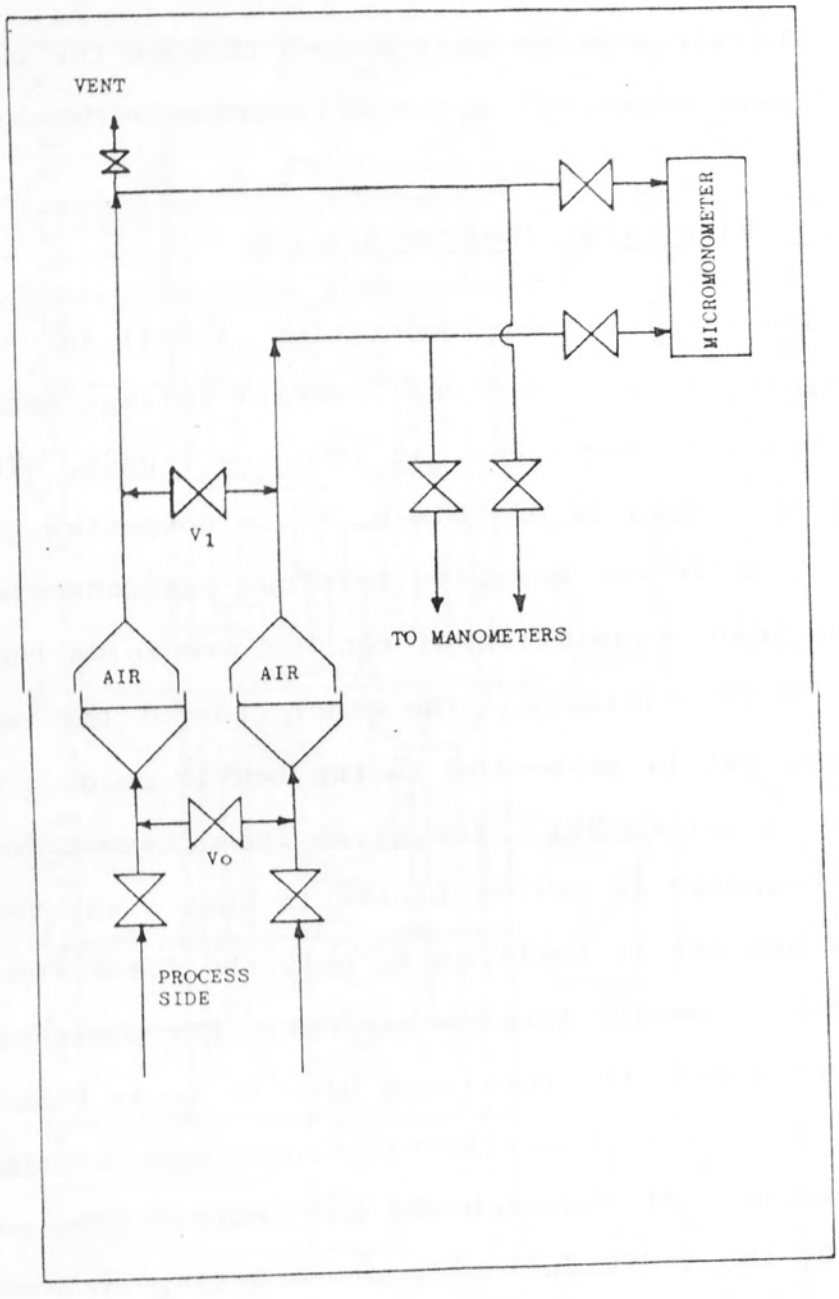

Figure IV.6 Pressure instrumentation diagram

with ten poles and one way, was used to bring a digital voltage meter (D.V.M.) parallel to the resistors. The D.V.M. had a very high impedence of the order of 10^{11} Ω compared to the precision resistors. Thus, the current flowing through each registor could be measured as the voltage drop across a 10 Ω precision resistor.

A 0-10 voltimeter was connected between the positive and negative terminals of the power pack.

During activation the above power pack was replaced by a two amperes at six voltage stabilised D.C. unit as the maximum limit on the Farnell L30B power pack was one ampere. The resistors were short circuited by switch SW3 during activation to protect them against high currents.

IV.3.5 Pressure Instrumentation

The pressure drops were measured by connecting the pressure tapping points in each nozzle via 6.3 mm p.v.c. flexible tubing to two 76 mm (3 inch) internal diameter glass vessels. This is illustrated in Figure IV.6 . These glass vessels were partly filled by the process fluid and converted the liquid pressure into a pneumatic pressure. This pressure was transmitted from the top of the vessels via 6.3 mm internal diameter pneumatic line to the pressure measuring instruments. The instruments used included three U-tube manometers and a micromanometer. The fluids used in these

manometers were mercury (s.g. = 13.6), chloroform (s.g. = 1.59) and water. Differential pressure drops of less than 100 mm wg were measured by a Furnace Controls model FM 589 micromanometer. At high flow rates this meter was isolated from the circuit by Hoffman clips.

The pressure and level in these vessels and manometers was equalised by opening valves V_1 and V_0 in Figure IV.6 . During the experimental run any of the three manometers could be used with others isolated from the circuit. The advantages of using this system were numerous and include:

(i) the corrosive nature of the process fluid could contaminate or change the physical properties of the manometer fluid if direct contact was made between the two fluids. This problem was removed by the present system.

(ii) because the process fluid was not in direct contact with the manometer fluid the process lines were shorter hence trapped gas was not a problem.

(iii) the use of pneumatic pressure enabled a micromanometer to be used hence small pressure drop measurements could be made.

One major disadvantage with this system compared against direct contact system was that a greater

response time was needed due to the sensitivity of the system. This system is discussed in greater detail by De Candappe (67).

No attempt was made to measure the individual compartment differential pressure drop as was done by Bergelin et al (20-25) and Mackley, only the overall pressure drop across the whole exchanger was measured.

IV.4 Experimental Procedure

The following section describes the features of experimental procedure leading up to and including the experimental run.

IV.4.1 Assembly of the Tube Bundle*

The baffles were assembled along the tie bars at the designated spacing. The nickel composite electrodes and p.v.c. dummy rods were then inserted into the assembly starting from the centre and working outwards. In case of no-leakage tests it was necessary to ice-cool and lubricate the rods before insertion as the fit was very tight. The rods and electrodes were gently tapped into position. The bundle was then inserted into the shell, again for the no-leakage case lubrication and constantly increasing pressure on one end were necessary. The bundle was held in position by support plates at each end (see section IV.3.2). A photo-graph of the assembled tube bundle is given in

* See footnote on page 70

Figure IV.7

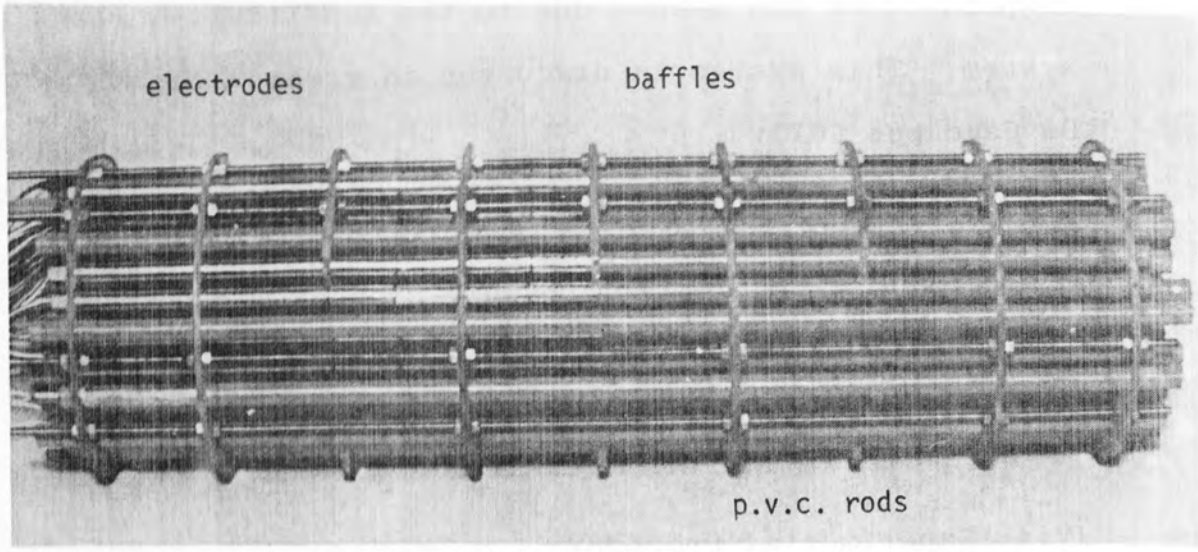

Photograph of assembled tube bundle

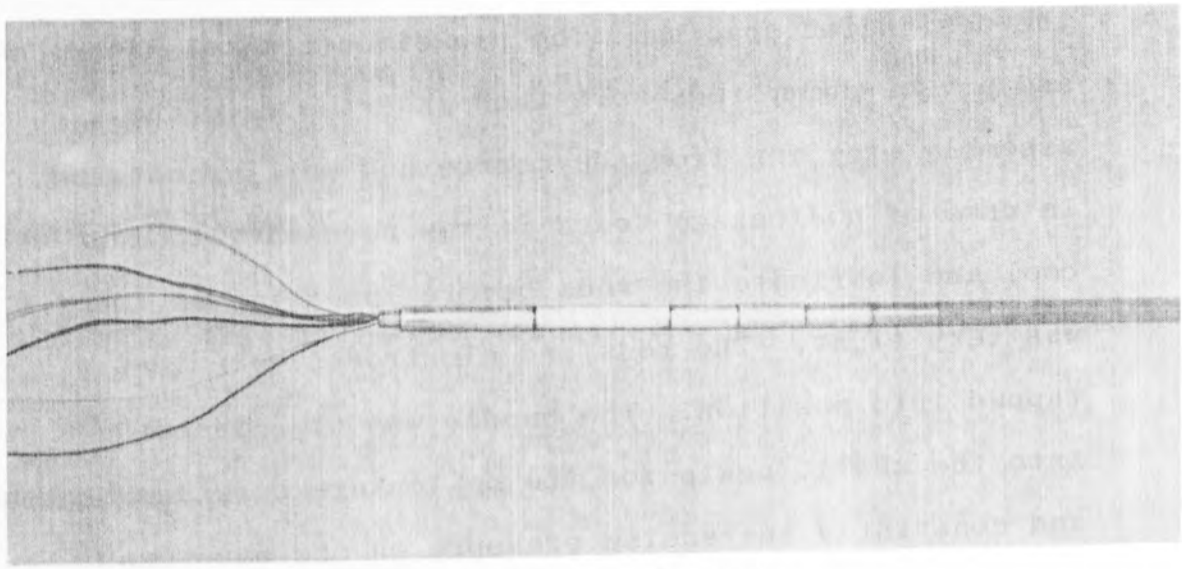

Photograph of multi-electrode.

Figure IV.7 .

IV.4.2 Making the Solutions

There were two types of solution used, the activation solution and the electrolyte. The activation solution comprised a molar aqueous solution of sodium hydroxide. The electrolyte also used the same composition of sodium hydroxide but it also contained a 0.01 molar mixture of potassium ferricyanide and potassium ferrocyanide. The volume of the solutions needed was approximately 75 l and 120 l respectively. The following procedure was adopted in making these solutions .

All valves except the drain valves were opened including the vent. Nitrogen was introduced into the system through valves NV_1 and NV_2 in Figure IV.2 . After a short time when most of the air had been displaced the vent was closed. With the nitrogen purge continuing, all the valves were closed except the electrolyte tank bottom valve V_1 and the drain valve DV_1. Through the latter valve approximately 200 litres of tap water were introduced into the storage tank.

The solution was circulated through the by-pass line with nitrogen purge displacing any dissolved gases, as they desorbed out of the water due to cavitation through the pump and valves. Solid commercial flake sodium hydroxide was added in small batches through the

storage vessel port holes into the solution. The heat of dissolution liberated caused the temperature to rise allowing more of the absorbed gases to desorb out of the solution. Circulating the liquid ensured homogeneity. Samples were taken and titrated against molar acid to determine the alkali concentration. A calculated amount of NaOH flake was then added to obtain the desired concentration of the solution. After the correct concentration was achieved approximately 75 l of the solution were transferred into the activation tank, and the pump was switched off with both tanks isolated. The required amounts of potassium ferricyanide and ferrocyanide were added through the storage port hole. The electrolyte solution in the storage tank was circulated through the by-pass line and samples were taken to be titrated. The titration technique used to measure the concentration of ferricyanide is described in Prowse (4).

When the desired concentration was attained the pump was stopped. Nitrogen pressure was used to transfer the remaining electrolyte in the model exchanger, pipe work and the pump back into the storage tank. The storage tank and the exchanger model were isolated. The circuit was washed by flowing tap water through valve DV_1 and with valves DV_2 and DV_3 open.

IV.4.3 Electrode Activation

The electrode surface needed microscopic cleaning

and removal of any oxide film prior to the experimental run. This was done by cathodically activating the electrode, which involved electrolysis of water using a current density of 0.1 mA/mm^2 (3). Hydrogen was evolved at the cathode and oxygen at the anode. The following procedure was used towards this end.

Air was removed from the flow circuit by nitrogen bleeding. All drains were closed and the activation tank isolation valves were opened. The flow through the exchanger was adjusted to 50 l/min and each cathode element separately activated for five minutes using the activation circuit (see section IV.3.4). An additional activation anode was placed in the activation tank. This was used to activate individually the two operational anodes. For this purpose these anodes were made negative poles in the circuit. The surface area of the activation anode was greater than that of the single operational anodes. The electrolysis of water produced oxygen which was removed to some extent by the nitrogen purge. The operational anodes were activated before the cathodes. At the end of the activation period the voltage was interrupted and the pump stopped. The activation solution from the exchanger and pipework were pressurised back into the activation tank using nitrogen.

The activation tank was then isolated and the electrodes were not exposed to air. The electrical circuit was then altered to permit the acquisition of experimental data.

IV.4.4 Experimental Run

The electrolyte isolation valves were opened with nitrogen still purging. The electrolyte was circulated through the exchanger model and by-pass line until the operating temperature of 25^{o}C was reached. The water through the cooling coils was adjusted in order to stabilise the fluid temperature.

The flow rate through the exchanger model was set at the desired value. The nitrogen purge was stopped as it affected both the flow rate and pressure drop; the latter quite significantly.

The power pack was switched on and the voltage adjusted until the ten test electrodes showed their limiting currents. The DVM readings were recorded for each element. The temperature and flow rate were randomly checked. Also, elements were chosen randomly and tested to see if they were exhibiting their limiting currents. This was obtained by adjusting significantly the voltage supplied by the power pack and observing how the current changed. A steady current suggested limiting conditions. The current values were remeasured if this was not the case. When all the electrodes had been measured the power pack was switched off.

The pressure drop was measured as discussed earlier in Section IV.3.5 .

The pump was stopped and nitrogen pressure used to pressurise the solution back into the storage tank. The tank was then isolated and the pipe work washed. The concentration of the ferricyanide used was as indicated in appendix AII .

Nitrogen pressure was maintained above both solutions.

CHAPTER V

V Shell-Side Investigation in Bundles without Leakage

V.1 Scope of Experimental Work

For the no-leakage work the baffles used were of such a diameter that they gave zero clearances, hence eliminating both tube-to-baffle and shell-to-baffle leakage streams.

Local mass transfer measurements were made for bundle configurations with an 18.4% baffle-cut and two baffle spacings of 47.6 mm and 149.2 mm. The size of the end compartments was the same for both bundles configurations, with a length of 47.6 mm. These measurements were made over the whole exchanger length for the 47.6 mm baffle-spacing and over half of it for the 149.2 mm spacing configuration. As the electrodes span half the exchanger length, the flow direction was reversed to enable overall examination of the bundle.

As Mackley (3) had shown a symmetrical distribution of the transfer coefficients about the vertical axis for horizontal baffle-cut, all twenty electrodes were installed in one half of the exchanger compartment.

The electrode positions are shown in Appendix (IV) together with the individual tube data.

An investigation was also made into a semi-leakage configuration in which the shell-to-baffle clearance was 0.5 mm and the tube-to-baffle clearance was negligible. The baffle-cut and baffle-spacing were 18.4% and 47.6 mm respectively. All the dimensions of configurations tested in this section are listed in Table V.1.

Table V.1 Geometrical Dimensions for Configurations Tested in Chapter V

RUN NO.	BC (%)	COMPARTMENT BS (mm)		S/B (mm)	T/B (mm)	COMPARTMENTS STUDIED
		END	INTERNAL			
1	18.4	47.6	47.6	0.5	0	1 to 4
2	18.4	47.6	47.6	0	0	1 to 4
3	18.4	47.6	47.6	0	0	5 to 8
4	18.4	47.6	149.2	0	0	1 to 4

The tube bundle was arranged in the shell with the flow entering and leaving at the top of the inlet and outlet compartments respectively.

The inside diamter of the shell in all above cases was equal to 133 mm. Investigations were carried out using Bergelin et el (18-25) type rectangular ports. Prowse had previously shown little difference between these and commercial circular ports, discussed earlier in Section II.5.4.

These investigations were carried out for electrolyte flow rates in the range of 3 to 95 litres per minute.

V.2 Repeatability of Experimental Data

The repeatability of the data was checked by comparing two runs performed on different days with similar bundle geometry and flow rate. Bundle-average transfer coefficients expressed in the form $(Sh/Sc^{1/3})$ are given in Table V.2 below. The percentage difference in the dimensionless transfer coefficients were less than 3%. This was well within the estimated experimental accuracy of ±6.5%, (see Appendix A3). The close agreement demonstrates the consistency of data obtained using this electrochemical technique.

Table V.2 Reproducability of Data

DATES	2/6/79	3/5/79
Rem	312	315
$Sh/Sc^{1/3}$	15.9	15.53

V.3 Individual Tube Coefficients

The individual tube dimensionless transfer coefficients ($Sh/Sc^{1/3}$) were studied to provide an insight into local flow behaviour within the exchanger compartments. Comparisons of the data were made against the internal compartment data of Mackley (3) and Williams (48).

This investigation provided information on the distribution of transfer coefficients and the characteristics of individual tubes. Thus providing useful information to explain the aggregate compartment and overall effects.

V.3.1 Variation of Transfer Coefficients within the Compartment

To fully illustrate the variation of transfer coefficient would require local point velocities. This is beyond the capability of the present equipment. However, averaged transfer coefficients over a segmental electrode within the compartment could be used to show velocity variation along the tube. The internal compartment data from Run 4 provides the best example for demonstrating the existence of lengthwise variation. The compartment contained multielectrodes, each consisting of five isolated segmental electrodes spanning the whole length of the compartment. These individual electrodes were not of the same length. The most upstream element (called Blue in Section IV.3.3) was

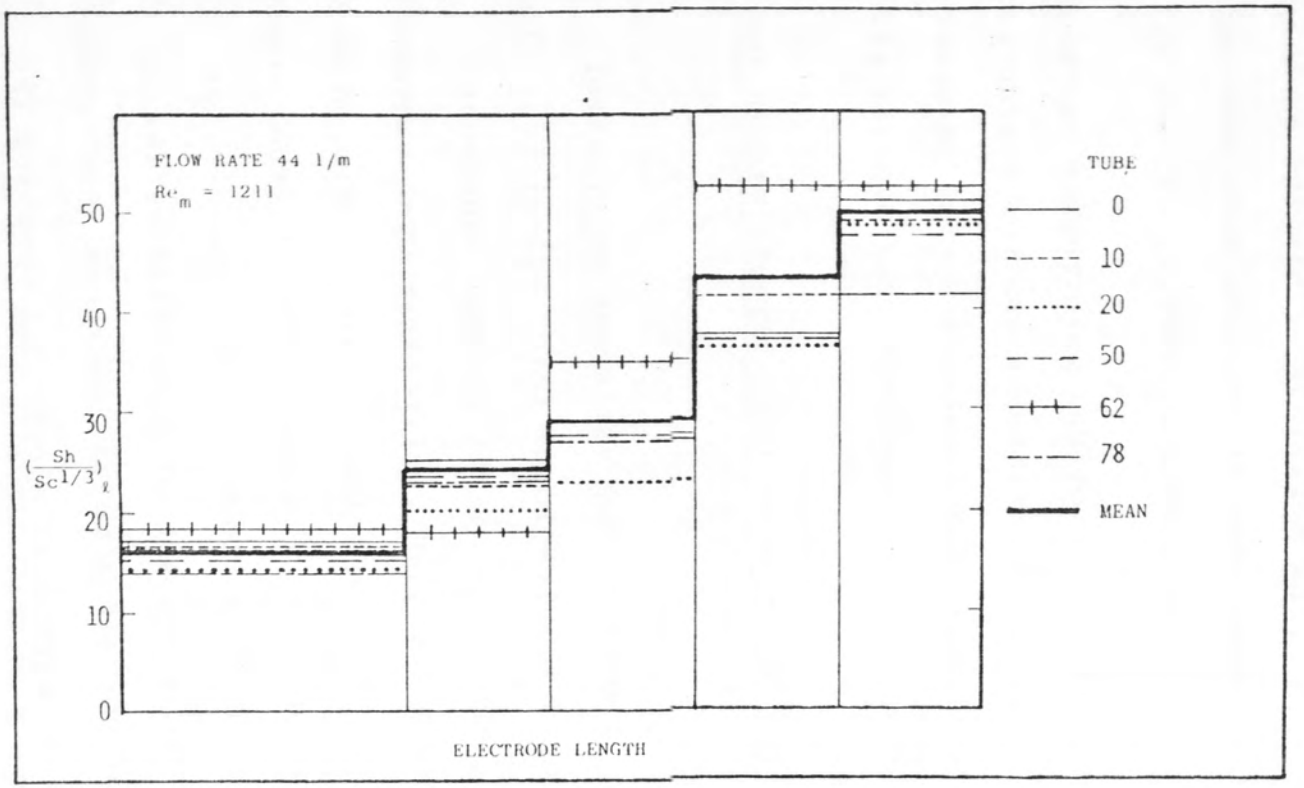

Figure V.1 Variation of transfer coefficient along the compartment length

twice the length of the remaining four electrodes.

A number of tubes from all sections of the compartment were chosen to show the variation of the transfer coefficients along the exchanger length, as illustrated in Figure V.1 for a particular Reynolds number. Although the magnitude and the variation would change with Reynolds number, this figure demonstrates the general trends. Also shown in Figure V.1 are the mean segmental electrode transfer coefficients.

All the tubes examined showed similar lengthwise variation, displaying initially lower dimensionless transfer coefficients in the upstream end of the compartment but increasing towards the downstream baffle. The mean value for all elements showed a similar variation increasing by 125% from the most upstream segment to the most downstream segment. This was consistent with the findings of Stachiewicz and Short (47), as discussed earlier in Section II.4.2.

This variation could be explained by two factors, firstly acceleration and deceleration by the baffles in the downstream and upstream sections respectively, and secondly, changes in fluid direction again caused by the presence of the baffles. Regions immediately after the baffles would have eddy flow also. A better understanding should emerge from the examination of flow characteristics over individual tubes as studied in Section V.3.3. This investigation suggested that a similar variation may

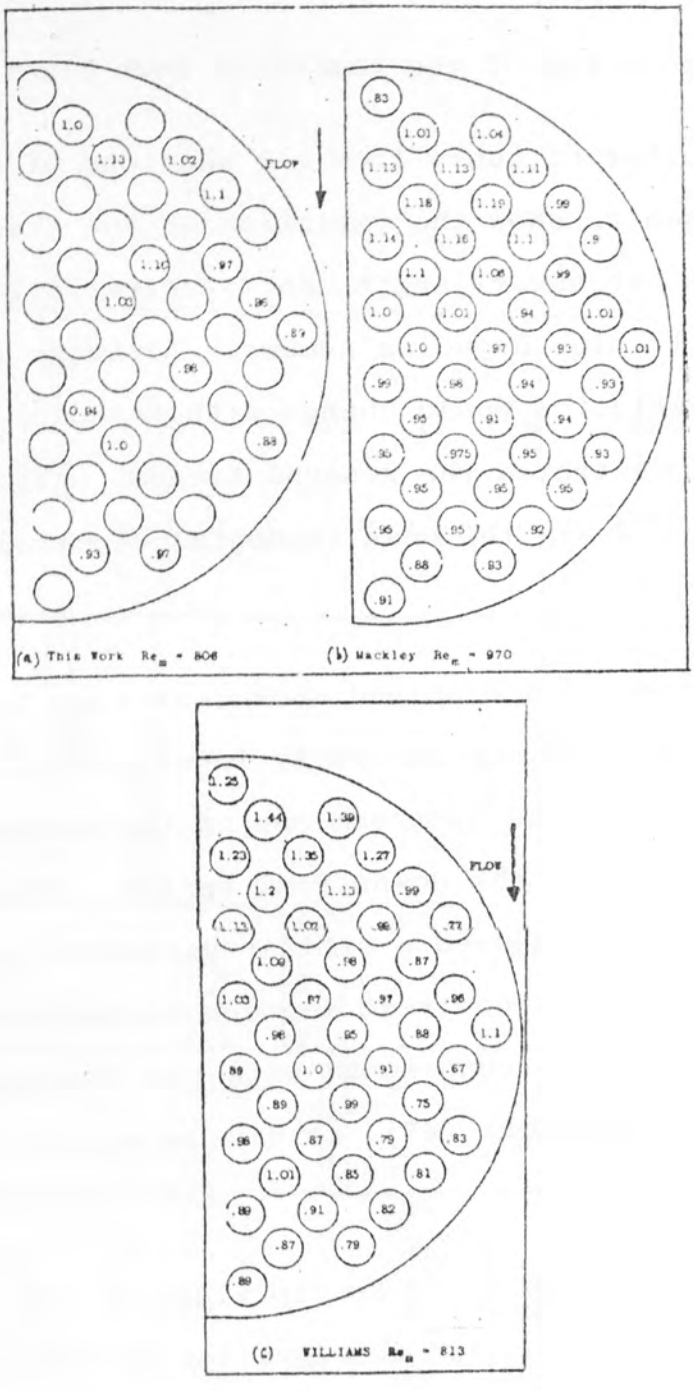

Figure V.2 Normalised distribution diagrams of the internal compartments

exist in the smaller baffle-spacing compartments, thus indicating the need for local velocity data.

V.3.2 Distribution of Transfer Coefficients

The distribution of transfer coefficients can be represented by a normalised form of the data within each compartment. The individual tube transfer coefficients were each divided by the respective compartment average transfer coefficient. Both Mackley (3) and Williams (48) presented their data in this manner. Distribution diagrams for the fifth compartment of the 47.6 mm baffle-spacing configuration are shown in Figure V.2 enabling a comparison to be made with similar data of Mackley and Williams .

For the lower flow rate, the spread of individual transfer coefficients for this work is seen to be within 20%. This was comparable to Mackley's value of 30%, but was much lower than Williams's value of 48%. The large spread in the latter data was due to the inaccuracies inherent in the use of the mercury evaporation technique (see Section II.4.3.1)

At a higher Reynolds number the spread of the present data was of the order of 34%, illustrated in Figure V.3. This maximum spread was due to tube 44 exhibiting an extremely low coefficient indicating local leakage. The spread of Mackley's data was slightly lower at 31%. There

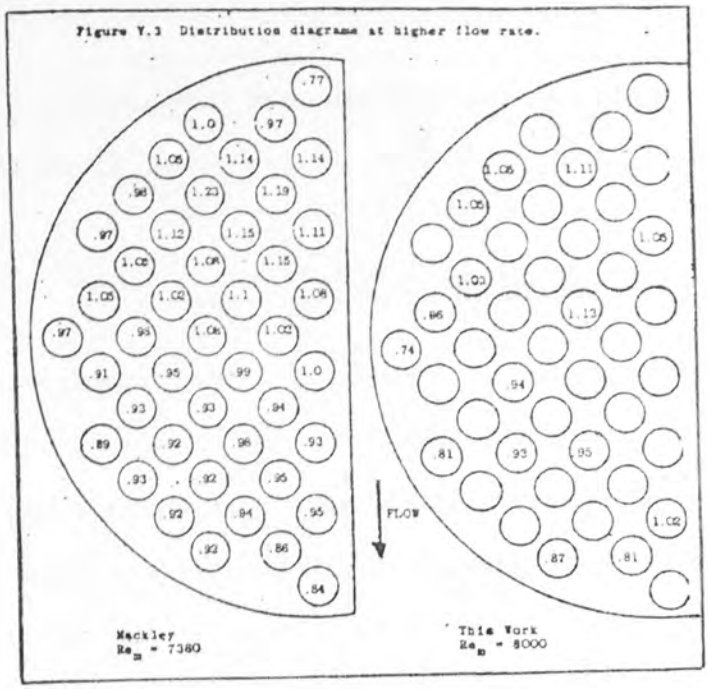

Figure V.3 Distribution diagrams at higher flow rate

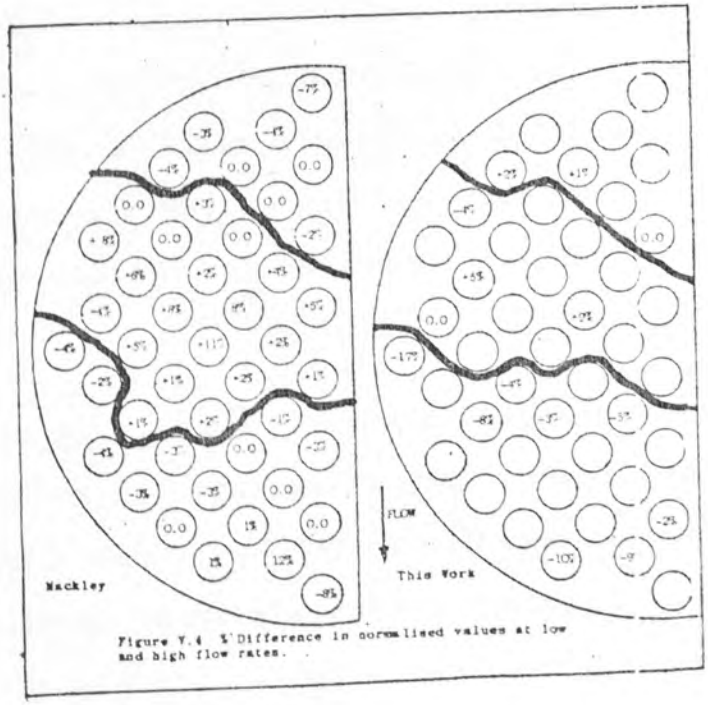

Figure V.4 The effect of flow rate on distribution values

was no Williams data at Reynolds numbers above 1500.

Comparing the normalised individual values of this work against Mackley's, showed agreement for individual tubes to within ± 10% for both Reynolds numbers, thus indicating that the distribution of flow was similar in both cases. However, a corresponding comparison with Williams's data showed much higher disagreement of the order of ± 25%. Deficiencies due to the mercury evaporation technique have already been mentioned.

The percentage differences due to flow rate in the distribution patterns were shown by comparing normalised individual values at lower and higher Reynolds numbers. This is shown in Figure V.4 for both the present and Mackley's data. The datum values were chosen at the lower Reynolds number. The maximum difference in the individual normalised values for this work were within ± 10% with the exception of tube 44. The comparable values in Mackley's case were +11% and -8%. This suggested that the normalised distribution pattern of transfer coefficients did not change greatly with flow rate. However, both the complete compartmental data of Mackley and the concise data of the present work indicated that the tubes in the window zones showed negative values while part of the baffle overlap region showed positive values. This suggested that the crossflow region received a greater penetration of flow at high Reynolds numbers than at lower Reynolds numbers, and the reverse for the window zones. This is discussed later in the section.

The distribution patterns over all the tubes obtained by Mackley (3) and Williams (48) were much more complete compared with the twenty tubes investigated in this study. This number was further reduced when some cathodes malfunctioned. The distribution pattern only provide an indication of general behaviour within the compartments so as to highlight regions with high and low transfer coefficients. This could satisfactorily be done by the available number of electrodes.

V.3.3 Characteristic Behaviour of Individual Tubes

The physical construction of the baffled compartment had led previous workers to subdivide the compartment into zones within which tubes experienced a particular flow mode, such as cross-flow in the baffle-overlap region and longitudinal flow in the window regions. Bergelin et al (22-25), Williams (48), Mackley (3) and Prowse (4) then all tried to use the distribution of transfer coefficients to show the presence of these flow modes. This simplification may be erroneous as the transfer coefficient is a function of both fluid flow magnitude and direction. Therefore, any study of the individual tubes needs to take into account variations in both fluid flow magnitude and direction over each tube in order to highlight zones of any specific characterisation.

The relationship between dimensionless heat or mass-transfer coefficients and Reynolds numbers was somewhat simplified to be expressed by equation V.1

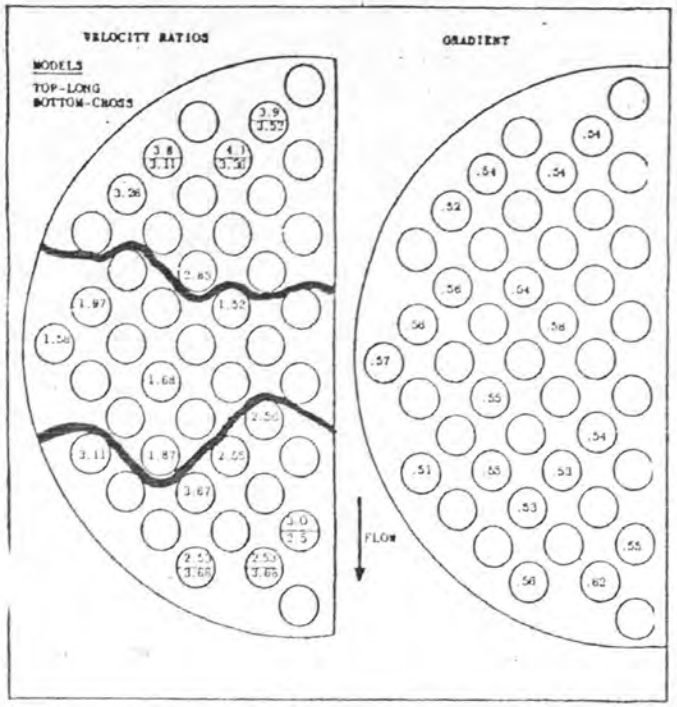

Figure V.7 Characteristic behaviour of individual tubes Compartment Third

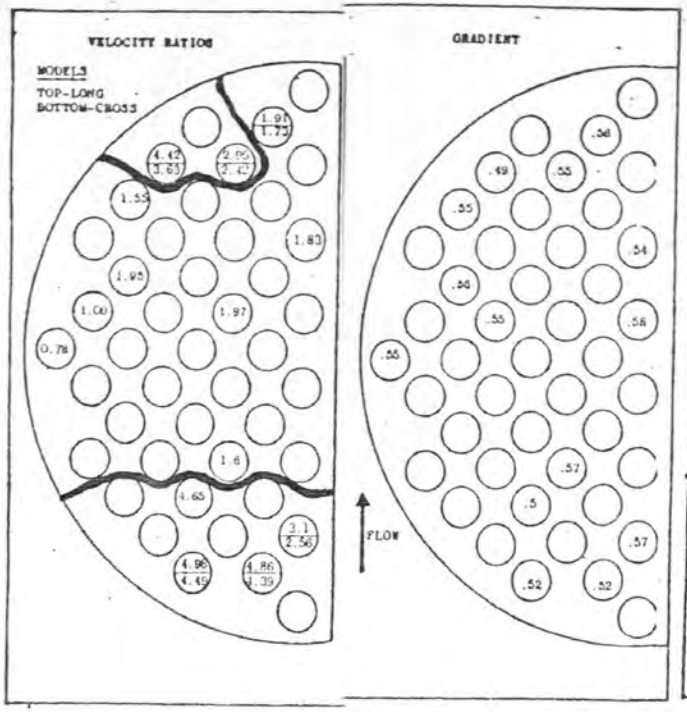

Figure V.6 Characteristic behaviour of individual tubes Compartment Second

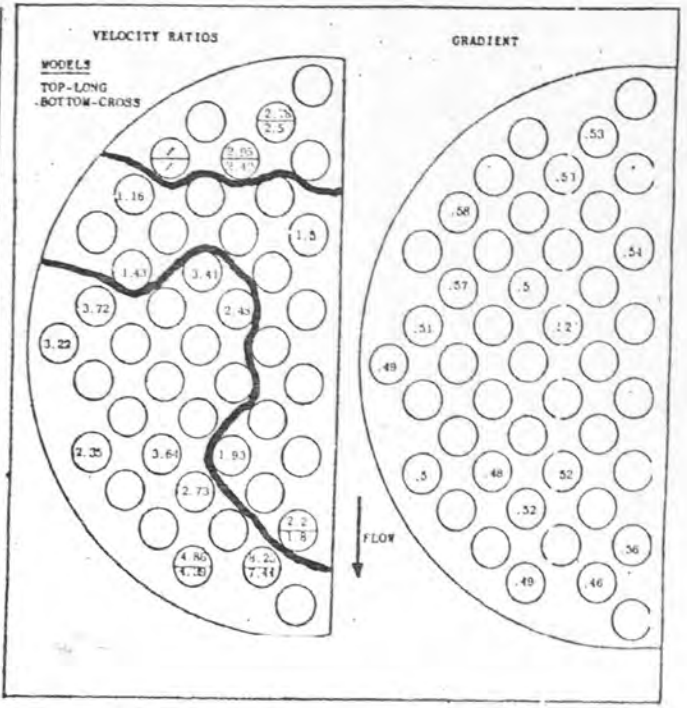

Figure V.5 Characteristic behaviour of individual tubes Compartment Inlet

$$(Sh/Sc^{1/3}) = a\ Re^{b} \qquad (V.1)$$

where the exponent and the equation coefficient would perhaps be modified to indicate flow direction and magnitude respectively.

Naturally the proper velocity in the Reynolds number would be the local velocity experienced by that surface. This is not obtainable from the present data. However, an arbitrary velocity such as that based on flow area A_M could be used, and later adapted to account for the local effects as explained later.

To investigate all the electrode surfaces a computer programme was used to fit equation V.1 through all the data points for each individual electrode. The least squares technique was used to find such a line. The fitted line correlated the experimental data to within ± 20%. The velocity used in the Reynolds number was based on the flow area A_m and the Sherwood number on tube diameter. The exponent and coefficient values obtained from each fitted curve of individual segments and for all experimental runs listed in Table V.1 are reported in the Appendix A4.

Characterisation by Exponent Values

The exponent values for the 47.6 mm baffle spacing configuration are diagrammatically shown in Figures V.5 to V.12 from the inlet to the outlet compartments.

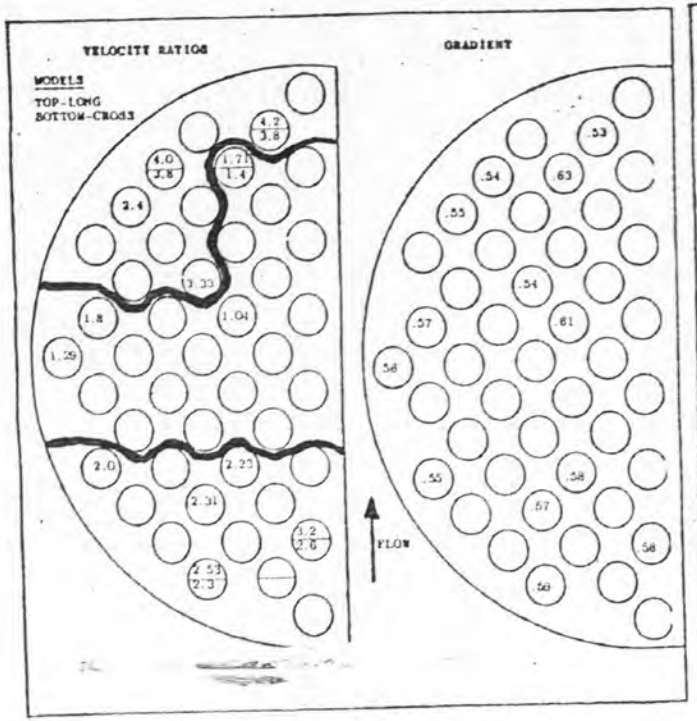

Figure V.10 Characteristic behaviour of individual tubes Compartment Six

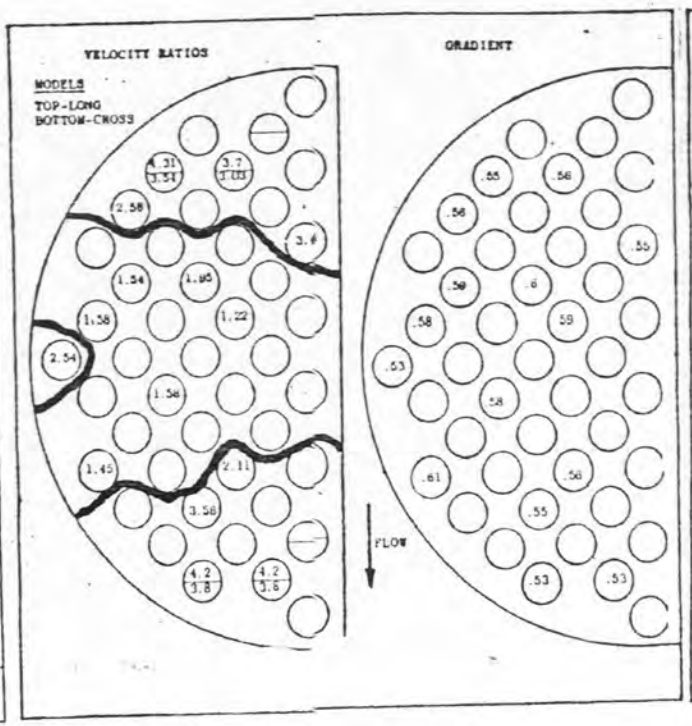

Figure V.9 Characteristic behaviour of individual tubes Compartment Five.

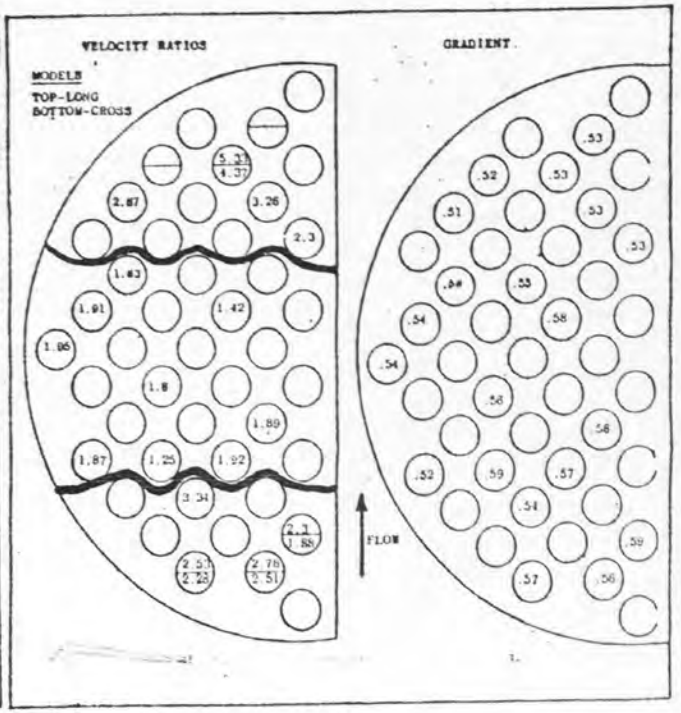

Figure V.8 Characteristic behaviour of individual tubes Compartment Four.

The individual tube values in the internal compartments from the third to the sixth were averaged over two half electrodes employed in these compartments (see Figure IV.4). Whenever possible the value of a faulty electrode in this pair was estimated from the surrounding tubes and the working half of the pair, and is indicated by an asterisk.

Closer examination of these figures revealed that the average compartment exponent values were slightly higher for the internal compartment as compared with the end compartments. This effect is discussed further in Section V.4.1.

Examination of individual tubes in Figures V.5-12 showed that the exponent values varied from 0.48 to 0.6. Thus the variation within the compartment of the exponent values was small being less than ± 11% from the compartment average value. Also there were no regions within any compartment which possessed distinctly different values, thus distinction between the window, cross or any other zone could not be made purely from the exponent values.

A similar analysis was carried out for run number 4 which constituted two end compartments geometrically the same as for the above case, and two internal compartments of 149.2 mm baffle-spacing.

The individual tube study, depicted in Figure V.13 for the inlet compartment again showed no region which possessed distinctive exponent values. The difference between the compartment average exponent values for this

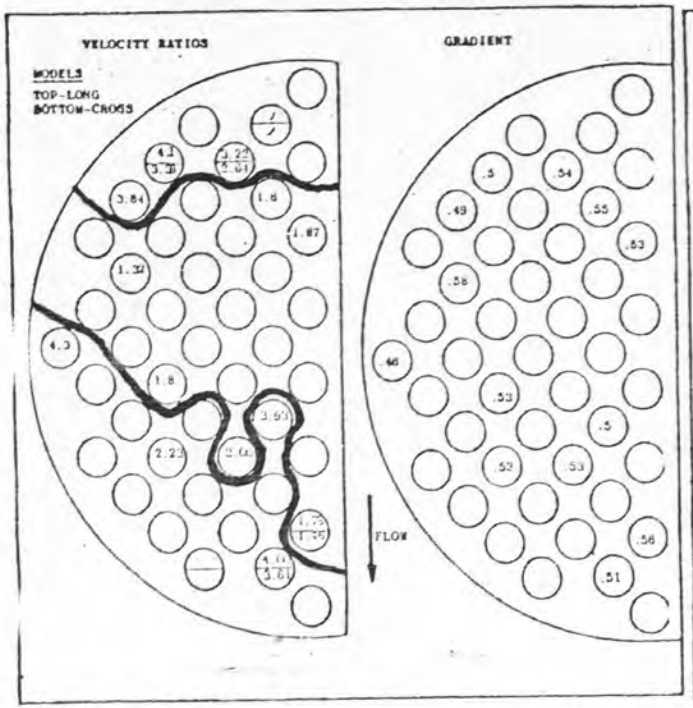

Figure V.13 Characteristic behaviour of individual tubes Compartment Inlet - Run 4.

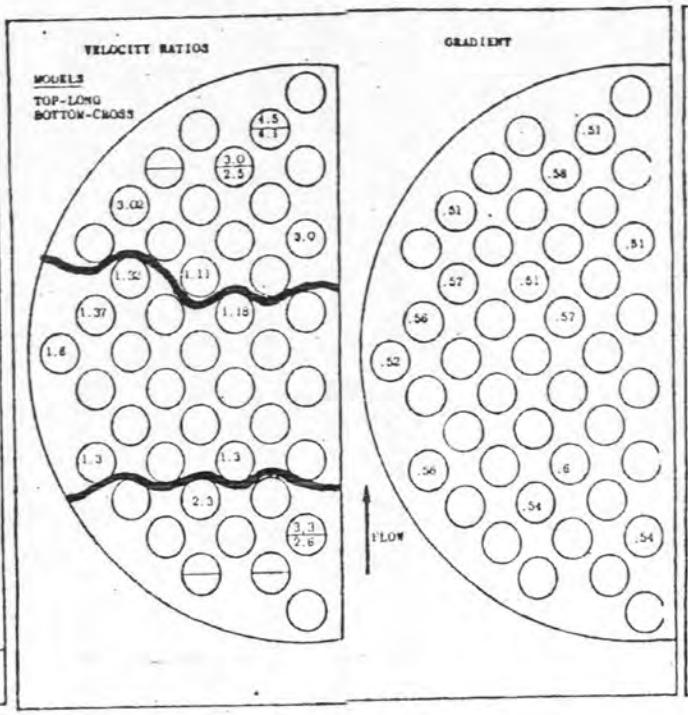

Figure V.12 Characteristic behaviour of individual tubes Compartment Outlet

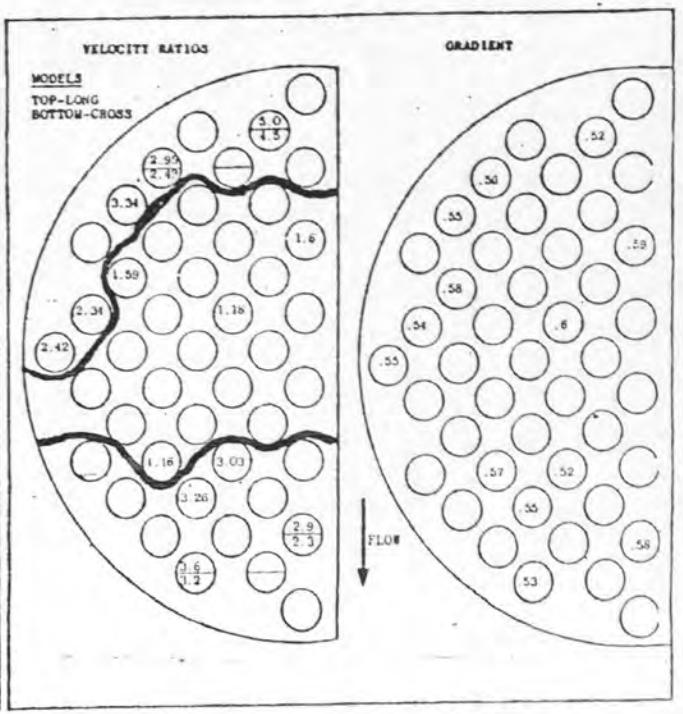

Figure V.11 Characteristic behaviour ofindividual tubes Compartment Seven

case and the inlet compartment studied earlier as shown in Figure V.5, was less than 2% and the individual values differed by less than ± 10% from each other, with the exception of tube 16. This tube differed by 15%, with the compartment investigated in run number 4 showing the lower value. This tube may be experiencing local shell-to-baffle leakage through the sealing strip. Apart from this tube, however, the two inlet compartments were indistinguishable in terms of their exponent values.

The main conclusions drawn from these vital compartment comparisons is that similar configuration compartments had similar exponent values regardless of the configuration of their adjacent compartments.

Investigation of the 149.2 mm internal compartment is discussed later in this section.

Nowhere did the exponent value reach near to 0.8, exponent representing longitudinal flow over a flat or curved surface in the turbulent regime (73). However, corresponding exponent value for longitudinal flow in the laminar range is 0.5 (8). Similarly, for crossflow to a cylinder, the exponent value varies from 0.466 to 0.618 as shown by Hilpert (6) for Reynolds numbers from 40 to 40,000. This suggested that the exponent values listed in Figures V.5 to V.13 could not differentiate between longitudinal flow in the laminar regime and crossflow in the Reynolds number range indicated above.

Characterisation by Equation Coefficients

The coefficient values (a) obtained from equation V.1 for each individual element should not be compared directly with the values of other tubes within the same compartment. This is due to two factors. The first is that the distribution of the fluid flow changes from row to row of the tube bank. The second is that, these coefficients have been determined by using an arbitrary velocity V_m, and therefore for any true comparison to be made correction to account for the different local velocities is needed. The following simple procedure was adopted to account for the above factors and so develop a method of discriminating between different types of flow zones.

Before the procedure is outlined an important assumption requiring the tubes to experience one type of flow throughout the compartment length is made. This is to simplify the procedure.

For flow perpendicular to a single cylinder, Ulsamer (7) correlated his data by equation V.2 for Reynolds number from 50 to 10,000.

$$\frac{hd}{k} = 0.6 \left(\frac{dv\rho}{\mu}\right)^{.5} Pr^{.31} \qquad (V.2)$$

A similar equation for fluid in laminar flow parallel to plane or moderately curved surfaces, being Pohlhausen's (8) theoretical equation, is

$$\frac{hL}{k} = 0.658 \left(\frac{Lv\rho}{\mu}\right)^{0.5} Pr^{.31} \qquad (V.3)$$

According to Van der Hegge Zijmen (78), laminar boundary layer ceases at around a length Reynolds number of 300 000, although values as low as 100 000 have also been observed (73).

Now consider a tube in the n^{th} row experiencing cross-flow, then the velocity in equation V.2 would be the local velocity V_ℓ experienced by that surface. Arranging equation V.2 to express the dimensionless heat transfer coefficient as a function of Reynolds number based on the free flow area at the n^{th} row centre-line, $A_{\ell,n}$, we get

$$\frac{Nu}{Pr^{1/3}} = 0.6 \left(\frac{V_\ell}{V_{\ell n}}\right)^{0.5} Re_{\ell n}^{0.5} \qquad (V.4)$$

Again by re-expressing Reynolds number on the basis of A_m, equation V.4 becomes

$$\frac{Nu}{Pr^{1/3}} = 0.6 \left(\frac{V_\ell}{V_{\ell n}}\right)^{0.5} \left(\frac{A_m}{A_{\ell n}}\right)^{0.5} R_{\ell m}^{0.5} \qquad (V.5)$$

The form of this equation is similar to that of the equation used to fit the data (equation V.1) thus equating them together we get

$$\frac{Sh}{Sc^{1/3}} \text{ or } \frac{Nu}{Pr^{1/3}} = 0.6\left(\frac{A_m}{A_{\ell m}}\right)^{0.5} \left(\frac{V_\ell}{V_{\ell m}}\right)^{0.5} \cdot Re_m^{0.5} = a\,Re_m^b \qquad (V.6)$$

It is shown in Figures V.5 to V.12 that the exponent 'b' varies from 0.48 to 0.6, differences of -4% to

20% if b=0.5. To simplify equation (V.6) the exponent values will be assumed to equal 0.5. The effect of not doing so will be discussed later in this section. Therefore

$$\left(\frac{V_\ell}{V_{\ell m}}\right) = \frac{2.78\, a^2}{\left(\frac{A_m}{A_{\ell m}}\right)} \qquad (V.7)$$

Similarly for a tube experiencing parallel flow in the window zones, an equation relating the ratio of local and overall fluid window velocities is obtained from equations V.3 and V.1 as:

$$\left(\frac{V_\ell}{V_w}\right) = \frac{2.3\, a^2}{(d/L_s)(A_m/A_w)} \qquad (V.8)$$

The magnitude of these velocity ratio terms indicates the distribution of fluid flow. Values of these velocity ratios near unity would suggest a better fit of the models, and excessive departure from unit would mean the model to be invalid.

The individual values of these ratios expressed by equations V.7 and V.8 are also depicted in Figure V.5-12, for the 47.6 mm uniform baffle spaced configuration. The parallel flow equation was restricted to tubes in the vicinity of the window zones as equation V.8 becomes meaningless in baffle overlap regions. Further, the parallel flow equation V.8 was applicable only in the laminar flow range, with the critical Reynolds number (based on baffle spacing as the characteristic length) of the order of 100 000 to 300 000. Calculating this

Reynolds number for the maximum flow rate used in this work showed a value of 277 000. It is noted that the flow in the window zone of a baffled exchanger would have much greater disturbance caused by the flow turn-round, interaction of boundary layer from surrounding cylindrical tubes, and the complex geometry of the window zone. Therefore, it would be highly unlikely that the flow in the window zone would be completely laminar over the whole length of the tube even at the lower flow rates. This would be even more unlikely in the baffle overlap. Hence application of equation V.8 was suspect.

The equation V.7 applicable for the crossflow region was however able to predict velocity ratio values in the window zones to within 20% of those predicted by equation V.8. Therefore, equation V.7 was applied throughout the compartment.

Closer examination of Figure V.5 showed that the inlet compartment could be divided into regions having extremely high and slightly high velocity ratios compared with unity. Most of the compartment showed high local to average row velocity ratios, although a small region of the bundle gave values for the velocity ratio slightly lower than those in the outlet window zone and peripheral tubes of the bundle. This region occupied the upper end of the crossflow region. There was also a clear difference between the extremely high values in the outlet window zone and the remaining regions.

This procedure was extended to the inlet compartment. Comparison of the two inlet compartments from two different tube bundle configurations showed some resemblance in the flow distribution patterns as determined from the velocity ratios, (see Figures V.5 and V.13). The majority of the compartment in both cases experienced high velocity ratios in the window zone and outer peripheral tubes. This was with the exception of tube 73 in the window zone and a region near the upper end of both inlet compartments. The velocity ratio region closer to unity however, were of different sizes for the two compartments. This difference could either be real and caused by their adjacent compartments, or artificial as the number of tubes defining the distribution patterns were small in both cases. More tubular data would be needed before a definite conclusion could be drawn. The remaining compartments , second to the outlet all showed similar distribution patterns, with lower velocity ratios within the baffle overlap region and higher values in the vicinity of the window regions. The second compartment showed the largest low flow distribution region while the remaining compartments all showed approximately similar sized regions.

In Figure V.3 it was suspected that tube 44 in the fifth compartment might have been experiencing local shell-to-baffle leakage. In Figure V.9 this tube uncharacteristically showed high velocity ratio term, indicating a high proportion of flow passing about this tube. Apart from this tube

there were no other tubes in the low flow distribution region which had significantly high velocity ratios, thus again indicating that there was no internal leakage within the bundle.

The comparison between the inlet and outlet flow distribution patterns of the uniform baffle-spacing compartments configuration showed them to be different. The outlet compartment showed a similar flow distribution pattern compared with other internal compartments. The flow entering from the bottom inlet zone and leaving at the top outlet port would not be expected to greatly effect the behaviour of the flow distribution. The reason for high velocity ratios at the compartment outlet was due to flow contracting because of the restriction downstream induced by the port. The inlet however, has flow expanding from the port and contracting towards the outlet window zone.

When examining the differences in the normalised dimensionless coefficient values at higher and lower flow rates, (see Figure V.4 in Section V.3.2), it was found that tubes in the crossflow zone had higher normalised transfer coefficient values at Reynolds number of 8,000 compared with Reynolds number of 784. The two window zones both showed the reverse trend to the crossflow zone. The present procedure, so far, expressed by equations V.7 and V.8, made no attempt to account for the effects of flow rate. In developing this procedure it

was also assumed that the exponent on the Reynolds number in the fitted equation was constant and equal to 0.5. Both of these points are now discussed further.

During the development of this method for calculating the individual tube ratios of local velocity against some mean velocity, the fitted equation was compared with published correlations for flow perpendicular and parallel to any surface. If now the exponent (b) on the Reynolds number in the fitted equation was not equated to 0.5 then for the crossflow zone equation V.7 becomes

$$\left(\frac{V_L}{V_{L,m}}\right) = \frac{2.78\ a^2\ Re_m^{2b-1}}{(A_m/A_{L,m})} \qquad (V.9)$$

This applies for Reynolds numbers up to 40 000. Taking data of compartment five as an example, depicted in Figure V.9, it can be seen that the values of the exponent are above 0.5 in the crossflow zone. Thus the exponent (2b-1) would be positive, suggesting that as Reynolds number was increased the velocity ratio expressed by equation V.9 would also increase. It follows that as the crossflow zone receives relatively greater penetration of the total flow, the ratio of the normalised values at high and low flow rates for the window zones would reduce. Hence supporting the conclusion obtained from the analysis of transfer coefficient data as shown in Figure V.4.

This however is a tentative approach as the models are not accurate enough to predict such a small change.

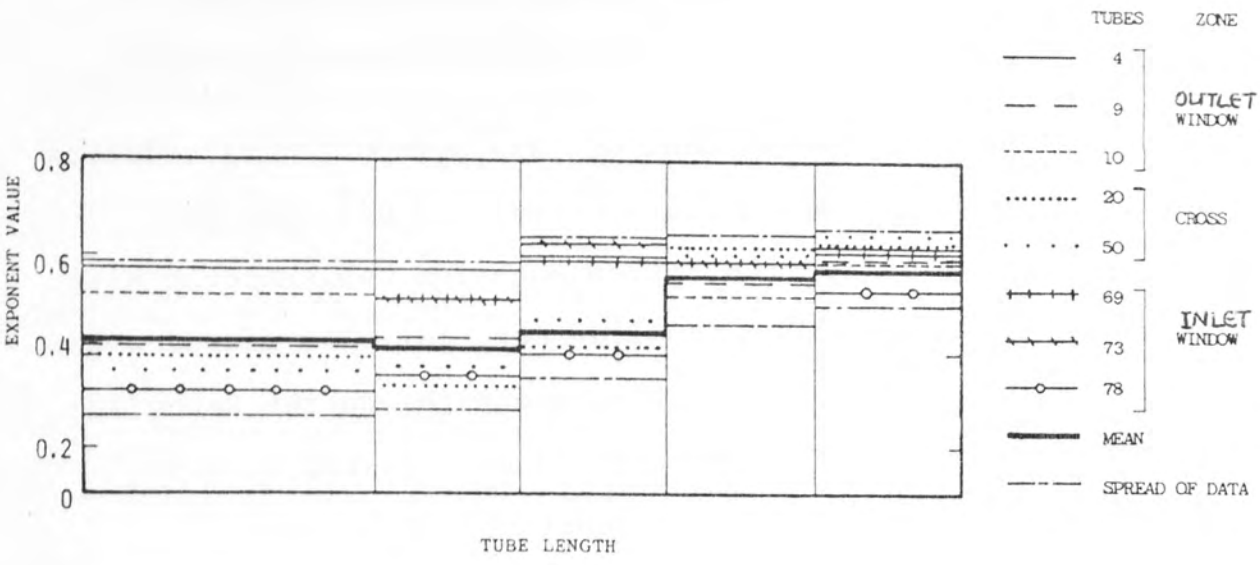

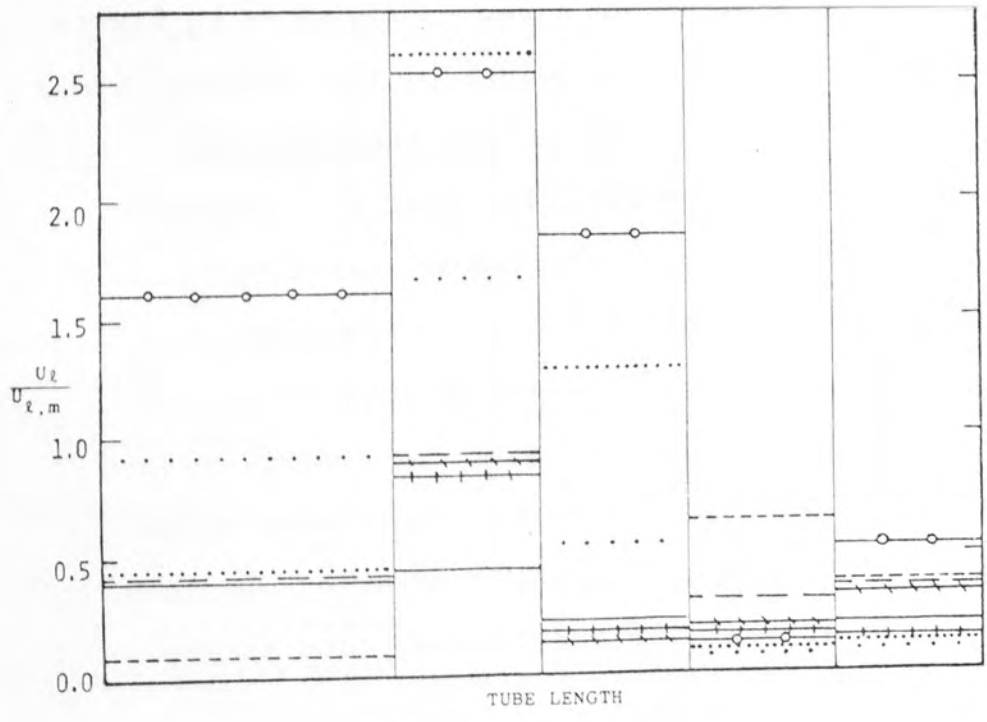

Figure V.14 Characteristic behaviour of individual electrodes showing the length-wise variation within the compartment

Flow Characteristics along the Tube Length

Variation of the transfer coefficent along the tube length was studied previously in Section V.3.1. The flow characeteristics over individual element electrodes are now investigated within the 149.2 mm baffle-spacing compartment. The average and some selected individual tube exponent values are shown in Figure V.14a.

The average exponent value is approximately 0.42 over two-thirds of the upstream end of the compartment. The remaining third of the compartment shows the average exponent value to be approximately 0.56. Thus, only the latter third of the compartment indicated exponent values associated with crossflow. The remaining two-thirds of the compartment may be under eddy flow regime. The spread of the exponent values about the compartment mean value is also found to decrease towards the outlet end of the compartment. This is also shown in the Figure V.14a and suggests even distribution of flow.

The individual values of some selected tubes shows that the exponent value increases downstream by as much as 45%. The pattern of the variation depends very much on the tube position. Tubes in the outlet window region of the compartment, numbers 4,9 and 10, generally show exponent values which are somewhat higher than others in the upstream section of the tube, and they increase marginally along the compartment. Tubes in the baffle overlap region, tube numbers 20, 50 and 69, show the

highest rate of increase in the exponent value along the tube length. The inlet window region indicated by the tube number 78, shows the lowest exponent value throughout, although tube 73 also in this zone has values always above average. The latter tube might be influenced by the baffle edge. However, not all the tubes within the compartment behave as described above. There are tubes which subscribe to neither of these patterns.

Figure V.14b shows the individual ratios of local to mean row velocities, as expressed by equation V.5. Thus showing a large variation in the velocity ratio, both along some tubes and between different tubes. The last third of the compartment had the lowest velocity ratio values in contrast to the exponent values. This suggests that the downstream electrodes achieved higher transfer coefficients by change in the flow direction rather than better flow distribution. As for the exponent case the spread of velocity ratio values is the lowest at the downstream end of the compartment. This suggests flow characteristics for the tubes in this position are similar. The largest variation in the velocity ratio is at the middle region of the compartment. Therefore, this suggested that the region was experiencing considerable amount of flow redistribution. The most upstream region showed the largest spread in the exponent values and also some variation in the velocity ratio values. This suggests that the upstream region is greatly affected by direction of fluid flow. All this means that the length-wise variation of transfer coefficients within this compartment

is caused by the three flow region outlined above. This is however a tentative conclusion and depends on the correctness of the assumption used in the model and insufficient data. An overall compartment study of the individual tube average exponent and velocity ratio values was also made and is shown in Figure V.15. As before the value for the faulty electrode segment was estimated whenever possible from general trends of surrounding tubes and the working elements in the multi-electrode. A weighted average was used to account for the most upstream electrode segment being twice the length of remaining segments within the multi-electrode.

Examination of Figure V.15 shows the variation of the exponent values for all the multi-electrodes to lie within ± 10% of the average value, when tubes 4 and 78 are omitted. The latter tubes exhibited the highest and the lowest values respectively, differing from the average value by ± 28%. The compartment average exponent value differed from the smaller baffle-spacing inlet compartment value by 16%, with the internal compartment showing the lower value. The low value for the large baffle-spacing compartment is attributed to the geometry of the large compartment producing greater eddy flow and less perpendicular flow compared with the short baffle spacing compartments.

The velocity ratios of the multiple electrodes shows a large variation between individual tubes. Both the crossflow and longitudinal flow model are used and

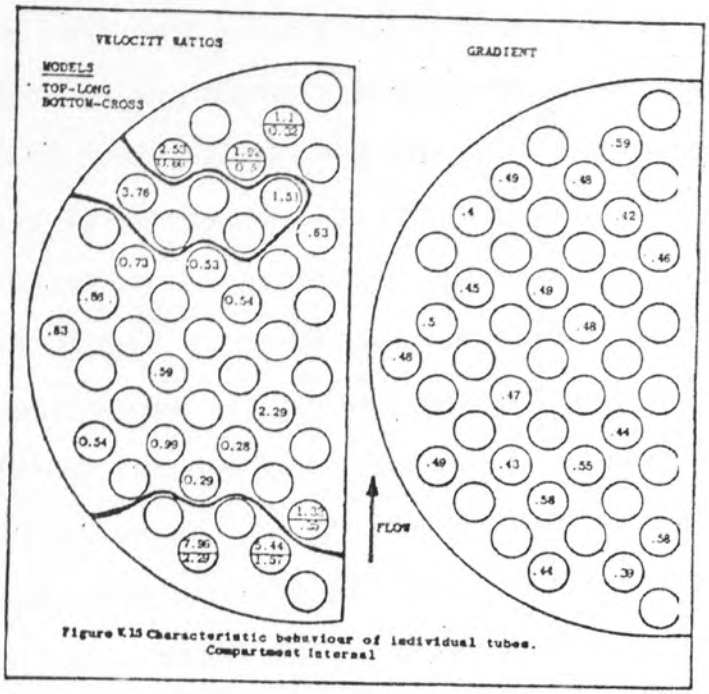

Figure V.15 Characteristic behaviour of individual tubes in a large baffle-spacing compartment

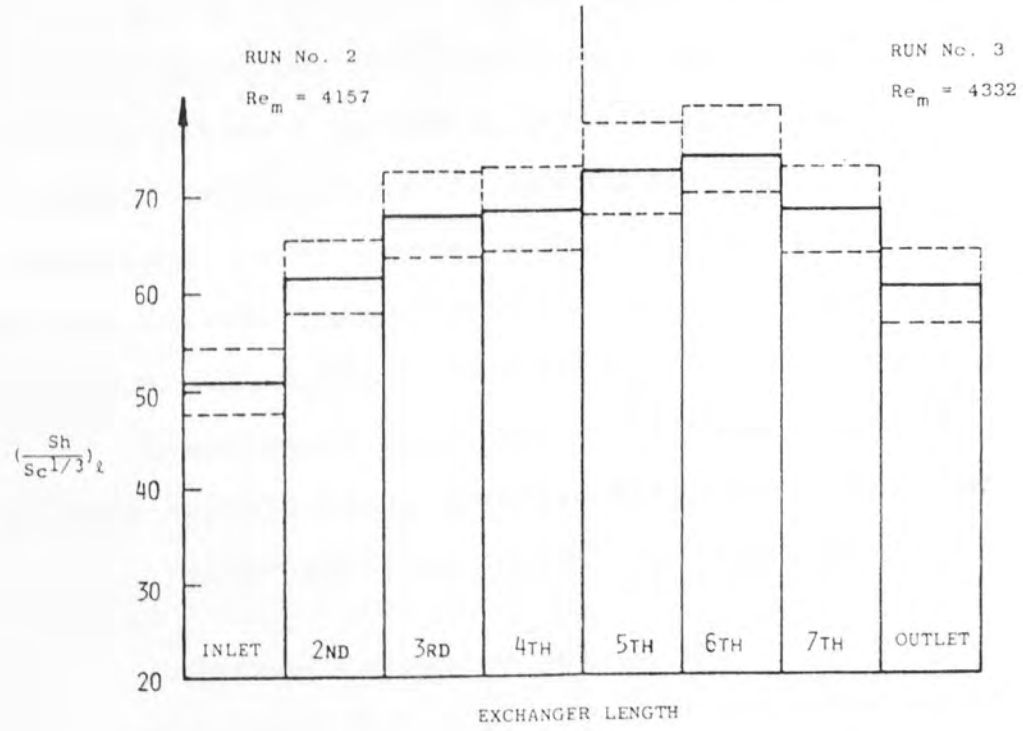

Figure V.16 Histogram showing the length-wise variation of the transfer coefficients along the exchanger length

their values calculated throughout the compartment. These values are however, in doubt because of the inability to estimate safely the coefficient of the fitted equation due to malfunctions of many elements. There is no clear region which shows values near unity, although the values are distributed about it. This perhaps suggests a better fit of the model but more data are needed before any further conclusions could be drawn.

The large variation in the transfer coefficient values and flow characteristics of individual elements within the compartment point out an important feature useful in design of commercial exchangers. In many pressure drop intensive exchangers the baffle-spacing is increased. The above investigation shows increased distortion results in the distribution of transfer coefficient in large baffle-spacing compartment. This could cause thermal stress to be set-up in the tubes and tube sheets, hence reducing the life of the unit. Such exchangers could also be under designed as the present desin methods do not allow for the existence of the length-wise variation of the transfer coefficient, discussed further in Section V.3.1. However, this would only apply for exchangers operating without internal leakage and small baffle cutdown, which is not the case in industrial units.

V.4 Compartment Coefficients

The individual tube coefficients were averaged within

each compartment to give overall compartment average transfer coefficient. This unweighted procedure was justified as the bulk and surface conditions remained constant.

These compartment average values were used to compare the present data with previous data, examine the behaviour of the end compartment and to study the effects of different compartment configurations. The compartment average transfer coefficients were also used to examine the length-wise variation along the exchanger length.

V.4.1 Length-wise Variation of Transfer Coefficients

The overall averaged dimensionless transfer coefficient for each compartment in the bundle were individually analysed in the form of dimensionless transfer coefficients against Reynolds number. As reported in Chapter III, the definition of the characteristic velocity used in the Reynolds number is an important correlating parameter. However, in this section only compartments of the same baffle-cut and -spacing are investigated, that is, they have the same configuration. Therefore, any characteristic velocity could be used to represent the data. The characteristic velocity chosen in this case is based on the minimum flow area at the centre of bundle, as often used in the past.

The 47.6 mm baffle-spacing compartment data are set out in Figures V.16 to V.18. The inlet half of the

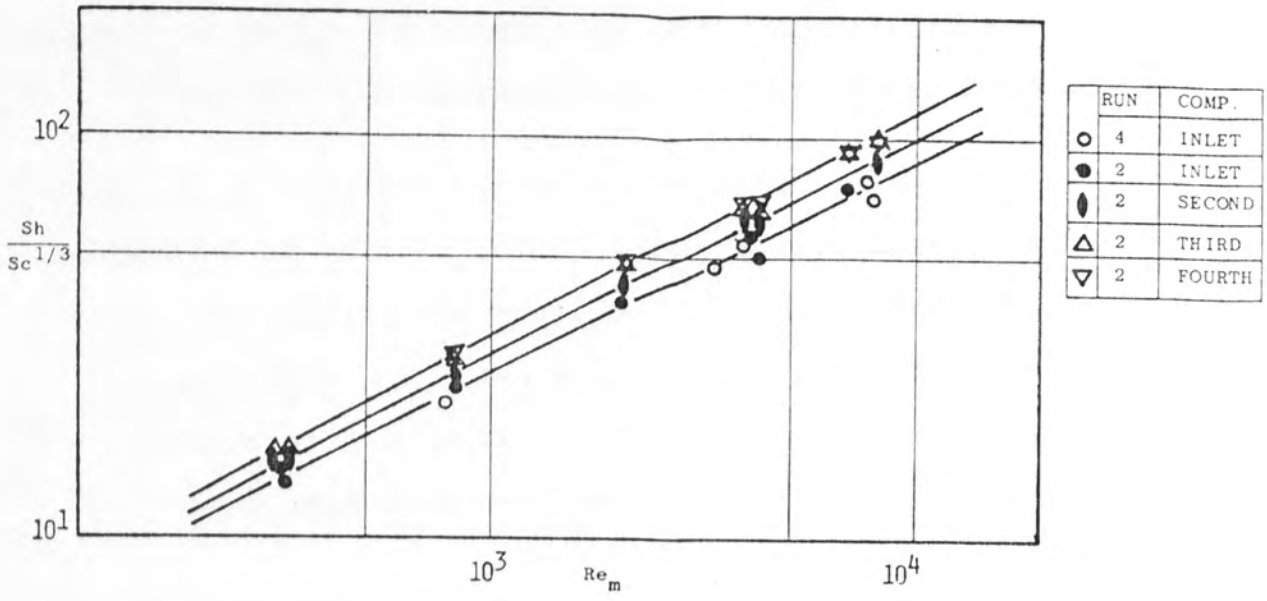

Figure V.17 Effect of flow rate on the length-wise variation of transfer coefficients in the first four compartments

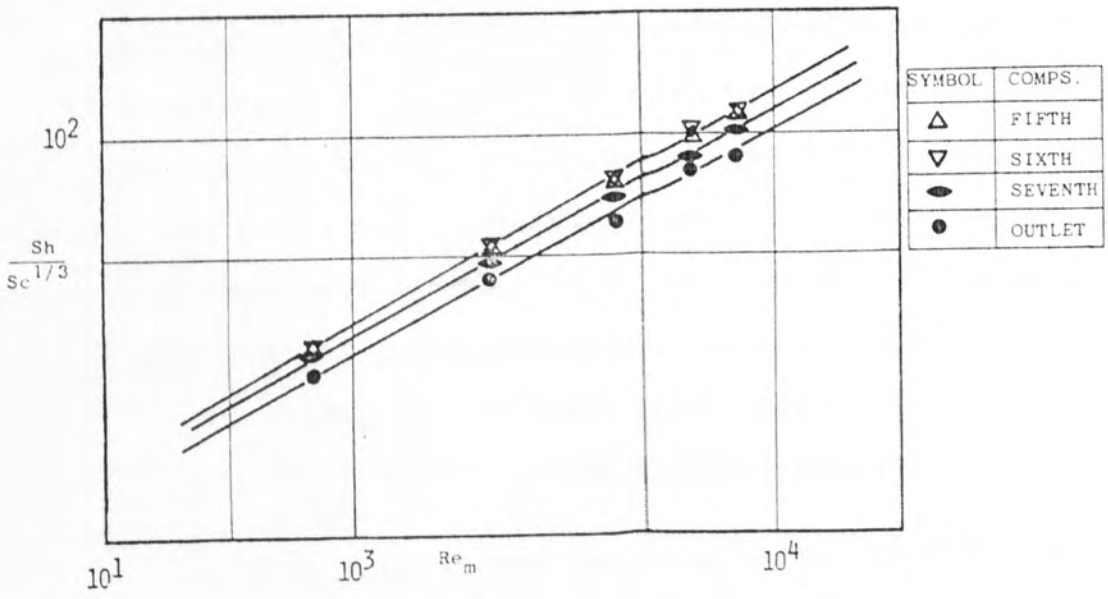

Figure V.18 Effect of flow rate on the length-wise variation of transfer coefficients in the last four compartments

bundle (i.e. first four compartments) and the outlet half of the bundle were plotted separately as two separate experiments were needed to investigate the complete length of the exchanger. The experimental measurements for each half of the bundle were made at the same operating conditions.

Figures V.16 to V.18 show for a no-leakage bundle, a distinct length-wise variation from compartment to compartment. This variation, in the form of a histogram at one flow rate, is depicted in Figure V.16, showing also the maximum experimental accuracy of the data as ± 6.5%. In spite of the error band encompassing some of the length-wise differences, the overall variation still exists especially between the end and internal compartments. Furthermore, the actual systems error in compartments studied at the same time would have a much lower value than the experimental accuracy of ± 6.5%. Thus emphasising the variation more strongly.

The compartment average transfer coefficients for the first four compartments against Reynolds number are shown in Figure V.17. The respective differences between the inlet compartment and second, third and fourth compartments were 13%, 26% and 26% at Reynolds number of 10^4. These differences changed to 12%, 15% and 15% respectively at a Reynolds number of 500. The difference between the internal compartments three and four was too small to be expressed by separate curves.

The second half of the bundle (compartments 5 to the outlet) also show negligible differences between central compartments five and six (see Figure V.18). The difference between the outlet compartment and compartments seven was 12% and that between five and six was 28% at a Reynolds number of 10^4. Again these differences reduced to 9% and 14% respectively at Reynolds number of 500. Thus the phenomena causing the length-wise variation increased in its effect with Reynolds number.

Both Mackley (3) and Prowse (4) postulated that because the end compartments possessed a different configuration to the other internal compartments, the behaviour of the end compartments would be different. This is discussed in detail in Section II.5.1. In the previous section it was shown that the inlet compartment did possess a different flow distribution compared to other internal compartments. This is shown in Figures V.5 to V.12. However, the flow characteristics of the outlet compartment are more akin to the internal compartments than to the inlet compartment. Thus, although it is quite plausible to explain the increase of transfer coefficient on moving from inlet compartment to the adjacent internal compartments, the decrease in transfer coefficients observed in the second half of the bundle is not so easily explained.

Comparing Figures V.17 and V.18 it can be seen that the data for internal compartments three to six have a scatter of

less than 6%, and a single curve could adequately represents all the data. The internal compartments, being geometrically similar, would be expected to behave similarly, if the incoming and outgoing fluid to each compartment had the same conditions. The compartment adjacent to the inlet compartment, although it is geometrically the same as internal compartments,it received a flow affected by the inlet compartment. Therefore, the transfer coefficients in the second compartment would reflect the type of flow it received. The geometry of the succeeding internal compartments would dampen the flow characteristics of the inlet compartment until their effects were removed.

But as stated earlier this simple explanation cannot account for the behaviour in the second half of the bundle. One possible hypothesis can be arrived at by observing, first that the remaining compartments have a similar distribution of flow but, second that the average compartment exponent values differ from compartment to compartment. This variation is similar in outline to the length-wise variation of transfer coefficient along the bundle. The compartment average exponent values are shown in Table V.3 below.

Table V.3 The Compartment Average Exponent Values

Compartment	Inlet	2	3	4	5	6	7	Outlet
Exponent Value	.516	.542	.55	.55	.565	.568	.555	.545

This variation in exponent values may reflect different flow vectors even though the distribution of flow is similar. The difference is however too small to extend the analysis any further.

The length-wise variation within a 149.2 mm baffle-spacing compartment was shown earlier in Section V.3.1. The dimensionless transfer coefficient of each segment changed along the compartment length. Therefore, this suggests that the variation exists both within the compartment and between compartments. Such a variation has been unobserved previously and designers have always assumed that the overall heat transfer coefficient remains constant along the tube bundle and lengths. With length-wise variation of the transfer coefficient, due purely to the fluid flow characteristics and not changes in the physical properties, this would result in some small size units being under designed. This is because exchangers with fewer compartments would reflect the effects of the end compartments in the overall transfer coefficient. In large exchangers with many internal compartments these end compartment effects would not be noticed in the overall aggregated transfer coefficient. However, the data reported in this chapter arefor no-leakage bundles, whereas all the commercial exchnagers have associated internal leakages. This indicated the importance of leakage data, which are examined in Section V.6 and in Chapter VI.

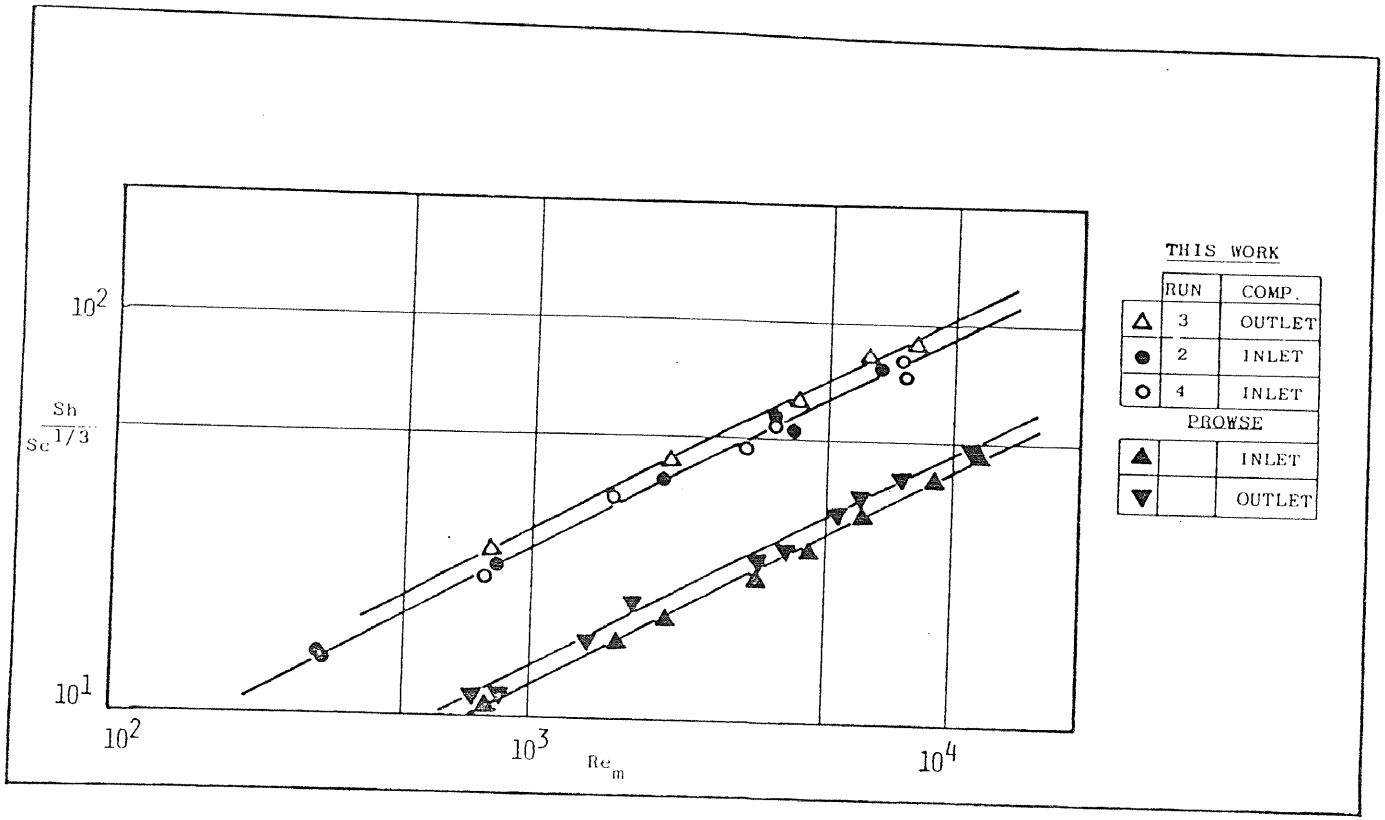

Figure V.19 Comparison with previous end compartment data.

V.4.2 Characteristics of the End Compartments

It is suspected in Section II.5 and shown in the above sections that the end compartments do behave differently from the internal compartment. It can be seen from Figures V.17-18 that the inlet and outlet compartments behave differently from each other. The inlet compartment shows coefficients which are constantly lower than the outlet compartment by about 10% over the Reynolds number range examined. The reason for this difference between two end compartments, which are geometrically the same, is that with respect to the fluid flow they are in fact different. The inlet compartment has the fluid entering from the nozzle and leaving from the outlet window zone, whereas the reverse situation is obtained in the outlet compartment. The different positions of flow entering and leaving affect the magnitude and direction of the flow. Thus resulting in different transfer coefficients.

The inlet compartment data for the 149.2 mm internal compartment baffle-spacing configuration are also plotted in Figure V.19. The data of both inlet compartments for the two different bundle configurations agreed to within the experimental accuracy and may be represented by a single curve. Therefore, the adjacent compartments had no effect on the inlet compartments. This same conclusion is echoed in Section V.3 and suggests that the down-stream compartments have negligible influence on the upstream compartment. (Note that the Reynolds number used

to represent to inlet data for both cases was based on the minimum free flow area of these compartments and not the internal compartments).

The tentative length-wise investigation as presented by Prowse (4), and set out in Figure II.3 showed a much larger variation between the end and internal compartments. The difference between the end compartments and the fifth compartment was of the order of 125%, with the latter showing inferior values. The differences observed by Prowse were much greater than those shown in this section.

V.4.3 Comparison with Previous Data

The data from this work are compared with the mass transfer data of Mackley (3), Prowse (4) and Williams (5).

End Compartments

The inlet and outlet compartmental data of Prowse (4) are compared with the end compartment data of this work In both cases the same experimental rig was used, and the baffle-spacing, baffle-cut, baffle-thickness, baffle-orientation, tube diameter, shell inside diameter, and port shape and size were all unchanged. The measuring technique was also the same in both cases.

All the available end compartment data, with Bergelin type ports and horizontal baffle-cut, are shown in Figure V.19. The difference between the inlet compartments of this work, represented by data from two

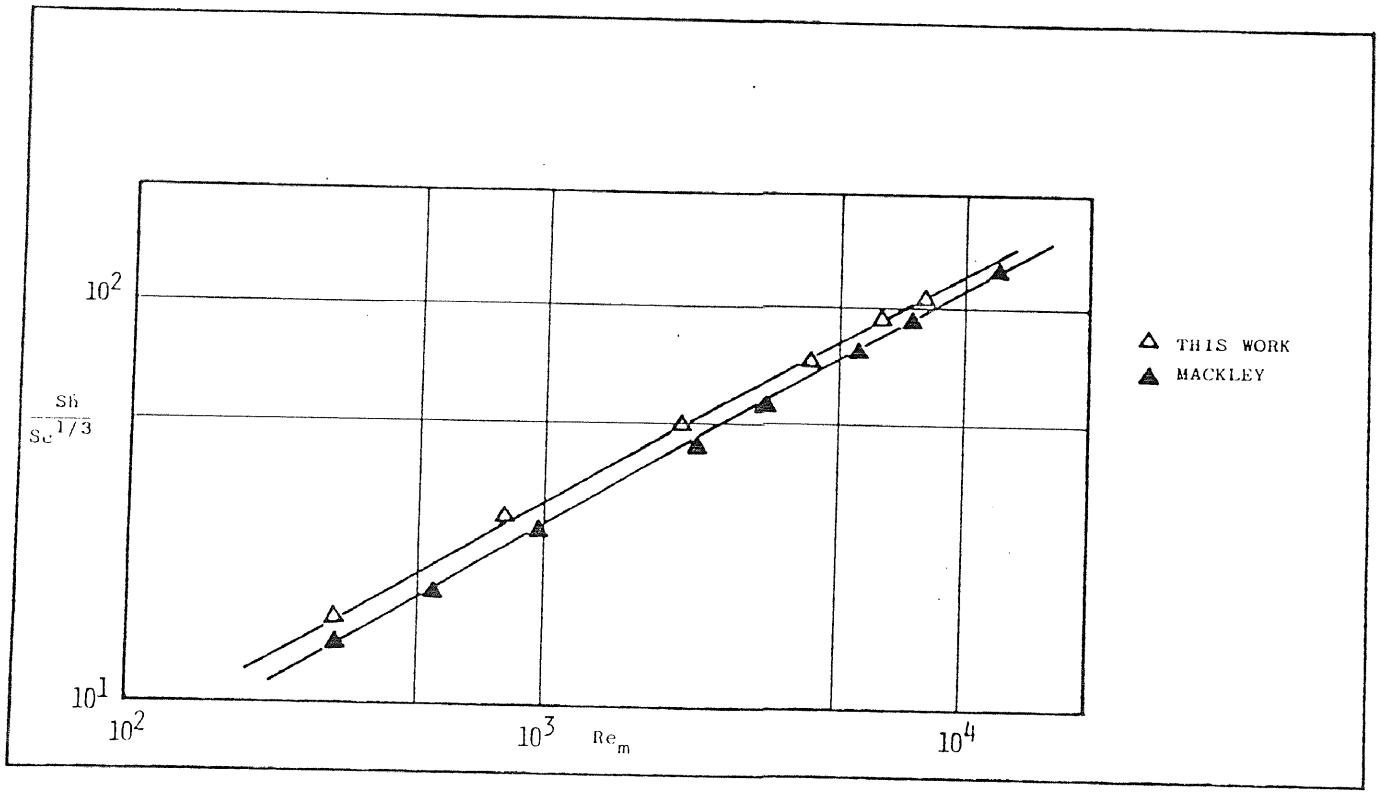

Figure V.20 Comparison with previous internal compartment data for nominal baffle-spacings of 50 mm.

configurations, and Prowse (4) was about 48%. This discrepancy was greater for the outlet compartments at about 59%. The data from this work were chosen as the base. For both cases the data obtained from this work were higher than those obtained by Prowse. These very large differences could not be explained by shell-to-baffle leakage which existed in the model of Prowse, or by any other physical means such as changes in fluid properties etc. Re-examination of Prowse's experimental procedure as set out in his Chapter V shows a serious misapplication of the activation procedure. The purpose of the activation process, (see Chapter IV.4.3), was to electrolytically clean the electrode surface and to remove the oxygen film by evolving hydrogen at its surface. Prowse however instead appeared to have evolved oxygen at the electrode surface, resulting in increasing further the thickness of the oxide film. Hence, this greater mass transfer resistance produced lower transfer coefficients. Therefore, the data of Prowse are probably in error.

Internal Compartments

The 18.4% baffle-cut compartment data of Mackley (3) are now compared with the corresponding data of this work. Since Mackley's data were for the fifth compartment from the inlet, the comparison is made for that compartment, as shown in Figure V.20. The difference between the data of Mackley and this work was 12%, with this work showing higher values. The combined error for both works ($\pm$ 8.6% for Mackley's data and $\pm$ 6.5% for this work) would

encompassed this difference, but an explanation was still considered to be necessary to explain this variation. The effect of local uncontrolled leakage could perhaps account for the variation, as this would reduce the effective mass transfer flow streams hence lowering transfer coefficients. The effects of shell-to-baffle leakage are discussed further in Section V.6. As was suggested in Section V.4.1 compartments three to six could all be represented by one curve, thus indicating the unlikelihood of compartment five having specifically high transfer coefficients. The low coefficients obtained by Mackley were also lower than for these internal compartments, thus suggesting that either Mackley's compartment exhibited local leakage or some other phenomena was causing this difference.

Mackley calibrated his variable area flow-meters with water as the flowing medium. In this work flowmeters were accurately calibrated with the electrolyte as the flowing medium. It is shown in Appendix A1 that the water calibration curve predicted flowrates which were 5% higher than those obtained from the eletrolyte calibration curve. Thus, this would add to Mackley's experimental error, increasing it to ±13.6%, and showing lower transfer coefficients.

A counter possibility could be that seeping of electrolyte into the inner surfaces of the multi-electrode, (see Section IV.3.3), could result in increasing the transfer coefficients. This however was unlikely to be

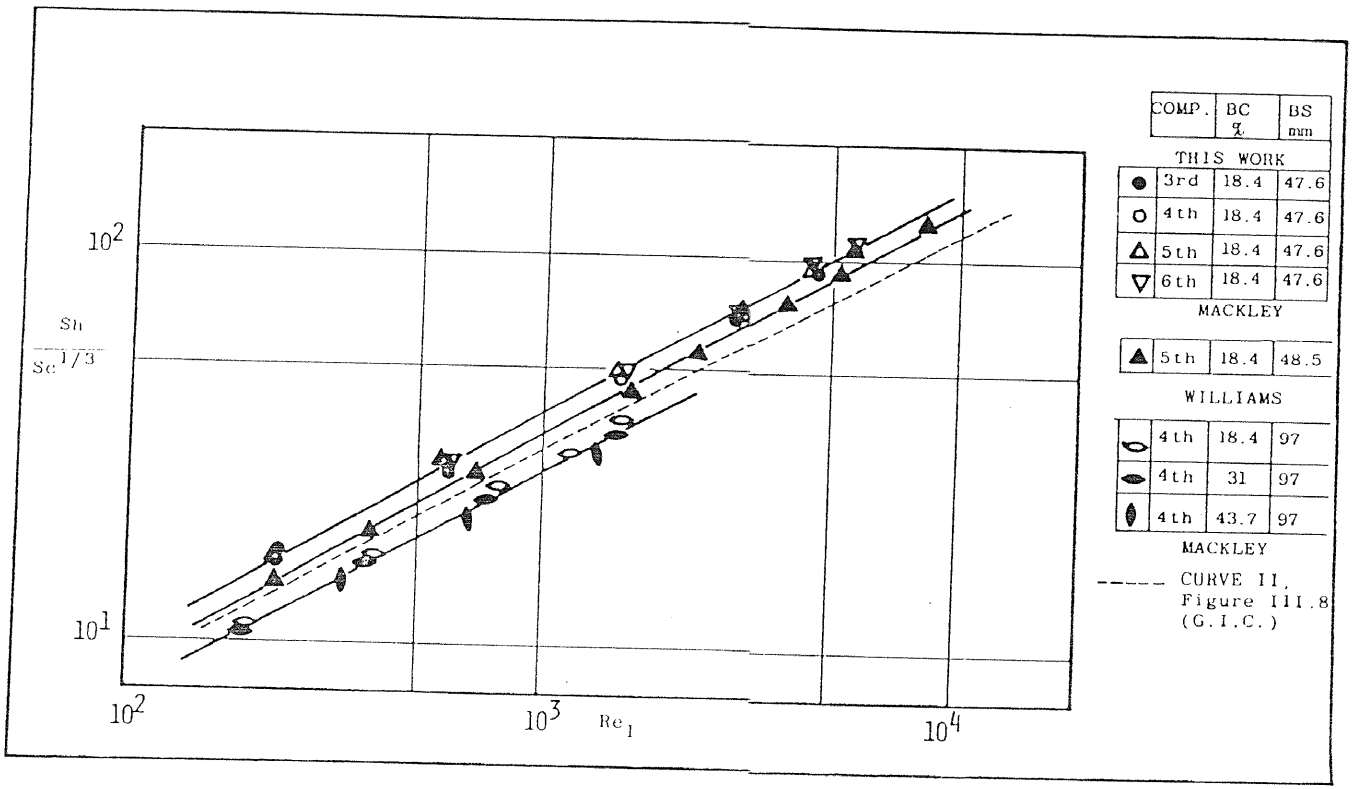

Figure V.21 Comparison with all the previous internal compartment data

significant as the relevant flow area and flow rate were small compared with the flow contacting the outer surface. Furthermore, these inside surface areas were coated with liquid Araldite.

The remaining baffle-cut and baffle-spacing configurations examined by Mackley and Williams are now compared by expressing the characteristic flow area by A_I. This comparison is shown in Figure V.21 together with other internal compartment data obtained in this work. The data of Williams throughout showed lower coefficients by 27%. This may be due to internal leakage and associated inaccuracies in Williams experiments. The data of Mackley correlated by the geometric independent correlation showed disagreement with the present work to be dependent on Reynolds numbers. The difference between the two curves was 14% and 27% at Reynolds number of 200 and 10^4. The geometrical independent correlation curve (G.I.C.) had lower gradient than the correlation curves for internal compartments with baffle-cut of 18.4% and baffle-spacing less than 50 mm. This difference in the gradients suggested that latter configurations had a greater alignment to crossflow phenomena than the former. Similar differences were also observed with the comparison of the overall bundle average data, see curve II in Figure III.9.

Large Baffle-Spacing Compartments

The effect of large baffle-spacing is demonstrated by the 149.2 mm long internal compartment shown in Figures V.22 and V.23. No other data were available for

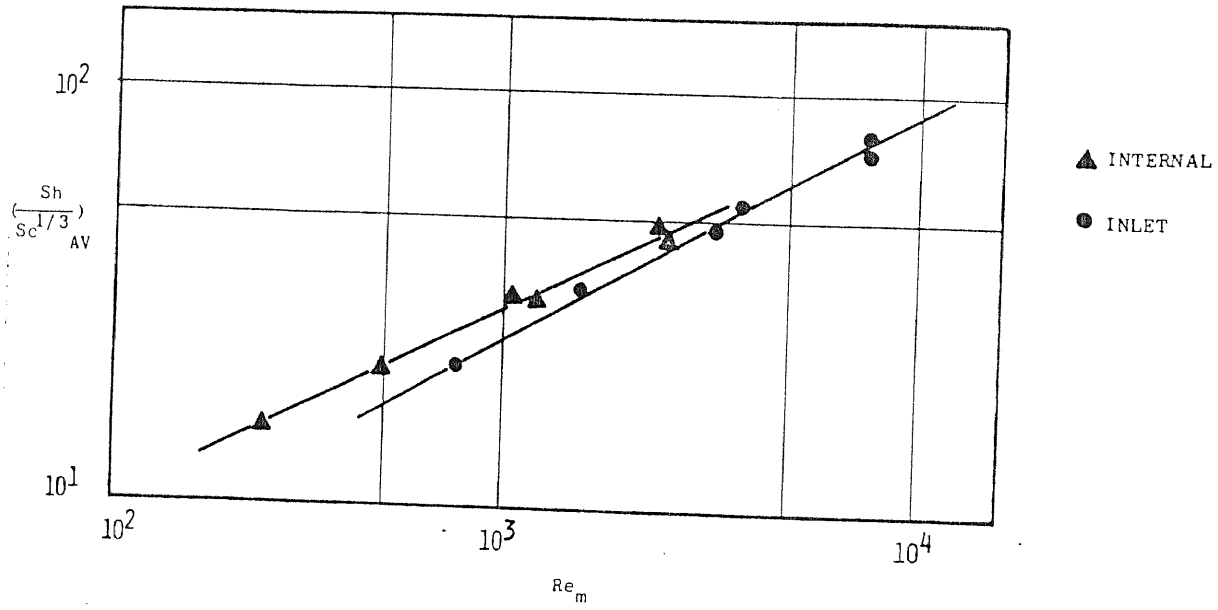

Figure V.22 Comparison of different size compartment in the same bundle

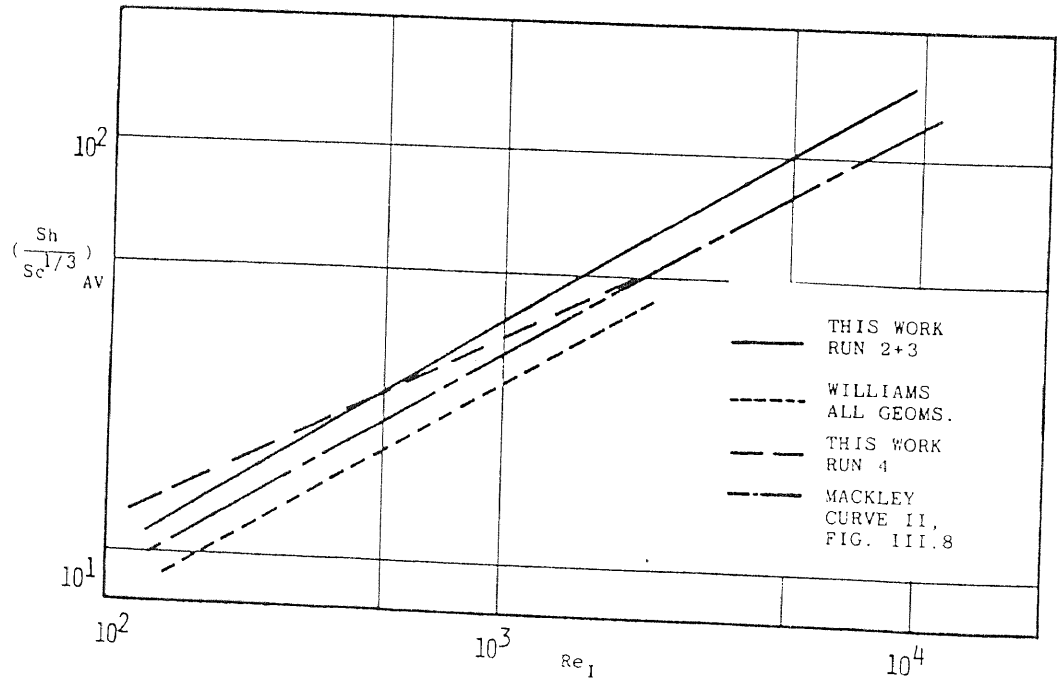

Figure V.23 Comparison of large baffle-spacing compartment with all the previous data

comparison at this baffle-spacing.

The surprising conclusion from Figure V.22 is that the 149.2 mm baffle-spacing compartment shows higher transfer coefficients than the 47.6 mm inlet compartment. The gradient of the former curve 0.48 is much smaller than the latter curve (0.56) suggesting that the large spacing compartment would become inferior at $Re_m > 10^4$. As the internal compartment data were only examined for Reynolds numbers less than 3000, the curve cannot be extrapolated much further beyond this Reynolds number.

The slope of this curve is also much smaller than the geometrical independent correlation of Mackley's and the 18.4 per cent baffle cut and 47.6 mm baffle-spacing internal compartment tested here. This is shown in Figure V.23. The large baffle-spacing configuration has a gradient of same magnitude as for the leakage cases.

The effect of parallel flow is further discussed in Chapter VI. It was stated in Section V.3.3 and V.4.2 that large internal compartment was only examined under laminar and transition flow. Therefore, the low gradient suggests a longitudinal flow over most parts of its surface.

V.5 Overall Bundle Average Characteristics

The pressure drop, heat and mass transfer data are now compared over the whole of the exchanger. The previously recorded data of Deleware University were

used in these comparisons.

No comparison had previously been made between the overall bundle average heat and mass transfer coefficient data, previous comparisons having been between the average transfer coefficients over a single compartment and overall bundle. In this work the overall transfer coefficients and pressure drops are determined for each Reynolds number examined. Hence the performance of the exchanger could be fully investigated.

V.5.1 Bundle Average Transfer Coefficient

As in the previous section the average transfer coefficient could be determined by simply averaging the transfer coefficients over segments or compartments. This is because of the constant mass transfer driving force existing at any point within the exchanger, as mentioned earlier in Section V.4. Therefore, the bundle average dimensionless mass transfer coefficients were determined by averaging the individual compartment values in the same proportion as the ratio of compartment length to the bundle length. These average transfer coefficient were then plotted against Reynolds number. The characteristic velocity incorporated in the Reynolds number was calculated by using the flow area A_I, as described in Section III.4.1. In order to compare mass transfer data with direct heat transfer data, it is necessary for the boundary conditions to be analogous, particularly the constant driving forces in both cases. The heat transfer coefficients were determined by using the logarithm Mean Temperature

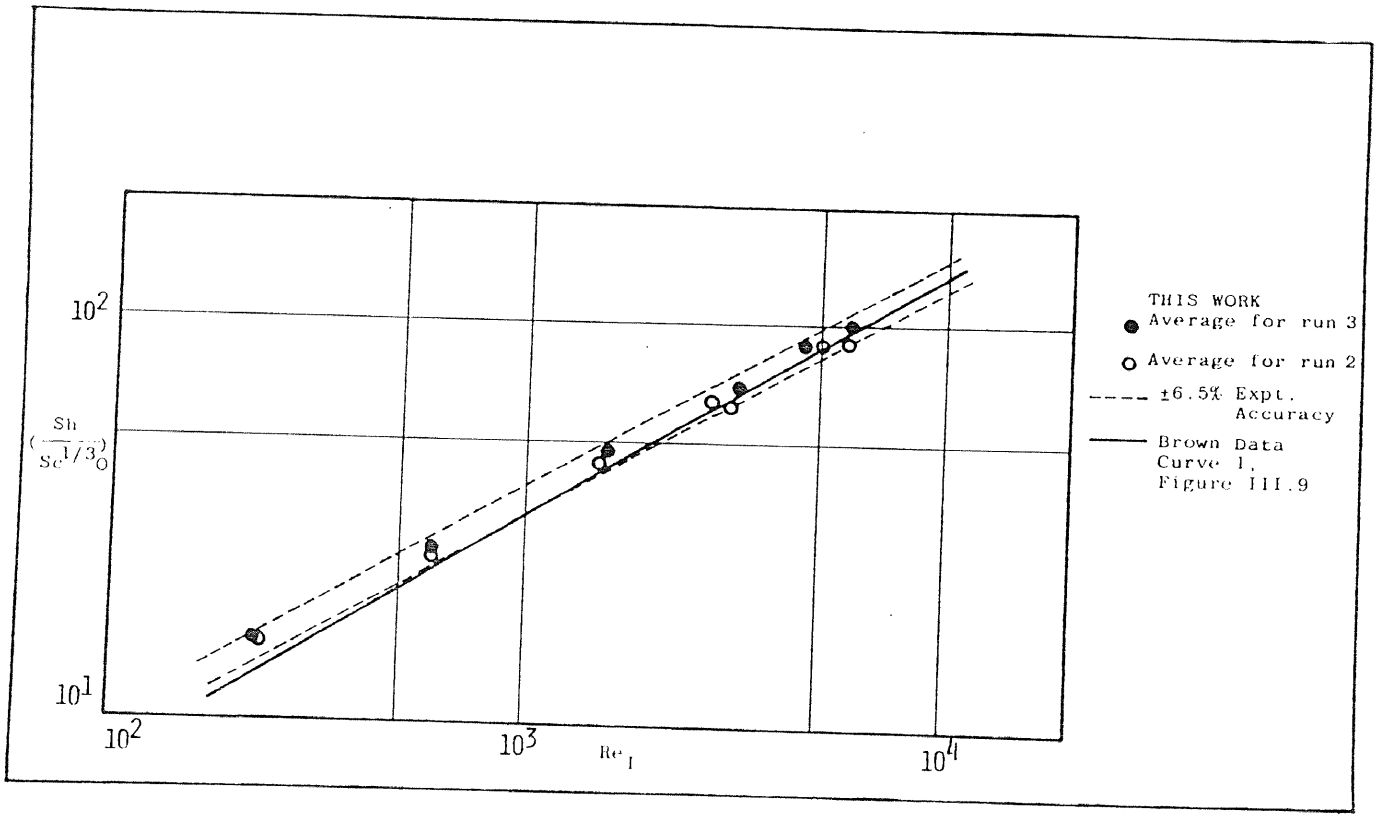

Figure V.24 Comparison of overall bundle average data with Deleware data for 18.4% baffle-cut and baffle-spacings less than 50 mm.

Difference (LMTD). Therefore, the heat transfer data could only be compared with the mass transfer data if the temperature changes for both streams were small. This would mean the (LMDT) and the arithmetic mean temperature, were almost comparable. In most of the heat transfer data these two temperatures were quite similar. This is discussed in greater detail in Section VI.5.1.

Uniform Baffle-Spacing Compartments

The data of Brown and the present study are displayed in Figure V.24 for configurations with 18.4% baffle cutdown and all baffle-spacings less than 50 mm. The two half-bundle average transfer coefficients for the present work were plotted and a mean line could be drawn through the points to indicate the overall bundle average values. Also shown is the experimental accuracy in this work. Figure V.24 reveals good agreement between the data of Brown and this work for Reynolds numbers above 800. However, below this Reynolds number the two data sets diverged with the present work showing higher coefficients. At a Reynolds number of 200, the difference between them was16%. The combined experimental error in the heat and mass transfer data would make this difference barely significant. In spite of this an explanation is needed especially since the agreementwas so good at higher Reynolds numbers. Mackley had also observed this when comparing his single compartment data against the bundle average coefficients of (23).

He attributed the discrepancy between heat and mass transfer data to many possible phenomena. These included, effects of comparing single compartment data with overall bundle data, suspected different flow characteristics in the end compartment, limitations of the heat and mass transfer analogy at low flow rate possibly due to natural correlation and uncontrolled leakage existing in the heat transfer data.

In this comparison of overall bundle average coefficients the first two effects had been considered, and the effect of leakage in Brown's bundles were discussed in Section V.5.2, thus leaving the influence of natural convection and the limitations of the analogy at low flow rates as possible explanations. Natural convection is produced in heat transfer by fluid motion brought about solely by differences of density created by temperature gradients. The analogous situation in mass transfer only exists where differences in density occur due to the concentration gradients, which is not the case in the present study. The analogy has been successfully applied at low Reynolds numbers and in free convection, to the electrchemical deposition of copper sulphate systems (67). Some workers (61) also employed the present electrochemical technique at low flow rates and achieved comparable results to the heat transfer data when using the Chilton-Colburn analogy. This was, however, for simple geometries such as Gauzes and Spheres.

For the heat and mass transfer analogies to apply, each system requires similar dynamic, geometric and kinematic conditions. At low Reynolds numbers the L.M.T.D.'s for Brown's data are different from the arithmetic average temperature, thus dynamic and kinematic conditions would be different for mass and heat transfer techniques. Therefore, the heat transfer data at low Reynolds number were influenced by both flow distribution and temperature distribution. Hence, the mass transfer and heat transfer data could not be compared at low Reynolds numbers.

Mixed Baffle-Spacing Compartments

The bundle average transfer coefficients are now examined for the configuration comprising of mixed baffle-spacing compartments. As the compartments were of different baffle-spacings (149.2 mm for the internal and 47.6 mm for the end compartments), they had different transfer coefficients and Reynolds numbers for the same flow rate. Therefore, a method was needed to enable calculation of the bundle average transfer coefficients. These methods are now developed.

The analytical method requires evaluation of overall bundle average transfer coefficient and Reynolds number from the compartmental values. As there is constant concentration driving force throughout the exchanger it is quite correct to aggregate the individual tube transfer coefficient and calculate the half-bundle mean value. The corresponding bundle average Reynolds number which

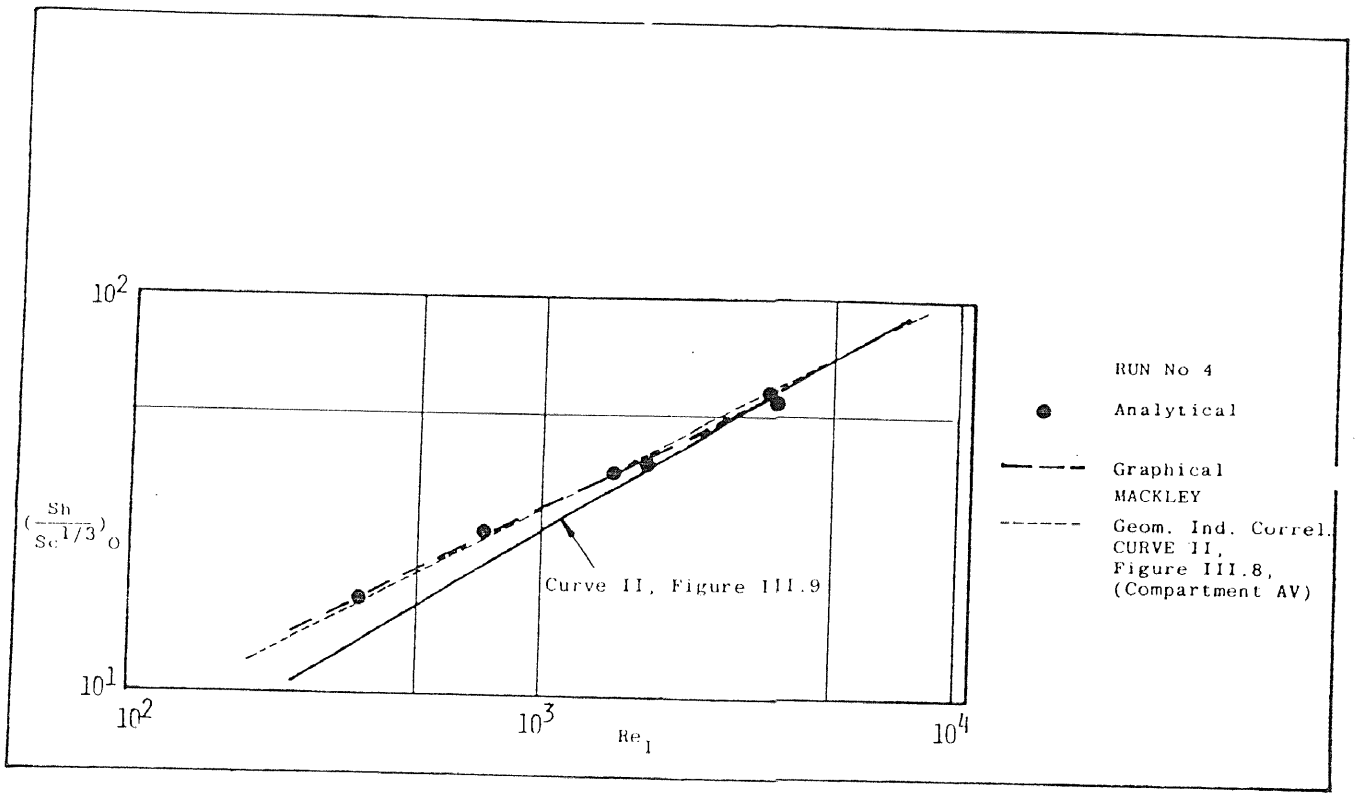

Figure V.25 Comparison of overall bundle average data for mixed compartment data and previous data of (23)

represents all compartments is then calculated from the weighted mean of the Reynolds numbers of individual compartments, this is further discussed in Section V.5.2.

The graphical procedure is now outlined. The end and internal compartment transfer coefficients are separately plotted against Reynolds number based on its compartment flow area, as depicted in Figure V.22. The average transfer coefficients for each compartment are then recorded from the curves at a single Reynolds number. The weighted average is evaluated by combining the compartment coefficients in the same proportion as the ratio of their sizes to the half-bundle length.

The half-bundle average transfer coefficients evaluated from both analytical and graphical methods are compared against the geometric independent curve of Brown (Curve II in Figure III.9). This is depicted in Figure V.25. The Reynolds number used in this case is based on the flow area A_I.

Both the analytical and the geographical methods produced similar coefficients. However, the analytical method is much easier to use and thus shall be utilised in later sections. The gradient of this curve (0.47) is smaller than for the Brown data. Also, at low Reynolds number the mass transfer data shows higher coefficients than the direct heat transfer data. The difference is however slightly higher for the mixed baffle-spacing configuration than the previous uniform spacing configuration,

shown in Figure V.24. For instance, at Reynolds number of 300 and 3000 the mixed baffle-spacing correlation showed transfer coefficients which were higher by 25% and 2% respectively compared with the data of Brown (23). At Reynolds number of 3500, the two curves were the same.

The difference could be due to comparing data at low Reynolds number. The large baffle spacing compartment has been shown to exhibit large variation in the distribution of flow and hence temperature gradient. Thus showing poor comparison between heat and mass transfer data. Also shown in Figure V.25 is Mackley's geometric independent correlation curve for compartment data. It can be seen that the agreement between this compartment average curve and the mixed baffle-spacing bundle average curve is good.

V.5.2 Overall Bundle Pressure Drop

Pressure drop measurements have been made for all the runs previously described. These are compared with the pressure drop data of Delaware University (23-25). The dimensionless pressure drop factor shall be expressed as:

$$F_p = \left(\frac{\Delta P}{L_s}\right) \frac{d^3 \rho}{\mu^2} \qquad (V.11)$$

where L_s represents the overall length of the exchanger. This parameter is plotted against Reynolds number based on flow area A_I. An advantage of this factor over other conventional friction factor is that F_p expressed in equation V.11 is independent of velocity.

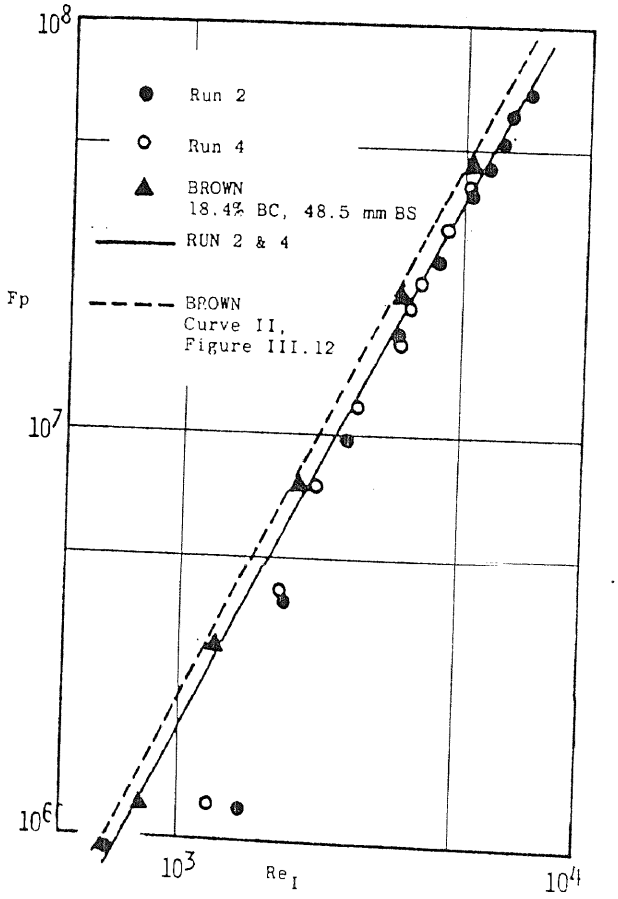

Figure V.26 Comparison of overall bundle pressure drop data with data of Brown (23)

Uniform Baffle-Spacing Compartments

The comparison of pressure drop data from similar configurations is shown in Figure V.26. It can be seen that the difference between the Brown data and this work is insignificantly small and a single curve could represent both sets of measurements. This difference is particularly good when considering the pressure drop techniques used were different. Mackley's explanation of low heat transfer coefficients existing in Brown's bundle being perhaps due to leakage is not supported. Figure V.26 also points to the usefulness of defining the pressure drop factor by equation V.11.

The only exceptions to this agreement are in the Reynolds number range of 10^3 to 2000. Two points in this range show uncharacteristically low values. No definite explanation could be found for this difference except that these points are erroneous. However, change of flow regime over the surface has been known to produce a sudden "dip" in the pressure drop versus Reynolds number curves (68). Additional data are required before this can be established.

These data are also compared with the geometrically independent correlation (curve 2 in Figure III.12) which represents three configurations. This is shown in Figure V.26. The maximum difference is 15% between the two curves with the present data showing lower values. However this difference should be within the combined experimental

error for the two correlations.

Mixed Baffle-Spacing Compartments

The configuration with mixed baffle-spacing compartments requires a particular Reynolds number which represents the overall pressure drop for such an exchanger. At same flow rate Reynolds numbers for the end compartment are higher than the 149.2 mm baffle-spacing internal compartments, by the inverse ratio of their lengths. Therefore, overall bundle weighted mean Reynolds numbers are determined by averaging the individual compartment Reynolds numbers throughout the exchanger length. This assumed that the ratio of the end compartment to internal compartment pressure drop is represented by the inverse ratio of their sizes.

These data are all shown in Figure V.26. It can be seen that the mixed spacing configuration surprisingly shows overall dimensionless pressure drop values in agreement with the configuration with the smaller spacings and thus greater number of compartments. Again, in agreement with the smaller baffle-spacing configuration data, the data from Run 4 shows low values of 'F_p' at low Reynolds number, thus indicating the presence of the 'dip' in the curve.

The 'dip' in the 149.2 mm baffle-spacing curve occurs in the Reynolds number range of 800 to 10^3. It is thought that perhaps the micromonometer used in this work

have improved the sensitivity of measuring pressure drop at low flow rates and hence detected the presence of this 'dip'. Similar equipment was not available to Brown (23) who used u-tube monometers which are known to be insensitive at low flow rate. This 'dip' is thought to show the change in flow regimes over the exchanger surface.

V.6 Influence of Shell-to-Baffle Leakage

In the previous sections of this chapter both tube-to-baffle and shell-to-baffle leakages have been prevented in the experiment discussed. However, numerous references have been made concerning their possible effects indicating their importance in any study of the shell-side transfer coefficients. In commercial exchangers leakages are necessary because of fibrication requirements and removal of bundle for cleaning purposes. The only reason for studying the no-leakage bundles was to understand fully the effects of baffle-cut and baffle-spacing, by making the flow distribution "simpler".

In this section exactly the same configiration was studied as in run numbers 2 and 3, but the shell-to-baffle seals were removed to give a clearance of 0.5 mm, thus making the flow distribution akin to that in the industrial exchangers. The reason for investigating only this leakage stream was to differentiate the effect from the combined leakage case. In Chapter III, it was shown that although

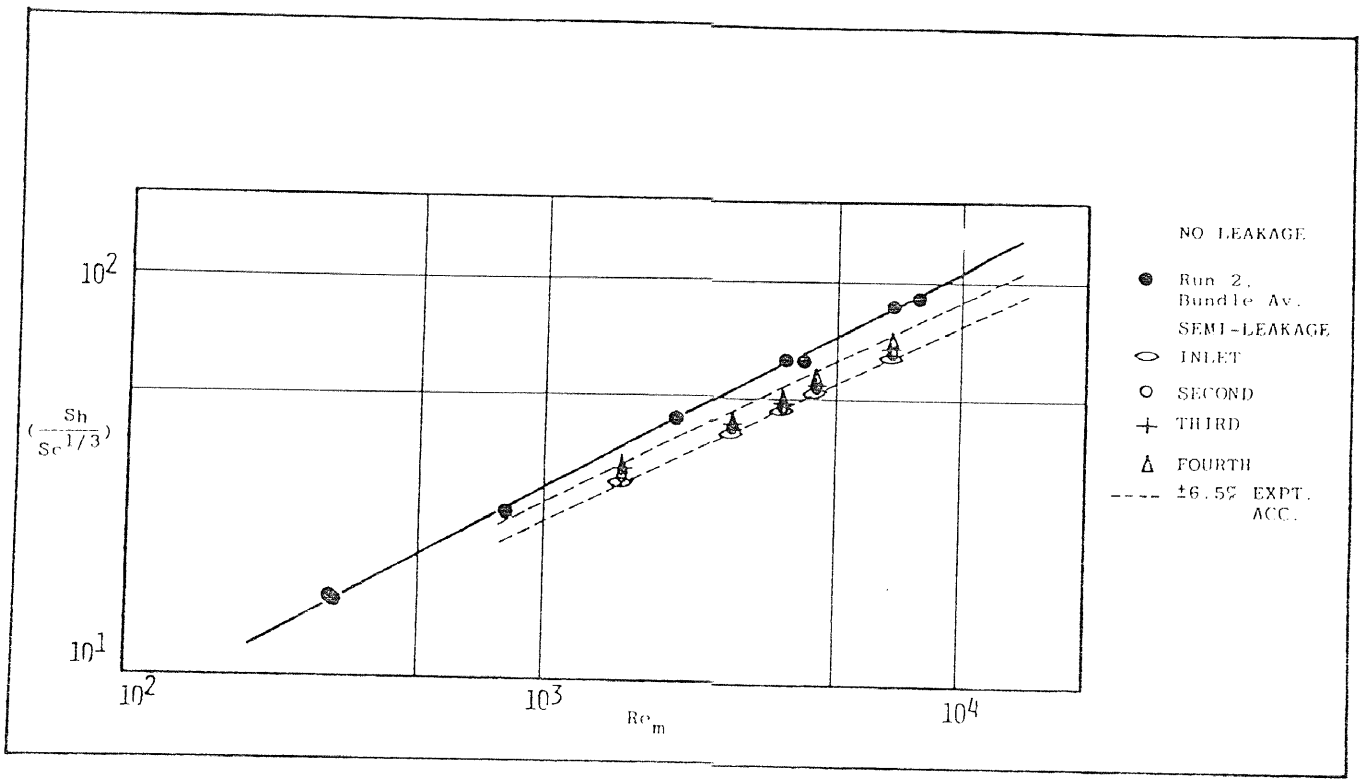

Figure V.27 Effect of shell-to-baffle leakage on length-wise variation of transfer coefficients

this stream contributed the least towards heat transfer, it is none the less the main stream reducing the pressure drop and heat transfer coefficient.

The dimensionless compartment average heat transfer coefficient for the leakage case are plotted against the Reynolds number based on flow area Am, as shown in Figure V.27. From this it can be conculded that, firstly leakage reduces the length-wise variation to within 10% for the first four compartments tested, secondly the coefficients are lower than in the no-leakage case and thirdly the gradient of the line (0.5) is lower than for the no-leakage cases.

It is shown in Figure V.20 that the compartments variation of transfer coefficients for the first four no-leakage compartments was 15 to 26% at Reynolds number of 500 and 10^4 respectively. With the introduction of shell-to-baffle leakage the length-wise variation was reduced by 16% at higher Reynolds numbers. It is suspected that this variation would reduce further with the introduction of tube-to-baffle leakage. One reason for the reduction of compartment variation with leakage could be that the increased longitudinal flow reduces the propagation of the end compartment effects through the exchanger.

In Figure V.27 the half bundle average for no-leakage and leakage configurations are both shown. The correlations differed by 10% to 22% at Reynolds numbers of 500 and 10^4 respectively, with leakage configuration showing lower

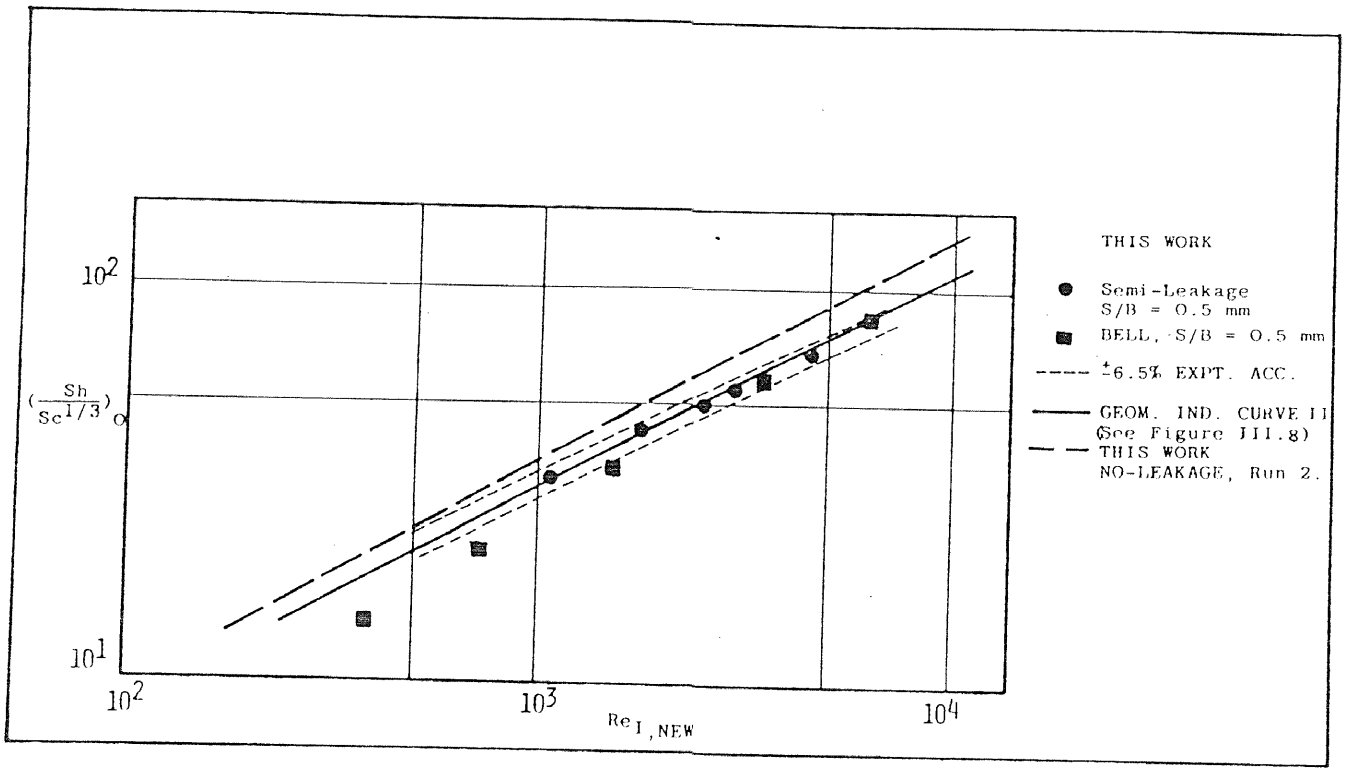

Figure V.28 Comparison of overall bundle average data for semi-leakage case with previous semi and total-leakage configurations

transfer coefficients. This was expected as part of the fluid would be 'lost' from the effective heat transfer streams (see Figure II.2) to the shell-to-baffle leakage stream. Also, the flow area used in the Reynolds number was no longer strictly applicable.

In equation (III.2) the leakage flow area was accounted for in the Reynolds number. This is used to modify the data shown in Figure V.28 together with the no-leakage data of this work, Bell's semi-leakage heat transfer data, and the no-leakage geometric independent correlation.

No significant improvement between the no-leakage and leakage correlations emerged when using the modified Reynolds number. The comparison of direct heat transfer data of Bell (37) (obtained from a configuration with shell-to-baffle clearance of 0.53 mm) with this leakage study, showed transfer coefficients in agreement for Reynolds numbers higher than 1500. Below this Reynolds number the two sets of data departed to the extent 22% at Re=500. This difference was suspected to be due to reasons outlined in Section V.5.1.

The comparison of the overall bundle no-leakage geometrically independent correlation and the shell-to-baffle leakage data of this work shows good agreement over all the Reynolds number range examined. Thus, by defining the flow area by equation III.2 the shell-to-baffle leakage is well accounted for by the no-leakage geometric independent correlation.

V.7 Conclusions

The following conclusions are made for the no-leakage tube bundle arrangements discussed in this chapter:

i) The repeatability of the experimental data is shown to be within the experimental accuracy of ± 6.5%.

ii) Comparison of individual tube transfer coefficient data against Mackleys data shows agreement to within ±10%, suggesting similar flow distributions. It is also shown that a greater proportion of flow penetrates the bundle as the flow rate increases. However, the distribution patterns of individual tubes obtained by Mackley and Williams are much more complete compared with the twenty tubes investigated in this study. This number was further reduced when some cathodes malfunctioned.

iii) Length-wise variation is shown to exist both within the compartment and between adjacent compartments of the bundle.

iv) A tentative model is outlined which discriminates between the different flow characteristic within a compartment. This showed the inlet compartment to possess different flow behaviour to the remaining compartments. This model also shows a large variation in the distribution of flow for large baffle-spacing compartments.

v) Examination of compartment average coefficients shows:

a) Inlet compartment with marginally higher transfer coefficients than the outlet compartment, less than 10%. This is explained by the acceleration and declaration of the fluid at different positions.

b) Comparison of the inlet and outlet compartments data with corresponding data of Prowse showed inferior transfer coefficients for the latter by 48% and 58% repectively.

c) The difference between Mackley's fifth compartment data and this work is about 12% and reduces at higher Reynolds number, with Mackley's data showing inferior values.

d) The length-wise variation between end and internal compartments is shown to depend on flow rate, and the difference increases from 12% at Re_m=500 to 26% at Rem=10^4.

vi) The overall bundle pressure drops and average transfer coefficients are compared with Deleware University data. These show:

a) good agreement for the transfer coefficient data when the Reynolds number is above 800. At lower Reynolds numbers the difference increases and this is explained by the unanalogous boundary conditions. The existence of temperature distribution becoming important at lower Reynolds number is limiting the analogy.

b) Comparison of pressure drop data also shows good agreement to within 5% of Deleware University data.

c) The 47.6 mm and 97 mm compartment data shows similar pressure drops.

vii) Some limited study is made for a configuration with shell-to-baffle leakage clearances. This shows;

a) the length-wise variation reduced by 10%, and

b) lower transfer coefficients obtained than for the no-leakage case.

CHAPTER VI

VI Shell-Side Investigation in Leakage Bundles

VI.1 Scope of Experimental Work

The baffles used here had clearances between the baffle holes and the tubes and between the baffle periphery and the shell-wall. The tube-to-baffle and shell-to-baffle diametrical clearances were 0.5 mm and 2.2 mm respectively.

The thickness of the baffle was the same as for the no-leakage case and equal to 3.18 mm. The inside diameter of the shell and the diameter of the baffle for all leakage runs were 134 mm and 131.8 mm respectively. The corresponding orifice shape factors for the tube-to-baffle and shell-to-baffle clearances were defined by:

$$Z = 2.\frac{\text{baffle plate thickness}}{\text{diametrical clearance}} \qquad \text{(VI.1)}$$

were equal to 12.72 and 2.89 respectively.

The tubes were allowed to settle on the bottom of the baffle hole and similarly for the baffles in the shell. The resultant eccentric baffle clearance are

typical of those used in commercial exchangers.

The leakage investigations were confined to a baffle-cut of 18.4% and, baffle-spacings of 47.6 mm, 66.6 mm, 97 mm and 149.2 mm. Mass transfer studies were made over the whole of the bundle with the shell-side flow weaving up and down and with side-to-side movement. As symmetry does not exist across the axis (3) for the latter case, the whole of the compartment was studied. This was easily achieved by rotating the bundle through 180 degrees. For up and down movement only one half of the compartments was studied, as symmetry exists across the vertical axis.

Overall pressure drops were also measured for all the configurations examined.

These investigations were carried out for electrolyte flow rates in the range of 2 to 127 ℓ/m.

VI.2 Repeatability of Experimental Data

The repeatability of experimental data was demonstrated by comparing two experimental runs performed at different times but with similar compartment geometry and flow rates. The average transfer coefficients for 50 mm nominal baffle-spacing end compartments in the form of $(Sh/Sc^{1/3})$ against Reynolds numbers are shown in Figure VI.14. The difference was within the experimental accuracy of ± 6.5%. Further demonstrations of the repeatability of the data are shown later in this section

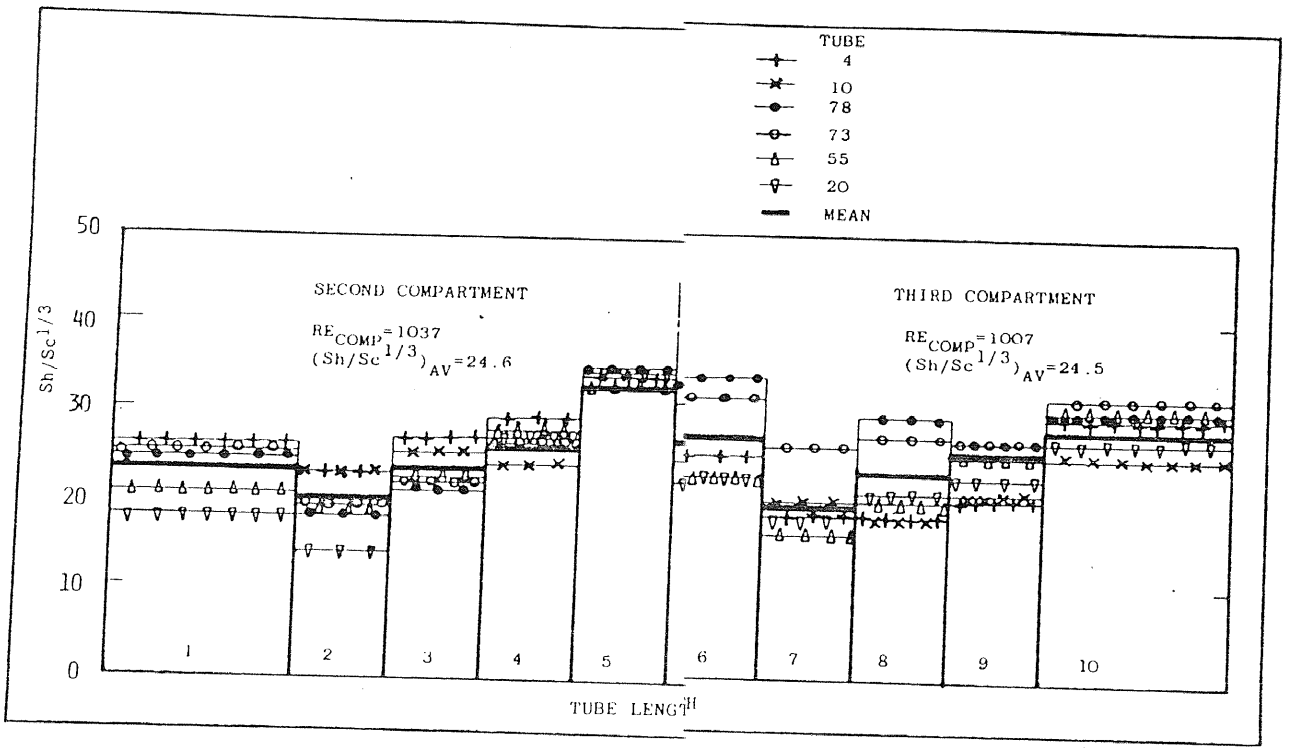

Figure VI.1 Variation of transfer coefficients along the compartment length

with close agreement obtained when comparing compartment data of similar geometry, hence demonstrating the consistency of data when using the electrochemical technique.

VI.3 Individual Tube Coefficients

Individual tube coefficients were studied to provide insight into local flow behaviour within the baffle compartment. These data were compared with previous leakage and no-leakage data. The no-leakage data are reported in Chapter V.

VI.3.1 Variation of Transfer Coefficient in the Compartments with Leakage

The average transfer coefficients over each element electrode within the compartment were used to show the existence of length-wise variation along the tube in the no-leakage case. The data from the 149.2 mm baffle-spacing configuration were used to demonstrate this effect. A similar study is now carried out for the leakage data.

A number of selected tubes[†] from all sections of the above compartment were chosen to show the individual electrode value, as depicted in Figure VI.1 at a constant flow rate. This figure also shows the average values for each element section over compartments two and three.

[†] Tube numbering diagram is shown inside back cover.

All the examined tubes showed similar length-wise behaviour, displaying higher transfer coefficients near the baffles and lower transfer coefficients away from the baffles. The comparable no-leakage investigation shows in Figure V.1 the extremely low transfer coefficient values in lee of the first baffle, but these increase quickly towards the downstream central baffle.

With the introduction of leakage, segments in lee of the first and second baffles (numbered 1 and 6 in Figure VI.1) both showed higher transfer coefficients than the mean value. This agreed with the findings of (45), (46) and (47), as explained in Section II.4.2. However, the remaining segments, 2 to 5 and 7 to 10 in Figure VI.1, all showed similar behaviour to the no-leakage case. That is, the transfer coefficients increased towards the downstream end of the compartment. This increase in the second and third compartments was of the order of 40% and 33% respectively. Thus, leakage had considerably reduced the length-wise variation.

The transfer coefficients for segments immediately upstream of the baffle (such as segments 5 and 10) showed higher values compared to segments immediately downstream of the baffle, such as segments 1 and 6. This could be explained by acceleration and deceleration upstream and downstream of the baffle respectively.

This study suggests that leakage reduces the length-wise variation along the exchanger length, although the local geometrical effects are not completely removed,

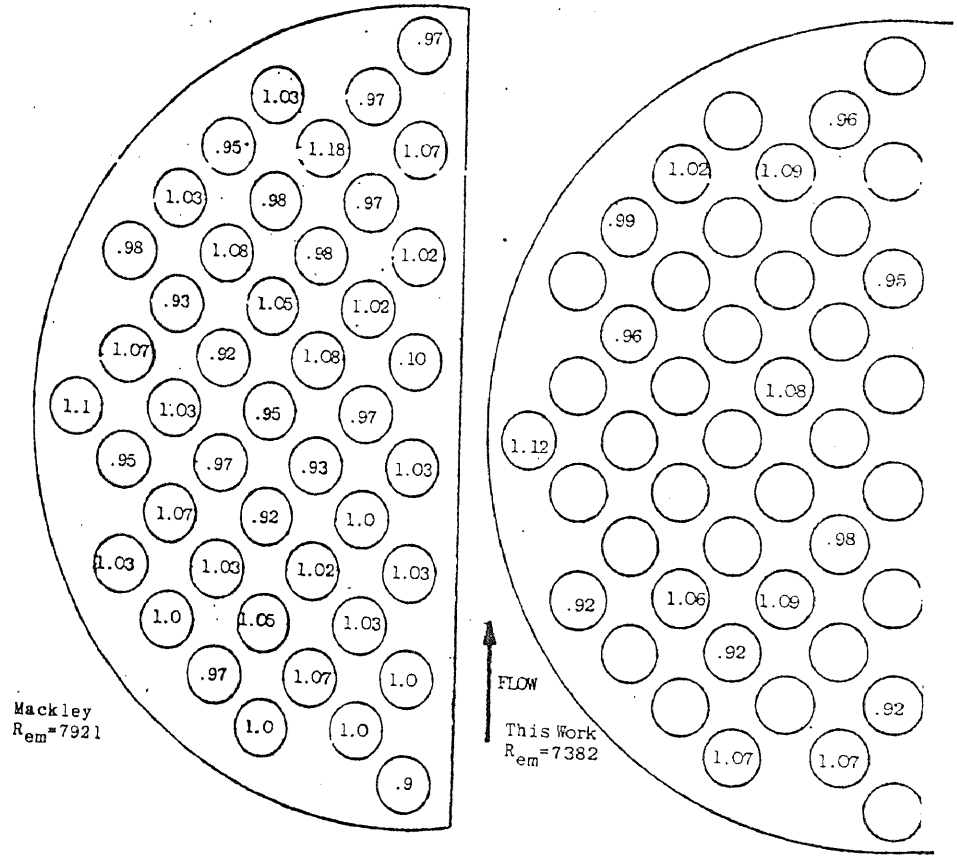

Figure VI.2 Distribution patterns. Comparison with Mackley Data.

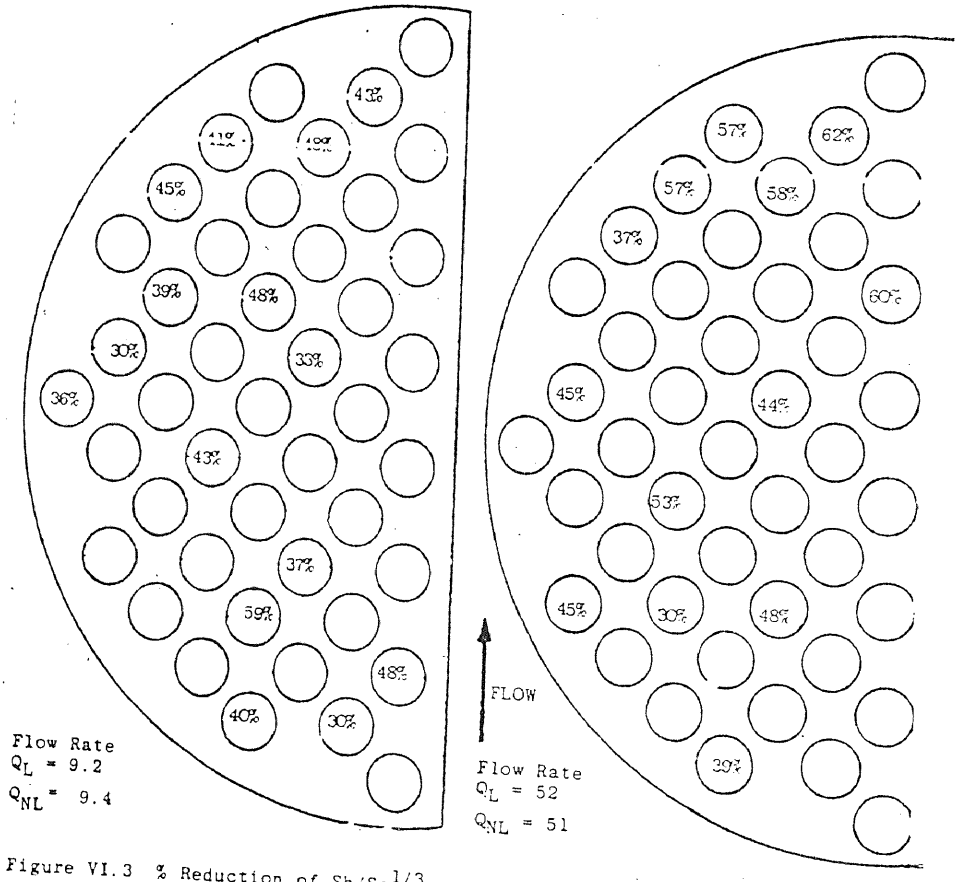

Figure VI.3 % Reduction of $Sh/Sc^{1/3}$ caused by leakage.

as the presence of baffle are clearly evident.

VI.3.2 Distribution of Transfer Coefficients

Comparison with Previous Leakage Data

The leakage data of Mackley and this work are compared in Figure VI.2. The agreement between the two data sets was within ± 10% inspite of the leakage clearances being different. The spread of data was also within ± 10%. Hence, suggesting that the flow distribution was even for the leakage case in comparison to the no-leakage case. This was also observed by (3).

Effect of Leakage

The effects of leakage are demonstrated in Figure VI.3, which shows for two flow rates, the percentage difference in the individual tube transfer coefficient values between leakage and no-leakage data. Figure VI.3 shows lower individual tube transfer coefficients with leakage at both Reynolds numbers. Furthermore, the difference between the leakage and no-leakage cases increased as the flow rate was increased. Similar observations were made by Mackley (3). This effect could be explained by two reasons; firstly, increased longitudinal flow in the leakage case distorts the no-leakage distribution patterns and, secondly, the overall flow area increases from the no-leakage case due to the presence of leakage clearances thus lowering the overall compartment average fluid velocity. These points are further studied in the following section (VI.4).

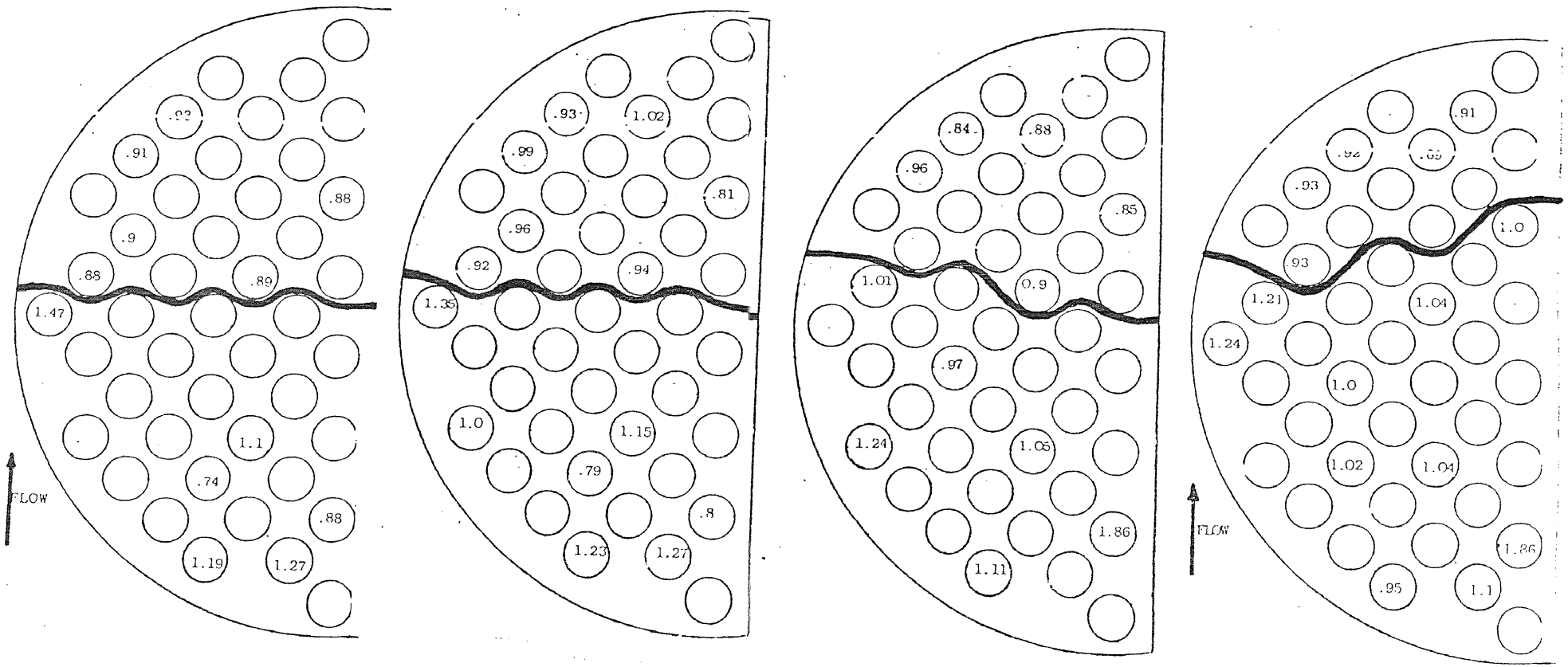

	NL	L
Flow Rate (l/m)	95	88.5

	NL	L
Flow Rate (l/m)	7.3	88.5

	NL	L
Flow Rate (l/m)	51	52
$Sh/Sc^{1/3}$ /av	73	33

	NL	L
Flow Rate (l/m)	9.4	9.2
$Sh/Sc^{1/3}$ /av	28.1	15.58

Figure VI.4 Distribution diagram showing ratio of leakage and no-leakage normalised values

Comparison of 47.6 mm Leakage and No-Leakage Data

The distribution of transfer coefficients for the no-leakage cases were represented by a normalised value within each compartment in Section V.3.2.

The present leakage data are compared with previous leakage and no-leakage data in this form.

The ratio of normalised values for the 47.6 mm baffle-spacing configuration are used to study the effects of leakage. This is shown in Figure VI.4 for four different flow rates. It can be seen in this Figure that the outlet window region and approximately the outlet half of the baffle overlap region shows lower values than the inlet half of the compartment. Furthermore, as the flow rate is increased, the lower value region also increases and encompasses approxiamtely half the compartment. This suggests leakage streams induce higher transfer coefficients relative to the compartment average in the inlet half of the compartment than for the corresponding no-leakage case. Thus, indicating the useful contribtion of the tube-to-baffle leakage stream by increasing the fluid velocity around the tube-to-baffle clearance it reduces the eddy zones near the baffle. However, the fluid lost from the main flow stream through the leakage clearances in the inlet half of the compartment results in lowering the transfer coefficients in the outlet half of the compartment.

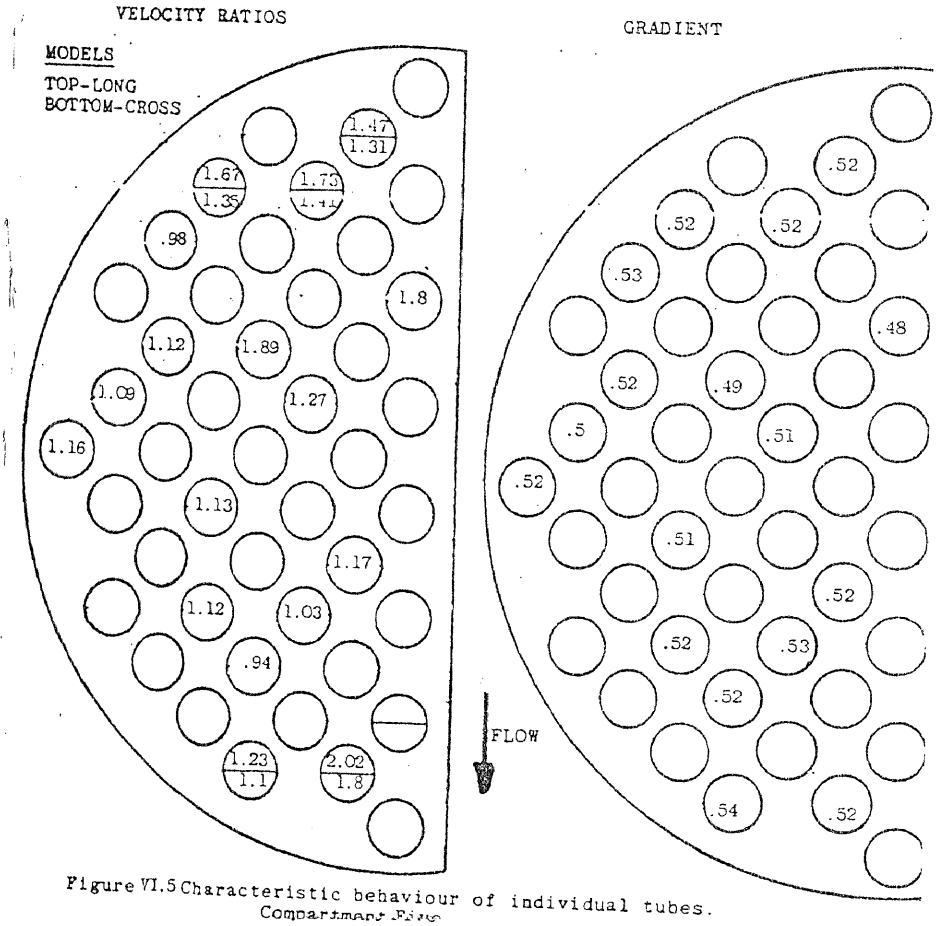

Figure VI.5 Characteristic behaviour of individual tubes.
Compartment Five

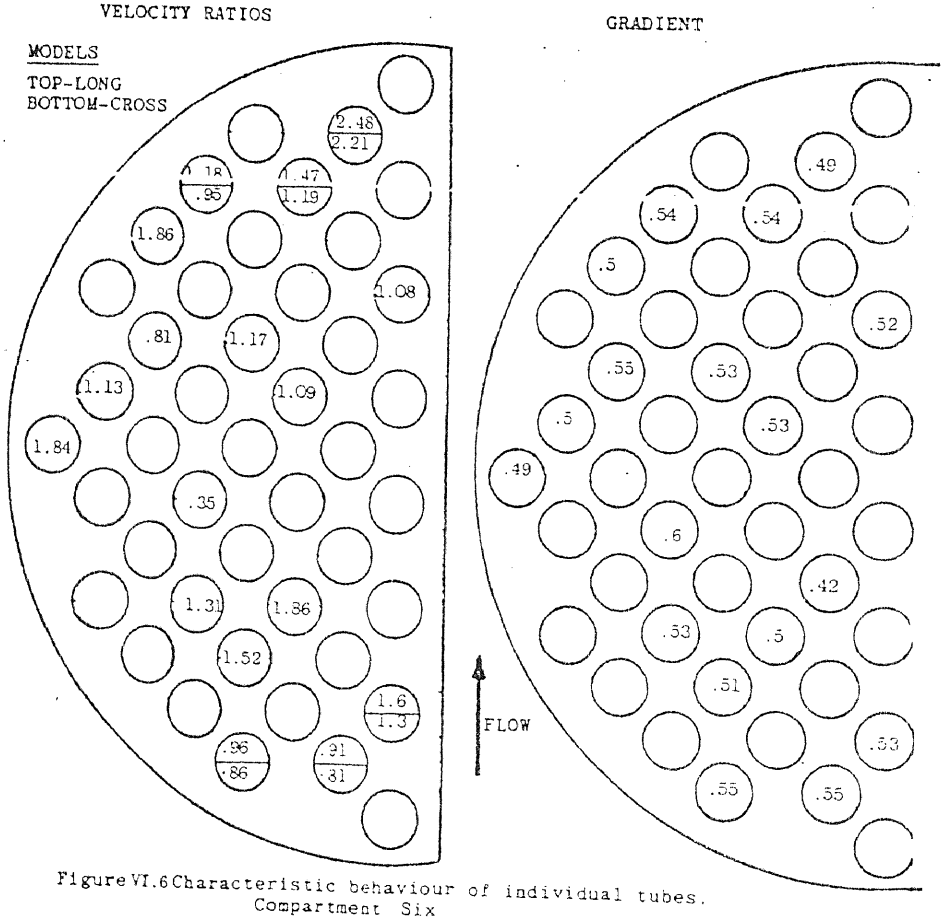

Figure VI.6 Characteristic behaviour of individual tubes.
Compartment Six

As the flow rate increased, the effect of leakage was shown to become more pronounced. This may be explained by a greater proportion of total flow being lost to the shell-to-baffle leakage stream and increasing longitudinal flow adversely effecting the distribution patterns in the leakage case, thus lowering the transfer coefficients further.

The distribution patterns were unable to show the flow character of individual tubes, thus the two possibilities above cannot be investigated further using this approach. The study of individual tube characteristics may provide further insight into the flow behaviour.

VI.3.3 Characteristic Behaviour of Individual Tubes

The characteristic behaviour of individual tubes was outlined in Section V.3.3 by fitting equation V.1 through each individual electrode element. A similar procedure was used to treat the leakage data to give the exponent and equation coefficient of equation V.1. The velocity used in the Reynolds number did not account for the leakage streams and was based on the flow area, A_m, as used for the no-leakage data.

Characterisation of Exponent Values

The exponent values for the 47.6 mm baffle-spacing configuration are diagrammatically shown in Figures VI.5 to VI.8 from the fifth to the outlet compartments. During

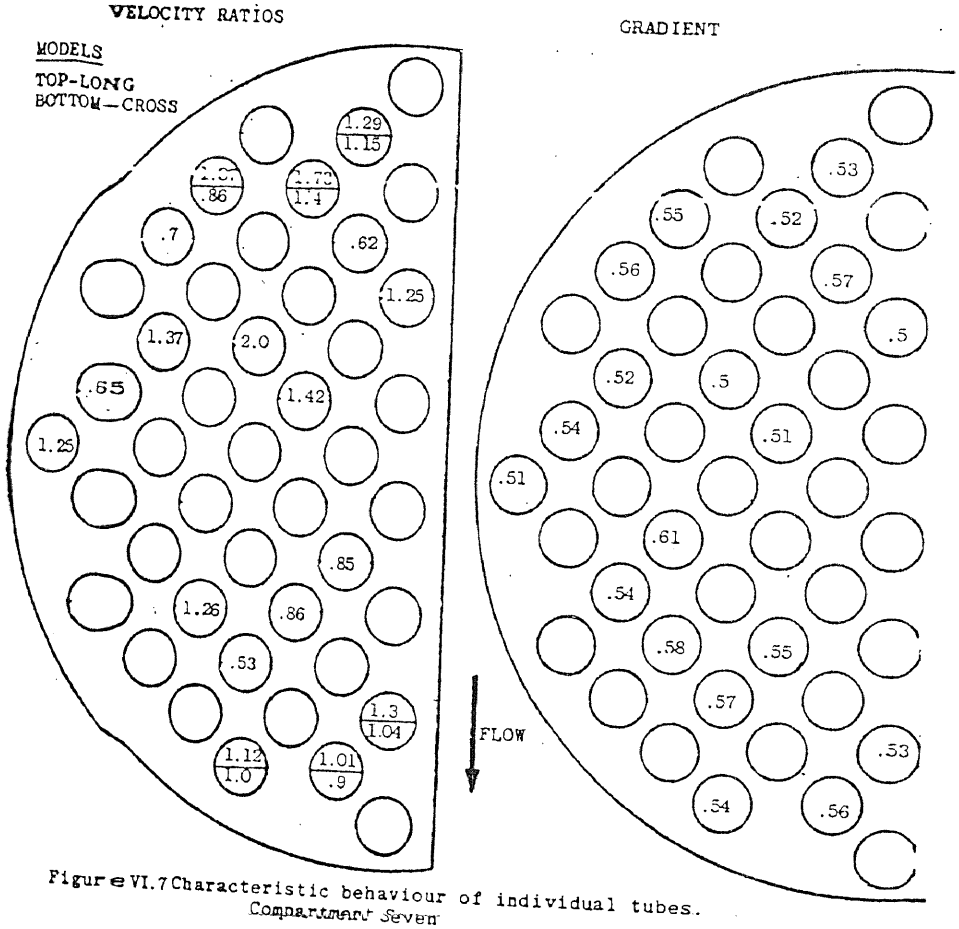

Figure VI.7 Characteristic behaviour of individual tubes.
Compartment Seven

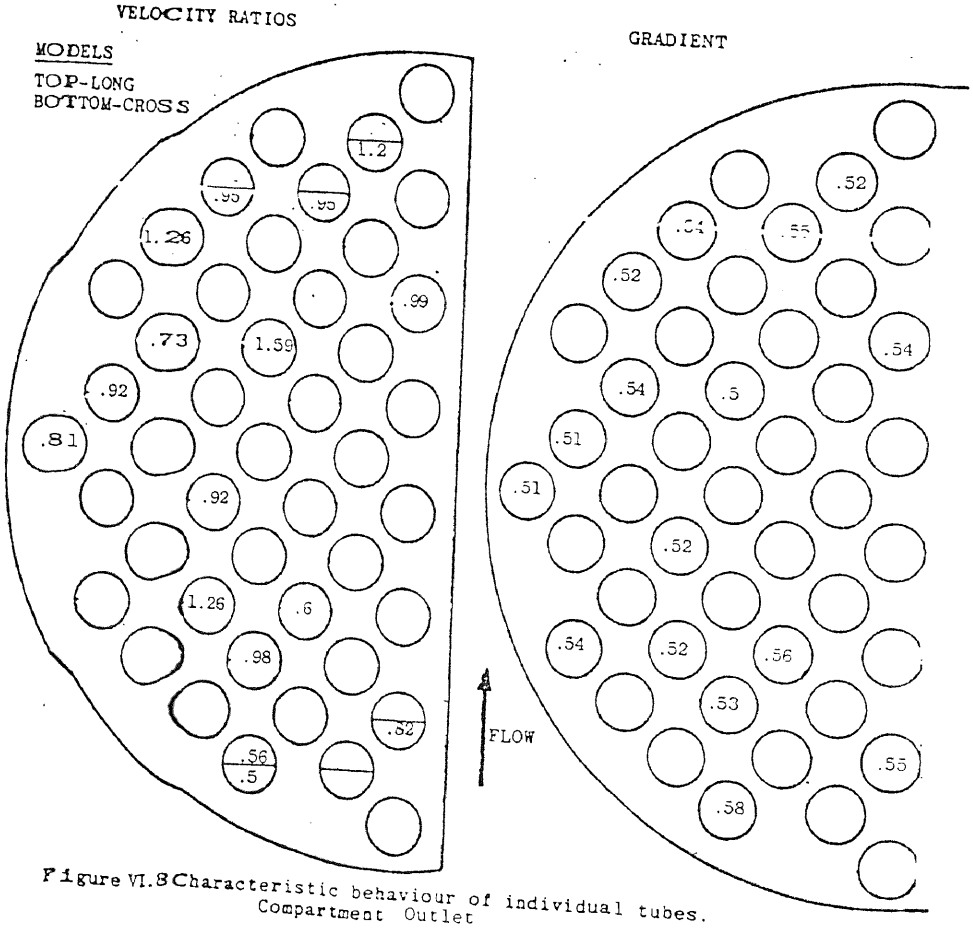

Figure VI.8 Characteristic behaviour of individual tubes.
Compartment Outlet

this experimental study the two 25.4 mm long electrode elements in compartments five and six were electrically connected together, thus each electrode was 50.4 mm long.

Examination of Figures VI.5 to VI.8 showed agreement for the average compartment exponent values of the four compartments to be within 5% of each other. Furthermore there was no obvious trend in the variation of the compartment average exponent values along the bundle. This is unlike the no-leakage study which showed compartment average exponent values falling from the internal compartments to the end compartments. This is further discussed in Section VI.4.1.

Examination of individual tubes in the above figures showed the majority of the tubes exhibiting exponent values between 0.49 and 0.55. Also, with a few exceptions, the variation of individual tube exponent values was small at ± 7% from the average compartment value. There were again no regions within a compartment which possessed distinctive exponent values. A similar conclusion was obtained for the no-leakage case.

A further effect of leakage can be seen by comparing the leakage and no-leakage data in Figures VI.5 to VI.8 and V.5 to V.12 respectively. It is found that the compartment average leakage exponent values are always lower than the corresponding no-leakage compartment values. This is further discussed in Section VI.4. The individual leakage values also shows less scatter than the

no-leakage values. Thus, leakage reduces the variation in the exponent values between individual tubes and also the overall compartment value.

However, examination of all the exponent values was unable to distinguish between crossflow and longitudinal-flow regimes. The reasons were similar to the no-leakage case outlined in Section V.3.3. Hence the type of flow existing within the various regions of the compartment could not be established.

Characterisation by Flow Magnitude

The coefficient values (a) for each electrode expressed by equation V.1 were used in Section V.3.3 to characterise the fluid flow patterns existing within the baffle compartment. These equation coefficients were expressed as the ratio of local velocity to either baffle tip crossflow velocity or window-flow velocity, and described by equations V.7 and V.8 respectively. These equations account for changing velocity from tube row to row and the arbitrary velocity V_m which was used to correlate the data in equation V.1.

During the development of these models it was also assumed that the exponents in equation V.1 were approximately equal to 0.5. Previously in this section it was shown that the leakage cases exponent values were lower than the no-leakage case and closer to 0.5. Thus, the above assumption is more valid for the leakage case than for the no-leakage case.

The crossflow and longitudinal window-flow velocity ratios, as described by equations V.7 and V.8 are also shown in Figures VI.5 to VI.8. Unlike the no-leakage study where different regions were outlined by contours of high and low velocity ratio values, the presence of leakage produced no such characteristic flow regions. All the compartments studies with leakage showed similar unsuccessful outcome using both Ulsamar's crossflow or Pohlhausen's (8) longitudinal-flow models. However, these velocity ratio values were reasonably well distributed about unity, hence suggesting that the models were better applicable for the leakage case than for the no-leakage case.

The leakage flow distribution diagrams showed the baffle overlap region as having similar flow distribution to the window zones. Whereas the no-leakage flow distribution diagrams showed part of the baffle overlap region having lower velocity ratio values than the window zones. This suggested that leakage caused fluid to penetrate equally into the bundle.

The compartment average velocity ratio values for the no-leakage case were approximately twice as high as those for the leakage configuration. This may be explained by two possibilities; firstly, the theoretical models may be better applicable to the leakage case as the exponent values were closer to 0.5 and, secondly the exclusion of leakage flow area from the model would artificially lower the ratio values by about 10%. Comparison of leakage and no-leakage individual tube values in the window zones

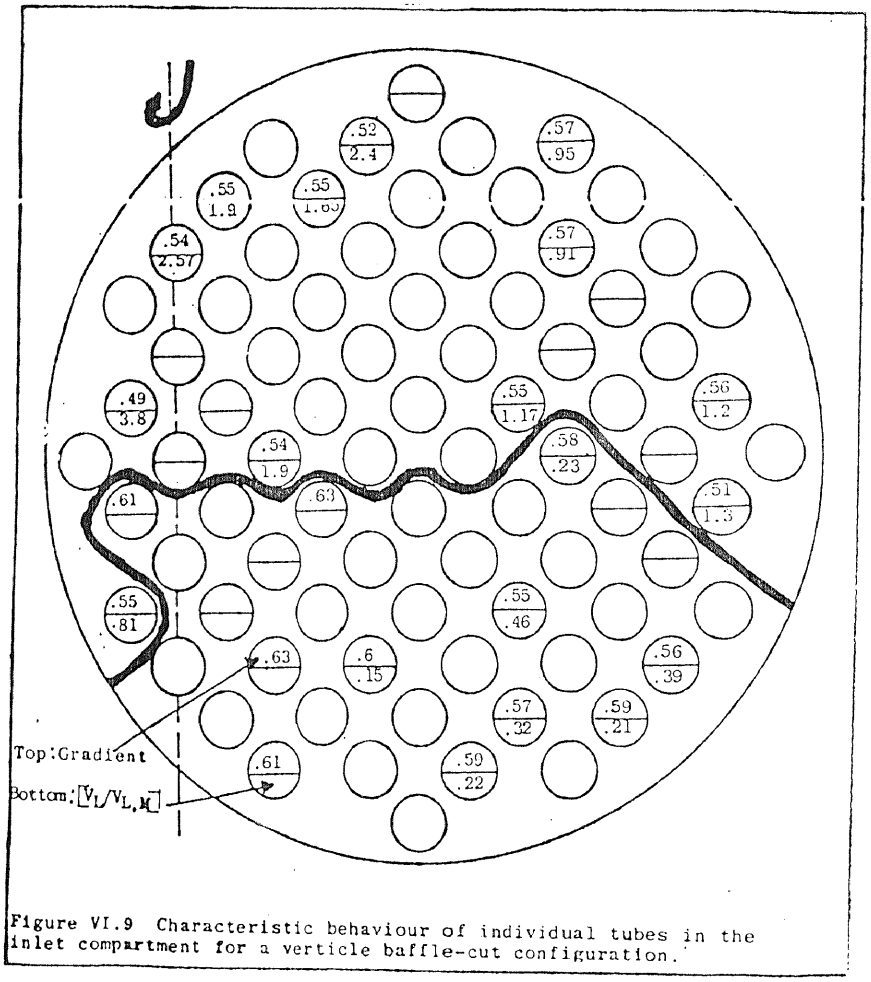

Figure VI.9 Characteristic behaviour of individual tubes in the inlet compartment for a verticle baffle-cut configuration.

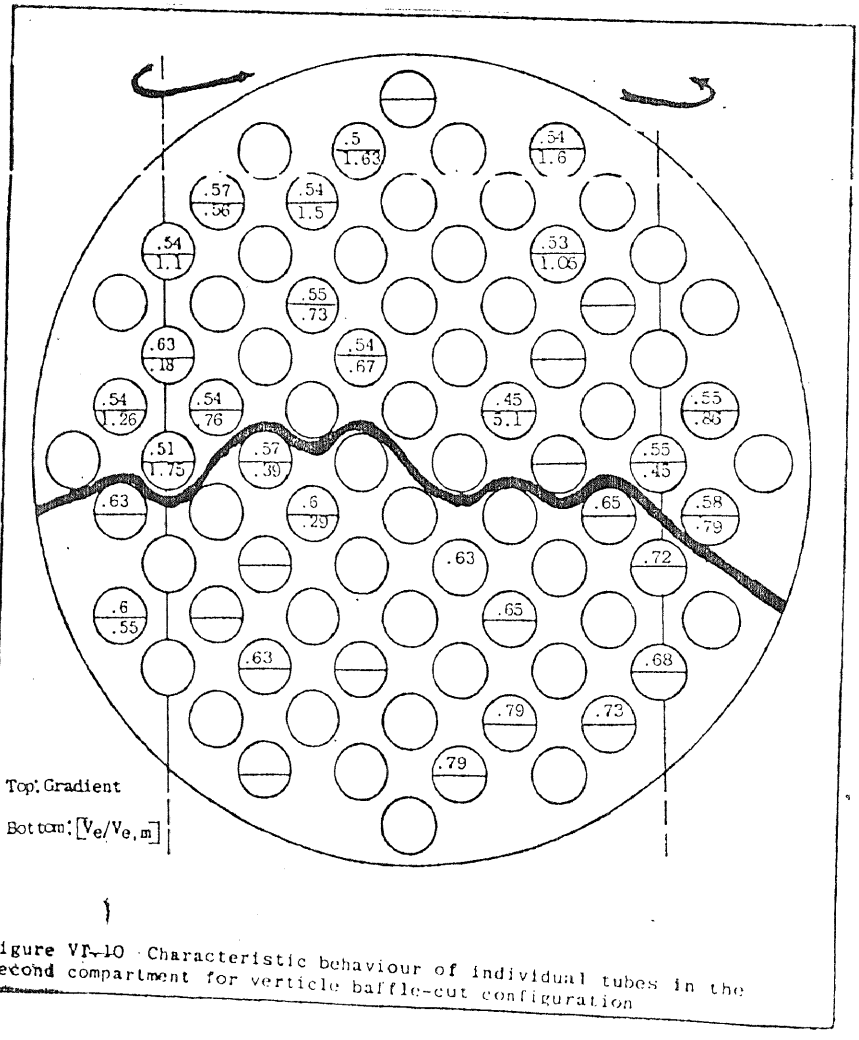

Figure VI-10 Characteristic behaviour of individual tubes in the second compartment for verticle baffle-cut configuration

also showed lower value for the former. However, the comparison of the leakage data with the no-leakage data in the baffle overlap regions, which exhibits lower velocity ration terms, showed similar magnitudes. This again indicates the effects of the leakage streams to produce uniform distributions, as the low velocity ratio region in the no-leakage case spread throughout the whole of the compartment with leakage.

There were no regions within any compartment which possessed distinct velocity ratio values consistently throughout the bundles. Although, it can be seen that the bottom window zone consistently showed lower velocity ratio values than the window zone at the top of the bundle. This may be explained by the excentric shell-to-baffle clearance due to the bundle resting at the bottom of the shell wall.

VI.3.4 Flow Behaviour for Verticle Baffle-Cut Configuration

The exponent and velocity ratio values for a configuration with verticle baffle cut were determined. Similar analysis as in the previous section were applied to obtain the flow distribution patterns. These patterns are shown in Figure VI.9 to VI.13.

Comparison of these Figures showed similar flow behaviour existing in all the compartments. As in the no-leakage compartments regions of high and low velocity ratios were outlined. But, unlike the no-leakage case,

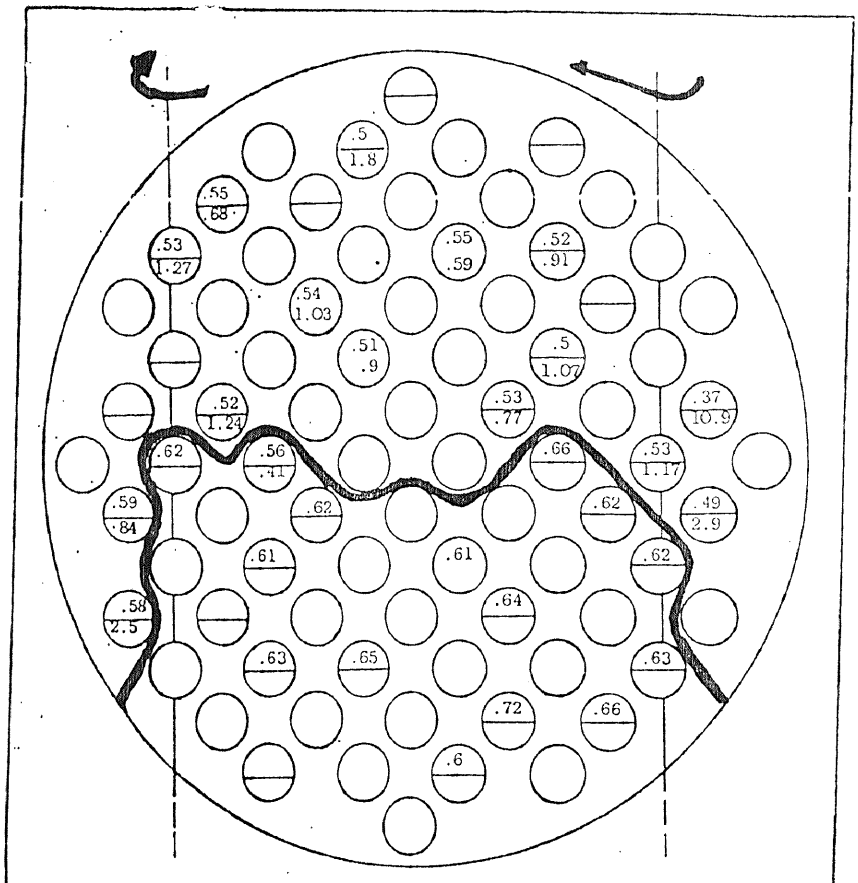

Figure VI.11 Characteristic behaviour of individual tubes in the third compartment for verticle baffle-cut configuration.

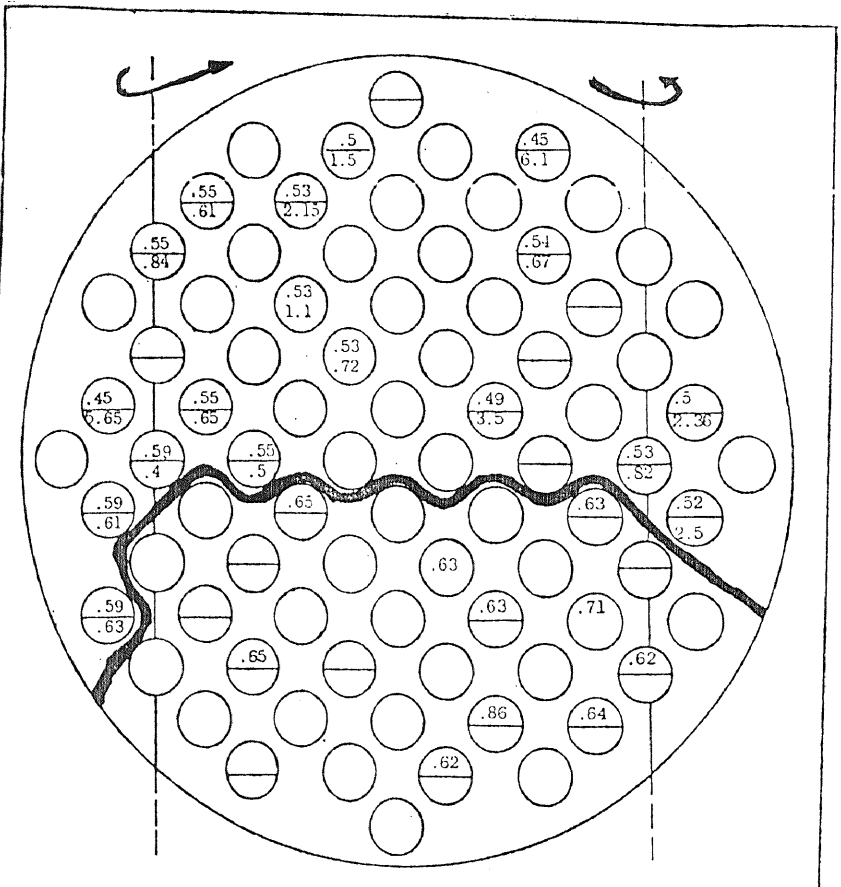

Figure VI.12 Characteristic behaviour of individual tubes in the fourth compartment for verticle baffle-cut configuration.

the exponent values for the leakage configuration with verticle baffle-cut were also able to distinguish flow behaviour within each compartment. Further, these regions were in agreement with those determined by examination of the velocity ratio values.

In the low velocity ratio region, which occurred at the bottom of every compartment, the exponent values on average were much higher than those in the high velocity ratio region, which occupied the window zones and remaining top part of each compartment. The percentage difference between average exponent values in these two regions was approximately 21%, and is the same for all three compartments. The same difference for the two end compartments was approximately 10%.

The exponent and velocity ratio values in the high region were similar to those in the no-leakage case. However, the values in the low region were much different with the exponent values being between 0.58 and 0.8 and velocity ratio values lower than 0.5. The velocity ratio model is only valid when the exponent value is around 0.5, (see Section V.3). Therefore, for some tubes in the low region the velocity ratio ($U_{\ell}/U_{\ell M}$) could not be determined. These very high exponent values suggest longitudinal or eddy flow existing in this region.

The existence of high and low regions indicates greater proportion of flow passing through the top part of the compartment and by-passing some tubes in the

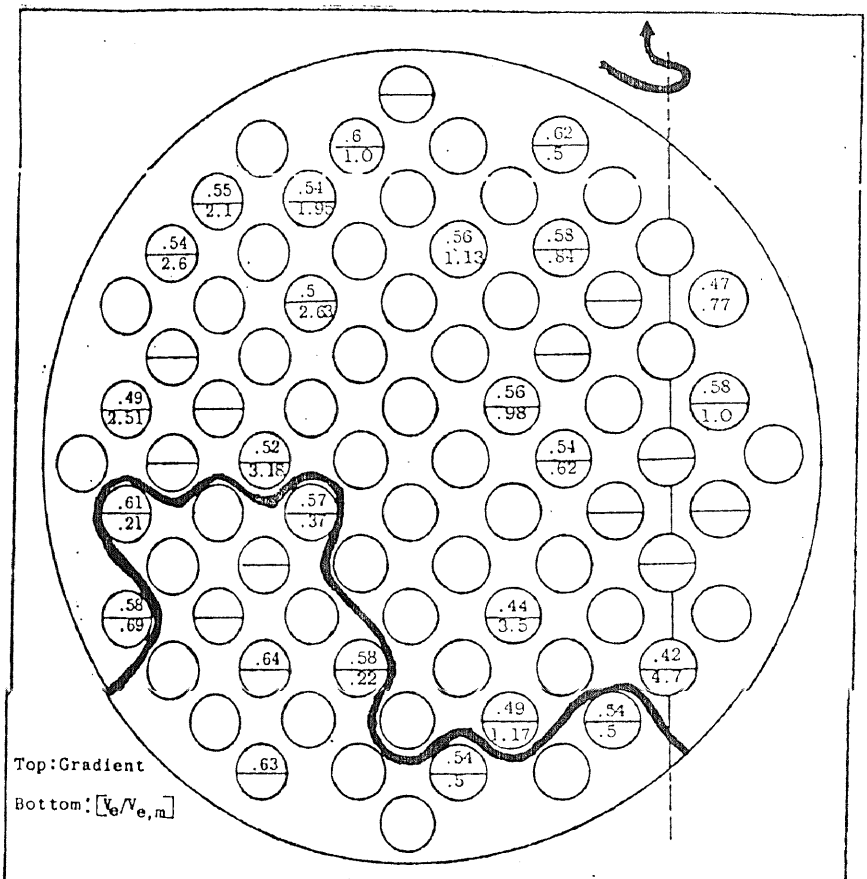

Figure VI.13 Characteristic behaviour of individual tubes in the outlet compartment for verticle baffle-cut configuration.

bottom of the compartment. The existence of these regions, inspite of the presence of leakage, suggests an uneven distribution of flow behaviour compared to the leakage case with horizontal baffle-cut. Prowse also observed this when analysing his data in the form of distribution of transfer coefficients.

VI.4 Compartment Average Coefficients

Similar to the no-leakage and semi-leakage cases reported in the last chapter, the overall compartment average transfer coefficients were determined for the leakage cases from the individual tube values. The average values were then compared with the previous leakage and no-leakage compartment data. The compartment coefficients showed the effects of tube-to-baffle and shell-to-baffle clearances on the length-wise variation of the transfer coefficient and effects of baffle-spacing. Also, an attempt to correlate the averaged coefficients from different compartment configurations was made.

VI.4.1 Length-Wise Variation of Transfer Coefficient

The variation of the transfer coefficient along the length of a bundle comprised of uniform baffle-spacing compartments were discussed earlier in Section V.4.1. Also, in Section V.3.1 the variation of the transfer coefficient along the tube but within the compartment was demonstrated. The above geometries had baffle-spacing of 47.6 mm and 149.2 mm respectively, and with

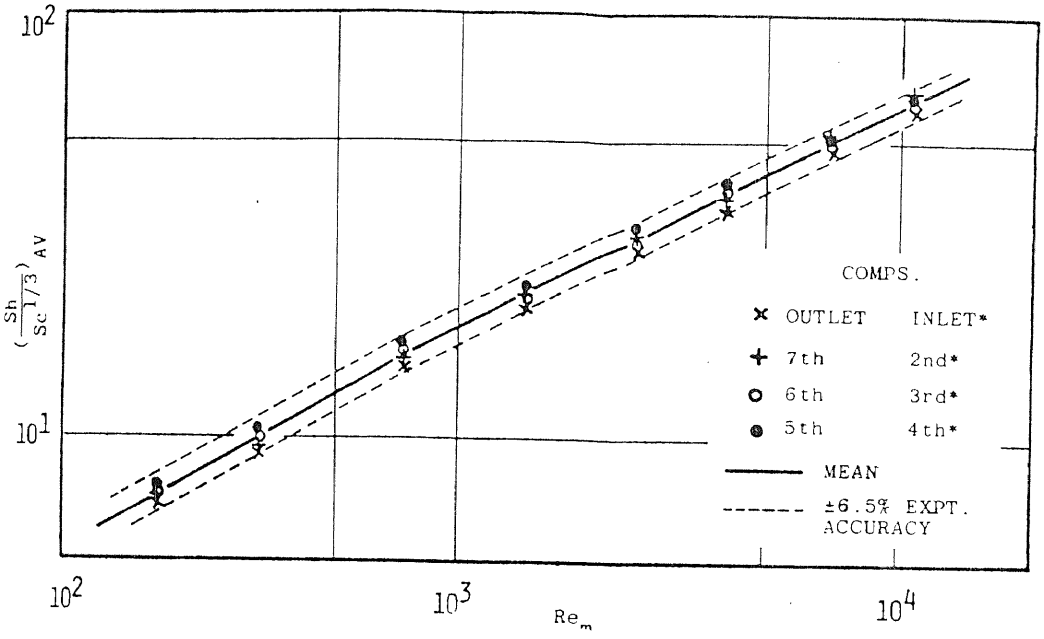

Figure VI.14 Effect of leakage on length-wise variation along the exchanger length - for Run no. 6

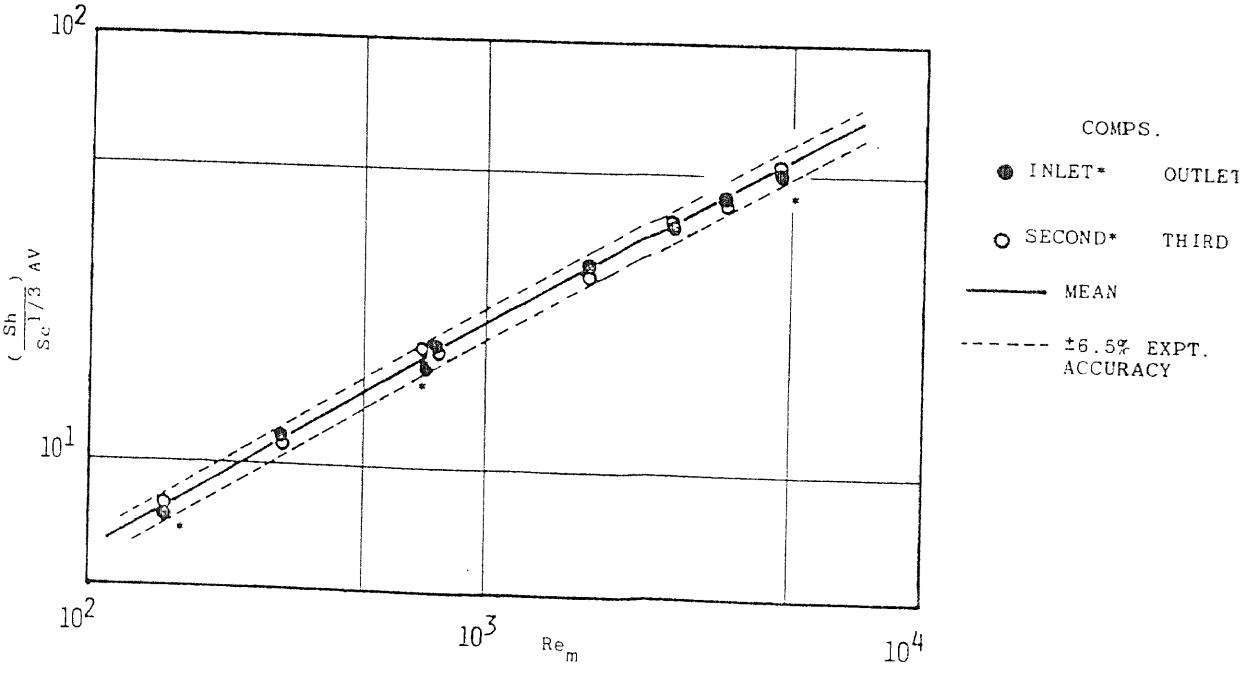

Figure VI.15 Effect of leakage on length-wise variation along the exchanger length for Run no. 8

leakage streams eliminated. However, in Section V.6 it was shown that the introduction of shell-to-baffle leakage reduced such a variation.

In this section leakage clearances were introduced to simulate commercial exchangers. The data for compartments with uniform baffle-spacing of 47.6 mm and 97 mm are shown in Figures VI.14 and VI.15 respectively. The variation of the transfer coefficient along the bundle length in the 47.6 mm baffle-spacing configuration is shown in Figure VI.14 to be within the experimental accuracy of ± 6.5%. A similar conclusion is also demonstrated in Figure VI.15 for the 97 mm baffle-spacing configuration. There was also little variation in the transfer coefficients for compartments in either the inlet and the outlet halves of the bundles. This is particularly evident from the overall bundle investigations at one flow rate; such as, at 88.5 L/M and 18 ℓ/m for 47.6 mm and 97 mm baffle-spacing configurations respectively. The former case is exemplified in the form of a histogram in Figure VI.16. Also shown in this figure is the experimental error at each elemental electrode. For this particular flow rate the length-wise variation of the transfer coefficent along the overall bundle length was within the experimental accuracy. In a similar comparison made for the no-leakage case the maximum difference was between -22% and +14% from the bundle average value (see Figure V.16).

Unlike the no-leakage case where the length-wise variation of transfer coefficient increased in this effect with flow rate, the leakage configurations showed no

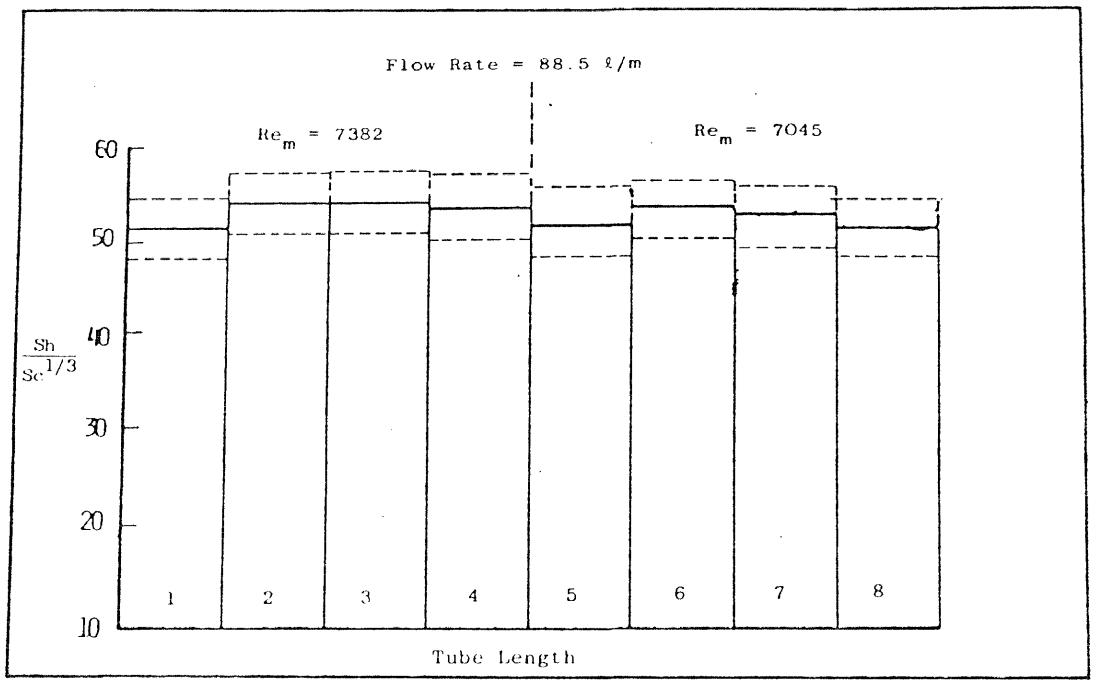

Figure VI.16 Histogram showing the length-wise variation

change with flow rate. The individual tube study in Section VI.3 also showed little variation in the gradient value between different compartments and tubes within the compartment. The value of the gradient for the leakage case was closer to 0.5 than for the no-leakage case suggesting possibly greater amount of longitudinal flow. Further, it was shown that the flow distribution between the compartments were similar and little variation existed between the tubes within any compartment. This suggested that the effect of the end compartments which were previously suspected of causing length-wise variation had been removed with the introduction of leakage. The increased longitudinal flow associated with the leakage configurations is suspected to cause this.

In no-leakage configurations it was also shown that the end compartments behaved differently from each other, although this difference was small and less than 10%. The effect of leakage was to reduce further this difference to well within the experimental accuracy.

Mackley had also shown that leakage reduced the effects of baffle-cut, i.e. the 18.4% and 25% baffle-cuts showed identical compartment transfer coefficients. Thus, further indicating the levelling of different geometric parameters affected by leakage streams.

VI.4.2 Comparison with Previous Leakage Data

The data from this study were compared with the

data of Mackley (3). The leakage runs carried out in this study are all tabulated in Table VI.1.

Mackley provided leakage data for two baffle-spacings of 48.5 mm and 97 mm and two different leakage area sizes. These data are depicted in Figures VI.17 and VI.18. The comparison of configurations with baffle-spacings less than 50 mm are shown in Figure VI.17. The data of Mackley from 25% and 37.5% baffle-cut configurations are also shown. It can be seen that the data from this work lie between the two cases of Mackley. The shell-to-baffle and tube-to-baffle clearances for this work were 2.2 mm and 0.5 mm respectively (see Table VI.1). This configuration showed transfer coefficients, consistently lower by 14% than Mackley's configuration with shell-to-baffle and tube-to-baffle clearances of 1.6 mm and 0.33 mm respectively, and constantly higher by 8% compared to Mackley's configuration with shell-to-baffle and tube-to-baffle clearances of 2.66 mm and 0.66 mm respectively. Mackley's data from 25% and 37.5% baffle-cut configurations with large clearances were also tested. They highlighted Mackley's conclusion that leakage reduced the effect of baffle-cuts, (see Section II.5). The corresponding data for the no-leakage case were not correlated by the same curve, as the data for 18.4% baffle-cut configuration showed higher values than the remaining baffle-cut cases, (see Figure III.8).

The differences between this work and Mackley's studies were expected as the leakage areas were different. These are further compared in Section VI.4.3. However, when comparing the data for 97 mm baffle-spacing

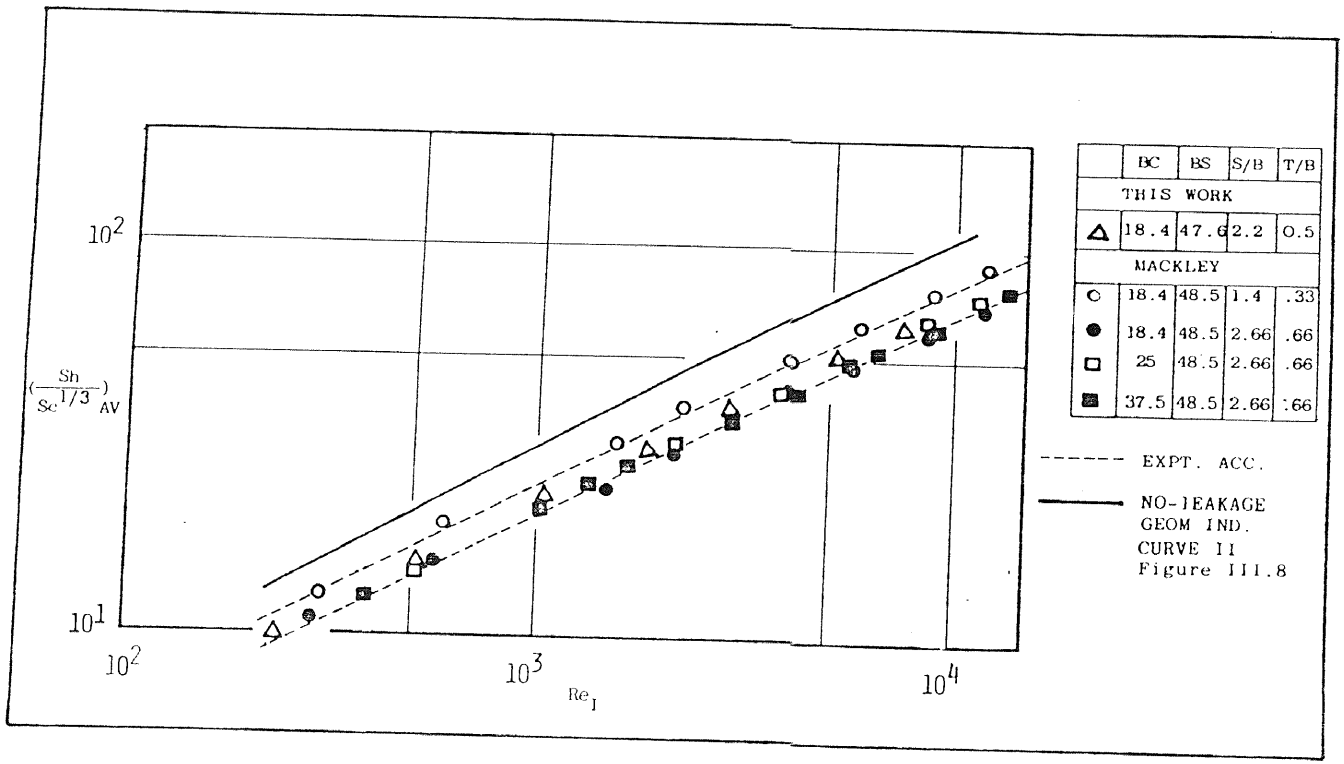

Figure VI.17 Comparison with previous leakage compartment data - for baffle-spacings less than 50 mm.

Table VI.1 Leakage Configurations Studied in this Chapter (VI)

Run No.	Baffle-Cut	BAFFLE SPACING		Comps. Studied	S/B	t/B	Flow
		END	INTERNAL				
6	18.4	47.6	47.6	1 to 4	2.2	0.5	Top-Bottom
7	18.4	47.6	66.6	1 to 5	2.2	0.5	Top-Bottom
8	18.4	97	97	1 to 4	2.2	0.5	Top-Bottom
*9	18.4	47.6	97	1 to 5	2.2	0.5	Side-Side
10	18.4	47.6	149.2	1 to 4	2.2	0.5	Top-Bottom

* Refers to bundle with verticle baffle-cut only.

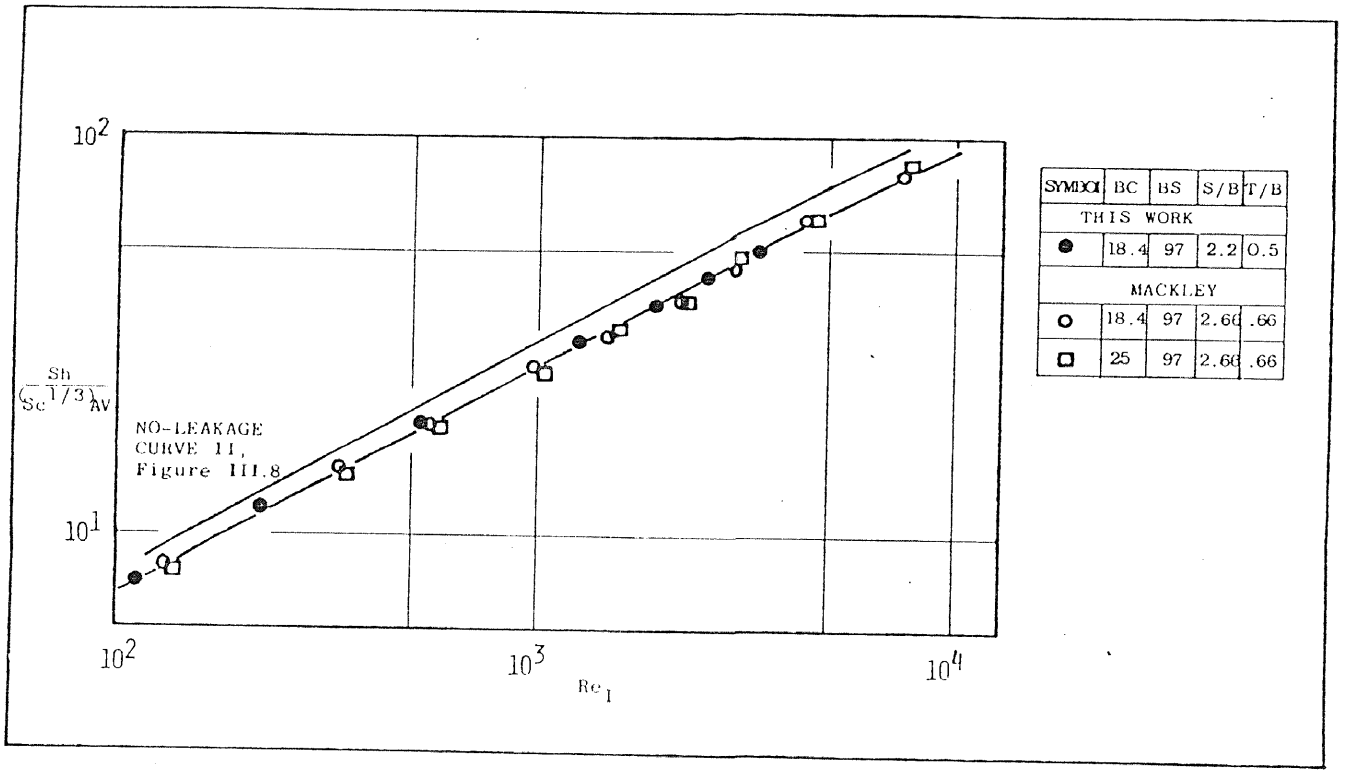

Figure VI.18 Comparison with previous leakage compartment data - for 97 mm baffle-spacing

configurations, the difference between this work and Mackley's was negligible and a single curve correlated all the data. Thus, large baffle-spacing had removed the effects of leakage clearances. Unfortunately, Mackley did not investigate configurations with small leakage clearances and large baffle-spacing, thus the conclusion of the effects of large baffle-spacing on leakage clearances could not be extended further.

If by increasing the baffle-spacing the effects of different leakage areas were removed, then this would suggest that the increased longitudinal flow caused by increasing the baffle-cut would also have a similar effect.

VI.4.3 Comparison with No-Leakage Data

The leakage data were compared with the no-leakage data discussed previously in Section V.4. As the lengthwise variation in the leakage configurations had been nullified, the average from all the compartments in the bundle was used in these comparisons. The techniques described in Chapter III to account for leakage streams were used.

The effect of semi-leakage clearances was discussed in Section V.6. It was shown there that the effects of shell-to-baffle leakage stream were comparable to the no-leakage configurations, listed in Table III.2, when the leakage area was accounted for within the Reynolds number. The configurations listed in Table III.2 were correlated by the geometric independent correlation

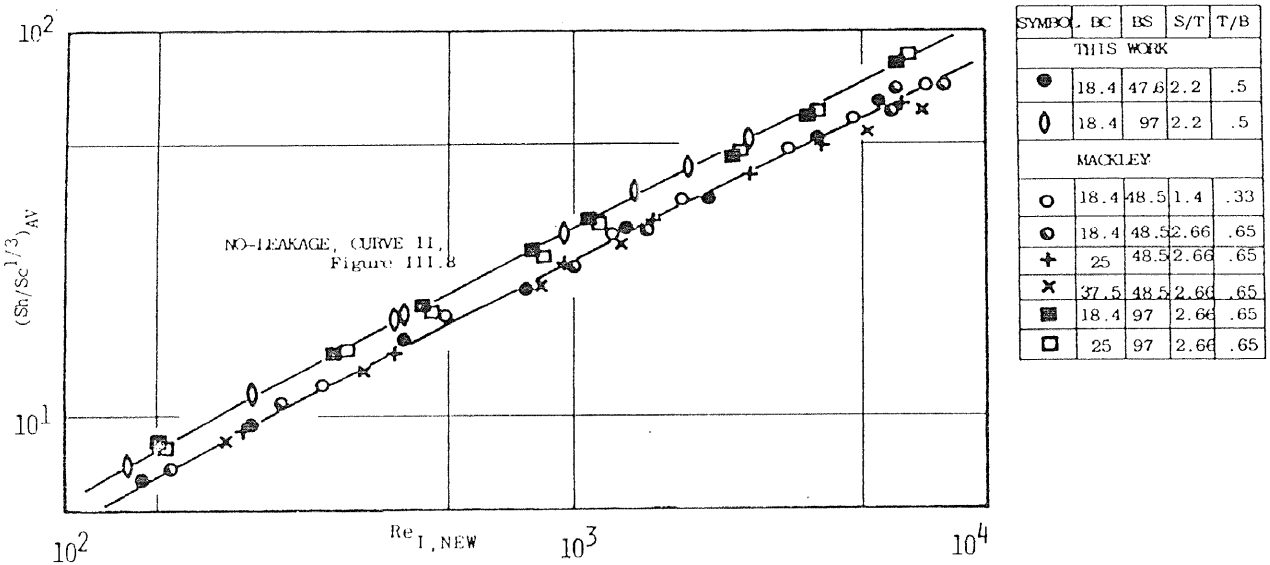

SYMBOL	BC	BS	S/T	T/B
THIS WORK				
●	18.4	47.6	2.2	.5
◊	18.4	97	2.2	.5
MACKLEY				
○	18.4	48.5	1.4	.33
◎	18.4	48.5	2.66	.65
+	25	48.5	2.66	.65
×	37.5	48.5	2.66	.65
■	18.4	97	2.66	.65
□	25	97	2.66	.65

Figure VI.19 Correlations of leakage streams

curve, and is also depicted in Figures IV.17 and IV.18. All the leakage data shown in these figures were recalculated by modifying the Reynolds number for each configuration by using equation III.2, and is shown in Figure VI.19. It can be seen that the large baffle-spacing geometries of both this work and Mackley's were correlated to within ± 5% of the geometric independent no-leakage curve.

The configurations with nominal baffle-spacing less than 50 mm were all correlated on a single curve different from the above geometric independent curve. Similar results were also obtained in Figure III.11. However, for the small baffle-spacing case semi-leakage data of both this work and Bell et al (37) were correlated with the geometric independent curve. This suggested that the tube-to-baffle leakage stream was causing this difference and was not satisfactorily accounted for when using equation III.2. Also, the small baffle-spacing correlation had a lower gradient than the geometric independent correlation curve. This meant that the stream affecting the correlation was doing so by re-distributing the flow and changing the flow pattern within the compartment. Thus the tube-to-baffle stream by the action of longitudinal jetting flow was much more likely to affect the flow distribution patterns away from the no-leakage configuration. As the Reynolds number was lowered, these longitudinal jetting flow streams through the tube-to-baffle clearances would result in smaller tube lengths being effected. This explained the smaller differences between the no-leakage and leakage cases at the lower Reynolds numbers, (see Figure VI.19). In large baffle-spacing

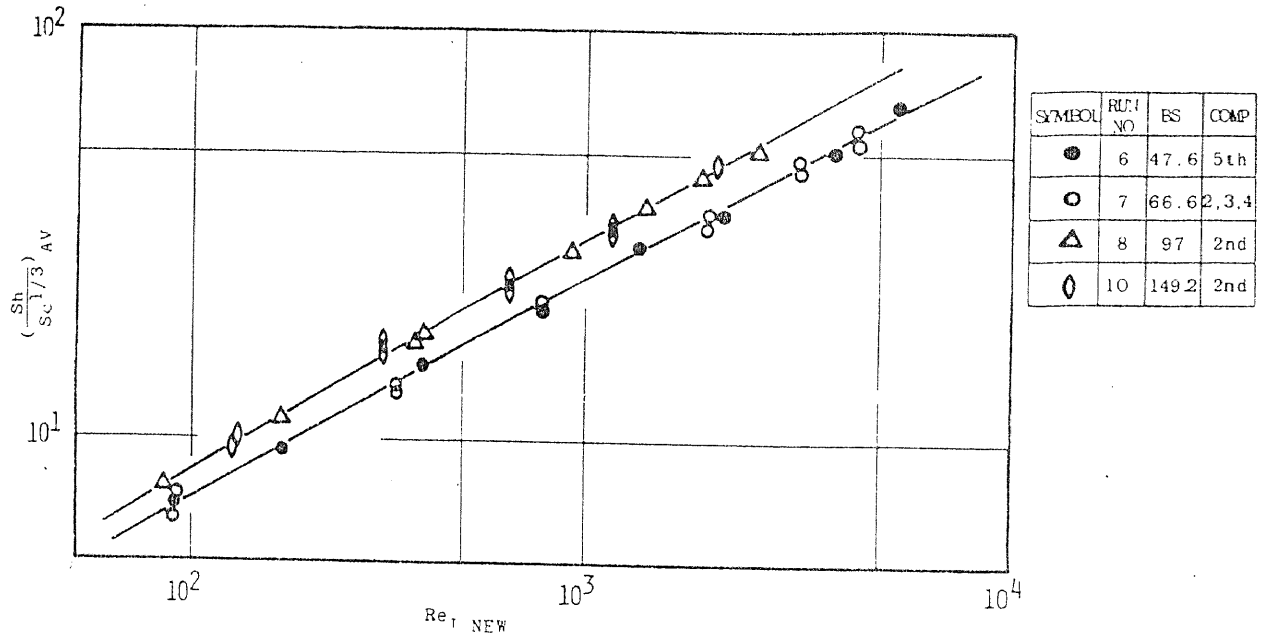

Figure VI.20 Correlation of different sized internal compartment data

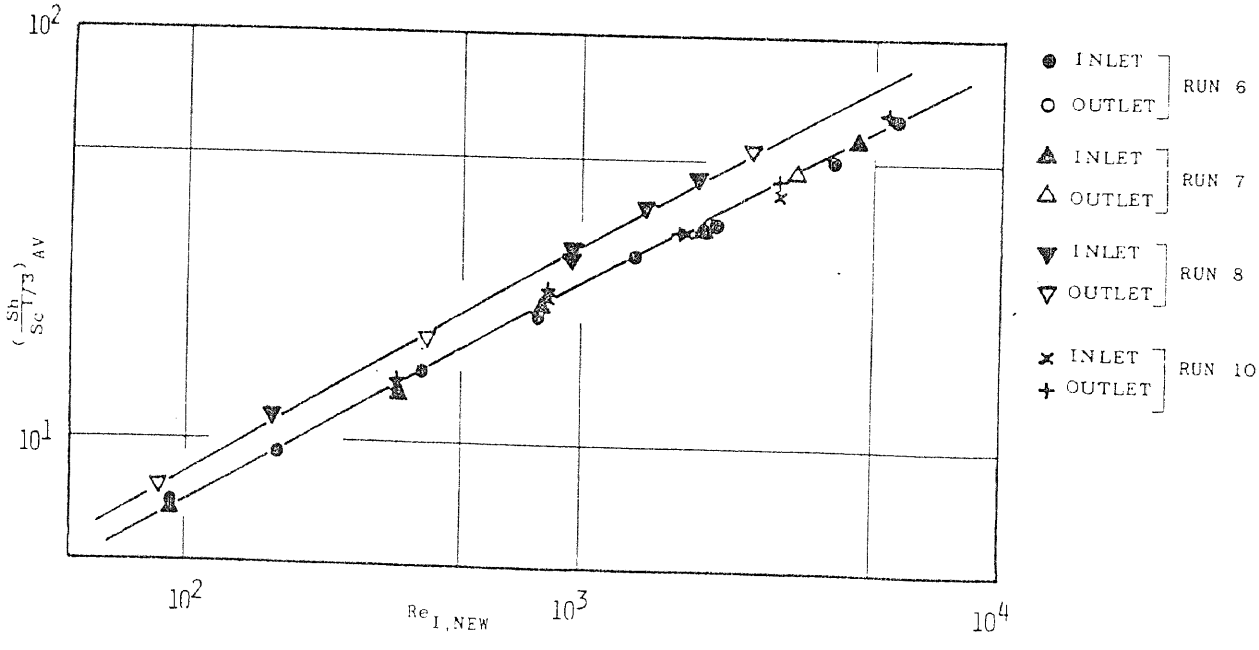

Figure VI.21 Comparison of end compartment data obtained from different configurations and position

compartment a smaller proportion of the tube length was effected; thus the resultant departure from the no-leakage correlation was negligible.

VI.4.4 Effects of Different Baffle-Spacing Compartments

The effects of baffle-spacing have already been discussed earlier in this section, however, only a few selected cases were introduced. In this section, all the leakage data with different configurations examined are reviewed and compared with the leakage and no-leakage data presented earlier in the form similar to Figure VI.19. Compartments with baffle-spacings equal to 47.6 mm, 66.6 mm, 97 mm and 149.2 mm are studied.

All internal compartment data outlined above are plotted in Figure VI.20 with the Reynolds number modified by equation III.2. It can be seen that all the data were again correlated onto two separate curves. Compartments with baffle-spacing higher than 97 mm were correlated with the no-leakage geometric independent curve. However, the data for a compartment with baffle-spacings less than 66.6 mm were correlated with the data for configurations with nominal baffle-spacing of 50 mm tested in Figure VI.19. This suggested that the 66.6 mm baffle-spacing compartment was also influenced greatly by the tube-to-baffle leakage stream. Hence compartments with baffle-spacing from 66.6 mm to 97 mm would possibly show the reduced effect of tube-to-baffle leakage streams.

The end compartment data were compared with the

no-leakage and leakage data discussed above. These are shown in Figure VI.21. Both the inlet and outlet compartments are indicated for each geometry. Again, all the data were correlated on two separate curves described earlier in Figure VI.20. The data for inlet and outlet compartments with baffle-spacing of 97 mm were correlated onto the geometric independent correlation curve. There was no difference between the inlet and outlet compartment values. Similarly, the inlet and outlet compartment data with 47.6 mm baffle-spacing were correlated on the same curve as the remaining leakage data with baffle-spacing less than 66.6 mm.

The above comparisons indicated two important features attributed to leakage bundles. Firstly, the difference between the inlet and the outlet compartments was negligible; whereas the no-leakage cases showed transfer coefficient for the former compartments higher by 10% than the latter compartment (see Section V.4.2). Secondly, the correlation of the 47.6 mm baffle-spacing compartment data, showed that the geometry of any compartment did not effect the flow behaviour of its adjacent compartments. A similar conclusion was also made in Section V.4.2.

VI.4.5 Effect of Baffle-Cut Orientation

An experimental investigation of baffle-cut orientation was made by rotating the bundle comprised of two end and three internal compartments with 47.6 mm and 97 mm baffle-spacings respectively. In each

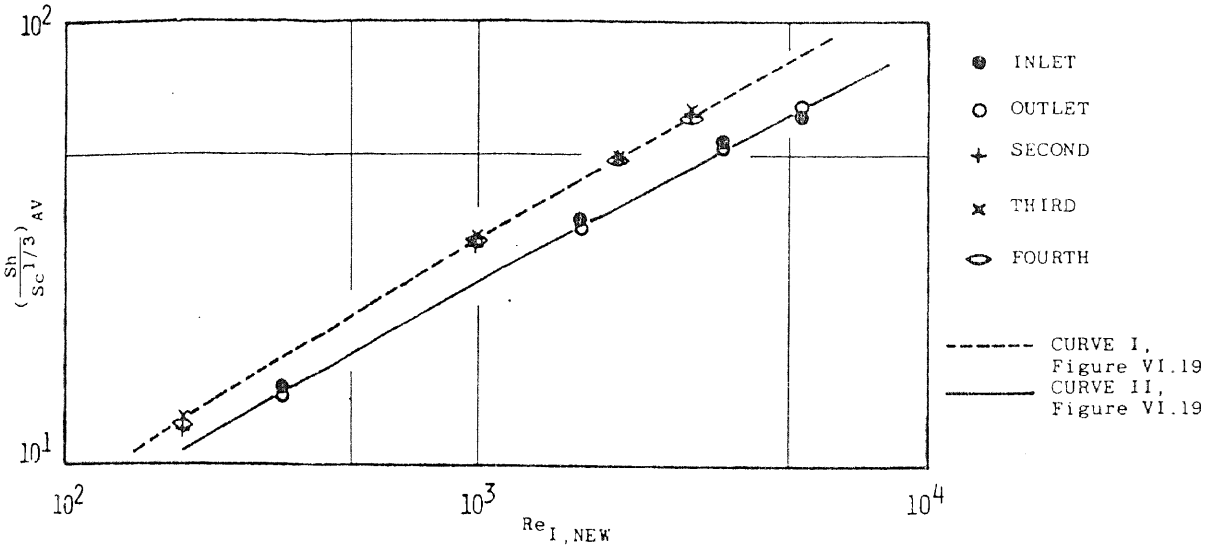

Figure VI.22 Effect of orientation of baffle-window

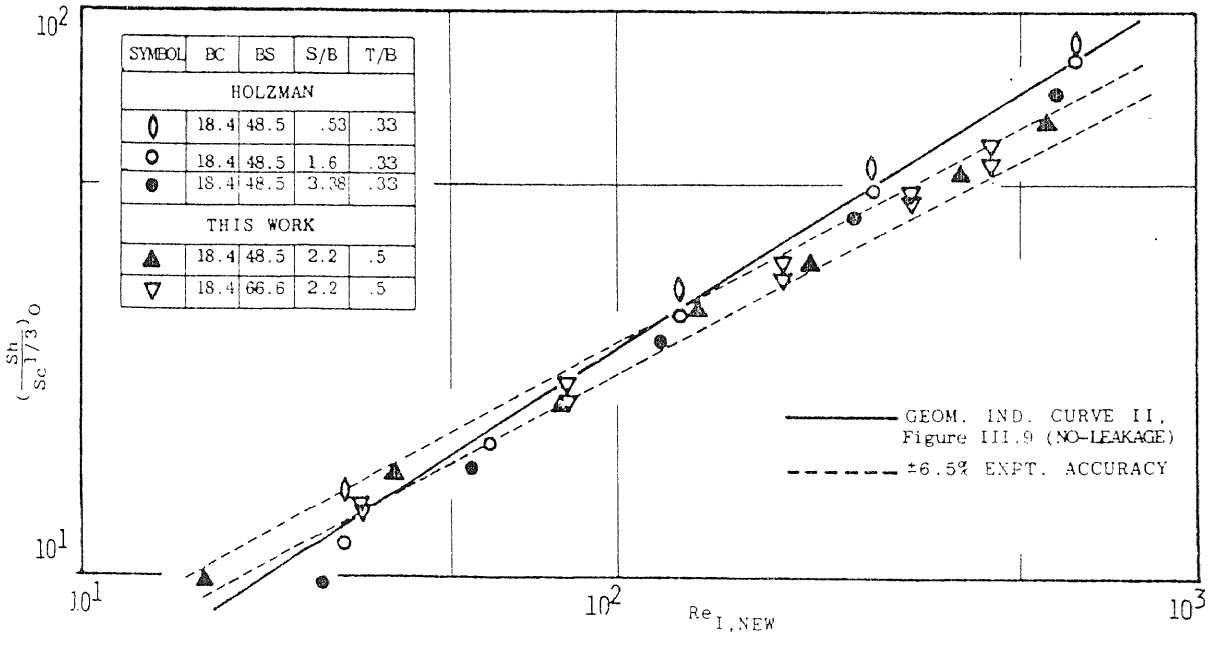

SYMBOL	BC	BS	S/B	T/B
HOLZMAN				
◊	18.4	48.5	.53	.33
○	18.4	48.5	1.6	.33
●	18.4	48.5	3.38	.33
THIS WORK				
▲	18.4	48.5	2.2	.5
▽	18.4	66.6	2.2	.5

Figure VI.23 Comparison of overall bundle average data with previous leakage and no-leakage data

compartment forty tubes were investigated instead of the twenty in all other experimental runs. The data for each of the internal and end compartments were plotted in the form of compartment average dimensionless transfer coefficient against Reynolds number based on flow area $A_{I,NEW}$, and is shown in Figure VI.22.

Figure VI.22 shows no length-wise variation of transfer coefficient along the bundle, as the agreement between compartment averages is within the experimental accuracy Thus, the inlet and the outlet compartments are defined by the same correlation.

Again the data for the end and internal compartments were correlated by the two separate curves shown in Figure VI.19. The internal compartments were represented by the geometric independent curve, Curve II, Figure II.8, while the end compartments were correlated by the leakage curve for compartments with baffle-spacings less than 66.6 mm. Therefore, the compartment average transfer coefficients for the horizontal and verticle baffle-cuts were similar and not influenced by baffle-cut orientation. Mackley (3) also obtained a similar conclusion.

The negligible effect of baffle-cut orientation on compartment average transfer coefficients highlights an important design feature. Baffle-cuts with side orientation are widely used in industrial exchangers in order to remove trapped liquid so as not to contaminate the following batch or cause build-up of pressure in upstream equipment. It is shown here that side orientation

would not reduce the compartmental average transfer coefficient. However, side orientation produces maldistribution of flow within the compartments (see Section VI.3.2) which may not be desirable. Hence distribution plates may be necessary to overcome this problem.

VI.5 Overall Bundle Examination

The overall bundle transfer coefficients are discussed in this section. It was shown in Section VI.4.1 that no significant length-wise variation existed along the bundle length, thus average compartment data could be compared against the overall bundle average data. The compartment average data of Mackley and the direct heat transfer bundle averages obtained by Deleware University workers were used in the comparisons.

The procedure outlined earlier in Section V.5 was used to determine the average coefficients for bundles with uniform and non-uniform baffle-spacings.

The correlation method discussed in Chapter III and Section VI.4 were used for correlating the data.

VI.5.1 Comparison with Previous Leakage Data

The leakage data of Mackley were previously plotted together with the no-leakage data in Figure VI.19. However, it was shown there that only large baffle-spacing leakage data were correlated with the no-leakage correlation curve while all the configurations with

baffle-spacings less than 66.6 mm were correlated by a single curve different from the no-leakage case.

The comparison with direct heat transfer data of Holzman (24,25) is now attempted. Unfortunately, Holzman's data were limited to one baffle-spacing equal to 48.5 mm. The data for configurations with nominal baffle-spacings less than 70 mm are plotted in Figure VI.23. The overall bundle average data for mixed baffle-spacing compartments in the bundle were obtained by a weighted average of the Reynolds number as described in Section V.5.2.

Figure VI.23 shows the mass transfer data to be represented on a same correlation curve. Further, this curve was the same as that shown in Figures VI.19 and VI.20, correlating all compartment data with nominal baffle-spacings less than 70 mm. Also shown in Figure VI.23 is the no-leakage heat transfer geometric independent correlation curve. Data from three different configurations studied by Holzman were in disagreement with the present work. These three cases of Holzman's were correlated within ± 16% and 19% at Reynolds numbers of 300 and 7000 respectively, about the geometric independent no-leakage heat transfer curve. A similar disagreement was also noticed by Mackley when comparing his data with Holzman's using j_m versus R_{em} diagrams. Mackley suggested this was perhaps due to the internal compartment showing different flow behaviour to the end compartments. Thus comparison between his data and

Holzman's would be inaccurate. In Sections VI.3.3 and VI.4.1 this hypothesis was dismissed as all compartments showed similar flow behaviour.

The difference between data of Holzman and this work was difficult to explain as all the mass transfer data of Mackley supported this work, while the heat transfer data of Bell (37) agreed with the former data. Further, the disagreement between the two sets of data was considerable showing particularly in the gradient of the correlation curves In view of the above factors the disagreement was considered to be between the mass and heat transfer mechanisms.

A possible explanation for this disagreement could be due to the boundary conditions not being analogous. In the case of mass transfer constant concentration driving force was ensured throughout the exchanger by the bulk and surface concentrations remaining unchanged. However, in the heat transfer case the temperature driving force was assumed constant throughout the bundle if the logarithmic mean temperature difference (L.M.T.D.) and arithmetic average temperature difference (M.T.D.) were approximately equal. At higher Reynolds numbers the maximum percentage difference between the two temperature differences was found to be quite small ($\lesssim$ 2.5%), while at lower Reynolds numbers this difference was of the order of 13%. When comparing the semi-leakage data of Bell and Fusco (37) they also showed similar values at high Reynolds number but a maximum difference at low Reynolds number was 17%.

The increase in difference at lower Reynolds numbers was also shown in the no-leakage data of Brown (23). The agreement between the no-leakage heat and mass transfer coefficient data was shown to decrease at lower Reynolds numbers, see Figure V.23. For higher Reynolds numbers in no-leakage configuration concordance of L.M.T.D. and M.T.D. (3%) was reflected in good agreement between the heat and mass transfer coefficient data, (see Section V.5.1). However, as was reported above for leakage configurations, the agreement between heat and mass transfer data was poor at high flow rates too, inspite of good agreement between the L.M.T.D. and M.T.D. A possible explanation for this irregularity is that at high flow rates, a greater proportion of flow passes through the shell-to-baffle leakage clearances. The enthalpy of this fluid stream remains unaltered from that of the inlet fluid stream. Therefore, this stream reduces the difference between the average temperature of outlet and inlet streams. Thus, although the difference between L.M.T.D. and M.T.D. is small, the local mean temperature difference would change considerably along the length.

The logarithmic mean temperature difference is strictly applied to countercurrent parallel flow, although the Deleware University workers and others have used it to determine heat transfer coefficients in their heat exchangers. For no-leakage bundles particularly at high flow rates the distribution of fluid magnitude and temperature are fully accountable by L.M.T.D. However, for

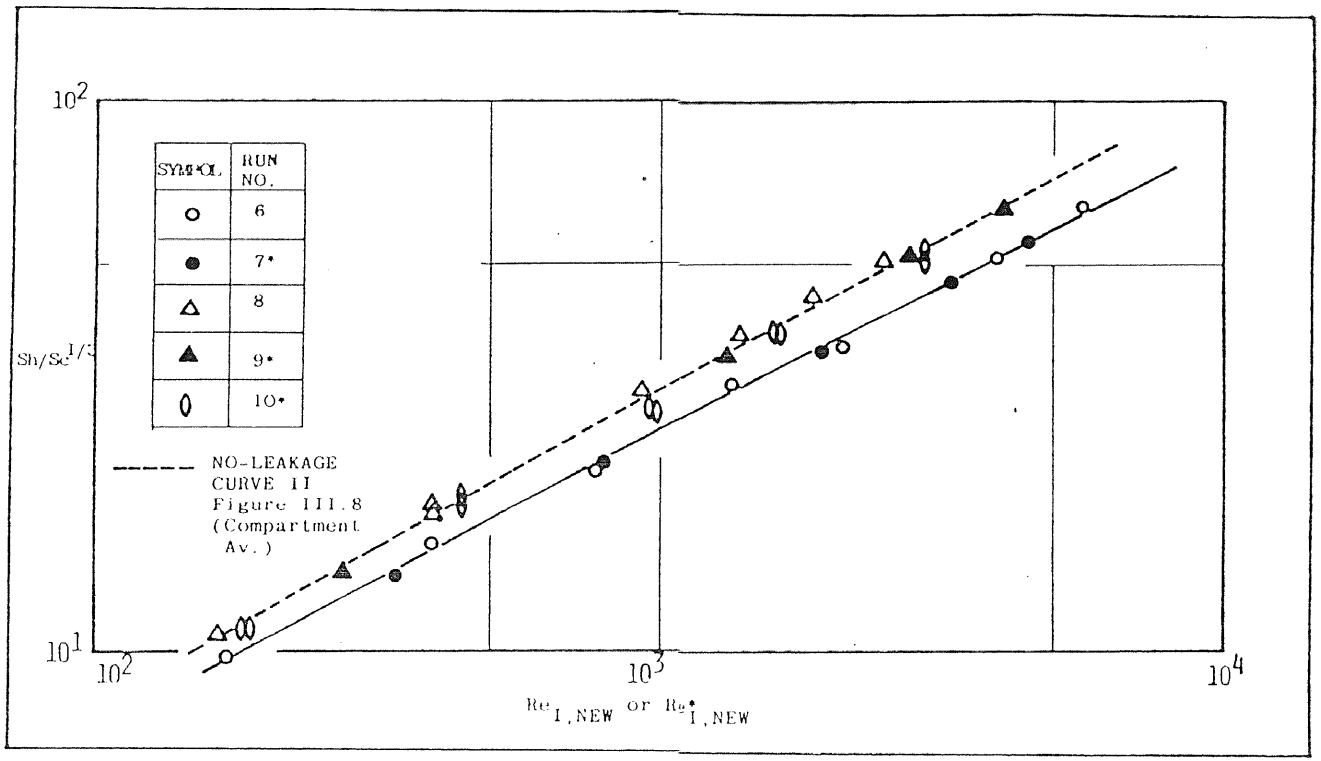

Figure VI.24 Effect of baffle-spacing on overall bundle average data

leakage and low flow rates the unpredictable by-passing of fluid between tube-to-baffle and shell-to-baffle clearances distorts the mean temperature driving force along the exchanger length. Therefore, unless the temperature driving force is constant throughout the bundle as for a theoretical isothermal heat exchange, the heat and mass transfer coefficient data cannot be compared. This shows that the heat transfer data are influenced by local flow and temperature distributions, with the latter distribution itself dependent on the local flow distribution.

VI.5.2 Effect of Baffle-Spacing on Overall Transfer Coefficients

The effects of different baffle-spacing configurations were studied by comparing overall transfer coefficients against no-leakage configurations. All the leakage configurations studied, including side orientation data are shown in Figure VI.24. The overall bundle transfer coefficients for the mixed baffle-spacing compartments was obtained by simply averaging all the transfer coefficient values within the exchanger, as described in Section V.5.2. A single average value for the Reynolds number at corresponding flow rate was also determined by a weighted average of the Reynolds numbers in all the compartments present in the bundle again as described in Section V.5.1.

Figure VI.24 shows all the leakage data examined in this work being correlated on two curves. This was

irrespective of the considerable diversity in the examined configurations including data from many different baffle-spacings compartments, for inlet and outlet halves of the bundle, uniform and mixed baffle-spacing compartments and two baffle-cut orientations. The two curves were as described in Figure VI.19 for a single compartment. Thus, the data were only separable by baffle-spacings between 66.6 mm and 97 mm. There was no effect of baffle-spacing outside this range.

As in Figure VI.19, the overall bundle average transfer coefficient data for baffle-spacings less than 66.6 mm were correlated on a lower curve, while the remaining configurations were correlated by the geometric independent curve, (see Table III.2). Bundles with mixed baffle-spacings did not affect the above conclusion. This was expected as a greater proportion of each tube was experiencing flow distribution similar to that in the internal compartments, hence the overall effect represented the internal compartments.

This supported the earlier conclusion that leakage reduced the length-wise variation along the bundle, thus bundle average data were comparable with compartment average.

This also suggests that Reynolds number based on flow area $A_{I,NEW}$ successfully correlated overall bundle average transfer coefficient data onto two curves. Different baffle-spacing compartments existing in one bundle were also correlated by determining the bundle mean

flow area.

VI.6 Overall Pressure Drop in Bundles

Overall pressure drop measurements were made for all the leakage runs previously described. These were compared with similar leakage data of previous workers, and also the no-leakage data discussed in Section V.5.2. The pressure drop meaasurements were re-expressed in the form of dimensionless pressure drop factors defined in equation V.11.

VI.6.1 Comparison with Previous Leakage Data

The leakage data were compared with the data obtained from a similar bundle geometry by Holzman (25). The pressure drop data of Holzman used in these comparisons were obtained from his isothermal runs.

Holzman investigated three different shell-to-baffle leakage clearance arrangements, however the baffle-cut, baffle-spacing and tube-to-baffle clearances were fixed at 18.4%, 48.5 mm and 0.33 mm respectively.

The comparison between the 50 mm nominal baffle-spacing data of the present work and Holzman's is shown in Figure VI.25. It can be seen that the present data agreed well with those from Holzman for the case with shell-to-baffle and tube-to-baffle clearances of 1.6 mm and 0.33 mm respectively. On average, the present data were approximately 20% higher than Holzman's configuration with largest shell-to-baffle clearances.

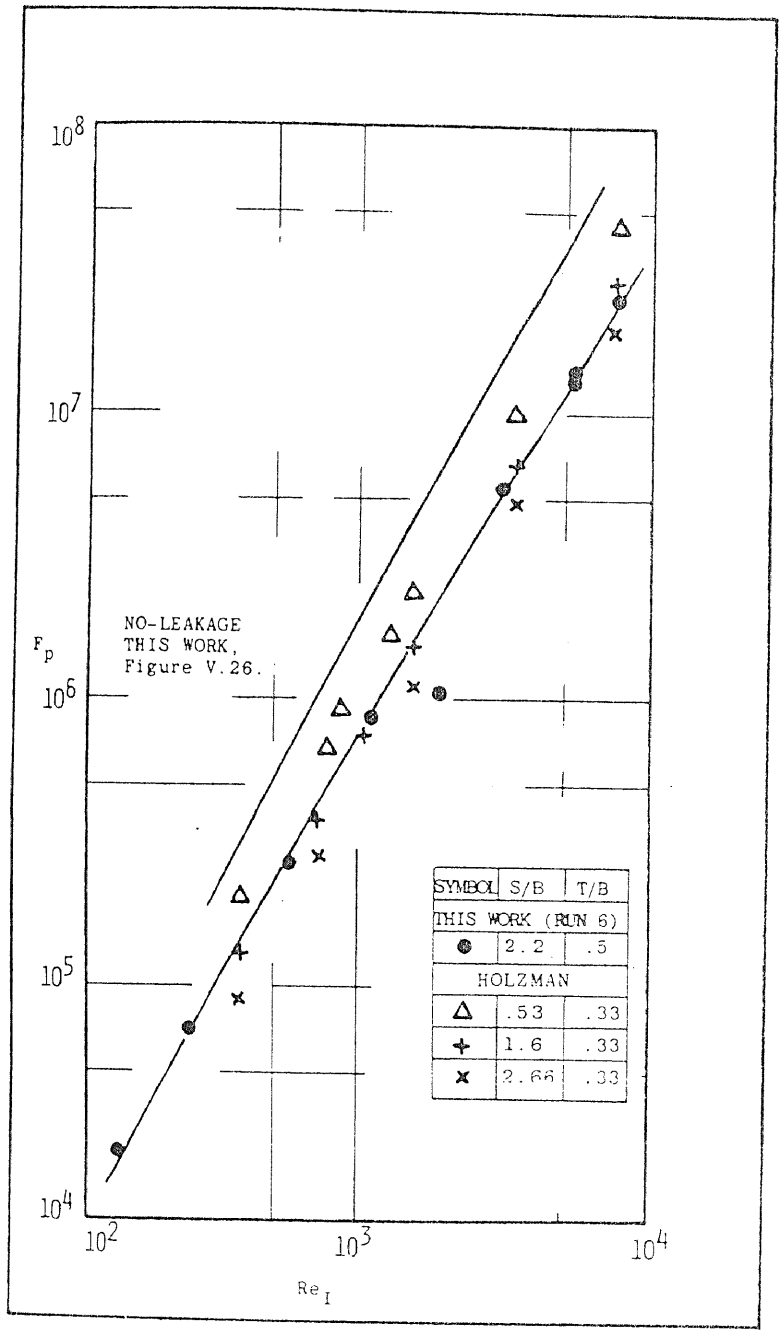

Figure VI.25 Comparison of overall pressure drop data with Deleware University data (24)

These comparisons suggested that the present configuration, with diametrical shell-to-baffle and tube-to-baffle clearances of 2.2 mm and 0.5 mm respectively had higher pressure drops than would be predicted by Holzman for the same configuration. This difference could be explained by numerous factors such as, uncontrolled leakage, trapped gas in the metal exchanger of Holzman, trapped gas in the pressure impulse lines, and tube-to-baffle leakage area. However, the experimental error existing in both measurements would encompass this difference.

Unfortunately, no other baffle-spacing data were available from similar exchanger arrangement for further comparison with the remaining configuration studied here.

VI.6.2 Comparison with No-Leakage Configurations

The no-leakage data for configurations with baffle-spacings of 47.6 mm and 149.2 mm were compared with corresponding data from leakage configurations.

Figure VI.25 also shows the no-leakage data for configurations with nominal baffle-spacings of 50 mm. This was discussed in Section V.5.2 and shown in Figure V.26. It can be seen that all the leakage cases showed lower pressure drops than the no-leakage case, and this difference increased with increasing leakage clearances. Similar conclusions were also drawn from Figure III.13 leakage and no-leakage data for this work was 67% at Re_I=8000. This difference reduced slightly at lower Reynolds numbers and was 55% at Re_I=500. The no-leakage case was chosen as

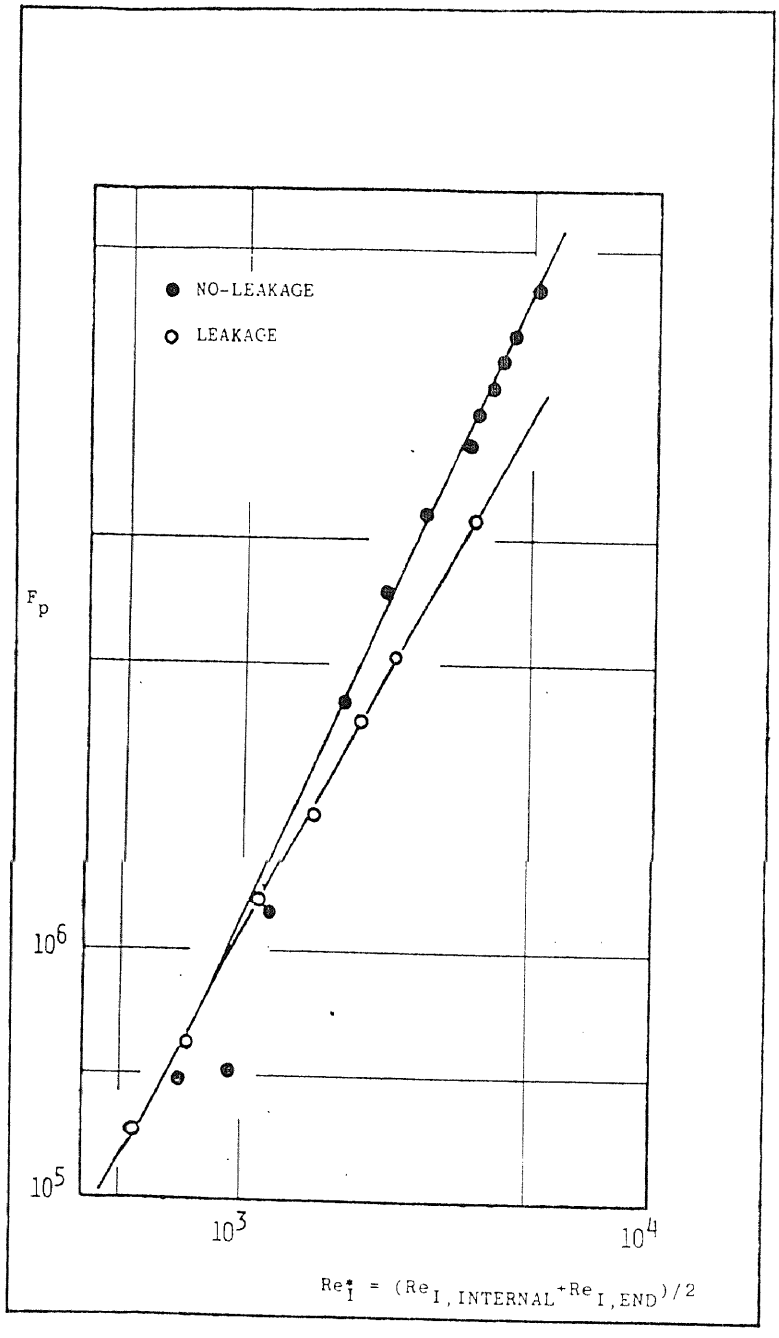

Figure VI.26 Comparison of leakage and no-leakage pressure drop data for large baffle-spacing configuration

the base. The increased departure at higher Reynolds numbers can be explained by greater proportion of the total flow being "lost" from the main stream (stream B in Figure II.2) through the leakage clearances which has low flow path reistance. Most of the "lost" fluid escaped through the shell-to-baffle clearance. At low flow rates the overall pressure drop through the exchanger was small, thus the differential resistance between leakage and no-leakage cases were indifferent. Therefore, same proportion of the total fluid did not pass through the leakage clearances at low flow rates compared with higher flow rates.

The leakage and no-leakage configurations with mixed baffle-spacing compartments were also compared, and are shown in Figure VI.26. Again, the procedure outlined in Section V.5.2 was used to account for different sized compartments existing in the same bundle. The overall bundle Reynolds numbers were calculated by a weighted average of the individual Reynolds numbers of every compartment in the bundle. The difference between the leakage and no-leakage pressure drops again changed with Reynolds number, and were 46% at Reynolds number of 4000 and almost insignificant at Reynolds number of 600. The no-leakage case was chosen as the base. These differences were much smaller in this case than for the 47.6 mm baffle-spacing configuration. Thus, suggesting configurations with large baffle-spacing compartments had smaller difference between the flow resistances of the leakage streams and

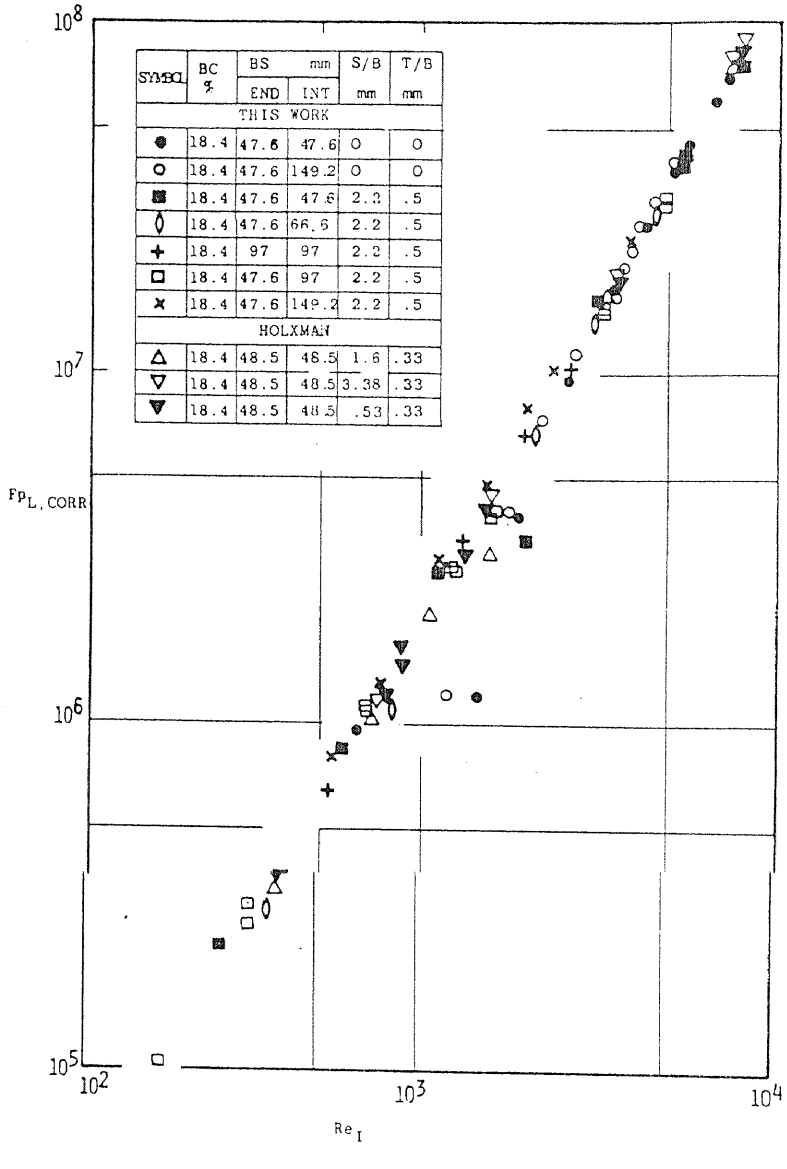

FIGURE VI.27. correlation of leakage and no-leakage data from past and present studies.

stream B in Figure II.2.

In Section III.3.2 an attempt was made to account for the leakage streams by modifying the measured pressure drop with equation III.4. The leakage data for 47.6 mm, 66.6 mm, 97 mm and 149.2 mm baffle-spacing configurations were re-expressed and are shown in Figure VI.27 by using a modified form of equation III.4:

$$Fp_{L,CORR} = \frac{Fp_L}{(1-(\frac{AL}{A_I}).4)^2} \qquad (VI.1)$$

the leakage area was for the shell-to-baffle leakage clearance only. For non-uniform baffle-spaced compartments the bundle average flow area A_I, was determined by a weighted average, similar to the Reynolds number, described above. All the cases examined showed remarkable agreement thus indicating the correctness of equation VI.1 in accounting for leakage. Another interesting pointer to the successful correlation was when comparing leakage and no-leakage configurations with baffle-spacings of 47.6 mm and 149.2 mm. These results indicate the presence of disturbance in the curve at approximately same Reynolds number range of 10^3 to 2000. This was also indicated to a small extent by the data of Holzman for the 1.6 mm shell-to-baffle clearance case. (Note: this method has increased the gradient of the leakage curves to agree with the no-leakage cases).

The success in correlating the leakage data whilst only using shell-to-baffle leakage area in equation VI.1

highlighted the importance of this leakage stream compared with the tube-to-baffle leakage stream. A similar conclusion was outlined in Figure III.13, where no significant difference resulted in the pressure drop even when the tube-to-baffle clearances were doubled. This attribution of the tube-to-baffle leakage stream was surprising, especially since the total leakage flow-area for this stream was always higher than for the shell-to-baffle leakage stream. One possible explanation for the apparent insensitivity of the tube-to-baffle clearance is that, as the flow-resistence is proportional to the frictional surface area, the total area for all the tubes was approximately five to six times greater than for the shell-to-baffle cases.

Figure VI.26 also shows correlation of data from different baffle-spacing configurations. Therefore, equation VI.1 not only accounts for leakage areas but also baffle-spacing.

VI.7 Conclusions

Following conclusions are made for the leakage tube bundle arrangements discussed in this Chapter.

i) The repeatability of the experimental data is shown to be well within the experimental accuracy of $\pm$ 6.5%.

ii) Leakage caused lower transfer coefficients by as much as 40% in places within the compartment compared to the no-leakage case. Leakage also produced much more even flow distribution compared to the no-leakage case.

iii) The flow characteristic model proposed in Section V.3.3 was unable to discriminate between different regions within the compartment, contrary to the no-leakage case. Although regions with high and low velocity ratios were shown for the verticle baffle-cut orientation. The model also showed how leakage caused the fluid to pen-trate equally into the bundle for the horizontal baffle-cut orientation, and uneven flow distribution for the verticle baffle-cut orientation. The latter case showed the bottom region of the compartments being by-passed by the flow.

iv) Examination of compartment average transfer coefficients showed the following:

a) No length-wise variation along the exchanger length, with comparison between compartments lying within the experimental accuracy. The length-wise variation within a compartment was shown to be reduced by the presence of leakage stream.

b) The effects on many parameter including, baffle-cut, baffle-cut orientation and compartment position (i.e. end or internal) were comparable with the no-leakage when Reynolds number was based on flow area $A_{I,NEW}$. Further, the effects of shell-to-baffle and tube-to-baffle clearances were also correlated when baffle-spacing was greater than

97 mm. For configurations with baffle-spacings less than 66.6 mm all the above parameters were correlated on a separate curve. Outside the range of 66.6 mm to 97 mm, the baffle-spacings had no effect and all the configurations examined lay on either of these two curves. This difference is due to the baffle-to-tube leakage.

v) Examination of the overall bundle average transfer coefficients showed the following.

a) All data lay on two curves outlined in IV above, when using $A_{I,NEW}$ as the flow area in the Reynolds number.

b) Comparison of this data with heat transfer data from Deleware University Research programme showed no agreement. This was expected to be due to non-analogous boundary conditions, particularly the mean driving forces and temperature distribution along the exchange length.

vi) Examination of overall bundle pressure drops showed the following:

a) All leakage cases showed lower pressure drops than the no-leakage case, and this was further lowered as the leakage areas increased. This difference was shown to depend on Reynolds number.

b) Comparison of all leakage and no-leakage data of Deleware workers and this study were correlated by a single curve, (see Figure VI.27) when Reynolds number and dimensionless pressure drop factor were based on flow area A_I. (This was corrected to A_I^* for configuration with mixed baffle-spacing compartments).

CHAPTER VII

GENERAL CONCLUSIONS

The suitability of the electrochemical technique for rapid data acquisition is demonstrated by approximately 10,000 local measurements of mass transfer coefficients. Thus, providing valuable information for the stream analysis computer models. The data has also highlighted some interesting conclusions.

VII.1 The No-Leakage Case

(a) The examination of compartment average transfer coefficients shows a length-wise variation of transfer coefficients between adjacent compartments of the bundle. The difference between the end and internal compartments is shown to be dependent on flow rate and increases from 12% to 26% as the Reynolds number increases from 500 to 10^4.

(b) The individual tube transfer coefficients and the flow characteristics as described by the model shows that:

(i) a greater proportion of flow penetrate the bundle as the flow rate is increased,

(ii) the inlet compartment possesses different flow characteristics compared with the remaining compartments.

(iii) a large variation exists in the distribution of flow within the large baffle-spacing compartments, and

(iv) the variation of transfer coefficient along

the compartment length.

(c) The comparison of both transfer coefficient and pressure drop data with previous data obtained from direct heat transfer work and the electrochemical techniques revealed the following:

(i) Agreement for the internal compartment mass transfer data of this work and similarly data of Mackley .

(ii) The overall bundle average mass transfer coefficients for this work and for the heat transfer studies also shows good agreement at Reynolds numbers above 800. This agreement became poor at lower Reynolds numbers and is explained by unanalogous boundary conditions.

(iii) The overall bundle pressure drop data for this work and Delaware University research programme shows an agreement to within 5% for similar geometries.

VII.2 The Leakage Case

(d) The effect of semi-leakage configuration shows the length-wise variation to reduce by 10% from the no-leakage case and further examination of two total leakage configurations shows no length-wise variation throughout the exchanger length.

(e) The individual tube transfer coefficients and the flow characteristics as described by the model shows:

(i) Leakage reduces the transfer coefficient value by as much as 40% in places compared with the no-leakage case.

(ii) Leakage streams also produced even flow distribution and thus the model was unable to discriminate between different regions of the compartment. This is unlike for the no-leakage configurations.

(iii) The flow characteristic model shows maldistribution of the flow in verticle baffle-cut configuration.

(d) The comparison of leakage transfer coefficient data with previous data shows:

(i) Good agreement for the compartment average transfer coefficients for this work and data of Mackley.

(ii) There is no comparison between the overall bundle average mass transfer coefficient data and corresponding direct heat transfer data. This is inspite of the very good agreement achieved between the overall pressure drops for all the flow rates. This disagreement is explained by unanalogous driving forces and is the extension of the no-leakage case at lower Reynolds number.

VII.3 Correlations for the Shell-side

The following conclusions are made about the correlation of present and past shell-side data.

(g) The compartment average transfer coefficient data from many configurations with different baffle-cuts, baffle orientations, compartment position (i.e. end or internal), compartments existing in non-uniform bundle, baffle-spacings (outside the range 66 mm to 97 mm), tube-to-baffle and shell-to-baffle clearances and baffle thickness for both leakage, semi-leakage and no-leakage are correlated on two curve when using flow area A_I,NEW. These curves are represented by baffle-spacings less than 66.6 mm and greater than 97 mm. The difference is attributed to the tube-to-baffle leakage stream effecting the flow patterns in smaller baffle-spacing compartments.

(h) The examination of overall bundle pressure drop data for a total of eighteen different configurations studied by two authors using different fluids for leakage and no-leakage cases shows a good correlation by the procedure outlined in Chapter III.

CHAPTER VIII

Recommendations For Future Work

The following recommendations are made for future work:

(1) More detailed investigations of different geometrical configurations in leakage and no-leakage bundles are required to show:

(i) if their data are correlated by methods described here,

(ii) more individual tube transfer coefficient data to improve the flow characteristic model,

(iii) the affects of length-wise variation and attempt to explian what is causing this (local velocities measured by L.D.V. technique may be useful)

(iv) what happens between baffle-spacings of 66 mm and 97 mm in the leakage case and how tube-to-baffle stream effects this,

(v) the effects of different port types on both pressure drop and transfer coefficient,

(vi) the effect of various commercially used impingement baffles on the distribution of flow particularly for the vertical baffle-cut.

(vii) the 'dip' in the pressure drop versus Reynolds number plot near the transition Reynolds numbers,

(viii) a model of local velocity profile calculated from the transfer coefficient data. This can then be used to determine the change in the analogous driving force gradient and hence account for the leakage heat transfer data. In this way a better mean temperature driving force might be found compared to LMTD.

Nomenclature

Symbol	Title	Units
a	Equation coefficient	
A	Shell-side flow area	m^2
A_I	Minimum crossflow area at the baffle edge	m^2
$A_{I,NEW}$	(A_I+A_L)	m^2
A_L	Baffle leakage area	m^2
$A_{\ell,n}$	Minimum crossflow area at n^{th} row of tubes	m^2
A_m	Minimum crossflow area at centre row of tubes	m^2
A_{max}	Maximum crossflow area m cross-flow zone	m^2
A_{min}	Minimum crossflow area in cross-flow	m^2
A_SB	Shell-to-baffle leakage area	m^2
A_TB	Tube-to-baffle leakage area	m^2
A_w	Free flow area in the window zone	m^2
b	Equation coefficient	
BC	Baffle cutdown	%
BS	Baffle-spacing	mm
C, C_p	Specific heat evaluated at bulk temperature	$KJ/K_g\,^oC$
C_b	Bulk ferricyanide ion concentration	Kg mole/m^3
d, d_o, d_t	Tube outside diameter	m
D_{ek}	Equivalent hydraulic diameter defined by Kern	m
D, D_v	Diffusion coefficient	m^2/s
D_i, D_s	Shell inside diameter	m
F	Faraday's constant	c/kg mole
F_B	Correction factor for bypass stream	

Symbol	Title	Units
F_L	Correction factor for leakage	
F_N	Correction factor for number of tube bundles	
F_w	Correction factor for window zone	
G	Shell-side fluid mass velocity	$kg/m^2/s$
G_c	Crossflow mass velocity	$kg/m^2/s$
G_k	Mass velocity defined by Kern	$kg/m^2/s$
h	Heat transfer coefficient	$kw/m^{2o}C$
h_o	Bundle average shell-side transfer coefficients	$kw/m^{2o}C$
i	Electrical current	A
i_L	Limiting (or diffusion) current	A
k	Thermal condictivity evaluated at bulk temperature	w/m^oC
k_c, k_m	Mass transfer coefficient	m/s
L, ℓ	Characteristic length	m
L_c	Baffle overlap	m
L_s	Baffle-spacing	m
L_T	Total exchanger length	m
m	Exponent	
n	Exponent	
N	Number of tube rows in crossflow zone	
N_A	Rate of mass transfer	kg mole/m^2s
n_e	Valency of an ion (equal to 1)	
p	Tube Pitch	m
ΔP	Overall pressure drop	N/m^2
$\Delta P_{L,CORR}$	Corrected overall bundle pressure drop for leakage	N/m^2
Q	Shell-side fluid volumetric flow rate	m^3/s

Symbol	Title	Units
S	Cathode surface area	m^2
S_L	Total surface area of tubes in exchanger	m^2
S/B	Shell-to-baffle leakage diametrical clearance	mm
t/b	Tube-to-baffle leakage diametrical clearance	mm
T	Temperature of fluid	^oC
V	Fluid velocity	m/s
V_{AV}	$1/3\ (V_{min} + V_{max} + V_w)$	m/s
V_G	Ideal bundle crossflow velocity	m/s
V_m	Shell-side velocity based on flow area A_m	m/s
V_w	Shell-side velocity based on flow area A_m	m/s
V_y	Shell-side velocity based on flow area $(A_m^2.A_w)^{1/3}$	m/s
V_Z	Shell-side velocity based on area $(A_m.A_w)^{\frac{1}{2}}$	m/s
W	Shell-side fluid mass flow rate	kg/s
Z	Orifice shape factors	

Greek Symbols

α	Effectiveness factor	
η	Kinematic viscosity, μ/ρ	m^2/s
μ	Fluid viscosity evaluated at bulk temperature	Ns/m^2
μw	Fluid viscosity evaluated at wall temperature	Ns/m^2
ρ	Fluid Density evaluated at bulk temperature	kg/m^3
σ	Standard deviation	

Symbol	Title	Units
	Angle between fluid flow and surface	Rad

Dimensionless Groups

$F_{\Delta p}$	Pressure drop factor $\Delta p \frac{d^3 \rho}{\mu L_T}$
j	Individual tube transfer j-factor
j_{av}	Compartment average transfer j-factor
jc	Crossflow zone average mass transfer j-factor
j_h	Heat transfer j-factor, $\frac{h}{C_p \rho v}.Pr^{2/3}$
j_m	Mass transfer j-factor, $\frac{K_c}{v} Sc^{2/3}$
Nu	Nusselt number, $\frac{hd}{k}$
Pr	Prandtl number, $\frac{C_p \mu}{k}$
Re	Shell-side Reynolds number, $\frac{dv\rho}{\mu}$
Re_I^*	Average Reynolds number over the bundle for the bundle with different baffle-spacing compartments
Sc	Schmidt number, $\frac{\mu}{\rho Dv}$
Sh	Sherwood number, $\frac{k_m d}{Dv}$
St	Stanton number, $\frac{h}{c\rho v}$

Subscripts

Av	Based on Vav
B	Bundle bypass stream
c	Based on Vc
Comp, Av	Compartment average value
eff	Effective value

Symbol	Title	Units
ek	Based on equivalent hydraulic diameter defined by Kern	
h	Heat transfer process	
I	Based on flow area A_I	
I,New	Based on flow area (A_I+A_L)	
K	Based on Kern's interpretation	
ℓ	Local effects	
L	Leakage case	
m	Mass transfer process	
m	Based on A_m	
max	Based on A_{max}	
min	Based on A_{min}	
NL	Without baffle leakage	
O	Overall value	
w	Based on A_w	
y	Based on V_y	
z	Based on V_z	

APPENDIX 1

Calibration of Flowmeters

Two variable area flowmeters of sizes 65 and 18 (metric) were used to measure the electrolyte flow rate. In order to increase the accuracy of the results, the error in the flow rate had to be reduced. This required calibration of the flowmeters with electrolyte as the flowing media. The previous users, Mackley, Macbeth and Prowse all used water for the calibration runs and applied the resulting curve for determining the electrolyte flow. The physical properties, especially viscosity of the two fluids would effect the accuracy of the flow rate. A better technique was needed to increase the accuracy of the flowmeters.

The following procedure was used to calibrate the flowmeter with electrolyte as the flowing medium. A direct calibration of the flowmeters using the electrolyte instead of water was hazardous and costly, especially because of the very high flow rates involved. The following indirect method was found to be satisfactory. The Rotameter Manufacturing Company calibration techniques (76) were used to generate calibration curves for the two flowmeters with the electrolyte physical properties. The two equations of interest were:

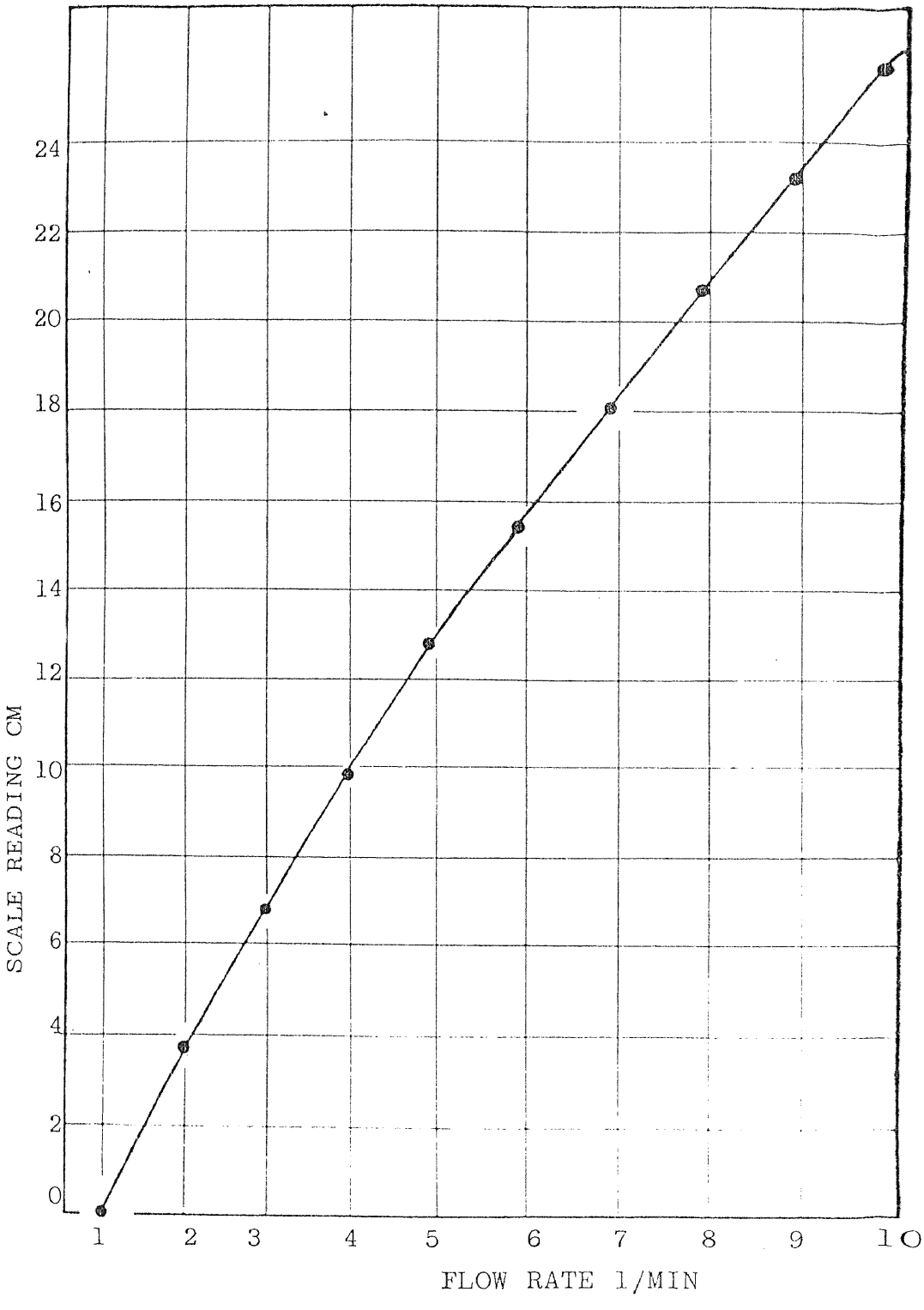

Figure A1.1 Calibration of Rotameter Size 18

$$I = \text{Log } \{K_i \nu \frac{\sigma\rho}{\omega(\sigma-\rho)} 10^4\} \qquad (A1.1)$$

and

$$F_r = K_2 \frac{\omega(\sigma-\rho)}{\sigma\rho} \qquad (A.1.2)$$

where ν ρ σ ω are the fluid kinematic viscosity, fluid density and float weight all in c.g.s. units. K_1 and K_2 are instrument constants which vary with its size. The co-ordinates I and F_r were used with the empirical correlations provided by (76) to produce the calibration curve. The points for calibration curves are shown in Tables A1.1 and A1.2 and the curves depicted in Figures A1.1-2 for Rotameter sizes 18 and 65.

Two tests were made to check the accuracy and the correctness of this technique. Firstly, the experimental calibration data of Mazar (77), using three different concentrations (1 m, 5.38 m, 7.62 m) of sodium hydroxide solution in Rotameter sizes 7 and 24, were compared with corresponding curves generated from the above technique (76). As the flow rates were small in Mazar's case, experimental investigation was safely attempted. The agreement between the analytical and experimental data of (76) and (77) respectively was within the experimental accuracy of 1%. Secondly, the present Rotameters were experimentally calibrated with water as the flowing medium, and compared with the corresponding curve obtained analytically. The agreement between the analytical and experimental data was again within the experimental accuracy of 1%. Hence the analytical procedure for each fluid and flowmeter tested accurately predicted the experimental calibration

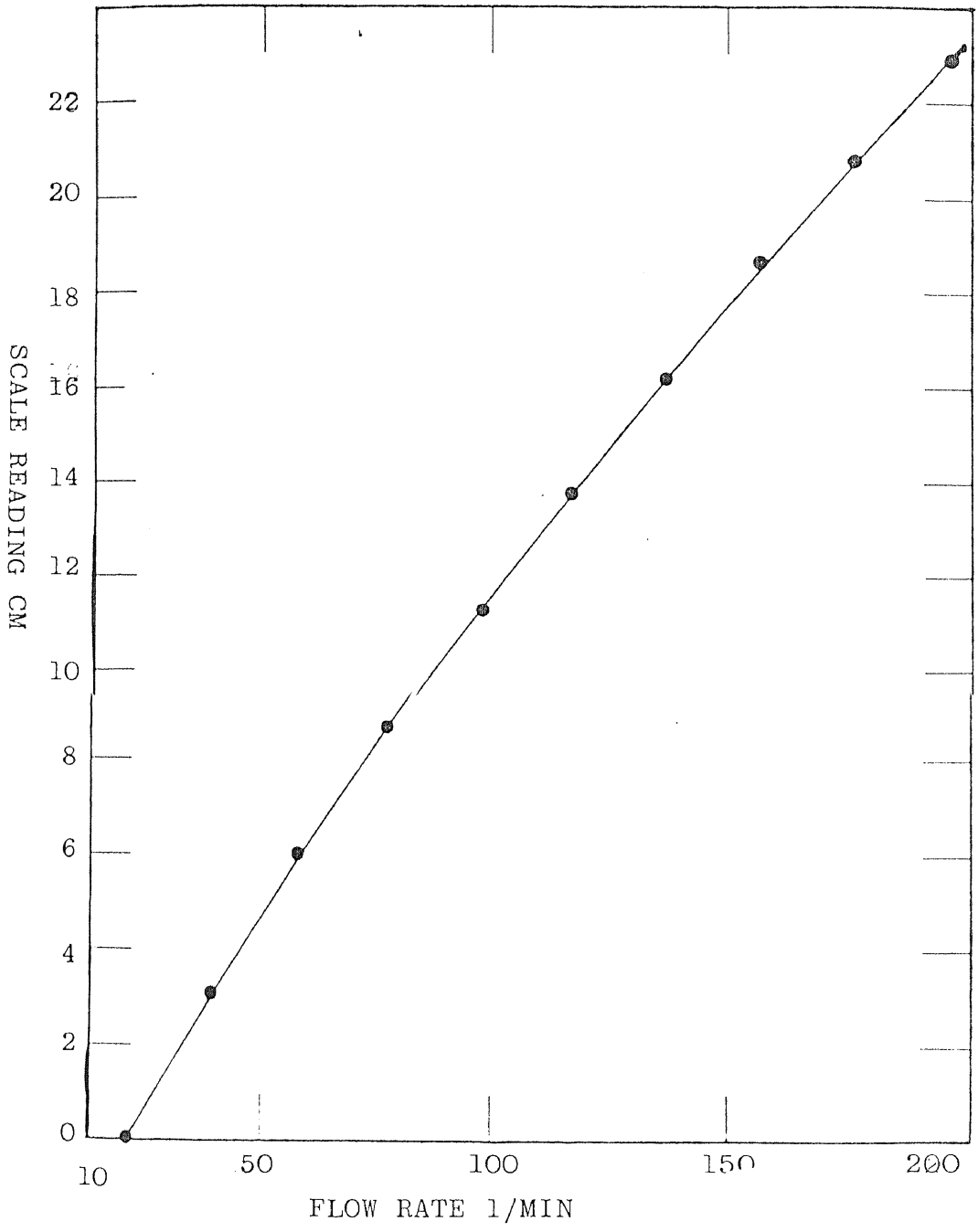

Figure A.1.2 Calibration of Rotameter Size 65

data.

The difference between the water and electrolyte calibration curves was of the order of 5% with the electrolyte showing lower values.

TABLE (A1.1) Analytical Calibration of Rotameter Size 18, using Electrolyte as Flow Medium

Scale Reading CM	0.1	6.8	9.9	12.8	15.4	18.1	23.2
Flow Rate L/M	1.0	2.9	3.9	4.8	5.8	6.9	8.8

TABLE (A1.2) Analytical Calibration of Rotameter Size 65, using Electrolyte as Flow Medium

Scale Reading CM	0.1	3.1	6	8.7	11.3	13.8	16.2	18.7	20.8
Flow Rate L/M	10.9	39	58	78	98	117	137	156	176

APPENDIX 1

Pretreatment of Electrodes

Previous users found that chemical polarisation was an occasional problem when operating with the ferri-ferrocyanide system, particularly if the electrode surfaces were not pretreated before operation. A series of pretreatment processes proposed by Eisenburg et al (75), have since been adopted. Mackley extended Eisenburg's procedure for the pretreatment of the nickel anode and cathodes. He found that satisfactory results were obtained by polishing the electrode surfaces with a fine emery paper. An activation process was then performed by evolving hydrogen at the electrode surface. The current density used for this cathode activation was 0.1 mA/mm^2 for five minutes. This same procedure was used in the present study. The operational anode was also pretreated by using an activation anode during the activation process. The former electrode being connected to the negative terminal.

After a series of experimental tests the tube bundles was removed. In order to pretreat the electrode surface an alternative to the polishing treatment was required so as to avoid disassembly of the bundle. This

was done by thoroughly rinsing the tube bundle with distilled water to remove any traces of electrolyte and then immersed in a 10% solution of hydrochloric acid for 1 to 2 minutes. After removal, the bundle was again thoroughly washed with distilled water prior to replacement in the shell.

APPENDIX A3

Accuracy of Experimental Data

The accuracy of the mass transfer coefficient and $(Sh/Sc^{1/3})$ data reported in this work were derived from the estimated accuracies of the electrolyte solution physical property data and of the experimental measurements made. The mass transfer coefficient is given by:

$$K_M = \frac{I_L}{SC_b neF} = \frac{I_L}{(\overline{A}L_c d)C_b neF} \qquad (A3.1)$$

and the dimensionless transfer coefficient groups by:

$$\left(\frac{Sh}{Sc^{1/3}}\right) = \frac{Kmd}{Dv} \; Sc^{-1/3} \qquad (A3.2)$$

The possible random and systemic error in each compartment term are now determined:

(1)	Concentration C_b	± 0.005	Mazar (77), Prowse (4)
(2)	Diffusivity D_v (Independent of Temperature)	± 0.03	Eisenberg (59)
(3)	Tube diamteter d	± 0.001	Micrometer limit
(4)	Limiting Current I_L	± 0.008	(Measurement and Fluctuation)
(5)	Electrode length L	± 0.003	Measuring Limit
(6)	Surface Area S	± 0.004	Measuring Limits
(7)	Velocity (i.e. Flow Rate) V	± 0.02	(Calibration accuracy and Fluctuations in Flow)

8)	Kiematic viscosity η (Independent of Temperature)	± 0.02	Mackley (3)

By summation of constituent errors, the accuracy of the mass transfer data is estimated.

9)	Schmidt number $Sc=(\frac{\eta}{D_v})$ Thus for $Sc^{1/3}$	± 5 per cent ± 1.7 per cent
10)	Mass transfer coefficient K_m	± 1.7 per cent
11)	Dimensionless transfer coefficient $(Sh/Sc^{1/3})$	± 6.5 per cent
12)	Reynolds number $(\frac{dV}{\eta})$	± 4.1 per cent

TABLE A4.1 CONFIGURATIONS EXAMINED IN THIS PRESENT WORK

RUN NO.	BC %	NO.OF COMPART-MENTS	NO.OF COMPS. STUDIED	FLOW TYPE	CLEARANCES		COMPARTMENT BS	
					S/B	T/B	END	INTERNAL
1	18.4	8	1 to 4	TOP - BOTTOM	0.5	0	47.6	47.6
2	18.4	8	1 to 4	"	0	0	47.6	47.6
3	18.4	8	5 to 8	"	0	0	47.6	47.6
4	18.4	4	1 to 2	"	0	0	47.6	149.2
6	18.4	8	1 to 4	"	2.2	0.5	47.6	47.6
7	18.4	6	1 to 6	"	2.2	0.5	47.6	66.6
8	18.4	4	1 to 4	"	2.2	0.5	97	97
9	18.4	5	1 to 5	SIDE - SIDE	2.2	0.5	47.6	97
10	18.4	4	1 to 4	TOP - BOTTOM	2.2	0.5	47.6	149.2

TABLE A4.2 RUN NUMBER 1

REYNOLDS NUMBER	COMPARTMENT AVERAGE $Sh/Sc^{1/3}$				BUNDLE Av. ($Sh/Sc^{1/3}$)
	INLET	SECOND	THIRD	FOURTH	
1596	29.9	32.8	33.3	31.9	32.0
2670	41.3	42.7	45.5	43.2	43.2
3730	48.0	48.5	49.9	45.1	47.9
4350	52.9	54.6	58.6	54.8	55.2
6750	64.9	70.7	72.9	65.2	68.4

TABLE A4.3 RUN NUMBER 2

Re_m	COMPARTMENT AVERAGE $Sh/Sc^{1/3}$				BUNDLE Av. ($Sh/Sc^{1/3}$)
	INLET	SECOND	THIRD	FOURTH	
312	14.4	16.2	16.9	16.2	15.9
316	13.7	15.8	16.5	16.2	15.5
811	23.4	25.5	26.8	26.9	25.6
2048	38.9	43.7	46.2	46.2	43.7
3755	57.8	64.2	66.7	67.1	63.9
4332	67.8	72.3	74.3	70.2	71.1
6750	76.4	-	94.6	96.3	89.1
7883	-	88.2	109.5	107	90.0

TABLE A4.5 RUN NUMBER 3

Re_m	COMPARTMENT AVERAGE $Sh/Sc^{1/3}$				BUNDLE Av. $Sh/Sc^{1/3}$
	OUTLET	SEVENTH	SIXTH	FIFTH	
805	24.1	27.5	28.2	28.1	26.9
2133	43.6	48.3	51.6	48.7	48.1
4332	60.5	68.6	75.2	72.8	69.3
6200	82.9	85.1	99.1	95.8	90.7
8070	87.5	103	111.6	107.5	102.4

TABLE A4.6 RUN NUMBER 4

Re_m END	$(Sh/Sc^{1/3})$Av.Comp. INLET	$(Sh/Sc^{1/3})$Av.Comp. SECOND	Re_m INTERNAL	$\frac{Sh}{Sc^{1/3}}_o$ *	Re_I*
768	21.9	15.5	245	17.1	368
1543	36.6	21.67	492	25.4	730
3286	47.6	32.2	1048	36.1	1554
3797	54.9	31.6	1210	37.4	1795
7510	80.0	49.0	2395	56.8	3551
7784	71.5	44.0	2483	50.9	3680

TABLE A4.7 RUN NUMBER 6

Re_m	$(Sh/Sc^{1/3})$av. COMPARTMENT *Inlet/Oulet	2nd*/7th	3rd*/6th	4th*/5th	$\frac{Sh}{Sc^{1/3}}_o$
171	6.96	7.07	7.27	7.33	7.16
318	9.54	9.85	10.3	9.63	9.83
732	14.9	15.9	16.1	15.4	15.6
1467	19.9	21.0	21.3	20.2	20.6
2468	29.3	30.4	30.9	29.6	30.0
4042	34.3	36.1	35.6	33.0	34.8
7046*	49.4	51.5	52.0	54.1	52.2
7382	50.9	52.3	52.8	50.3	51.6
10350	62.8	67.7	63.6	63.3	64.3

TABLE A4.8 RUN NUMBER 7

Re_m END	COMPARTMENT $(Sh/Sc^{1/3})$ *INLET/OUT	2nd*/5th	3rd*/4th	Re_m INTERNAL	$\frac{Sh}{Sc^{1/3}}_o$	$Re_{I,NEW}$*
171	6.76	6.64	7.46	122	6.98	92
638	12.9	12.2	13.6	455	12.9	343
1467	21.9	20.6	22.2	1047	21.6	787
3668	34.3	32.0	35.0	2618	33.7	1970
6091*	45.6	45.9	47.2	4347	46.3	3670
8396*	56.1	52.1	56.7	5990	54.8	4500

TABLE A4.9 RUN NUMBER 8

Re_m	INLET*/OUTLET	2nd*/3rd	$(Sh/Sc^{1/3})_o$
	$(Sh/Sc^{1/3})$ Av.		
158*	7.47	8.0	7.79
309	10.5	9.98	10.2
726*	17.6	19.0	18.3
735	18.6	18.5	18.5
1735	30.2	28.6	29.4
2633	37.3	36.2	36.7
3510	43.7	42.1	42.9
4690*	50.1	53	51.6

TABLE A4.10 RUN NUMBER 9

Re_m END	$(Sh/Sc^{1/3})$ Av.					Re_m INTERNAL	$\frac{Sh}{Sc^{1/3}}_b$	Re_I*
	INLET	SECOND	THIRD	FOURTH	OUTLET			
653	14.4	14.75	13.4	13.4	14.8	320	13.9	328
3170	36.0	31.2	31.8	32.3	39.6	1555	33.3	1591
6673	52.8	51.0	50.0	49.7	57.4	3275	51.5	3350
9927	65.4	65.3	63.7	63.8	59.9	4870	63.7	4980

TABLE A4.11 RUN NUMBER 10

Re_m END	$(Sh/Sc^{1/3})$ Av.		Re_m INTERNAL	$\frac{Sh}{Sc^{1/3}_o}$	$Re^*_{I,NEW}$
	INLET/OUTLET	SECOND/THIRD			
624	14.3	9.86	198	10.97	186
1500	24.8	17.7	477	18.7	447
3170	33.7	24.75	1007	27.0	1177.5
5505	45.6	33.1	1750	36.2	1640
9927	69.2	49.3	3154	54.3	2960
638*	13.6	10.1	203	11.3	190
1500*	23.0	16.7	477	18.3	447
5570*	39.3	32.4	1769	34.2	1660
3265*	33.2	25.2	1037	27.2	973
9810*	58.9	45.4	3118	48.6	2925

TABLE A4.12 RUN NUMBER 2 - PRESSURE DROP DATA

REYNOLDS NUMBER Re_m	PRESSURE DROP N/M^2 x 10^3	$\frac{\Delta P d^3}{L\mu^2}$ x 10^{-7}
900	0.53	0.096
2044	0.66	0.12
2586	2.126	.387
3670	5.32	.968
4879	9.56	1.74
6089	14.61	2.66
7298	21.3	3.88
7966	24.7	4.5
8591	28.3	5.15
9258	33.1	6.02
9926	37.61	6.85

TABLE A4.13 RUN NUMBER 4 - PRESSURE DROP

REYNOLDS NUMBER		ΔP N/M^2 x 10^{-3}	Re_I*	Fp x 10^{-6}
END	INTERNAL			
1440	480	-	688	-
1956	652	-	935	-
2475	825	.667	1183	1.21
3797	1170	2.20	1781	4.0
4629	1543	4.13	2213	7.5
5826	1942	6.33	2785	11.5
7509	2328	9.20	3527	16.7
7784	2541	11.20	3702	20.4
8223	2741	12.80	3931	23.3
8859	2953	14.67	4235	26.7
9498	3166	17.20	4540	31.3
10695	3565	22.13	5112	40.3

TABLE A4.14 RUN NUMBER 6 - PRESSURE DROP

Re_m	ΔP (N/M^2)	FL x 10^{-6}	FL_{corr} x 10^{-6}
179.4	14.7	0.027	0.084
353	39	0.071	0.222
811.7	147	0.268	0.838
1538	4 70	0.855	2.68
2649	580	1.056	3.32
4444	29 00	5.280	16.50
7562	6911	12.580	39.5
7562	7460	13.580	42.55
10852	13220	24.07	

TABLE A4.15 RUN NUMBER 7 - PRESSURE DROP

Re_m END	Re_I*	ΔP N/M^2 x 10^{-3}	F_L x 10^{-6}	$F_{L,corr}$ x 10^{-6}
171	99	.0137	0.025	0.068
624	362	.055	0.10	0.274
1470	852	.219	0.40	1.09
3670	2130	1.316	2.39	6.55
6240	3622	3.480	6.33	17.30
8403	4877	5.923	10.78	29.33

$$Re_I^* = \tfrac{1}{3}\,(2Re_{I,INTERNAL} - Re_{I,END})$$

$$F_{L,CORR} = \frac{F_L}{\left[1 - \frac{A_{SB}}{0.33(2A_{I,INT.} - A_{I,END})}\right]}$$

TABLE A4.16 RUN NUMBER 8 - PRESSURE DROP

Re_m	Re_I	F_L x 10^{-6}	$F_{L,corr}$ x 10^{-6}	ΔP N/M^2 x 10^{-3}
165	118	0.018	0.04	0.01
315	226	0.04	-	0.022
743	533	0.286	0.637	0.157
743*	533	0.375	0.834	0.206
1815	1302	1.48	3.3	0.814
1815*	1302	1.37	3.05	0.752
2723	1953	2.97	6.61	1.63
3630*	2600	4.28	9.53	2.35
3630	2600	4.48	9.97	2.46

TABLE A4.17 RUN NUMBER 9 - PRESSURE DROP

Re_m END	Re_m INTERNAL	Re_I*	ΔP N/M^2 x 10^{-3}	F_L x 10^{-6}	$F_{L,corr}$ x 10^{-6}
328	161	163	0.024	.0437	0.106
636	308	317	0.059	.107	0.261
636	308	317	0.058	.107	0.26
1395	684	694	0.255	.464	1.13
1395	684	694	0.26	.473	1.15
2543	1248	1266	0.628	1.14	2.78
2543	1248	1266	0.642	1.17	2.84
3160	1530	1573	0.883	1.61	3.9
3160	1530	1573	0.9	1.65	4.02
6672	3232	3322	3.4	6.19	15.04
9925	4808	4940	6.973	12.7	30.8
9925	4808	4940	7.21	13.1	31.9

$$Re_I^* = 0.2\ (3Re_{I,INTERNAL} + 2Re_{I,END})$$

TABLE A4.18 RUN NUMBER 10 - PRESSURE DROP

Re_m END	Re_m INTERNAL	Re_I*	ΔP N/M^2 x 10^{-3}	F_L x 10^{-6}	$F_{L,corr}$ x 10^{-6}
1503	480	540	.200	0.364	0.8
2080	667	745	.325	0.592	1.3
3170	1015	1136	.721	1.31	4.8
4240	1360	1520	1.187	2.16	4.8
5505	1765	1974	1.99	3.62	8.0
6652	2133	2390	2.844	5.18	11.5
10770	3170	3865	6.017	11.0	23.55

$$Re_I^* = \tfrac{1}{2}(Re_{I,END} + Re_{I,INTERNAL})$$

$$F_{L,corr} = \frac{F_L}{\left[1 - \left(\frac{A_{SB}}{\frac{1}{2}(A_{I,END} + A_{I,INTERNAL})}\right)^{0.4}\right]^2}$$

TABLE A4.19 FLOW AREAS

BC(%)	18.4	25	31	37.5	43.7	BS(mm)
FLOW AREA						
AM	1896	1896	1896	1896	1896	48.5
AI	2543	2740	2693	3395	3105	48.5
AW	1152	1660	2220	2870	3400	48.5

For different baffle spacings the flow area is determined by multiplying the above flow areas by the ratio (BS/48.5).

TABLE A4.20 FLOW AREAS - LEAKAGE

$Re_{I,NEW}$	BS(mm)	BC(%)	S/B mm	t/b mm	A_{TB}	A_{SB}	A_L
3217	48.5	18.4	1.4	0.33	361	209	574
3776	48.5	18.4	2.66	0.66	741	392	1133
3790	48.5	25	2.66	0.66	685	364	1050
4265	48.5	37.5	2.66	0.66	552	317	870
3088	48.5	18.4	0.53	0.33	365	80	445
3508	48.5	18.4	3.38	0.33	365	504	865
3246	48.5	18.4	1.6	0.33	365	238	603
3481	47.6	18.4	2.2	0.5	557	330	887

TABLE A4.21 FLOW AREAS - SEE FIG. III.4

BS(mm)	BC(%)	A_A'	A_B'	A_C'	A_I
48.5	18.4	2955	3380	2083	2643
48.5	25.0	3250	4690	1928	2740
48.5	37.5	4550	9298	2310	3395

10
BAFFLE SPACING (MM) =149.8 BAFFLE CUT (%) =18.4
B/S CLEARANCE (MM) =0.00 T/B CLEARANCE (MM) =0.00
FLOW RATE = 119.0 TEMP (DEG C) =25.0 VELOCITY =1.096
REYNOLDS NO. =4.1194E 04 SCHMIDT NO. =1560. END COMP REYNOLDS NO. =4.9927E 04

INDIVIDUAL TUBE COEFFICIENTS (SH/(SC)1/3)

TUBE						
75	6.52E 01	5.13E 01	4.03E 01	3.49E 01	3.16E 01	4.92E 01
71	6.43E 01	5.38E 01	5.07E 01	5.39E 01	0.00E 00	6.77E 01
79	6.38E 01	7.42E 01	0.00E 00	5.57E 01	5.40E 01	6.63E 01
9	0.00E 00	5.40E 01	0.00E 00	3.18E 01	3.23E 01	4.80E 01
55	7.65E 01	5.79E 01	4.40E 01	3.22E 01	2.98E 01	5.34E 01
4	6.23E 01	4.50E 01	3.99E 01	3.17E 01	3.88E 01	0.00E 00
64	6.75E 01	6.30E 01	1.20E 02	3.92E 01	3.94E 01	0.00E 00
10	6.75E 01	5.34E 01	3.72E 01	3.27E 01	3.37E 01	5.63E 01
44	6.52E 01	6.18E 01	0.00E 00	0.00E 00	0.00E 00	0.00E 00
50	6.30E 01	0.00E 00	4.40E 01	3.47E 01	3.16E 01	6.05E 01
28	6.52E 01	4.89E 01	3.47E 01	3.25E 01	3.51E 01	5.82E 01
67	7.76E 01	6.18E 01	0.00E 00	1.00E 02	0.00E 00	1.00E 02
73	0.00E 00	5.73E 01	5.18E 01	5.13E 01	4.72E 01	6.36E 01
34	6.30E 01	0.00E 00	3.73E 01	2.87E 01	3.16E 01	4.87E 01
14	0.00E 00	5.12E 01	3.68E 01	2.84E 01	3.41E 01	5.07E 01
36	6.41E 01	4.95E 01	3.60E 01	3.94E 01	4.36E 01	4.52E 01
62	0.00E 00	0.00E 00	4.83E 01	3.89E 01	3.79E 01	5.18E 01
16	5.69E 01	5.51E 01	3.82E 01	3.15E 01	4.25E 01	5.79E 01
29	6.86E 01	5.03E 01	0.00E 00	0.00E 00	3.83E 01	0.00E 00
63	6.63E 01	5.96E 01	5.04E 01	0.00E 00	4.30E 01	4.95E 01

AVE	6.52E 01	5.52E 01	4.23E 01	4.07E 01	3.79E 01	5.00E 01
LE	47.6	47.6	23.8	23.8	23.8	23.8
COMP	OUTLET	THIRD				

10

BAFFLE SPACING (MM) =149.8 BAFFLE CUT (%) =18.4

B/S CLEARANCE (MM) =0.00 T/B CLEARANCE (MM) =0.00

FLOW RATE (KG/S) = [illegible] TEMP (DEG C) =24.5 VELOCITY =1.096

REYNOLDS NO = [illegible] SCHMIDT NO =1600. END COMP REYNOLDS NO. =9.9813E 04

INDIVIDUAL TOWER COEFFICIENTS (SH/(SC)1/3)

CUT						
35	5.79E 01	3.92E 01	4.87E 01	5.48E 01	4.85E 01	6.40E 01
78	7.25E 01	4.00E 01	3.27E 01	3.62E 01	0.00E 00	6.32E 01
29	5.73E 01	0.00E 00	0.00E 00	3.77E 01	4.30E 01	6.35E 01
9	0.00E 00	4.02E 01	0.00E 00	5.37E 01	4.71E 01	5.30E 01
55	7.25E 01	4.15E 01	2.78E 01	3.93E 01	5.16E 01	6.42E 01
4	5.17E 01	0.00E 00	4.14E 01	5.11E 01	4.39E 01	0.00E 00
64	6.91E 01	0.00E 00	0.00E 00	0.00E 00	4.70E 01	4.79E 01
10	5.16E 01	5.01E 01	4.00E 01	4.43E 01	5.49E 01	6.20E 01
44	0.00E 00	0.00E 00	0.00E 00	0.00E 00	0.00E 00	0.00E 00
50	5.67E 01	0.00E 00	3.62E 01	5.61E 01	4.16E 01	5.83E 01
28	5.04E 01	5.05E 01	5.10E 01	5.07E 01	4.87E 01	5.46E 01
69	0.00E 00	4.15E 01	0.00E 00	8.31E 01	0.00E 00	8.42E 01
73	0.00E 00	4.94E 01	3.36E 01	3.65E 01	4.43E 01	6.69E 01
34	5.51E 01	0.00E 00	0.00E 00	3.84E 01	4.77E 01	5.64E 01
14	0.00E 00	4.36E 01	4.83E 01	4.90E 01	4.46E 01	5.38E 01
36	6.24E 01	3.64E 01	0.00E 00	0.00E 00	4.34E 01	6.14E 01
62	0.00E 00	0.00E 00	3.17E 01	3.65E 01	4.69E 01	5.99E 01
16	5.34E 01	3.79E 01	2.58E 01	3.76E 01	5.50E 01	6.54E 01
29	5.39E 01	3.90E 01	0.00E 00	0.00E 00	4.18E 01	0.00E 00
63	6.04E 01	0.00E 00	3.10E 01	0.00E 00	4.39E 01	5.44E 01
AVE	5.69E 01	4.11E 01	3.78E 01	4.71E 01	4.67E 01	6.08E 01
LE	47.6	47.6	23.8	23.8	23.8	23.8
COMP	INLET	SECOND				

10

BAFFLE SPACING (MM) =*149.8 BAFFLE CUT (%) =18.4

B/S CLEARANCE (MM) =0.00 T/B CLEARANCE *(MM) =0.00

FLOW RATE =66.0 TEMP (DEG.C) =25.0 VELOCITY =0.608

REYNOLDS NO. =*.1749E 04 SCHMIDT NO. =1560. END COMP REYNOLDS NO. =*.5505E 04

INDIVIDUAL TUBE COEFFICIENTS (SH/(SC)1/3)

*TUBE						
20	4.05E 01	3.62E 01	2.92E 01	2.60E 01	2.21E 01	3.43E 01
78	0.00E 00	3.88E 01	3.51E 01	3.80E 01	0.00E 00	4.72E 01
79	0.00E 00	0.00E 00	4.08E 01	3.89E 01	3.94E 01	4.71E 01
9	0.00E 00	3.84E 01	0.00E 00	2.19E 01	2.14E 01	3.23E 01
55	4.27E 01	4.27E 01	3.22E 01	2.35E 01	2.06E 01	3.38E 01
4	4.10E 01	3.31E 01	2.69E 01	2.33E 01	2.59E 01	0.00E 00
64	4.77E 01	0.00E 00	0.00E 00	2.79E 01	2.78E 01	0.00E 00
10	4.77E 01	3.94E 01	2.70E 01	2.35E 01	2.45E 01	3.72E 01
44	0.00E 00	0.00E 00	0.00E 00	0.00E 00	0.00E 00	0.00E 00
50	4.37E 01	0.00E 00	3.01E 01	2.55E 01	2.01E 01	3.81E 01
28	4.65E 01	3.59E 01	2.59E 01	2.36E 01	2.41E 01	3.90E 01
69	0.00E 00	4.08E 01	0.00E 00	0.00E 00	0.00E 00	0.00E 00
73	0.00E 00	4.16E 01	3.60E 01	3.72E 01	3.38E 01	4.31E 01
34	4.76E 01	0.00E 00	2.75E 01	2.20E 01	2.25E 01	3.40E 01
14	0.00E 00	3.66E 01	2.70E 01	2.18E 01	2.07E 01	3.44E 01
36	4.50E 01	3.53E 01	3.11E 01	3.49E 01	2.59E 01	3.23E 01
62	0.00E 00	0.00E 00	3.46E 01	2.81E 01	2.21E 01	3.47E 01
16	4.60E 01	3.92E 01	2.92E 01	2.48E 01	2.48E 01	3.94E 01
29	4.78E 01	3.55E 01	0.00E 00	0.00E 00	2.05E 01	0.00E 00
63	4.69E 01	4.05E 01	3.43E 01	0.00E 00	2.35E 01	3.36E 01

AVE	4.06E 01	3.77E 01	3.14E 01	2.78E 01	2.47E 01	3.74E 01
LE	47.6	47.6	23.8	23.8	23.8	23.8
COMP	OUTLET	THIRD				

10

BAFFLE SPACING (MM)=*149.8 BAFFLE CUT (%) =18.4

B/S CLEARANCE (MM) =0.00 T/B CLEARANCE *(MM) =0.00

FLOW RATE =45.0 TEMP (DEG C) =25.5 VELOCITY =0.608

REYNOLDS NO. =* 1.20E 04 SCHMIDT NO. =1522. END COMP REYNOLDS NO. =*.5569E 04

INDIVIDUAL TUBE COEFFICIENTS (SH/(SC)1/3)

TUBE						
30	4.85E 01	2.50E 01	1.66E 01	2.35E 01	3.65E 01	4.56E 01
70	0.00E 00	0.00E 00	2.09E 01	2.59E 01	0.00E 00	4.56E 01
79	0.00E 00	2.80E 01	0.00E 00	3.80E 01	3.35E 01	3.81E 01
9	0.00E 00	2.83E 01	2.22E 01	2.92E 01	3.68E 01	4.53E 01
55	3.72E 01	0.00E 00	2.98E 01	3.47E 01	3.03E 01	0.00E 00
4	0.00E 00	3.65E 01	0.00E 00	3.36E 01	3.46E 01	0.00E 00
64	3.59E 01	3.45E 01	2.92E 01	3.20E 01	3.84E 01	4.40E 01
10	0.00E 00	0.00E 00	0.00E 00	0.00E 00	0.00E 00	0.00E 00
44	4.07E 01	0.00E 00	1.79E 01	2.23E 01	3.06E 01	4.07E 01
50	3.67E 01	3.73E 01	3.75E 01	3.71E 01	3.60E 01	4.21E 01
28	0.00E 00	3.04E 01	0.00E 00	6.22E 01	0.00E 00	6.38E 01
49	0.00E 00	3.47E 01	2.45E 01	2.75E 01	3.34E 01	4.93E 01
73	3.67E 01	7.51E 00	1.54E 01	3.12E 01	3.54E 01	4.27E 01
34	0.00E 00	3.17E 01	3.81E 01	3.56E 01	3.31E 01	4.00E 01
14	4.42E 01	2.41E 01	1.75E 01	2.25E 01	3.34E 01	4.62E 01
36	0.00E 00	0.00E 00	2.08E 01	2.83E 01	3.54E 01	4.44E 01
62	3.83E 01	2.61E 01	2.14E 01	3.18E 01	3.87E 01	4.73E 01
16	3.90E 01	2.41E 01	4.78E 01	0.00E 00	3.14E 01	0.00E 00
29	4.39E 01	3.06E 01	2.08E 01	0.00E 00	3.34E 01	3.97E 01
63	0.00E 00	0.00E 00	0.00E 00	0.00E 00	0.00E 00	0.00E 00

AVE	[illegible]	[illegible]	[illegible]	3.02E 01	3.44E 01	4.50E 01
LE	47.6	47.6	23.8	23.8	23.8	23.8
COMP	INLET	SECOND				

10
BAFFLE SPACING (MM)= *149.8 BAFFLE CUT (%) =18.4
B.S CLEARANCE (MM) = 0.60 T/B CLEARANCE (MM) =0.00
FLOW RATE =33.0 TEMP (DEG C) =25.0 VELOCITY =0.350
REYNOLDS NO. =4.1007E 04 SCHMIDT NO =1560. END COMP REYNOLDS NO. =*.317.0E 04

INDIVIDUAL TUBE COEFFICIENTS (SH/(SC)1/3)

NO.						
59	3.27E 01	2.66E 01	2.20E 01	2.02E 01	1.71E 01	2.20E 01
78	3.65E 01	2.87E 01	2.66E 01	2.89E 01	0.00E 00	3.37E 01
79	0.00E 00	0.00E 00	3.04E 01	2.83E 01	2.98E 01	3.49E 01
9	0.00E 00	2.75E 01	0.00E 00	1.69E 01	1.56E 01	2.14E 01
55	3.30E 01	3.00E 01	2.40E 01	1.89E 01	1.54E 01	2.17E 01
4	3.02E 01	2.48E 01	2.00E 01	1.65E 01	1.91E 01	0.00E 00
54	3.45E 01	3.18E 01	0.00E 00	2.17E 01	2.15E 01	0.00E 00
10	3.52E 01	2.95E 01	2.02E 01	1.75E 01	1.74E 01	2.44E 01
44	0.00E 00	0.00E 00	0.00E 00	0.00E 00	0.00E 00	0.00E 00
50	3.16E 01	0.00E 00	2.15E 01	1.99E 01	1.52E 01	2.54E 01
28	3.43E 01	2.71E 01	1.98E 01	1.75E 01	1.79E 01	2.54E 01
69	3.49E 01	3.21E 01	0.00E 00	5.05E 01	0.00E 00	3.15E 01
73	0.00E 00	3.17E 01	2.63E 01	2.68E 01	2.56E 01	3.13E 01
34	3.49E 01	1.50E 01	2.10E 01	1.70E 01	1.61E 01	2.18E 01
14	0.00E 00	2.72E 01	2.02E 01	1.63E 01	1.55E 01	2.28E 01
36	3.30E 01	2.54E 01	2.80E 01	2.81E 01	1.91E 01	2.28E 01
62	0.00E 00	0.00E 00	2.59E 01	2.25E 01	1.66E 01	2.17E 01
16	3.30E 01	2.91E 01	2.11E 01	1.81E 01	1.80E 01	2.70E 01
29	3.49E 01	2.59E 01	5.06E 01	0.00E 00	1.48E 01	0.00E 00
63	3.32E 01	3.09E 01	0.00E 00	0.00E 00	1.80E 01	2.11E 01

AVE	3.37E 01	2.91E 01	2.09E 01	2.27E 01	1.84E 01	2.56E 01
IE	47.6	47.6	23.8	23.8	23.8	23.8
COMP	OUTLET	THIRD				

TO

BAFFLE SPACING (MM) =149.0 BAFFLE CUT (%) =18.4

B.S. CLEARANCE (MM) 0.00 T/B CLEARANCE (MM) =0.00

FLOW RATE 88.0 TEMP (DEG C) =26.3 VELOCITY =0.350

REYNOLDS NO. =*.3265E 04 SCHMIDT NO =1464. END COMP REYNOLDS NO. =*.3265E 04

INDIVIDUAL TUBE COEFFICIENTS (SHZ/(SC)1/3)

TUBE						
76	3.05E 01	1.70E 01	1.36E 01	2.11E 01	2.68E 01	3.43E 01
78	3.89E 01	2.41E 01	1.93E 01	2.08E 01	0.00E 00	3.51E 01
79	0.00E 00	3.21E 01	0.00E 00	2.07E 01	2.58E 01	3.70E 01
9	0.00E 00	2.04E 01	0.00E 00	2.76E 01	2.50E 01	2.90E 01
55	3.71E 01	2.04E 01	1.82E 01	2.24E 01	2.76E 01	3.31E 01
4	2.69E 01	3.36E 01	2.77E 01	2.68E 01	2.35E 01	0.00E 00
64	3.92E 01	2.40E 01	4.32E 01	5.01E 01	2.65E 01	0.00E 00
10	2.72E 01	2.04E 01	2.29E 01	2.49E 01	2.89E 01	3.41E 01
44	0.00E 00	0.00E 00	0.00E 00	0.00E 00	0.00E 00	0.00E 00
50	3.34E 01	0.00E 00	1.42E 01	1.89E 01	2.24E 01	3.95E-01
38	2.95E 01	2.84E 01	2.80E 01	2.83E 01	2.83E 01	3.10E 01
69	4.32E 01	2.21E 01	0.00E 00	2.37E 01	0.00E 00	2.41E 01
73	0.00E 00	2.49E 01	1.09E 01	2.14E 01	2.58E 01	3.72E 01
34	3.26E 01	0.00E 00	1.46E 01	2.43E 01	2.61E 01	3.16E 01
14	0.00E 00	2.45E 01	2.05E 01	2.57E 01	2.49E 01	2.97E 01
35	3.17E 01	1.63E 01	1.30E 01	1.96E 01	2.54E 01	3.51E 01
62	0.00E 00	0.00E 00	1.85E 01	2.15E 01	2.62E 01	3.37E 01
16	2.83E 01	1.81E 01	1.91E 01	2.57E 01	2.89E 01	3.59E 01
29	3.02E 01	1.70E 01	3.02E 01	0.00E 00	2.37E 01	0.00E 00
67	3.43E 01	0.00E 00	1.70E 01	0.00E 00	2.52E 01	2.90E 01
AVE	3.02E 01	2.24E 01	2.19E 01	2.49E 01	2.59E 01	3.07E 01
LE	47.6	47.6	23.8	23.8	23.8	23.8
COMP	INLET	SECOND				

10

BAFFLE SPACING (MM)=*149.8 BAFFLE CUT (%) =18.4

B/S CLEARANCE (MM) =0.00 T/B CLEARANCE (MM) =0.00

FLOW RATE =18.0 TEMP (DEG C) =25.0 VELOCITY =0.166

REYNOLDS NO. =* 4.77E 03 SCHMIDT NO. =1560. END COMP REYNOLDS NO. =*.1501E 04

INDIVIDUAL TUBE COEFFICIENTS (SH/(SC)1/3)

TUBE						
20	2.27E 01	1.80E 01	1.61E 01	1.37E 01	1.23E 01	1.37E 01
78	2.72E 01	2.28E 01	2.17E 01	2.21E 01	0.00E 00	2.55E 01
79	2.96E 01	3.34E 01	0.00E 00	2.18E 01	2.23E 01	2.47E 01
9	0.00E 00	1.87E 01	0.00E 00	1.41E 01	1.05E 01	1.20E 01
55	2.64E 01	2.15E 01	1.88E 01	1.71E 01	1.15E 01	1.25E 01
4	2.21E 01	1.83E 01	1.36E 01	1.26E 01	1.21E 01	0.00E 00
64	2.46E 01	2.53E 01	0.00E 00	1.79E 01	1.72E 01	0.00E 00
10	2.46E 01	2.06E 01	1.53E 01	1.35E 01	1.25E 01	1.53E 01
44	0.00E 00	0.00E 00	0.00E 00	0.00E 00	0.00E 00	0.00E 00
50	2.24E 01	0.00E 00	1.61E 01	1.50E 01	1.17E 01	1.57E 01
28	2.47E 01	1.92E 01	1.41E 01	1.23E 01	1.26E 01	1.57E 01
69	3.15E 01	2.27E 01	0.00E 00	3.49E 01	0.00E 00	3.44E 01
73	0.00E 00	2.00E 01	1.88E 01	1.97E 01	2.18E 01	2.33E 01
34	2.38E 01	0.00E 00	1.54E 01	1.19E 01	9.78E 00	1.43E 01
14	0.00E 00	1.89E 01	1.42E 01	1.19E 01	1.17E 01	1.34E 01
36	2.34E 01	1.70E 01	1.51E 01	1.66E 01	1.42E 01	1.53E 01
62	0.00E 00	0.00E 00	1.83E 01	1.72E 01	1.39E 01	1.41E 01
16	2.30E 01	1.89E 01	1.53E 01	1.30E 01	1.34E 01	1.81E 01
24	2.36E 01	1.74E 01	0.00E 00	0.00E 00	1.05E 01	0.00E 00
63	2.30E 01	0.00E 00	1.63E 01	0.00E 00	1.47E 01	1.29E 01

AVE	[illegible]	[illegible]	1.64E 01	1.68E 01	1.37E 01	1.76E 01
LE	47.6	47.6	23.8	23.8	23.8	23.8
COMP	OUTLET	THIRD				

10
BAFFLE SPACING (MM)=*149.8 BAFFLE CUT (%) =18.4
B/S CLEARANCE (MM) =0.00 T/B CLEARANCE ¶MM) =0.00
FLOW RATE =18.0 TEMP (DEG.C) =25.0 VELOCITY =0.166
REYNOLDS NO =*.4771E 03 SCHMIDT NO. =1560. END COMP REYNOLDS NO.=*.1501E 04

INDIVIDUAL TUBE COEFFICIENTS (SH/(SC)1/3)

TUBE						
20	2.23E 01	1.06E 01	1.10E 01	1.55E 01	1.78E 01	2.26E 01
78	2.59E 01	1.64E 01	1.27E 01	1.42E 01	0.00E 00	2.52E 01
79	3.04E 01	0.00E 00	0.00E 00	1.47E 01	1.83E 01	2.65E 01
9	0.00E 00	1.44E 01	0.00E 00	2.06E 01	1.79E 01	2.04E 01
55	2.51E 01	1.31E 01	1.30E 01	1.62E 01	1.87E 01	2.21E 01
4	2.03E 01	0.00E 00	1.62E 01	1.88E 01	1.60E 01	0.00E 00
64	2.46E 01	1.65E 01	0.00E 00	1.87E 01	1.89E 01	0.00E 00
10	1.91E 01	1.78E 01	1.68E 01	1.91E 01	1.91E 01	2.13E 01
44	0.00E 00	0.00E 00	0.00E 00	0.00E 00	0.00E 00	0.00E 00
50	2.20E 01	0.00E 00	1.23E 01	1.39E 01	1.57E 01	2.02E 01
28	2.02E 01	1.92E 01	1.97E 01	1.92E 01	1.97E 01	2.16E 01
69	0.00E 00	1.48E 01	0.00E 00	0.00E 00	0.00E 00	1.65E 01
73	0.00E 00	1.62E 01	1.23E 01	1.45E 01	1.82E 01	2.60E 01
34	2.27E 01	0.00E 00	1.44E 01	1.71E 01	1.77E 01	2.10E 01
14	0.00E 00	1.63E 01	1.93E 01	1.78E 01	1.74E 01	2.01E 01
36	2.29E 01	9.33E 00	1.01E 01	1.46E 01	1.77E 01	2.36E 01
62	0.00E 00	0.00E 00	1.30E 01	1.51E 01	1.81E 01	2.33E 01
16	2.02E 01	1.14E 01	1.59E 01	1.83E 01	1.89E 01	2.38E 01
29	2.12E 01	1.09E 01	2.23E 01	0.00E 00	1.62E 01	0.00E 00
63	2.47E 01	0.00E 00	1.35E 01	0.00E 00	1.72E 01	1.87E 01

AVE	2.30E 01	1.11E 01	1.48E 01	1.68E 01	1.78E 01	2.21E 01
LE	47.6	47.6	23.8	23.8	23.8	23.8
COMP	INLET	SECOND				

BAFFLE CUT (%) =18.4

I/B CLEARANCE (MM) = 0.00

VELOCITY =0.070

SCHMIDT NO. =1640. END COMP REYNOLDS NO =# 6236E 03

3	1.41E 01	3.93E 01	7.11E 01	8.86E 00	7.50E 00	6.93E 00
6	1.34E 01	1.[illegible] 01	1.27E 01	1.34E 01	0.00E 00	1.51E 01
7	1.41E 01	1.39E 01	1.40E 01	1.25E 01	1.42E 01	1.64E 01
2	0.00E 00	0.00E 00	0.00E 00	0.00E 00	0.00E 00	0.00E 00
35	1.27E 01	1.11E 01	9.77E 00	9.31E 00	8.06E 00	7.72E 00
4	1.32E 01	1.04E 01	7.16E 00	7.50E 00	7.27E 00	0.00E 00
64	1.41E 01	8.97E 00	0.00E 00	9.54E 00	9.77E 00	0.00E 00
10	1.58E 01	1.19E 01	9.31E 00	7.61E 00	6.59E 00	7.72E 00
44	0.00E 00	0.00E 00	0.00E 00	0.00E 00	0.00E 00	0.00E 00
19	1.33E 01	0.00E 00	8.06E 00	7.95E 00	7.16E 00	8.63E 00
21	1.52E 01	1.16E 01	8.43E 00	7.38E 00	7.04E 00	8.29E 00
24	1.50E 01	1.28E 01	0.00E 00	1.67E 01	0.00E 00	1.67E 01
28	0.00E 00	1.22E 01	1.06E 01	1.11E 01	1.25E 01	1.24E 01
31	1.42E 01	0.00E 00	8.18E 00	7.72E 00	6.81E 00	8.18E 00
14	0.00E 00	1.11E 01	8.06E 00	7.50E 00	6.70E 00	6.93E 00
36	1.35E 01	1.01E 01	8.97E 00	1.04E 01	7.27E 00	8.18E 00
42	0.00E 00	0.00E 00	9.09E 00	8.63E 00	8.75E 00	7.72E 00
46	1.09E 01	1.07E 01	8.18E 00	7.72E 00	7.16E 00	8.75E 00
29	1.40E 01	1.08E 01	0.00E 00	0.00E 00	6.59E 00	0.00E 00
53	1.23E 01	0.00E 00	1.04E 01	0.00E 00	7.72E 00	7.72E 00

AVE	[illegible]	[illegible]	[illegible] 01	9.[illegible]E 00	8.19E 00	9.09E 00
LE	47.6	47.6	23.8	23.8	23.8	23.8
COMP	OUTLET	THIRD				

BAFFLE [illegible] (NO) =1492.0 BAFFLE CUT (%) =18.4

B/S CLEARANCE (MM) =0.00 T/B CLEARANCE (MM) =0.00

FLOW RATE [illegible] TEMP (DEG C) =25.0 VELOCITY =0.070

REYNOLDS NO. [illegible] SCHMIDT NO =1560. END COMP REYNOLDS NO. =*.6381E 03

[illegible] TYPE COEFFICIENTS (SHIRCO/1/3)

Comp						
20	1.09E 01	7.03E 00	8.95E 00	9.44E 00	9.67E 00	1.30E 01
78	1.51E 01	8.27E 00	9.43E 00	9.33E 00	0.00E 00	1.60E 01
79	1.66E 01	0.00E 00	0.00E 00	9.44E 00	1.16E 01	1.65E 01
9	0.00E 00	7.73E 00	0.00E 00	1.27E 01	1.01E 01	1.19E 01
25	1.44E 01	7.87E 00	8.30E 00	9.78E 00	1.08E 01	1.28E 01
4	1.15E 01	0.00E 00	7.33E 00	1.10E 01	9.67E 00	0.00E 00
24	1.51E 01	1.06E 01	0.00E 00	1.17E 01	1.19E 01	0.00E 00
10	1.11E 01	1.06E 01	1.17E 01	1.08E 01	1.08E 01	1.08E 01
44	0.00E 00	0.00E 00	0.00E 00	0.00E 00	0.00E 00	0.00E 00
50	1.30E 01	0.00E 00	8.21E 00	8.77E 00	9.56E 00	1.16E 01
38	1.34E 01	1.23E 01	1.12E 01	1.15E 01	1.18E 01	1.20E 01
69	1.64E 01	8.10E 00	0.00E 00	1.06E 01	0.00E 00	1.07E 01
75	0.09E 00	8.38E 00	7.43E 00	9.11E 00	1.14E 01	1.59E 01
34	1.29E 01	7.99E 00	9.11E 00	8.99E 00	9.56E 00	1.16E 01
14	0.00E 00	1.04E 01	1.14E 01	1.00E 01	9.89E 00	1.14E 01
18	1.36E 01	6.41E 00	7.11E 00	9.11E 00	1.00E 01	1.36E 01
47	0.00E 00	0.00E 00	8.50E 00	9.44E 00	1.09E 01	1.41E 01
14	1.15E 01	7.34E 00	1.14E 01	9.78E 00	1.26E 01	1.44E 01
29	1.29E 01	7.31E 00	1.46E 01	0.00E 00	9.11E 00	0.00E 00
73	1.47E 01	0.00E 00	8.79E 00	0.00E 00	1.05E 01	1.00E 01
AVE	[illegible]	[illegible]	[illegible]	1.01E 01	1.06E 01	1.29E 01
LE	47.6	47.6	23.8	23.8	23.8	23.8
COMP	INLET	SECOND				

CORR NO = 7

FULL SPACING (MM)=97.0 BAFFLE CUT (%) =18.4

B/S CLEARANCE (MM) =0.00 T/B CLEARANCE (MM)=0.00

FLOW RATE =*119.0 TEMP (DEG.C) =25.0 VELOCITY =1.096

REYNOLDS NO =0.4871E 04 SCHMIDT NO. =1560. END COMP REYNOLDS NO. =*.9927E 04

INDIVIDUAL TUBE COEFFICIENTS SH/SC(1/3)

	0.00E 00	5.20E 01	8.10E 01	5.33E 01	7.53E 01	5.94E 01	6.83E 01	0.00E 00
	6.[illegible]E 01	6.5[illegible] 01	6.44E 01	8.38E 01	6.39E 01	7.65E 01	7.29E 01	5.25E 01
	0.[illegible]E 00	5.4[illegible] 01	4.71E 01	6.19E 01	8.06E 01	7.79E 01	6.22E 01	0.00E 00
	0.[illegible]E 00	6.1[illegible] 01	7.73E 01	6.40E 01	7.90E 01	6.40E 01	5.91E 01	0.00E 00
	0.[illegible]E 00	5.91E 01	0.00E 00	0.00E 00	0.00E 00	0.00E 00	8.60E 01	0.00E 00
	4.[illegible]E 01	8.2[illegible] 01	8.59E 01	6.69E 01	7.87E 01	6.75E 01	5.64E 01	3.63E 01
	5.[illegible]E 01	0.00E 00	0.00E 00	0.00E 00	0.00E 00	0.00E 00	0.00E 00	4.53E 01
	4.[illegible]E 01	9.07E 01	9.10E 01	6.36E 01	7.85E 01	8.32E 01	8.34E 01	3.62E 01
	0.00E 00	5.45E 01	0.00E 00	0.00E 00	0.00E 00	0.00E 00	6.28E 01	0.00E 00
	4.97E 01	5.50E 01	9.09E 01	5.25E 01	6.83E 01	6.23E 01	5.64E 01	3.91E 01
	6.11E 01	7.59E 01	6.86E 01	0.00E 00	0.00E 00	8.15E 01	6.67E 01	6.33E 01
	4.83E 01	8.20E 01	7.34E 01	7.14E 01	8.26E 01	6.70E 01	6.16E 01	3.69E 01
	0.00E 00	7.05E 01	8.66E 01	8.23E 01	7.82E 01	8.82E 01	8.38E 01	0.00E 00
	4.49E 01	0.00E 00	8.90E 01	6.20E 01	8.06E 01	5.38E 01	0.00E 00	3.32E 01
	5.[illegible]E 01	6.08E 01	6.89E 01	5.27E 01	7.65E 01	6.09E 01	9.02E 01	4.00E 01
	4.[illegible]E 01	5.9[illegible] 01	9.[illegible]E 01	6.54E 01	8.12E 01	6.40E 01	5.28E 01	0.00E 00
	4.[illegible]E 01	0.0[illegible] 00	6.42E 01	5.92E 01	7.68E 01	5.33E 01	0.00E 00	3.44E 01
	0.[illegible]E 00	0.0[illegible] 00	6.33E 01	5.16E 01	7.17E 01	5.86E 01	0.00E 00	0.00E 00
	5.[illegible]E 01	7.64E 01	0.00E 00	0.00E 00	5.52E 01	5.47E 01	5.89E 01	3.90E 01
	4.49E 01	6.02E 01	6.47E 01	5.75E 01	7.36E 01	6.03E 01	7.85E 01	4.27E 01
	0.00E 00	5.38E 01	5.53E 01	4.49E 01	6.09E 01	4.82E 01	6.39E 01	0.00E 00
	6.[illegible]E 01	5.78E 01	5.42E 01	5.98E 01	5.02E 01	6.09E 01	6.05E 01	8.18E 01
	0.00E 00	5.17E 01	4.04E 01	5.14E 01	6.50E 01	6.51E 01	6.19E 01	0.00E 00
	0.00E 00	5.25E 01	6.96E 01	5.38E 01	6.42E 01	5.17E 01	5.92E 01	0.00E 00
	0.00E 00	5.59E 01	0.00E 00	0.00E 00	0.00E 00	0.00E 00	7.36E 01	0.00E 00
	9.77E 01	6.39E 01	5.94E 01	5.36E 01	5.91E 01	5.49E 01	6.16E 01	9.27E 01
	9.03E 01	1.01E 02	1.02E 02	0.00E 00	0.00E 00	0.00E 00	0.00E 00	1.05E 02
	9.09E 01	7.60E 01	7.65E 01	0.00E 00	0.00E 00	8.17E 01	8.18E 01	8.99E 01
	0.00E 00	5.77E 01	0.00E 00	0.00E 00	0.00E 00	0.00E 00	6.08E 01	0.00E 00
	8.73E 01	5.53E 01	5.30E 01	5.08E 01	5.38E 01	5.61E 01	5.64E 01	0.00E 00
	3.15E 01	3.44E 01	0.00E 00	0.00E 00	0.00E 00	0.00E 00	3.26E 01	2.76E 01
	7.59E 01	6.08E 01	6.12E 01	5.81E 01	6.65E 01	5.28E 01	5.64E 01	7.56E 01
	0.00E 00	5.83E 01	7.17E 01	6.37E 01	6.16E 01	6.64E 01	6.83E 01	0.00E 00
	9.64E 01	5.44E 01	5.14E 01	4.97E 01	6.33E 01	4.99E 01	6.16E 01	9.07E 01
	7.16E 01	5.81E 01	4.78E 01	4.67E 01	6.19E 01	3.82E 01	7.95E 01	7.82E 01
	9.82E 01	5.49E 01	5.77E 01	5.53E 01	5.92E 01	5.49E 01	6.11E 01	0.00E 00
	8.10E 01	0.00E 00	4.60E 01	4.91E 01	6.47E 01	4.39E 01	0.00E 00	8.54E 01
	0.00E 00	0.00E 00	5.05E 01	4.53E 01	5.84E 01	4.22E 01	0.00E 00	0.00E 00
	7.32E 01	6.20E 01	8.08E 01	8.91E 01	6.79E 01	6.70E 01	5.00E 01	5.95E 01
	9.01E 01	6.2[illegible]E 01	4.80E 01	4.96E 01	6.24E 01	4.71E 01	7.29E 01	9.19E 01

AVE	[illegible]E 01	[illegible]E 01	[illegible]E 01	5.60E 01	6.84E 01	6.10E 01	6.55E 01	5.99E 01
LE	47.6	47.6	47.6	47.6	47.6	47.6	47.6	47.6
COMP	INLET	SECOND		THIRD		FOURTH		OUTLET

RUN NO = 9

T-T-S SPACING (MM)=97.0 BAFFLE CUT (%) =18.4

B/S CLEARANCE (MM) =0.00 T/B CLEARANCE (MM)= =0.00

FLOW RATE =80.0 TEMP (DEG.C) =25.0 VELOCITY =0.737

REYNOLDS NO. =0.3275E 04 SCHMIDT NO. =1560. END COMP REYNOLDS NO. =*.6673E 04

INDIVIDUAL TUBE COEFFICIENTS SH/SC(1/3)

50	0.00E 00	4.15E 01	6.70E 01	4.32E 01	6.09E 01	4.52E 01	5.38E 01	0.00E 00
51	7.18E 01	4.97E 01	9.36E 01	3.35E 01	2.54E 01	6.03E 01	5.86E 01	5.77E 01
6	0.00E 00	4.13E 01	3.70E 01	5.03E 01	6.59E 01	3.13E 01	4.99E 01	0.00E 00
52	0.00E 00	4.94E 01	6.78E 01	5.19E 01	6.22E 01	4.92E 01	4.74E 01	4.83E 01
53	0.00E 00	4.60E 01	0.00E 00	0.00E 00	0.00E 00	0.00E 00	5.22E 01	0.00E 00
20	5.15E 01	6.70E 01	6.84E 01	5.31E 01	6.26E 01	5.10E 01	4.38E 01	4.29E 01
25	4.19E 01	0.00E 00	0.00E 00	0.00E 00	0.00E 00	0.00E 00	0.00E 00	5.27E 01
1	3.24E 01	7.32E 01	7.36E 01	0.00E 00	0.00E 00	6.48E 01	6.48E 01	4.30E 01
54	0.00E 00	4.30E 01	0.00E 00	0.00E 00	0.00E 00	0.00E 00	5.19E 01	0.00E 00
43	4.03E 01	4.35E 01	7.43E 01	4.19E 01	5.45E 01	4.53E 01	4.38E 01	4.41E 01
58	5.02E 01	6.26E 01	4.83E 01	4.85E 01	5.25E 01	0.00E 00	5.47E 01	6.90E 01
62	4.00E 01	6.64E 01	6.06E 01	5.75E 01	6.78E 01	5.33E 01	4.82E 01	4.71E 01
57	0.00E 00	5.38E 01	3.58E 01	6.69E 01	6.44E 01	3.58E 01	6.76E 01	0.00E 00
42	3.34E 01	0.00E 00	7.46E 01	4.85E 01	6.67E 01	4.44E 01	0.00E 00	3.97E 01
47	4.26E 01	4.83E 01	3.48E 01	4.19E 01	6.28E 01	4.72E 01	5.69E 01	4.83E 01
33	3.75E 01	4.99E 01	7.67E 01	5.38E 01	6.69E 01	4.97E 01	4.21E 01	3.58E 01
67	3.50E 01	0.00E 00	5.47E 01	4.71E 01	6.31E 01	4.11E 01	0.00E 00	4.32E 01
63	0.00E 00	0.00E 00	5.33E 01	4.22E 01	5.87E 01	4.58E 01	0.00E 00	0.00E 00
41	4.37E 01	6.20E 01	6.48E 01	6.54E 01	9.04E 01	9.04E 01	4.77E 01	4.83E 01
46	3.99E 01	4.62E 01	5.49E 01	4.63E 01	6.00E 01	4.69E 01	6.39E 01	4.97E 01
29	0.00E 00	4.19E 01	4.57E 01	3.54E 01	4.99E 01	3.83E 01	5.06E 01	0.00E 00
38	6.34E 01	4.53E 01	4.35E 01	2.37E 01	2.07E 01	4.80E 01	4.82E 01	6.42E 01
43	0.00E 00	4.08E 01	3.27E 01	3.99E 01	5.28E 01	2.62E 01	4.86E 01	0.00E 00
31	0.00E 00	4.10E 01	5.22E 01	4.24E 01	5.27E 01	4.15E 01	4.72E 01	0.00E 00
55	0.00E 00	4.44E 01	0.00E 00	0.00E 00	0.00E 00	0.00E 00	5.89E 01	0.00E 00
11	7.48E 01	5.10E 01	4.72E 01	4.24E 01	4.74E 01	4.36E 01	4.97E 01	7.48E 01
5	7.17E 01	7.98E 01	8.07E 01	0.00E 00	0.00E 00	8.65E 01	8.65E 01	7.98E 01
7	7.32E 01	6.12E 01	6.19E 01	0.00E 00	0.00E 00	6.54E 01	6.54E 01	7.09E 01
1	0.00E 00	4.53E 01	0.00E 00	0.00E 00	0.00E 00	0.00E 00	4.83E 01	0.00E 00
3	7.01E 01	4.21E 01	4.30E 01	3.90E 01	4.29E 01	4.44E 01	4.44E 01	8.80E 01
23	2.06E 01	2.77E 01	0.00E 00	0.00E 00	0.00E 00	0.00E 00	2.74E 01	2.26E 01
19	6.08E 01	4.83E 01	4.97E 01	4.66E 01	5.42E 01	4.19E 01	4.61E 01	6.00E 01
24	0.00E 00	4.60E 01	2.96E 01	5.16E 01	5.03E 01	2.70E 01	5.53E 01	0.00E 00
39	7.65E 01	4.22E 01	4.11E 01	4.05E 01	5.06E 01	4.00E 01	4.94E 01	8.62E 01
34	5.01E 01	4.66E 01	2.23E 01	3.60E 01	5.02E 01	3.35E 01	6.31E 01	6.16E 01
6	7.34E 01	4.30E 01	4.69E 01	4.39E 01	4.78E 01	4.38E 01	4.99E 01	8.62E 01
14	6.56E 01	0.00E 00	3.74E 01	3.90E 01	5.19E 01	3.60E 01	0.00E 00	6.61E 01
26	0.00E 00	0.00E 00	4.24E 01	3.69E 01	4.77E 01	3.41E 01	0.00E 00	0.00E 00
30	5.81E 01	4.94E 01	5.38E 01	5.41E 01	5.38E 01	5.30E 01	4.16E 01	4.82E 01
35	7.14E 01	5.14E 01	4.04E 01	3.93E 01	5.13E 01	3.86E 01	5.92E 01	7.25E 01

AVE	[illegible]	[illegible]	[illegible]	4.32E 01	5.51E 01	4.30E 01	5.26E 01	5.74E 01
LE	47.6	47.6	47.6	47.6	47.6	47.6	47.6	47.6
COMP	INLET	SECOND		THIRD		FOURTH		OUTLET

RUN NO. = 9

TUBE SPACING (MM)=97.0 BAFFLE CUT (%) =18.4

B/B CLEARANCE (MM) =0.00 T/B CLEARANCE (MM) =0.00

FLOW RATE =23.0 TEMP (DEG.C) =25.0 VELOCITY =0.350

REYNOLDS NO. =0.1559E 04 SCHMIDT NO. =1560. END COMP REYNOLDS NO. =*.3170E 04

TRUE THERMAL MODE COEFFICIENTS SH/SC(1/3)

	0.00E 00	2.46E 01	3.75E 01	2.37E 01	3.45E 01	2.53E 01	3.41E 01	0.00E 00
	0.00E 00	2.70E 01	3.04E 01	3.16E 01	3.05E 01	3.43E 01	3.47E 01	3.05E 01
	0.00E 00	2.03E 01	2.13E 01	2.86E 01	3.80E 01	3.53E 01	3.45E 01	0.00E 00
	0.00E 00	3.76E 01	3.45E 01	2.80E 01	3.63E 01	2.78E 01	3.22E 01	0.00E 00
	0.00E 00	2.41E 01	0.00E 00	0.00E 00	0.00E 00	0.00E 00	4.15E 01	0.00E 00
	3.71E 01	3.94E 01	3.71E 01	2.80E 01	3.77E 01	2.77E 01	3.18E 01	3.51E 01
	2.00E 01	4.45E 01	4.91E 01	4.45E 01	4.97E 01	5.00E 01	5.04E 01	2.65E 01
	2.34E 01	3.64E 01	3.91E 01	2.65E 01	3.58E 01	4.04E 01	4.12E 01	3.05E 01
	0.00E 00	2.32E 01	0.00E 00	0.00E 00	0.00E 00	0.00E 00	3.50E 01	0.00E 00
	2.64E 01	2.31E 01	4.13E 01	2.70E 01	3.12E 01	2.43E 01	2.98E 01	2.80E 01
	3.73E 01	3.43E 01	4.52E 01	4.04E 01	3.71E 01	3.71E 01	3.27E 01	3.33E 01
	2.67E 01	3.65E 01	3.04E 01	3.77E 01	3.94E 01	2.62E 01	3.13E 01	3.33E 01
	0.00E 00	2.82E 01	0.00E 00	3.70E 01	3.50E 01	3.21E 01	3.84E 01	0.00E 00
	2.51E 01	0.00E 00	4.08E 01	2.36E 01	3.51E 01	2.08E 01	0.00E 00	2.77E 01
	2.74E 01	2.61E 01	3.16E 01	2.33E 01	3.41E 01	2.08E 01	4.11E 01	3.05E 01
	2.48E 01	2.40E 01	4.16E 01	2.05E 01	3.58E 01	2.43E 01	2.90E 01	2.85E 01
	3.13E 01	0.00E 00	3.04E 01	2.51E 01	3.29E 01	2.08E 01	0.00E 00	2.32E 01
	0.00E 00	0.00E 00	2.92E 01	2.24E 01	3.18E 01	2.04E 01	0.00E 00	0.00E 00
	2.50E 01	3.57E 01	2.25E 01	2.32E 01	2.47E 01	0.00E 00	0.00E 00	3.06E 01
	1.79E 01	2.47E 01	3.16E 01	2.39E 01	3.16E 01	2.08E 01	0.00E 00	0.00E 00
	0.00E 00	2.78E 01	3.13E 01	2.51E 01	3.59E 01	2.72E 01	3.53E 01	0.00E 00
	4.34E 01	2.90E 01	3.00E 01	3.31E 01	3.18E 01	3.46E 01	3.49E 01	4.41E 01
	0.00E 00	2.73E 01	2.19E 01	2.88E 01	3.82E 01	1.80E 01	3.39E 01	0.00E 00
	0.00E 00	2.85E 01	3.62E 01	3.04E 01	3.88E 01	2.96E 01	3.37E 01	0.00E 00
	0.00E 00	2.92E 01	0.00E 00	0.00E 00	0.00E 00	0.00E 00	4.12E 01	0.00E 00
	5.31E 01	3.30E 01	3.30E 01	2.89E 01	3.54E 01	3.05E 01	3.46E 01	5.16E 01
	4.77E 01	2.73E 01	2.77E 01	0.00E 00	0.00E 00	3.02E 01	3.02E 01	5.28E 01
	4.84E 01	4.19E 01	4.22E 01	0.00E 00	0.00E 00	4.64E 01	4.65E 01	4.85E 01
	0.00E 00	2.86E 01	0.00E 00	0.00E 00	0.00E 00	0.00E 00	3.20E 01	0.00E 00
	4.85E 01	2.74E 01	3.02E 01	2.56E 01	3.06E 01	3.45E 01	3.39E 01	5.93E 01
	0.00E 00	0.00E 00	0.00E 00	0.00E 00	0.00E 00	0.00E 00	0.00E 00	0.00E 00
	4.19E 01	3.18E 01	3.45E 01	3.16E 01	3.86E 01	3.04E 01	3.34E 01	4.31E 01
	0.00E 00	3.08E 01	2.13E 01	3.57E 01	3.63E 01	1.94E 01	3.92E 01	0.00E 00
	5.21E 01	2.66E 01	2.01E 01	2.73E 01	3.45E 01	3.12E 01	3.22E 01	5.90E 01
	3.96E 01	3.06E 01	3.18E 01	2.49E 01	3.49E 01	2.45E 01	4.32E 01	4.34E 01
	5.34E 01	2.72E 01	3.26E 01	3.05E 01	3.23E 01	3.26E 01	3.25E 01	5.89E 01
	4.51E 01	0.00E 00	2.77E 01	2.57E 01	3.61E 01	2.55E 01	0.00E 00	4.65E 01
	0.00E 00	0.00E 00	3.10E 01	2.59E 01	3.34E 01	2.51E 01	0.00E 00	0.00E 00
	4.16E 01	3.31E 01	2.47E 01	2.48E 01	2.65E 01	2.65E 01	3.08E 01	3.57E 01
	4.91E 01	3.08E 01	2.88E 01	2.76E 01	3.63E 01	2.72E 01	3.96E 01	5.00E 01

AVE	2.93E 01	2.95E 01	3.27E 01	2.88E 01	3.49E 01	2.89E 01	3.58E 01	3.96E 01
LE	47.6	47.6	47.6	47.6	47.6	47.6	47.6	47.6
COMP	INLET	SECOND		THIRD		FOURTH		OUTLET

RUN NO. = 9

[illegible] SPACING (MM)=97.0 BAFFLE CUT (%) =18.4

B/S CLEARANCE (MM) =0.00 T/B CLEARANCE (MM) =0.00

[illegible] RATE = 7.7 TEMP (DEG.C) =26.0 VELOCITY =0.070

[illegible] NO. =0.3203E 03 SCHMIDT NO. =1485. END COMP REYNOLDS NO. =* .6528E 03

IN, OUT OF TUBE COEFFICIENTS SH/SC(1/3)

[illegible]	1.62E 01	1.34E 01	1.08E 01	1.38E 01	1.05E 01	1.26E 01	0.00E 00
[illegible]	1.62E 01	1.34E 01	9.19E 00	1.36E 01	1.56E 01	1.48E 01	1.08E 01
[illegible]	1.52E 01	1.30E 01	1.14E 01	1.52E 01	1.17E 01	1.27E 01	0.00E 00
[illegible]	1.14E 01	1.29E 01	1.12E 01	1.56E 01	9.71E 00	1.26E 01	0.00E 00
[illegible]	9.71E 00	0.00E 00	0.00E 00	0.00E 00	0.00E 00	1.60E 01	0.00E 00
[illegible]	1.51E 01	1.30E 01	1.09E 01	1.60E 01	1.02E 01	1.23E 01	1.29E 01
[illegible]	9.64E 00	9.97E 00	9.97E 00	1.23E 01	1.21E 01	1.19E 01	9.58E 00
[illegible]	8.40E 00	8.53E 00	1.23E 01	8.14E 00	8.27E 00	8.14E 00	1.08E 01
[illegible]	1.15E 01	1.05E 01	1.10E 01	1.31E 01	1.31E 01	1.46E 01	0.00E 00
[illegible]	8.92E 00	8.97E 00	1.02E 01	1.40E 01	1.02E 01	1.17E 01	1.02E 01
[illegible]	1.49E 01	1.36E 01	1.85E 01	1.02E 01	1.43E 01	1.51E 01	1.48E 01
[illegible]	1.36E 01	1.33E 01	1.13E 01	1.63E 01	9.58E 00	1.34E 01	1.30E 01
[illegible]	1.01E 01	9.19E 00	1.52E 01	1.50E 01	7.87E 00	1.54E 01	0.00E 00
[illegible]	0.00E 00	1.44E 01	1.01E 01	1.36E 01	9.45E 00	0.00E 00	9.45E 00
[illegible]	1.03E 01	1.26E 01	1.05E 01	1.34E 01	1.01E 01	1.46E 01	9.84E 00
[illegible]	1.06E 01	8.53E 00	9.84E 00	1.59E 01	9.19E 00	1.14E 01	1.05E 01
[illegible]	0.00E 00	1.26E 02	1.04E 01	1.35E 01	9.58E 00	0.00E 00	8.53E 00
[illegible]	0.00E 00	1.53E 01	1.08E 01	1.34E 01	1.05E 01	0.00E 00	0.00E 00
[illegible]	1.34E 01	1.49E 01	1.73E 01	2.02E 01	1.98E 01	1.25E 01	1.26E 01
[illegible]	1.01E 01	1.30E 01	1.05E 01	1.33E 01	9.19E 00	1.51E 01	8.79E 00
[illegible]	1.15E 01	1.35E 01	1.12E 01	1.51E 01	1.15E 01	1.42E 01	0.00E 00
[illegible]	1.12E 01	1.38E 01	1.57E 01	1.39E 01	1.52E 01	1.59E 01	1.69E 01
[illegible]	1.21E 01	8.40E 00	1.14E 01	1.61E 01	1.29E 01	1.34E 01	0.00E 00
[illegible]	1.25E 01	1.42E 01	1.17E 01	1.67E 01	1.05E 01	1.42E 01	0.00E 00
[illegible]	1.21E 01	0.00E 00	0.00E 00	0.00E 00	0.00E 00	1.86E 01	0.00E 00
[illegible]	1.42E 01	1.44E 01	1.08E 01	1.59E 01	1.13E 01	1.50E 01	2.14E 01
[illegible]	2.09E 01	2.44E 01	0.00E 00	0.00E 00	2.57E 01	2.59E 01	1.90E 01
[illegible]	1.76E 01	1.77E 01	1.26E 01	1.76E 01	1.94E 01	1.94E 01	2.05E 01
[illegible]	1.19E 01	0.00E 00	0.00E 00	0.00E 00	0.00E 00	1.40E 01	0.00E 00
[illegible]	1.22E 01	1.56E 01	1.09E 01	1.63E 01	1.34E 01	1.50E 01	2.22E 01
[illegible]	8.79E 00	0.00E 00	0.00E 00	0.00E 00	0.00E 00	9.84E 00	7.61E 00
[illegible]	1.33E 01	1.09E 01	1.21E 01	1.65E 01	1.10E 01	1.50E 01	1.89E 01
[illegible]	1.17E 01	9.02E 00	1.54E 01	1.50E 01	8.01E 00	1.57E 01	0.00E 00
[illegible]	1.01E 01	1.23E 01	1.10E 01	1.33E 01	1.13E 01	1.31E 01	2.35E 01
[illegible]	1.27E 01	1.47E 01	1.13E 01	1.36E 01	1.42E 01	1.59E 01	1.67E 01
[illegible]	1.05E 01	1.38E 01	1.12E 01	1.44E 01	1.18E 01	1.38E 01	2.39E 01
[illegible]	0.00E 00	1.29E 01	1.13E 01	1.40E 01	1.08E 01	0.00E 00	1.84E 01
[illegible]	0.00E 00	1.36E 01	1.21E 01	1.40E 01	1.12E 01	0.00E 00	0.00E 00
[illegible]	1.48E 01	1.04E 01	1.08E 01	2.23E 01	2.24E 01	1.25E 01	1.55E 01
[illegible]	1.37. 01	1.39E 01	1.21E 01	1.48E 01	1.10E 01	1.61E 01	1.89E 01

AVE	[illegible]	1.27E 01	1.24E 01	1.20E 01	1.48E 01	1.23E 01	1.44E 01	1.48E 01
IP	47.6	47.6	47.6	47.6	47.6	47.6	47.6	47.6
COMP	INLET	SECOND		THIRD		FOURTH		OUTLET

B

BAFFLE SPACING (MM)=98.4 BAFFLE CUT (%) =18.4
B/S CLEARANCE (MM) =0.00 T/B CLEARANCE (MM) =0.00
FLOW RATE =88.0 TEMP (DEG.C) =24.5 VELOCITY =0.011
REYNOLDS NO. =0.3510E 04 SCHMIDT NO =1600

INDIVIDUAL TUBE COEFFICIENTS

TUBE				
28	4.83E 01	4.45E 01	4.63E 01	4.72E 01
14	0.00E 00	3.97E 01	3.69E 01	4.30E 01
20	5.04E 01	3.23E 01	4.71E 01	3.79E 01
73	0.00E 00	4.20E 01	0.00E 00	3.00E 01
69	0.00E 00	4.75E 01	0.00E 00	0.00E 00
10	5.22E 01	4.22E 01	4.51E 01	4.14E 01
29	4.90E 01	3.28E 01	3.80E 01	0.00E 00
62	4.02E 01	0.00E 00	0.00E 00	3.26E 01
44	0.00E 00	3.96E 01	4.46E 01	0.00E 00
67	4.02E 01	4.55E 01	4.11E 01	4.03E 01
79	4.04E 01	3.40E 01	0.00E 00	0.00E 00
78	5.51E 01	5.37E 01	5.13E 01	3.19E 01
34	0.00E 00	3.93E 01	5.30E 01	4.40E 01
9	0.00E 00	4.13E 01	0.00E 00	4.27E 01
55	5.19E 01	4.89E 01	0.00E 00	3.75E 01
16	5.26E 01	3.35E 01	4.72E 01	4.40E 01
50	4.34E 01	0.00E 00	3.15E 01	4.35E 01
35	4.90E 01	0.00E 00	4.44E 01	4.22E 01
64	4.21E 01	3.87E 01	3.09E 01	3.56E 01
8	4.22E 01	3.36E 01	3.13E 01	3.37E 01

AVE.	4.49E 01	4.05E 01	3.99E 01	3.92E 01
ELEC. LENGTH MM	48.5	48.5	48.5	48.5
COMPS.	OUTLET		THIRD	

0

BAFFLE SPACING (MM)=98.4 BAFFLE CUT (%) =18.4
B/S CLEARANCE (MM) =0.00 T/B CLEARANCE (MM) =0.00
FLOW RATE =4119.0 TEMP (DEG.C) =24.0 VELOCITY =1.096
REYNOLDS NO. =0.4695E 04 SCHMIDT NO =1640

INDIVIDUAL TUBE COEFFICIENTS

TUBE				
28	7.49E 01	0.00E 00	6.25E 01	6.04E 01
14	0.00E 00	5.13E 01	3.36E 01	7.19E 01
20	5.49E 01	4.68E 01	4.61E 01	6.15E 01
73	0.00E 00	0.00E 00	0.00E 00	6.13E 01
69	0.00E 00	6.24E 01	0.00E 00	0.00E 00
10	4.13E 01	4.87E 01	5.99E 01	4.74E 01
29	4.13E 01	6.42E 01	6.46E 01	3.31E 01
62	0.00E 00	0.00E 00	5.60E 01	6.74E 01
44	0.00E 00	5.57E 01	0.00E 00	5.08E 01
67	5.19E 01	5.35E 01	7.51E 01	5.15E 01
79	0.00E 00	0.00E 00	0.00E 00	5.19E 01
78	3.45E 00	6.21E 01	5.30E 01	5.13E 01
34	0.00E 00	5.13E 01	4.66E 01	4.98E 01
9	0.00E 00	4.93E 01	0.00E 00	6.38E 01
55	5.31E 01	5.29E 01	5.41E 01	6.07E 01
16	3.98E 01	4.91E 01	4.72E 01	6.23E 01
50	4.66E 01	5.09E 00	4.78E 01	5.34E 01
35	4.52E 01	6.11E 01	4.53E 01	6.05E 01
64	5.30E 01	0.00E 00	0.00E 00	4.58E 01
8	5.48E 01	5.13E 01	6.80E 00	0.00E 00

AVE.	4.11E 01	5.01E 01	4.48E 01	5.47E 01
Le. MM	48.5	48.5	48.5	48.5
COMP	INLET		SECOND	

S

BAFFLE SPACING (MM)=98.4 BAFFLE CUT (%) =18.4
B/S CLEARANCE (MM) =0.00 T/B CLEARANCE (MM) =0.00
FLOW RATE =44.0 TEMP (DEG.C) =24.0 VELOCITY =0.405
REYNOLDS NO =0.1735E 04 SCHMIDT NO =1640.

INDIVIDUAL TUBE COEFFICIENTS

TUBE				
28	3.19E 01	0.00E 00	3.19E 01	2.64E 01
14	0.00E 00	2.70E 01	2.10E 01	2.75E 01
20	3.28E 01	2.04E 01	3.19E 01	2.45E 01
73	0.00E 00	3.36E 01	2.30E 01	3.30E 01
69	3.14E 01	3.19E 01	3.19E 01	3.22E 01
10	3.29E 01	2.76E 01	3.09E 01	2.54E 01
29	3.06E 01	3.67E 01	3.77E 01	2.61E 01
62	0.00E 00	0.00E 00	0.00E 00	2.30E 01
44	0.00E 00	0.00E 00	3.16E 01	0.00E 00
63	2.53E 01	0.00E 00	2.04E 01	2.74E 01
79	3.66E 01	3.64E 01	3.66E 01	3.57E 01
78	3.45E 01	3.47E 01	3.48E 01	2.06E 01
34	0.00E 00	2.63E 01	3.58E 01	2.80E 01
9	0.00E 00	2.80E 01	3.16E 01	2.70E 01
55	3.25E 01	3.17E 01	0.00E 00	2.37E 01
16	3.39E 01	2.22E 01	3.18E 01	2.71E 01
50	2.81E 01	0.00E 00	3.47E 01	2.70E 01
36	3.18E 01	0.00E 00	3.01E 01	2.69E 01
64	0.00E 00	2.39E 01	2.41E 01	2.43E 01
4	2.78E 01	2.32E 01	2.30E 01	2.37E 01

AV.	3.16E 01	2.88E 01	3.02E 01	2.70E 01
LE	48.5	48.5	48.5	48.5
	OUTLET COMP.		THIRD COMP.	

S

BAFFLE SPACING (MM)=98.4 BAFFLE CUT (%) =18.4
B/S CLEARANCE (MM) =0.00 T/B CLEARANCE (MM) =0.00
FLOW RATE =66.0 TEMP (DEG.C) =24.5 VELOCITY =0.608
REYNOLDS NO =0.2633E 04 SCHMIDT NO =1600

INDIVIDUAL TUBE COEFFICIENTS

TUBE				
28	4.02E 01	3.80E 01	3.95E 01	3.40E 01
14	0.00E 00	3.41E 01	2.61E 01	3.57E 01
20	4.16E 01	2.74E 01	3.99E 01	3.27E 01
73	0.00E 00	0.00E 00	0.00E 00	4.25E 01
69	0.00E 00	3.88E 01	0.00E 00	0.00E 00
10	4.29E 01	3.57E 01	3.93E 01	3.29E 01
29	4.01E 01	3.56E 01	3.79E 01	3.34E 01
62	0.00E 00	0.00E 00	3.43E 01	3.19E 01
44	0.00E 00	0.00E 00	0.00E 00	0.00E 00
63	3.43E 01	3.70E 01	4.14E 01	3.44E 01
79	0.00E 00	0.00E 00	0.00E 00	0.00E 00
78	4.45E 01	4.34E 01	4.40E 01	2.72E 01
34	0.00E 00	3.17E 01	4.40E 01	3.63E 01
9	0.00E 00	3.46E 01	0.00E 00	3.57E 01
55	4.22E 01	3.80E 01	3.56E 01	3.16E 01
16	4.34E 01	2.64E 01	3.90E 01	3.61E 01
50	3.63E 01	0.00E 00	4.30E 01	3.56E 01
36	4.16E 01	2.53E 01	3.66E 01	3.50E 01
64	3.56E 01	0.00E 00	3.72E 01	3.25E 01
4	3.61E 01	4.10E 01	3.53E 01	3.47E 01

AVE.	3.90E 01	3.43E 01	3.91E 01	3.44E 01
Le. mm	48.5	48.5	48.5	48.5
COMP	OUTLET		THIRD.	

8

BAFFLE SPACING (MM)=98.4 BAFFLE CUT (%) =18.4
B/S CLEARANCE (MM) =0.00 T/B CLEARANCE (MM) =0.00
FLOW RATE =18.0 TEMP (DEG.C) =25.5 VELOCITY =0.166
REYNOLDS NO. =0.7347E 03 SCHMIDT NO. =1522

INDIVIDUAL TUBE COEFFICIENTS

TUBE				
28	2.06E 01	0.00E 00	2.01E 01	1.54E 01
14	0.00E 00	1.75E 01	1.29E 01	1.59E 01
20	2.00E 01	1.09E 01	1.90E 01	1.50E 01
73	0.00E 00	2.00E 01	1.44E 01	2.18E 01
69	1.93E 01	1.92E 01	1.90E 01	1.90E 01
10	2.13E 01	1.72E 01	1.89E 01	1.51E 01
29	1.90E 01	2.16E 01	2.20E 01	1.59E 01
62	0.00E 00	0.00E 00	2.45E 01	1.62E 01
44	0.00E 00	0.00E 00	1.95E 01	0.00E 00
63	1.55E 01	0.00E 00	2.47E 01	1.62E 01
79	2.29E 01	2.31E 01	2.35E 01	2.27E 01
78	2.10E 01	2.11E 01	2.27E 01	2.37E 01
34	0.00E 00	1.69E 01	2.16E 01	1.69E 01
9	0.00E 00	1.83E 01	1.75E 01	1.50E 01
55	1.95E 01	1.94E 01	2.62E 01	1.65E 01
16	2.17E 01	1.27E 01	2.02E 01	1.57E 01
50	1.77E 01	0.00E 00	1.93E 01	1.63E 01
36	2.03E 01	0.00E 00	1.93E 01	1.63E 01
64	1.52E 01	1.52E 01	1.52E 01	1.53E 01
4	1.80E 01	1.49E 01	1.49E 01	1.49E 01

AVE.	1.94E 01	1.47E 01	1.98E 01	1.71E 01
ELEC MM	48.5	48.5	48.5	48.5
COMP.	OUTLET		THIRD.	

8

BAFFLE SPACING (MM)=98.4 BAFFLE CUT (%) =18.4
B/S CLEARANCE (MM) =0.00 T/B CLEARANCE (MM) =0.00
FLOW RATE =18.0 TEMP (DEG.C) =25.0 VELOCITY =0.166
REYNOLDS NO. =0.7263E 03 SCHMIDT NO. =1560.

INDIVIDUAL TUBE COEFFICIENTS

TUBE				
28	1.11E 01	0.00E 00	2.12E 01	2.22E 01
14	0.00E 00	1.80E 01	1.86E 01	2.31E 01
20	1.30E 01	1.71E 01	1.29E 01	2.15E 01
73	0.00E 00	1.77E 01	1.66E 01	2.09E 01
69	1.78E 01	1.74E 01	1.47E 01	1.43E 01
10	1.31E 01	1.76E 01	1.89E 01	2.41E 01
29	1.20E 01	2.21E 01	2.28E 01	2.20E 01
62	0.00E 00	0.00E 00	0.00E 00	1.64E 01
44	0.00E 00	0.00E 00	1.51E 01	1.81E 01
63	1.72E 01	0.00E 00	1.65E 01	1.69E 01
79	2.40E 01	1.82E 01	1.03E 01	2.14E 01
78	2.37E 01	2.02E 01	1.60E 01	1.30E 01
34	0.00E 00	1.70E 01	1.46E 01	2.31E 01
9	0.00E 00	1.71E 01	1.90E 01	2.35E 01
55	1.71E 01	1.73E 01	1.65E 01	2.13E 01
16	1.15E 01	1.76E 01	1.43E 01	2.46E 01
50	1.54E 01	0.00E 00	2.02E 01	2.20E 01
36	1.49E 01	0.00E 00	1.17E 01	2.20E 01
64	1.87E 01	2.68E 01	1.86E 01	1.98E 01
4	1.30E 01	2.43E 01	2.20E 01	2.30E 01

AVE.	1.52E 01	1.92E 01	1.77E 01	2.09E 01
ELECTRODE MM	48.5	48.5	48.5	48.5
COMP	INLET		SECOND	

8

BAFFLE SPACING (MM)= 98.4 BAFFLE CUT (%) =18.4
B/S CLEARANCE (MM) =0.00 T/B CLEARANCE (MM) =0.00
FLOW RATE = 4.0 TEMP (DEG.C) =24.0 VELOCITY =0.037
REYNOLDS NO. =0.1577E 03 SCHMIDT NO. =1640.

INDIVIDUAL TUBE COEFFICIENTS

TUBE				
28	5.50E 00	0.00E 00	1.07E 01	9.90E 00
14	0.00E 00	8.64E 00	5.16E 00	9.42E 00
20	6.84E 00	8.19E 00	6.84E 00	9.20E 00
73	0.00E 00	6.84E 00	6.84E 00	9.65E 00
69	7.74E 00	7.07E 00	7.74E 00	7.74E 00
10	5.50E 00	8.52E 00	8.97E 00	9.65E 00
29	6.39E 00	5.83E 00	5.72E 00	4.71E 00
62	0.00E 00	0.00E 00	7.85E 00	8.86E 00
44	0.00E 00	0.00E 00	4.82E 00	4.49E 00
63	7.40E 00	6.84E 00	7.85E 00	7.85E 00
79	1.04E 01	7.18E 00	7.07E 00	9.31E 00
78	1.05E 01	8.52E 00	6.73E 00	1.17E 01
34	0.00E 00	8.08E 00	7.40E 00	8.64E 00
9	0.00E 00	7.96E 00	7.40E 00	8.41E 00
55	7.51E 00	7.74E 00	7.85E 00	8.30E 00
16	5.83E 00	8.41E 00	7.51E 00	1.07E 01
50	7.07E 00	0.00E 00	7.29E 00	8.08E 00
36	6.62E 00	7.74E 00	6.51E 00	9.65E 00
64	8.08E 00	8.41E 00	8.41E 00	0.00E 00
4	5.39E 00	8.08E 00	9.08E 00	9.19E 00

AVE.	7.13E 00	7.44E 00	7.05E 00	9.45E 00
Le MM	48.5	48.5	48.5	48.5
COMP.	INLET		SECOND	

BAFFLE SPACING (MM)= 98.4 BAFFLE CUT (%) =18.5
B/S CLEARANCE (MM) =0.00 T/B CLEARANCE (MM) =0.00
FLOW RATE = 7.0 TEMP (DEG.C) =25.0 VELOCITY =0.070
REYNOLDS NO. =0.2682E 03 SCHMIDT NO. =1560

INDIVIDUAL TUBE COEFFICIENTS

TUBE				
3	1.25E 01	0.00E 00	1.27E 01	8.99E 00
14	0.00E 00	1.11E 01	7.93E 00	9.09E 00
20	1.13E 01	7.63E 00	1.18E 01	8.99E 00
73	0.00E 00	8.79E 00	9.20E 00	9.09E 00
69	9.99E 00	9.99E 00	9.99E 00	9.99E 00
10	7.93E 00	1.11E 01	1.18E 01	8.87E 00
29	8.79E 00	7.63E 00	7.19E 00	1.10E 01
62	0.00E 00	0.00E 00	1.11E 01	1.09E 01
44	0.00E 00	0.00E 00	6.51E 00	6.45E 00
63	9.99E 00	8.79E 00	9.99E 00	1.03E 01
79	1.36E 01	9.09E 00	8.99E 00	0.00E 00
78	1.36E 01	1.11E 01	1.27E 01	8.14E 00
34	0.00E 00	1.05E 01	1.21E 01	9.09E 00
9	0.00E 00	1.11E 01	0.00E 00	9.20E 00
55	1.11E 01	1.11E 01	1.36E 01	9.62E 00
16	9.87E 00	0.00E 00	1.21E 01	9.10E 00
50	1.24E 01	0.00E 00	1.24E 01	8.99E 00
36	1.25E 01	8.35E 00	1.15E 01	9.03E 00
64	1.25E 01	9.65E 00	9.19E 00	0.00E 00
4	1.25E 01	1.25E 01	8.99E 00	8.99E 00

AVE.	9.99E 00	9.99E 00	9.99E 00	9.99E 00
Le MM	48.5	48.5	48.5	48.5
COMP.	OUTLET		THIRD	

BAFFLE CUT (%) =18.4
T/B CLEARANCE (MM) =0.00
TEMP (DEG.C) =24.0 VELOCITY =0.949
SCHMIDT NO =1640. END COMP REYNOLDS NO. =*.8396E 04

	0 [illegible] 00	6 [illegible] 01	0 00E 00	6 75E 01	5.66E 01
	[illegible]	[illegible]	4 [illegible] 01	6 29E 01	5 61E 01
	[illegible]	[illegible]	4 00E 01	7 14E 01	5 06E 01
	5 78E 01	4 [illegible] 01	4 06E 01	6.75E 01	4.49E 01
	5 [illegible] 01	[illegible]	4 00E 01	6 35E 01	5.81E 01
	0 [illegible] 00	4 [illegible] 01	0 00E 01	0.00E 00	5.35E 01
	5 [illegible] 01	[illegible] 00	5 60E 01	5.77E 01	5.22E 01
	0 00E 00	[illegible] 00	4 30E 01	6 12E 01	5 72E 01
	6 [illegible] 01	5 [illegible] 01	4 08E 01	0.00E 00	0.00E 00
	4 75E 01	4 30E 01	0 00E 00	5 70E 01	4 44E 01
	5 04E 01	4 06E 01	5.13E 01	7.14E 01	5 69E 01
	0 00E 00	5 09E 01	5 37E 01	7.70E 01	4.99E 01
	6 57E 01	6 28E 01	5 46E 01	5.48E 01	6.43E 01
	5 67E 01	4 35E 01	5.02E 01	6.56E 01	5.51E 01
	0 [illegible] 00	5 48E 01	6 17E 01	6.43E 01	6.81E 01
	5 67E 01	6 21E 01	5 31E 01	6.77E 01	6.04E 01
	5 68E 01	5 01E 01	5 31E 01	5.79E 01	4.89E 01
	0 00E 00	4 67E 01	0 00E 00	0.00E 00	5.18E 01
	4 47E 01	5 [illegible] 01	0 00E 00	6.37E 01	3 16E 01
	5 25E 01	4 [illegible] 01	5 40E 01	5.40E 01	4.84E 01

AVE	[illegible]	[illegible] 01	5 [illegible] 01	6 40E 01	5 31E 01
LE	47.6	47.6	23.8	23.8	47.6
COMP	INLET	SECOND		THIRD	

[illegible] SPACING (MM) [illegible] 7 BAFFLE CUT (%) =18.4
[illegible] CLEARANCE (MM) [illegible] T/B CLEARANCE (MM) =0.00
[illegible] RATE [illegible] TEMP (DEG C) =20.0 VELOCITY =0.705
[illegible] SCHMIDT NO =1725 END COMP REYNOLDS NO.=#.6091E 04

[illegible]

1	[illegible]	[illegible]	5.29E 01	5.16E 01	5.51E 01
55	[illegible]	[illegible]	5.25E 01	4.11E 01	5.68E 01
[illegible]	[illegible]	[illegible]	5.74E 01	4.28E 01	4.25E 01
16	[illegible]	[illegible]	4.04E 01	4.47E 01	4.72E 01
79	[illegible]	[illegible]	0.00E 00	5.08E 01	5.92E 01
14	0.00E 00	[illegible]	5.40E 01	0.00E 00	4.61E 01
50	4.44E 01	0.00E 00	4.47E 01	4.24E 01	5.10E 01
52	0.00E 00	0.00E 00	5.01E 01	3.76E 01	5.89E 01
64	0.00E 00	5.14E 01	4.84E 01	0.00E 00	0.00E 00
4	[illegible]	4.53E 01	3.61E 01	4.07E 01	4.86E 01
28	[illegible]	[illegible]	5.14E 01	4.63E 01	4.27E 01
34	0.00E 00	0.00E 00	3.87E 01	4.32E 01	5.23E 01
67	3.92E 01	4.23E 01	3.72E 01	3.79E 01	3.76E 01
10	0.00E 00	0.00E 00	3.85E 01	0.00E 00	0.00E 00
78	5.42E 01	4.67E 01	4.79E 01	4.99E 01	4.99E 01
63	4.63E 01	4.44E 01	4.49E 01	4.04E 01	5.35E 01
29	[illegible]	[illegible]	0.00E 00	4.15E 01	4.11E 01
73	0.00E 00	4.38E 01	0.00E 00	0.00E 00	4.42E 01
44	4.22E 01	4.04E 01	0.00E 00	0.00E 00	0.00E 00
36	4.54E 01	4.46E 01	4.95E 01	4.95E 01	4.20E 01
AVE	[illegible]	[illegible]	[illegible]	4.10E 01	4.88E 01
LE	47.6	47.6	23.8	23.8	47.6
COMP	FIRST	SECOND		THIRD	

BAFFLE CUT (%) =18.4

T/B CLEARANCE (MM) =0.00

TEMP (DEG C) =24.0 VELOCITY =0.415

SCHMIDT NO =1640 END COMP REYNOLDS NO. =*.3668E 04

	0.00E 00	3.29E 01	0.00E 00	4.25E 01	3.42E 01
	3.47E 01	3.27E 01	2.90E 01	3.94E 01	3.53E 01
	3.38E 01	2.01E 01	3.19E 01	4.25E 01	2.85E 01
	0.00E 00	0.00E 00	0.00E 00	0.00E 00	0.00E 00
	4.04E 01	3.26E 01	3.03E 01	4.05E 01	4.03E 01
	0.00E 00	3.11E 01	1.24E 01	0.00E 00	3.34E 01
	3.38E 01	0.00E 00	3.09E 01	3.53E 01	3.34E 01
	0.00E 00	0.00E 00	3.29E 01	3.76E 01	3.51E 01
	0.00E 00	3.3E 01	4.00E 01	4.20E 01	3.34E 01
	3.12E 01	3.04E 01	3.74E 01	3.70E 01	2.82E 01
	3.10E 01	3.08E 01	2.92E 01	4.42E 01	3.47E 01
	0.00E 00	0.00E 00	3.15E 01	4.48E 01	3.07E 01
	3.91E 01	3.95E 01	0.00E 00	3.70E 01	3.68E 01
	2.41E 01	2.77E 01	0.00E 00	0.00E 00	2.31E 01
	4.18E 01	3.42E 01	3.03E 01	4.00E 01	3.83E 01
	3.07E 01	3.24E 01	2.79E 01	3.52E 01	3.57E 01
	3.38E 01	2.78E 00	0.00E 00	0.00E 00	2.19E 01
	0.00E 00	3.01E 01	0.00E 00	3.15E 01	3.92E 01
	2.78E 01	3.26E 01	0.00E 00	0.00E 00	3.92E 01
	3.19E 01	3.91E 01	2.88E 01	2.79E 01	3.02E 01

AVE	3.4	3.1	3.32E 01	3.80E 01	3.32E 01
IE	47.6	47.6	23.8	23.8	47.6
COMP	OUTLET	5TH		4TH	

[illegible] SPACING (MM) = 66.7 BAFFLE CUT (%) =18.4
B/B CLEARANCE (MM) =0.00 T/B CLEARANCE (MM) =0.00
[illegible] RATE =1E 0 TEMP (DEG C) =24.0 VELOCITY =0.166
[illegible] NO =0.1047E 04 SCHMIDT NO. =1640. END COMP REYNOLDS NO. =*.1467E 04

[illegible] FILM COEFFICIENTS

[illegible]	[illegible]	2.78E 01	2.59E 01	2.14E 01
[illegible]	[illegible]	1.67E 01	2.09E 01	2.18E 01
[illegible]	[illegible]	0.00E 00	2.57E 01	1.71E 01
[illegible]	[illegible]	2.07E 01	2.72E 01	1.71E 01
[illegible]	[illegible]	2.91E 01	2.76E 01	2.31E 01
[illegible]	[illegible]	1.91E 01	0.00E 00	2.20E 01
[illegible]	[illegible]	1.43E 01	2.09E 01	2.07E 01
[illegible]	[illegible]	1.67E 01	2.24E 01	2.07E 01
[illegible]	[illegible]	1.67E 01	0.00E 00	2.20E 01
[illegible]	[illegible]	2.08E 01	2.42E 01	1.94E 01
[illegible]	[illegible]	1.72E 01	2.81E 01	2.29E 01
[illegible]	[illegible]	1.78E 01	2.50E 01	1.95E 01
[illegible]	[illegible]	1.74E 01	1.74E 01	2.59E 01
[illegible]	[illegible]	0.00E 00	0.00E 00	0.00E 00
[illegible]	[illegible]	2.52E 01	2.70E 01	2.31E 01
[illegible]	[illegible]	1.78E 01	2.25E 01	2.17E 01
[illegible]	[illegible]	3.78E 01	2.61E 01	2.13E 01
[illegible]	[illegible]	2.37E 01	2.37E 01	2.11E 01
[illegible]	[illegible]	0.00E 00	0.00E 00	2.41E 01
[illegible]	[illegible]	2.00E 01	2.04E 01	1.84E 01
AVE	[illegible]	[illegible]	[illegible]	2.12E 01

LE	47.6	47.6	23.8	23.8	47.6
COMP	OUTLET	5TH		4TH	

BAFFLE SPACING (MM)=66.7 BAFFLE CUT (%) =18.4
B/S CLEARANCE (MM) =0.00 T/B CLEARANCE (MM) =0.00
FLOW RATE = 7.7 TEMP (DEG C) =25.0 VELOCITY =0.070
REYNOLDS NO =0.4054E 04 SCHMIDT NO =1560 END COMP REYNOLDS NO. =*.6381E 03

	[illegible]	[illegible]	1.43E 01	1.60E 01	1.19E 01
2	1.39E 01	1.30E 01	1.05E 01	1.43E 01	1.25E 01
3	1.13E 01	1.10E 01	1.07E 01	1.49E 01	9.93E 00
4	1.23E 01	1.04E 01	0.00E 00	1.66E 01	1.02E 01
5	1.56E 01	1.47E 01	1.15E 01	1.70E 01	1.26E 01
6	0.00E 00	1.34E 01	1.05E [illegible]	0.00E 00	1.26E 01
7	1.19E 01	0.00E 00	1.03E 01	1.24E 01	1.17E 01
8	[illegible]	0.00E 00	1.01E 01	1.30E 01	1.02E 01
9	1.42E 01	[illegible]	9.93E 00	1.24E 01	1.44E 01
10	1.30E 01	9.93E 00	1.47E 01	1.49E 01	1.75E 01
11	1.21E 01	1.15E 01	9.36E 00	1.68E 01	1.38E 01
12	0.00E 00	0.00E 00	0.00E 00	1.47E 01	1.18E 01
13	1.60E 01	1.51E 01	9.55E 00	1.34E 01	1.84E 01
14	1.37E 01	1.07E 01	9.17E 00	1.66E 01	1.25E 01
15	1.40E 01	1.37E 01	1.50E 01	1.59E 01	1.20E 01
16	1.05E 01	1.05E 01	9.93E 00	1.39E 01	1.18E 01
17	1.25E 01	1.13E 01	1.75E 01	1.57E 01	1.26E 01
18	0.00E 00	1.16E 01	0.00E 00	1.34E 01	1.23E 01
19	1.09E 01	1.07E 01	0.00E 00	1.28E 01	1.24E 01
20	1.15E 01	4.69E-01	4.43E 01	2.22E 01	1.15E 01

AVE	1.24E 01	1.10E 01	1.53E 01	1.51E 01	1.28E 01
LB	47.6	47.6	23.8	23.8	47.6
COMP	OUTLET	5TH		4TH	

BAFFLE SPACING (MM)=66.7 BAFFLE CUT (%) =18.4
B/B CLEARANCE (MM) =0.00 T/B CLEARANCE (MM) =0.00
[illegible] TEMP (DEG.C) =24.0 VELOCITY =0.019
[illegible] SCHMIDT NO. =1640. END COMP REYNOLDS NO.=*.1712E 05

[illegible] RESULTS

[illegible]	[illegible]	7.14E [illegible]	7.71E 00	0.00E 00	6.07E 00
[illegible]	[illegible]	6.57E 00	6.75E 00	7.72E 00	6.75E 00
[illegible]	[illegible]	6.05E 00	6.71E 00	7.91E 00	6.56E 00
[illegible]	[illegible]	8.04E 00	9.65E 00	8.49E 00	6.46E 00
[illegible]	[illegible]	[illegible]E 00	7.72E 00	9.26E 00	6.95E 00
[illegible]	[illegible]	6.34E 00	5.79E 00	0.00E 00	6.85E 00
[illegible]	[illegible]	6.05E 00	6.17E 00	7.03E 00	6.75E 00
[illegible]	[illegible]	[illegible]E 00	6.56E 00	7.72E 00	6.85E 00
[illegible]	[illegible]	8.04E 00	5.79E 00	6.75E 00	8.01E 00
[illegible]	[illegible]	0.00E 00	0.00E 00	0.00E 00	9.36E 00
[illegible]	[illegible]	5.92E 00	0.00E 00	9.07E 00	7.04E 00
[illegible]	[illegible]	[illegible]E 00	6.07E 00	7.91E 00	6.66E 00
[illegible]	[illegible]	[illegible]E 00	7.72E 00	9.69E 00	9.94E 00
[illegible]	[illegible]	[illegible]E 00	0.00E 00	7.91E 00	7.04E 00
[illegible]	[illegible]	6.55E 00	8.10E 00	9.07E 00	6.95E 00
[illegible]	[illegible]	6.37E 00	[illegible]E 00	8.68E 00	5.89E 00
[illegible]	[illegible]	[illegible]E 00	[illegible]E 00	7.72E 00	7.14E 00
[illegible]	[illegible]	[illegible]E 00	0.00E 00	0.00E 00	7.04E 00
[illegible]	[illegible]	[illegible]E 00	0.00E 00	7.91E 00	6.75E 00
[illegible]	[illegible]	[illegible]E 00	0.00E 00	0.00E 00	6.46E 00

AVE	[illegible]	[illegible]	[illegible]	8.72E 00	7.09E 00
1E	47.6	47.6	23.8	23.8	47.6
COMP	OUTLET	5TH		4TH	

6

BAFFLE SPACING (MM)= 47.6 BAFFLE CUT (%) =18.4
B/S CLEARANCE (MM) =0.00 T/B CLEARANCE (MM) =0.00
FLOW RATE =*127.0 TEMP (DEG.C) =24.0 VELOCITY) 1/0
REYNOLDS NO. =0.10336E 05 SCHMIDT NO. =1640.

INDIVIDUAL TUBE COEFFICIENTS

TUBE				
73	6.36E 01	6.36E 01	6.66E 01	5.69E 01
79	6.44E 01	6.53E 01	6.53E 01	6.93E 01
9	0.00E 00	6.97E 01	6.93E 01	6.78E 01
78	0.00E 00	0.00E 00	0.00E 00	0.00E 00
69	5.99E 01	6.49E 01	6.08E 01	5.77E 01
10	6.88E 01	6.66E 01	6.58E 01	6.48E 01
29	5.76E 01	0.00E 00	6.54E 01	6.05E 01
62	6.36E 01	7.10E 01	5.40E 01	6.71E 01
44	6.14E 01	6.93E 01	6.97E 01	6.97E 01
4	5.92E 01	6.23E 01	6.10E 01	6.12E 01
34	0.00E 00	6.54E 01	6.69E 01	6.17E 01
20	0.00E 00	0.00E 00	0.00E 00	5.77E 01
55	0.00E 00	6.36E 01	3.92E 01	6.10E 01
14	0.00E 00	0.00E 00	4.07E 01	0.00E 00
28	0.00E 00	7.21E 01	0.00E 00	0.00E 00
16	6.56E 01	6.49E 01	6.69E 01	6.03E 01
50	6.39E 01	8.60E 01	8.94E 01	6.99E 01
63	0.00E 00	7.25E 01	6.92E 01	6.46E 01
64	7.14E 01	0.00E 00	0.00E 00	0.00E 00
36	5.46E 01	5.81E 01	0.00E 00	0.00E 00

AVE	[illegible]	[illegible]	[illegible]	[illegible]
LE	47.6	47.6	47.6	47.6
COMP	OUTLET	7TH	6TH	5TH

BAFFLE SPACING (MM)= 1
B/S CLEARANCE (MM) =0
FLOW RATE =88.5
REYNOLDS NO. =0.73828

BAFFLE CUT (%) =18.4 =0.00
T/B CLEARANCE (MM =0.315
TEMP (DEG.C) =25.0 VELOCITY
SCHMIDT NO. =1060.

INDIVIDUAL TUBE COEFFICIENTS

TUBE				
73	0.00E 00	5.18E 01		
79	5.02E 01	5.44E 01	5.37E 01	4.65E 01
9	5.81E 01	4.77E 01	5.22E 01	5.38E 01
78	0.00E 00	5.84E 01	5.65E 01	5.47E 01
69	4.79E 01	5.18E 01	5.17E 01	5.38E 01
10	5.54E 01	5.53E 01	5.53E 01	4.59E 01
27	4.61E 01	4.57E 01	5.26E 01	5.11E 01
62	5.07E 01	5.88E 01	5.13E 01	4.83E 01
44	4.96E 01	5.65E 01	5.98E 01	5.49E 01
4	4.71E 01	5.04E 01	5.72E 01	5.64E 01
34	0.00E 00	5.06E 01	4.02E 01	4.82E 01
20	6.39E 01	0.00E 00	5.38E 01	5.17E 01
55	0.00E 00	5.02E 01	0.00E 00	4.79E 01
14	4.39E 01	0.00E 00	5.36E 01	4.95E 01
28	0.00E 00	5.89E 01	0.00E 00	0.00E 00
16	5.16E 01	5.18E 01	0.00E 00	0.00E 00
50	4.76E 01	4.99E 01	5.44E 01	4.99E 01
63	5.64E 01	5.90E 01	5.12E 01	0.00E 00
64	5.57E 01	4.53E 01	5.68E 01	5.34E 01
36	3.94E 01	4.52E 01	4.53E 01	4.61E 01
			4.35E 01	4.34E 01
AVE	5.04E 01	5.21E 01	5.28E 01	5.07E 01
LE	47.6	47.6	47.6	47.6
COMP	OUTLET	7TH	6TH	5TH

BAFFLE SPACING (MM)= 47.6
B/S CLEARANCE (MM) = 0.00
FLOW RATE =88.5
REYNOLDS NO. =0.7046E 04

BAFFLE CUT (%) =18.4
T/B CLEARANCE (MM) = 0.00
TEMP (DEG.C) =23.0
SCHMIDT NO. =1725.
VELOCITY =0.315

INDIVIDUAL TUBE COEFFICIENTS

TUBE				
73	0.00E 00	5.61E 01	5.17E 01	5.36E 01
79	4.78E 01	5.44E 01	5.20E 01	5.60E 01
9	5.72E 01	5.69E 01	5.02E 01	5.63E 01
78	0.00E 00	0.00E 00	0.00E 00	0.00E 00
69	4.09E 01	5.73E 01	5.44E 01	5.09E 01
10	4.83E 01	6.16E 01	5.27E 01	5.17E 01
29	4.40E 01	0.00E 00	5.40E 01	5.20E 01
62	5.02E 01	5.46E 01	5.76E 01	5.83E 01
44	5.37E 01	5.36E 01	5.77E 01	5.70E 01
4	4.86E 01	4.90E 01	5.54E 01	4.89E 01
34	0.00E 00	5.24E 01	5.29E 01	5.43E 01
20	5.98E 01	5.41E 01	5.46E 01	5.32E 01
55	0.00E 00	5.44E 01	5.47E 01	5.56E 01
14	0.00E 00	0.00E 00	0.00E 00	0.00E 00
28	6.16E 01	0.00E 00	6.51E 01	6.52E 01
16	4.29E 01	5.31E 01	5.29E 01	5.31E 01
50	3.97E 01	6.16E-01	1.76E-01	0.00E 00
63	0.00E 00	6.17E 01	6.15E 01	5.31E 01
64	5.76E 01	5.81E 01	0.00E 00	0.00E 00
36	3.87E 01	4.90E 01	4.59E 01	4.56E 01

AVE	[illegible]	[illegible]	[illegible]	[illegible]
LE	47.6	47.6	47.6	47.6
COMP	INLET	2ND	3RD	4TH

6

BAFFLE SPACING (MM)=47.6 BAFFLE CUT (%) =18.4
B/S CLEARANCE (MM) =0.00 T/B CLEARANCE (MM) =0.00
FLOW RATE =52.0 TEMP (DEG.C) =22.0 VELOCITY =0.479
REYNOLDS NO. =0.4042E 04 SCHMIDT NO. =1815.

INDIVIDUAL TUBE COEFFICIENTS

TUBE				
73	0.00E 00	3.57E 01	3.54E 01	3.35E 01
79	4.14E 01	3.73E 01	3.73E 01	3.11E 01
9	0.00E 00	3.40E 01	3.78E 01	3.11E 01
78	0.00E 00	0.00E 00	0.00E 00	0.00E 00
69	3.70E 01	4.11E 01	3.64E 01	0.00E 00
10	3.63E 01	3.53E 01	3.75E 01	3.75E 01
29	3.33E 01	4.44E 01	4.41E 01	0.00E 00
62	0.00E 00	4.14E 01	3.72E 01	3.40E 01
44	3.68E 01	2.84E 01	2.84E 01	0.00E 00
4	2.80E 01	2.95E 01	2.68E 01	2.79E 01
34	0.00E 00	0.00E 00	3.47E 01	3.12E 01
20	3.26E 01	3.51E 01	3.47E 01	3.43E 01
55	3.83E 01	3.80E 01	3.73E 01	3.42E 01
14	0.00E 00	0.00E 00	0.00E 00	0.00E 00
28	3.27E 01	3.38E 01	3.65E 01	2.98E 01
16	3.57E 01	3.64E 01	3.56E 01	3.39E 01
50	3.00E 01	0.00E 00	3.38E 01	3.16E 01
63	3.30E 01	3.92E 01	3.71E 01	3.79E 01
64	3.28E 01	3.67E 01	3.56E 01	3.06E 01
36	3.10E 01	3.18E 01	3.02E 01	3.16E 01
AVE	3.43E 01	3.41E 01	3.56E 01	3.36E 01
LE	47.6	47.6	47.6	47.6
COMP	OUTLET	7TH	6TH	5TH

6

BAFFLE SPACING (MM)= 47.5 BAFFLE CUT (%) =18.4
B/S CLEARANCE (MM) =0.00 T/B CLEARANCE (MM)= 0.00
FLOW RATE =31.0 TEMP (DEG. C) =23.0 VELOCITY = 1.93
REYNOLDS NO. =0.2460E 04 SCHMIDT NO. =1725.

INDIVIDUAL TUBE COEFFICIENTS

TUBE				
73	2.77E 01	2.94E 01	3.09E 01	2.77E 01
79	2.74E 01	2.98E 01	2.94E 01	3.03E 01
9	3.16E 01	3.12E 01	3.16E 01	3.12E 01
78	0.00E 00	0.00E 00	0.00E 00	0.00E 00
69	2.78E 01	2.89E 01	3.22E 01	2.82E 01
10	2.91E 01	3.01E 01	2.91E 01	2.99E 01
29	0.00E 00	0.00E 00	2.90E 01	2.93E 01
62	2.75E 01	3.36E 01	3.01E 01	3.12E 01
44	2.71E 01	3.04E 01	3.14E 01	3.10E 01
4	2.62E 01	2.92E 01	2.80E 01	2.90E 01
34	0.00E 00	3.19E 01	3.10E 01	3.03E 01
20	3.49E 01	0.00E 00	3.12E 01	3.20E 01
55	0.00E 00	3.30E 01	3.10E 01	3.20E 01
14	0.00E 00	0.00E 00	0.00E 00	0.00E 00
28	3.03E 01	3.41E 01	3.16E 01	3.40E 01
16	3.10E 01	3.20E 01	3.17E 01	3.03E 01
50	2.93E 01	3.00E 01	3.09E 01	2.96E 01
63	0.00E 00	3.39E 01	3.26E 01	3.06E 01
64	3.27E 01	0.00E 00	0.00E 00	0.00E 00
36	2.71E 01	2.78E 01	2.90E 01	2.90E 01

AVE	3.00E 01	3.20E 01	3.09E 01	3.04E 01
LE	47.6	47.6	47.6	47.6
COMP	OUTLET	7TH	6TH	5TH

6

BAFFLE SPACING (MM)=47.6 BAFFLE CUT (%)=18.4

B/S CLEARANCE (MM) =0.00 T/D CLEARANCE (MM) =7.00

FLOW RATE =18.0 TEMP (DEG.C) =24.0 VELOCITY (FT/S)

REYNOLDS NO =0.1467E+04 SCHMIDT NO. =1640.

INDIVIDUAL TUBE COEFFICIENTS

TUBE				
73	0.00E 00	2.02E 01	2.04E 01	1.89E 01
79	1.81E 01	2.01E 01	1.98E 01	1.94E 01
9	2.14E 01	2.11E 01	2.14E 01	2.10E 01
78	0.00E 00	0.00E 00	0.00E 00	0.00E 00
69	1.94E 01	1.98E 01	2.20E 01	1.88E 01
10	2.01E 01	2.05E 01	2.00E 01	2.01E 01
29	1.71E 01	0.00E 00	1.99E 01	1.88E 01
62	1.89E 01	2.04E 01	2.11E 01	2.12E 01
44	1.90E 01	2.10E 01	2.08E 01	2.08E 01
4	1.88E 01	1.93E 01	2.07E 01	1.98E 01
34	0.00E 00	1.97E 01	2.11E 01	2.09E 01
20	2.07E 01	2.09E 01	2.18E 01	2.14E 01
55	0.00E 00	1.99E 01	2.09E 01	2.08E 01
14	2.09E 01	2.13E 01	2.11E 01	2.07E 01
28	2.31E 01	2.40E 01	2.17E 01	2.38E 01
16	2.10E 01	2.07E 01	2.19E 01	1.97E 01
50	1.84E 01	2.09E 01	2.26E 01	1.81E 01
63	0.00E 00	2.04E 01	2.20E 01	2.11E 01
64	2.19E 01	0.00E 00	0.00E 00	0.00E 00
36	1.89E 01	1.96E 01	1.99E 01	1.79E 01

AVE	1.97E 01	2.04E 01	2.13E 01	1.98E 01
LE	47.6	47.6	47.6	47.6
COMP	OUTLET	7TH	6TH	5TH

6

BAFFLE SPACING (MM)= 47.6 BAFFLE CUT (%) =18.4
B/S CLEARANCE (MM) =0.00 T/B CLEARANCE (MM) =0.00
FLOW RATE = 9.2 TEMP (DEG.C) =23.0 VELOCITY =0.085
REYNOLDS NO. =0.7325E 03 SCHMIDT NO. =1725.

INDIVIDUAL TUBE COEFFICIENTS

TUBE				
73	1.32E 01	1.50E 01	1.61E 01	1.38E 01
79	1.26E 01	1.49E 01	1.41E 01	1.43E 01
9	1.59E 01	1.58E 01	1.63E 01	1.58E 01
78	0.00E 00	1.59E 01	1.62E 01	1.64E 01
69	1.52E 01	1.47E 01	1.58E 01	1.40E 01
10	1.53E 01	1.48E 01	1.50E 01	1.46E 01
29	1.31E 01	0.00E 00	1.45E 01	1.47E 01
62	1.37E 01	1.60E 01	1.54E 01	1.62E 01
44	1.45E 01	1.58E 01	1.76E 01	1.71E 01
4	1.41E 01	1.39E 01	1.47E 01	1.42E 01
34	0.00E 00	1.64E 01	1.54E 01	1.62E 01
20	1.59E 01	1.46E 01	1.44E 01	1.48E 01
55	0.00E 00	1.43E 01	1.41E 01	1.47E 01
14	1.47E 01	1.64E 01	1.50E 01	0.00E 00
28	1.58E 01	1.02E 01	1.58E 01	1.58E 01
16	1.64E 01	1.41E 01	1.53E 01	1.12E 01
50	1.53E 01	1.71E 01	1.58E 01	1.51E 01
63	1.60E 01	1.46E 01	1.68E 01	1.60E 01
64	1.41E 01	1.95E 01	1.50E 01	0.00E 00
36	1.12E 01	1.02E 01	1.62E 01	1.02E 01

AVE	[illegible]	[illegible]	[illegible]	[illegible]
LE	47.6	47.6	47.6	47.6
COMP	OUTLET	7TH	6TH	5TH

6

BAFFLE SPACING (MM) 47.6 B/S CLEARANCE (MM) 0.00 FLOW RATE = 4.0 REYNOLDS NO. =9.3102E 03

BAFFLE CUT (%) =18.4 T/B CLEARANCE (MM) = 0.00 TEMP (DEG C) =23.0 VELOCITY =0.03 SCHMIDT NO. =1725

INDIVIDUAL TUBE COEFFICIENTS

TUBE				
73	9.06E 00	9.50E 00	1.00E 01	9.06E 00
79	8.18E 00	9.50E 00	9.06E 00	9.50E 00
9	1.00E 01	1.01E 01	1.00E 01	9.94E 00
78	0.00E 00	0.00E 00	0.00E 00	0.00E 00
69	9.69E 00	8.99E 00	1.00E 01	8.88E 00
10	1.01E 01	9.50E 00	9.50E 00	9.94E 00
29	8.46E 00	8.88E 00	9.47E 00	9.94E 00
62	9.34E 00	1.00E 01	1.00E 01	1.00E 01
44	1.01E 01	1.01E 01	1.03E 01	1.03E 01
4	9.95E 00	9.94E 00	1.06E 01	8.99E 00
34	0.00E 00	1.07E 01	1.03E 01	1.05E 01
20	1.11E 01	1.01E 01	1.04E 01	1.02E 01
55	0.00E 00	9.94E 00	1.12E 01	9.10E 00
14	0.00E 00	0.00E 00	0.00E 00	0.00E 00
28	0.00E 00	1.13E 01	0.00E 00	0.00E 00
16	1.01E 01	9.50E 00	1.11E 01	9.94E 00
50	9.42E 00	9.48E 00	9.50E 00	9.06E 00
63	0.00E 00	1.03E 01	1.05E 01	9.94E 00
64	1.00E 01	0.00E 00	0.00E 00	0.00E 00
36	8.48E 00	9.00E 00	8.42E 00	9.42E 00

AVE	[illegible]	[illegible]	[illegible]	[illegible]
LE	47.6	47.6	47.6	47.6
COMP	OUTLET	7TH	6TH	5TH

6

BAFFLE SPACING (MM)= 47.6 BAFFLE CUT (%) =18.4
B/S CLEARANCE (MM) =0.00 T/B CLEARANCE (MM) = 0.00
FLOW RATE = 2.1 TEMP (DEG. C) =24.0 VELOCITY = 0.019
REYNOLDS NO. =0.1712E 03 SCHMIDT NO. =1640.

INDIVIDUAL TUBE COEFFICIENTS

TUBE				
73	6.97E 00	7.06E 00	7.49E 00	7.14E 00
79	6.19E 00	7.14E 00	6.97E 00	7.49E 00
9	7.23E 00	7.49E 00	7.58E 00	7.75E 00
78	0.00E 00	0.00E 00	0.00E 00	0.00E 00
69	6.62E 00	6.27E 00	8.10E 00	6.79E 00
10	7.06E 00	6.97E 00	7.06E 00	7.49E 00
29	6.45E 00	7.23E 00	7.23E 00	7.40E 00
62	6.71E 00	7.40E 00	8.01E 00	7.49E 00
44	7.67E 00	8.01E 00	0.00E 00	8.36E 00
4	6.62E 00	6.97E 00	6.97E 00	7.06E 00
34	6.62E 00	7.49E 00	7.49E 00	6.62E 00
20	7.32E 00	7.06E 00	7.06E 00	7.93E 00
55	0.00E 00	6.89E 00	0.00E 00	7.23E 00
14	8.71E 00	6.97E 00	7.84E 00	0.00E 00
28	7.14E 00	8.36E 00	7.14E 00	7.23E 00
16	7.14E 00	6.71E 00	8.01E 00	6.97E 00
50	6.71E 00	5.23E 00	5.40E 00	7.84E 00
63	0.00E 00	8.10E 00	7.93E 00	7.75E 00
64	7.32E 00	0.00E 00	0.00E 00	0.00E 00
36	5.84E 00	5.84E 00	6.01E 00	6.10E 00

AVE	[illegible]	[illegible]	[illegible]	[illegible]
LE	47.6	47.6	47.6	47.6
COMP	OUTLET	7TH	6TH	5TH

BAFFLE CUT (%) =10.4

I/B CLEARANCE (MM) = 0.00

TEMP (DEG C) =24.0 VELOCITY =0.080

SCHMIDT NO =1640 END COMP REYNOLDS NO = .7784E 04

HEAT TRANSFER COEFFICIENTS

TUBE						
2	0.00E 00	2.00E 01	2.74E 01	3.75E 01	5.52E 01	7.47E 01
26	0.00E 00	0.73E 01	0.00E 00	4.53E 01	6.68E 01	7.63E 01
30	7.31E 01	1.96E 01	2.70E 01	2.97E 01	0.00E 00	7.47E 01
62	7.00E 01	2.01E 01	3.69E 01	4.38E 01	8.46E 01	7.93E 01
64	0.00E 00	2.70E 01	3.27E 01	0.00E 00	7.81E 01	8.25E 01
29	8.25E 01	1.88E 01	2.44E 01	3.35E 01	4.87E 01	7.40E 01
4	0.00E 00	0.00E 00	0.00E 00	0.00E 00	0.00E 00	6.87E 01
16	6.95E 01	0.00E 00	3.66E 01	3.87E 01	7.43E 01	0.00E 00
50	7.35E 01	1.87E 01	2.56E 01	3.78E 01	0.00E 00	0.00E 00
14	7.22E 01	1.88E 01	0.00E 00	3.75E 01	5.31E 01	8.49E 01
69	0.00E 00	7.35E 01	6.78E 01	7.47E 01	7.27E 01	7.13E 01
73	0.00E 00	5.98E 01	6.16E 01	7.37E 01	7.37E 01	7.27E 01
44	5.99E 01	2.46E 01	2.92E 01	3.88E 01	6.24E 01	7.24E 01
34	0.00E 00	0.00E 00	2.42E 01	4.27E 01	5.75E 01	5.31E 01
79	0.00E 00	0.00E 00	0.00E 00	3.21E 01	4.13E 01	0.00E 00
10	6.47E 01	2.30E 01	0.00E 00	0.00E 00	4.78E 01	5.43E 01
78	6.36E 01	1.68E 01	2.93E 01	3.27E 01	0.00E 00	5.16E 01
63	6.50E 01	1.66E 01	2.81E 01	4.02E 01	5.56E 01	6.44E 01
38	0.00E 00	2.37E 01	4.44E 01	5.80E 01	0.00E 00	5.66E 01
55	6.86E 01	0.00E 00	0.00E 00	3.72E 01	5.28E 01	6.41E 01
AVE	7.11E 01	2.76E 01	1.66E 01	4.32E 01	6.16E 01	6.92E 01
LE	47.6	47.6	23.8	23.8	23.8	23.8
COMP	INLET	SECOND				

BAFFLE CUT (%) =18.4

TIP CLEARANCE (MM) =0.00

VELOCITY =0.811

SECTION NO. - 1485 END COMP REYNOLDS NO. - 7509E 04

			0.00E 00	7.54E 01	9.58E 01	
			4.03E 01	0.00E 00	0.00E 00	
			4.47E 01	7.80E 01	9.46E 01	
			5.54E 01	5.26E 01	5.58E 01	
			4.17E 01	8.13E 01	9.48E 01	
			4.31E 01	6.53E 01	9.32E 01	
			0.00E 00	0.00E 00	8.47E 01	
			4.41E 01	8.57E 01	1.01E 02	
			4.59E 01	7.74E 01	9.22E 01	
			4.59E 01	7.74E 01	9.22E 01	
			0.00E 00	6.39E 01	8.57E 01	
			0.00E 00	8.59E 01	7.52E 01	
			4.45E 01	7.94E 01	7.90E 01	
			5.30E 01	8.51E 01	8.39E 01	
			5.74E 01	9.20E 01	0.00E 00	
			4.47E 01	6.00E 01	8.47E 01	
			0.00E 00	7.58E 01	8.81E 01	
			4.55E 01	0.00E 00	7.54E 01	
			4.65E 01	6.57E 01	7.20E 01	
			5.20E 01	7.22E 01	8.27E 01	
			4.53E 01	6.67E 01	8.80E 01	

AVE			4.72E 01	7.43E 01	8.51E 01	
LE mm	47.6	47.6	23.8	23.8	23.8	23.8
COMP	INLET	SECOND				

[illegible] BAFFLE CUT (%) =18.4

[illegible] T/B CLEARANCE (MM) =0.00

[illegible] TEMP (DEG C) =26.9 VELOCITY =0.405

[illegible] SCHMIDT NO. =1450. END COMP. REYNOLDS NO =.3797E 04

[illegible] TUBE VIBRATION

TUBE						
2	[illegible]	[illegible]	2.21E 01	0.00E 00	3.74E 01	5.18E 01
25	[illegible]	[illegible]	0.00E 00	3.18E 01	4.49E 01	5.06E 01
26	[illegible]	[illegible]	[illegible]	2.30E 01	3.65E 01	4.86E 01
62	5.46E 01	[illegible]	1.65E 01	3.52E 01	5.32E 01	5.33E 01
64	[illegible]	[illegible]	[illegible]	0.00E 00	4.85E 01	5.32E 01
29	6.08E 01	[illegible]	2.19E 01	2.41E 01	3.38E 01	4.96E 01
4	0.00E 00	0.00E 00	4.74E 01	0.00E 00	0.00E 00	4.74E 01
16	5.08E 01	0.00E 00	[illegible]	3.03E 01	5.06E 01	0.00E 00
50	[illegible]	[illegible]	[illegible]	2.71E 01	3.67E 01	4.80E 01
14	[illegible]	[illegible]	[illegible]	0.00E 00	3.65E 01	4.86E 01
69	[illegible]	0.00E 00	[illegible]	[illegible]	4.76E 01	4.58E 01
73	[illegible]	0.00E 00	[illegible]	[illegible]	4.86E 01	5.01E 01
44	[illegible]	[illegible]	[illegible]	[illegible]	5.06E 01	5.23E 01
34	[illegible]	[illegible]	[illegible]	[illegible]	5.05E 01	6.41E 01
79	[illegible]	0.00E 00	0.00E 00	2.78E 01	3.36E 01	4.96E 01
10	[illegible]	[illegible]	[illegible]	0.00E 00	4.17E 01	4.90E 01
78	[illegible]	[illegible]	[illegible]	[illegible]	0.00E 00	4.13E 01
63	[illegible]	[illegible]	[illegible]	[illegible]	[illegible]	4.46E 01
36	0.00E 00	[illegible]	[illegible]	4.59E 01	5.27E 01	4.90E 01
55	[illegible]	[illegible]	0.00E 00	2.89E 01	[illegible]	5.10E 01

AVE	[illegible]	[illegible]	[illegible]	[illegible]	[illegible]	[illegible]
LE mm	47.6	47.6	23.8	23.8	23.8	23.8
COMP	INLET	SECOND				

BAFFLE SPACING (MM)=*142.2 BAFFLE CUT (%) =18.4
B/S CLEARANCE (MM) =0.00 T/B CLEARANCE (MM) =0.00
FLOW RATE 37.0 TEMP (DEG.C) =27.8 VELOCITY =0.341
REYNOLDS NO. = 1043E 04 SCHMIDT NO. =1362. END COMP. REYNOLDS NO. =.3206E 04

INDIVIDUAL TUBE COEFFICIENTS

TUBE						
9	5.44E 01	1.43E 01	2.44E 01	0.00E 00	5.04E 01	6.24E 01
28	0.00E 00	1.41E 01	2.27E 01	3.16E 01	5.04E 01	5.64E 01
20	4.96E 01	1.16E 01	2.05E 01	3.16E 01	4.78E 01	5.10E 01
62	4.54E 01	1.61E 01	1.73E 01	3.91E 01	6.11E 01	5.50E 01
64	0.00E 00	1.74E 01	0.00E 00	3.24E 01	3.96E 01	5.20E 01
29	5.31E 01	1.34E 01	2.25E 01	2.91E 01	4.29E 01	5.47E 01
4	4.85E 01	4.80E 01	4.62E 01	4.60E 01	0.00E 00	4.82E 01
16	4.53E 01	1.96E 01	2.05E 01	3.11E 01	5.18E 01	5.64E 01
50	4.29E 01	1.36E 01	2.03E 01	2.98E 01	4.53E 01	4.96E 01
14	4.62E 01	3.14E 01	2.24E 01	2.87E 01	3.91E 01	5.02E 01
69	0.00E 00	0.00E 00	0.00E 00	4.49E 01	4.00E 01	4.11E 01
73	4.94E 01	0.00E 00	4.69E 01	4.47E 01	4.34E 01	4.50E 01
44	4.24E 01	0.00E 00	2.25E 01	3.49E 01	4.85E 01	4.64E 01
34	0.00E 00	0.00E 00	2.36E 01	3.89E 01	5.22E 01	4.71E 01
79	0.00E 00	0.00E 00	2.18E 01	2.96E 01	0.00E 00	0.00E 00
10	4.30E 01	1.41E 01	1.95E 01	0.00E 00	4.56E 01	4.91E 01
78	5.14E 01	1.14E 01	2.16E 01	2.82E 01	0.00E 00	4.29E 01
63	4.94E 01	1.59E 01	2.49E 01	2.94E 01	3.98E 01	4.11E 01
36	0.00E 00	0.00E 00	3.31E 01	4.24E 01	5.20E 01	4.67E 01
55	5.31E 01	0.00E 00	0.00E 00	2.91E 01	3.98E 01	5.13E 01

AVE	4.74E 01	1.43E 01	2.15E 01	3.45E 01	4.65E 01	4.79E 01
LE	47.6	47.6	23.8	23.8	23.8	23.8
COMP	INLET		SECOND			

BAFFLE CUT (%) =18.4

T/B CLEARANCE (MM) =0.00

TEMP (DEG C) =27.0 VELOCITY =0.081

SCHMIDT NO =1415 END COMP. REYNOLDS NO = 7679E 03

TUBE						
9	[illegible]	2.17E 00	1.70E 01	0.00E 00	1.74E 01	2.19E 01
28	[illegible]	[illegible]	0.00E 00	1.57E 01	1.95E 01	2.04E 01
30	[illegible]	[illegible]	1.74E 01	1.39E 01	1.76E 01	1.91E 01
62	2.15E 01	[illegible]	1.72E 01	1.74E 01	1.98E 01	2.10E 01
64	[illegible]	[illegible]	1.46E 01	0.00E 00	2.10E 01	2.23E 01
29	[illegible]	8.24E 00	1.10E 01	1.27E 01	1.70E 01	2.38E 01
4	0.00E 00	[illegible]	2.06E 01	1.93E 01	0.00E 00	1.80E 01
16	[illegible]	[illegible]	1.90E 01	1.85E 01	2.19E 01	0.00E 00
50	2.12E 01	[illegible]	1.70E 01	1.37E 01	1.70E 01	0.00E 00
14	2.16E 01	[illegible]	1.16E 01	0.00E 00	1.72E 01	2.19E 01
69	0.00E 00	0.00E 00	2.13E 01	1.91E 01	1.93E 01	1.80E 01
73	2.17E 01	0.00E 00	2.13E 01	1.89E 01	1.89E 01	2.00E 01
44	2.14E 01	8.24E 00	1.67E 01	2.10E 01	2.10E 01	2.00E 01
34	0.00E 00	0.00E 00	1.78E 01	2.00E 01	2.00E 01	1.89E 01
79	0.00E 00	0.00E 00	0.00E 00	1.72E 01	1.70E 01	2.43E 01
10	2.20E 01	6.93E 00	1.27E 01	1.83E 01	1.82E 01	1.85E 01
78	2.20E 01	[illegible]	1.16E 01	0.00E 00	0.00E 00	1.82E 01
63	2.20E 01	[illegible]	1.72E 01	1.78E 01	1.80E 01	1.87E 01
36	0.00E 00	[illegible]	0.00E 00	2.10E 01	2.12E 01	1.95E 01
55	[illegible]	0.00E 00	0.00E 00	1.91E 01	1.87E 01	2.36E 01

AVE	[illegible]	[illegible]	[illegible]	1.77E 01	1.89E 01	2.05E 01
LE mm	47.6	47.6	23.8	23.8	23.8	23.8
COMP	INLET	SECOND				

BAFFLE CUT (%) =18.4

T/B CLEARANCE (MM) =0.00

TEMP (DEG C) =26.2 VELOCITY =0.166

SCHMIDT NO =1471. END COMP. REYNOLDS NO =.1543E 04

TUBE						
9	[illegible]	1.14E 01	1.88E 01	0.00E 00	2.63E 01	3.37E 01
28	[illegible]	[illegible]	0.00E 00	2.20E 01	3.08E 01	3.22E 01
30	[illegible]	[illegible]	1.88E 01	1.95E 01	2.81E 01	3.26E 01
62	3.61E 01	[illegible]	[illegible]	2.77E 01	3.59E 01	3.41E 01
64	[illegible]	[illegible]	[illegible]	0.00E 00	3.49E 01	3.72E 01
29	[illegible]	[illegible]	1.94E 01	1.79E 01	2.65E 01	3.69E 01
4	0.00E 00	0.00E 00	3.70E 01	0.00E 00	0.00E 00	3.08E 01
16	[illegible]	[illegible]	1.98E 01	0.00E 00	3.80E 01	4.00E 01
50	[illegible]	[illegible]	1.72E 01	2.05E 01	2.79E 01	3.26E 01
14	[illegible]	[illegible]	1.64E 01	0.00E 00	2.79E 01	3.45E 01

AVE	[illegible]	[illegible]	1.87E 01	2.15E 01	3.07E 01	3.45E 01
LE mm	47.6	47.6	23.8	23.8	23.8	23.8
COMP	INLET	SECOND				

3

BAFFLE SPACING (MM) 47.6 BAFFLE CUT (%) =18.4
B/S CLEARANCE (MM) =0.00 T/B CLEARANCE (MM) =0.00
FLOW RATE =73.0 TEMP (DEG.C) =25.8 VELOCITY =0.673
REYNOLDS NO. =0.62018 04 SCHMIDT NO. =1500.

INDIVIDUAL TUBE COEFFICIENTS

TUBE						
69	8.18E 01	1.05E 02	1.09E 02	8.24E 01	1.18E 02	1.02E 02
73	8.91E 01	8.63E 01	1.24E 02	1.05E 02	0.00E 00	7.95E 01
44	6.71E 01	8.05E 01	9.14E 01	7.01E 01	8.11E 01	7.75E 01
34	8.05E 01	1.01E 02	1.17E 02	8.52E 01	1.33E 02	7.67E 01
79	8.63E 01	7.09E 01	1.07E 02	1.02E 02	9.75E 01	6.93E 01
29	7.62E 01	9.61E 01	0.00E 00	8.36E 01	1.26E 02	6.64E 01
78	0.00E 00	0.00E 00	1.04E 02	0.00E 00	9.22E 01	6.97E 01
63	0.00E 00	8.07E 01	0.00E 00	7.70E 01	0.00E 00	7.58E 01
36	7.07E 01	8.36E 01	9.63E 01	8.32E 01	1.02E 02	7.75E 01
55	0.00E 00	0.00E 00	0.00E 00	0.00E 00	0.00E 00	0.00E 00
9	1.11E 02	8.20E 01	1.44E 02	1.43E 02	1.00E 02	1.05E 02
28	8.59E 01	0.00E 00	1.06E 02	8.97E 01	1.33E 02	0.00E 00
20	7.23E 01	1.02E 02	1.00E 02	0.00E 00	1.17E 02	1.00E 02
62	1.04E 02	8.36E 01	1.36E 02	8.48E 01	9.67E 01	8.48E 01
64	8.28E 01	0.00E 00	1.23E 02	5.94E 01	8.01E 01	8.77E 01
10	0.00E 00	1.03E 02	1.04E 02	7.79E 01	1.16E 02	7.43E 01
4	7.50E 01	9.28E 01	9.63E 01	7.50E 01	0.00E 00	9.02E 01
16	7.75E 01	9.32E 01	1.02E 02	8.24E 01	1.24E 02	8.08E 01
50	0.00E 00	0.00E 00	0.00E 00	8.07E 01	9.79E 01	8.69E 01
14	0.00E 00	0.00E 00	0.00E 00	0.00E 00	0.00E 00	0.00E 00

AVE	9.2[illegible] 01	9.[illegible] 01	1.1[illegible] 02	9.[illegible] 01	1.08E 02	8.[illegible] 01
LE	47.6	47.6	23.8	23.8	23.8	23.8
COMP	OUTLET	7TH	6TH		5TH	

3

BAFFLE SPACING (MM) 47.6 BAFFLE CUT (%) =18.4
B/S CLEARANCE (MM) =0.00 T/B CLEARANCE (MM) =0.00
FLOW RATE =95.0 TEMP (DEG.C) =25.8 VELOCITY =0.875
REYNOLDS NO. =0.80706 04 SCHMIDT NO. =1500.

INDIVIDUAL TUBE COEFFICIENTS

TUBE						
69	9.81E 01	1.[illegible] 02	1.09E 02	1.01E 02	1.44E 02	1.14E 02
73	1.07E 02	1.[illegible] 02	1.44E 02	1.21E 02	1.20E 02	9.81E 01
44	8.[illegible] 01	8.[illegible] 01	9.40E 01	8.[illegible] 01	7.81E 01	8.21E 01
34	9.15E 01	1.[illegible] 02	1.36E 02	1.00E 02	1.34E 02	8.93E 01
79	0.00E 00	9.[illegible] 01	1.21E 02	1.14E 02	1.08E 02	8.05E 01
29	8.19E 01	1.[illegible] 02	0.00E 00	9.49E 01	1.44E 02	7.97E 01
78	0.00E 00	0.00E 00	1.15E 02	0.00E 00	9.89E 01	7.73E 01
63	0.00E 00	8.51E 01	1.55E 02	0.00E 00	0.00E 00	8.57E 01
36	7.58E 01	8.[illegible] 01	1.12E 02	8.[illegible] 01	1.17E 02	8.93E 01
55	0.00E 00	0.[illegible] 01	0.00E 00	0.00E 00	0.00E 00	0.00E 00
9	0.00E 00	9.[illegible] 01	1.48E 02	1.15E 02	1.24E 02	0.00E 00
28	9.32E 01	0.00E 00	1.26E 02	1.04E 02	1.54E 02	1.20E 02
20	8.0[illegible] 01	1.18[illegible] 02	1.15E 02	0.00E 00	1.3[illegible] 02	[illegible].35E 01
62	1.1[illegible] 02	9.[illegible] 01	1.55E 02	9.45E 01	1.11E [illegible]	9.61E 01
64	8.[illegible] 01	0.00E 00	1.32E 02	6.41E 01	1.00E 02	0.00E 00
10	0.00E 00	1.1[illegible] 02	1.15E 02	8.13E 01	1.31E 02	9.73E 01
4	8.1[illegible] 01	1.0[illegible] 02	1.11E 02	7.89E 01	0.00E 00	9.[illegible] 01
16	7.[illegible] 01	1.[illegible] 02	1.14E 02	9.01E 01	1.36E 02	9.9[illegible] 01
50	0.00E 00	0.[illegible] 01	0.00E 00	8.74E 01	1.15E 02	9.7[illegible] 01
14	0.00E 00	0.[illegible] 01	0.00E 00	0.00E 00	0.00E 00	0.00E 00

AVE	8.[illegible] 01	1.[illegible]	[illegible] 02	9.[illegible] 01	1.[illegible] 02	9.[illegible] 01
LE	47.6	47.6	23.8	23.8	23.8	23.8
COMP	OUTLET	7TH	6TH		5TH	

3

BAFFLE SPACING (MM)=47.6 BAFFLE CUT (%) =18.4
B/S CLEARANCE (MM) =0.00 T/B CLEARANCE (MM) =0.00
FLOW RATE =25.0 TEMP (DEG C) =26.0 VELOCITY =0.230
REYNOLDS NO. =0.21306 04 SCHMIDT NO. =1485.

INDIVIDUAL TUBE COEFFICIENTS

TUBE						
69	4.65E 01	5.81E 01	6.01E 01	4.40E 01	6.31E 01	5.45E 01
73	5.00E 01	4.74E 01	6.25E 01	5.08E 01	5.36E 01	4.20E 01
44	3.52E 01	4.27E 01	4.50E 01	3.43E 01	4.07E 01	4.29E 01
34	4.29E 01	4.78E 01	5.47E 01	4.40E 01	6.05E 01	3.86E 01
79	0.00E 00	4.05E 01	5.23E 01	5.19E 01	5.02E 01	3.77E 01
29	3.92E 01	4.87E 01	0.00E 00	4.56E 01	5.70E 01	3.65E 01
78	0.00E 00	0.00E 00	0.00E 00	0.00E 00	4.72E 01	3.69E 01
63	0.00E 00	4.24E 01	0.00E 00	1.00E 00	0.00E 00	0.00E 00
36	3.71E 01	4.40E 01	4.76E 01	4.09E 01	4.89E 01	3.99E 01
55	0.00E 00	0.00E 00	0.00E 00	0.00E 00	0.00E 00	0.00E 00
9	0.00E 00	4.70E 01	7.01E 01	5.19E 01	5.70E 01	4.50E 01
28	4.95E 01	0.00E 00	7.92E 01	5.10E 01	6.86E 01	4.80E 01
20	4.27E 01	5.45E 01	7.52E 01	0.00E 00	6.05E 01	5.15E 01
62	5.34E 01	4.41E 01	7.16E 01	4.46E 01	5.15E 01	4.20E 01
64	4.10E 01	0.00E 00	6.31E 01	3.80E 01	4.09E 01	4.30E 01
10	0.00E 00	0.00E 00	5.66E 01	4.07E 01	0.00E 00	0.00E 00
4	4.40E 01	5.12E 01	5.45E 01	4.07E 01	0.00E 00	4.68E 01
16	4.14E 01	5.17E 01	5.47E 01	4.30E 01	6.26E 01	3.47E 01
50	0.00E 00	0.00E 00	0.00E 00	4.46E 01	4.89E 01	4.30E 01
14	0.00E 00	0.00E 00	0.00E 00	0.00E 00	0.00E 00	0.00E 00

AVE	4.[illegible] 01	4.[illegible] 01	5.[illegible] 01	4.40E 01	5.47E 01	4.[illegible] 01
LE	47.6	47.6	23.8	23.8	23.8	23.8
COMP	OUTLET	7TH	6TH		5TH	

3

BAFFLE SPACING (MM)=47.6 BAFFLE CUT (%) =18.4
B/S CLEARANCE (MM) =0.00 T/B CLEARANCE (MM) =0.00
FLOW RATE =51.0 TEMP (DEG.C) =25.8 VELOCITY =0.470
REYNOLDS NO. =0.43722E 04 SCHMIDT NO. =1500

INDIVIDUAL TUBE COEFFICIENTS

TUBE						
69	5.63E 01	8.11E 01	9.11E 01	5.99E 01	9.67E 01	8.11E 01
73	6.74E 01	6.21E 01	9.34E 01	8.06E 01	7.38E 01	2.46E 00
44	4.69E 01	6.05E 01	7.40E 01	5.98E 01	6.56E 01	6.56E 01
34	5.72E 01	7.19E 01	8.52E 01	6.39E 01	9.84E 01	5.50E 01
79	6.03E 01	5.51E 01	7.95E 01	8.03E 01	7.29E 01	5.00E 01
29	5.38E 01	7.03E 01	0.00E 00	6.52E 01	9.51E 01	4.96E 01
78	0.00E 00	0.00E 00	7.70E 01	0.00E 00	7.17E 01	5.30E 01
63	0.00E 00	5.03E 01	1.06E 02	6.07E 01	0.00E 00	5.45E 01
36	4.94E 01	6.29E 01	6.10E 01	6.64E 01	7.91E 01	5.78E 01
55	0.00E 00	0.00E 00	0.00E 00	0.00E 00	0.00E 00	0.00E 00
9	8.67E 01	6.45E 01	1.10E 02	7.75E 01	8.20E 01	7.30E 01
28	6.76E 01	0.00E 00	8.25E 01	7.05E 01	1.07E 02	0.00E 00
20	5.84E 01	8.01E 01	7.58E 01	0.00E 00	9.34E 01	8.52E 01
62	0.00E 00	6.40E 01	1.08E 02	6.52E 01	7.66E 01	6.52E 01
64	6.21E 01	0.00E 00	9.42E 01	4.47E 01	6.04E 01	6.04E 01
10	0.00E 00	8.18E 01	7.99E 01	5.49E 01	9.47E 01	7.62E 01
4	5.78E 01	7.43E 01	7.50E 01	5.29E 01	0.00E 00	7.25E 01
16	5.75E 01	7.26E 01	7.82E 01	5.97E 01	1.01E 02	5.41E 01
50	0.00E 00	0.00E 00	0.00E 00	6.47E 01	7.23E 01	6.76E 01
14	0.00E 00	0.00E 00	0.00E 00	0.00E 00	0.00E 00	0.00E 00

AVE	4.[illegible] 01	6.[illegible] 01	8.[illegible] 01	6.[illegible] 01	8.47E 01	6.[illegible] 01
LE	47.6	47.6	23.8	23.8	23.8	23.8
COMP	OUTLET	7TH	6TH		5TH	

2

BAFFLE SPACING (MM)=47.6 BAFFLE CUT (%) =18.4
B/S CLEARANCE (MM) =0.00 T/B CLEARANCE (MM) =0.00
FLOW RATE =94.5 TEMP (DEG.C) =25.0 VELOCITY =0.871
REYNOLDS NO =0.7883E 04 SCHMIDT NO. =1560.

INDIVIDUAL TUBE COEFFICIENTS

TUBE						
69	0.00E 00	7.05E 01	8.83E 01	9.22E 01	0.00E 00	0.00E 00
73	0.00E 00	0.00E 00	8.83E 01	1.08E 02	1.23E 02	1.19E 02
44	5.21E 01	8.88E 01	1.05E 02	1.28E 02	8.69E 01	1.02E 02
34	6.62E 01	9.33E 01	8.83E 01	1.04E 02	1.10E 02	1.11E 02
79	5.38E 01	8.09E 01	0.00E 00	1.17E 02	1.24E 02	1.05E 02
29	0.00E 00	9.07E 01	8.27E 01	1.41E 02	9.18E 01	1.08E 02
78	4.96E 01	8.95E 01	1.71E 02	0.00E 00	1.13E 02	9.64E 01
63	4.62E 01	9.21E 01	0.00E 00	1.01E 02	1.05E 02	1.37E 02
24	6.02E 01	9.99E 01	7.77E 01	1.02E 02	8.69E 01	9.54E 01

AVE	5.47E 01	8.83E 01	1.00E 02	1.19E 02	1.05E 02	1.09E 02
LE	47.6	47.6	23.8	23.8	23.8	23.8
COMP	INLET	SECOND	THIRD		FOURTH	

3

BAFFLE SPACING (MM)=47.6 BAFFLE CUT (%) =18.4
B/S CLEARANCE (MM) =0.00 T/B CLEARANCE (MM) =0.00
FLOW RATE = 9.4 TEMP (DEG.C) =26.2 VELOCITY =0.087
REYNOLDS NO. =0.8057E 03 SCHMIDT NO =1471.

INDIVIDUAL TUBE COEFFICIENTS

TUBE						
69	2.52E 01	3.29E 01	3.08E 01	2.53E 01	3.05E 01	3.23E 01
73	2.74E 01	2.67E 01	3.40E 01	3.12E 01	3.23E 01	2.55E 01
44	1.95E 01	2.55E 01	2.57E 01	2.04E 01	2.36E 01	2.53E 01
34	2.27E 01	2.75E 01	3.02E 01	2.43E 01	3.34E 01	2.36E 01
79	0.00E 00	2.46E 01	3.00E 01	2.73E 01	3.06E 01	2.20E 01
29	2.14E 01	2.66E 01	0.00E 00	2.57E 01	3.15E 01	2.21E 01
78	0.00E 00	0.00E 00	0.00E 00	0.00E 00	2.94E 01	2.21E 01
63	0.00E 00	0.00E 00	0.00E 00	0.00E 00	0.00E 00	0.00E 00
36	2.06E 01	2.54E 01	2.60E 01	2.60E 01	2.85E 01	2.40E 01
55	0.00E 00	0.00E 00	0.00E 00	0.00E 00	0.00E 00	0.00E 00
9	3.24E 01	2.62E 01	3.07E 01	2.94E 01	3.39E 01	2.09E 01
28	2.69E 01	0.00E 00	3.08E 01	2.93E 01	3.74E 01	2.89E 01
20	2.36E 01	2.24E 01	2.97E 01	0.00E 00	3.29E 01	0.00E 00
62	0.00E 00	0.00E 00	0.00E 00	2.59E 01	3.09E 01	2.45E 01
64	2.26E 01	0.00E 00	3.27E 01	1.92E 01	2.71E 01	1.96E 01
10	0.00E 00	0.00E 00	3.19E 01	2.70E 01	0.00E 00	2.84E 01
4	2.38E 01	2.57E 01	3.00E 01	2.76E 01	0.00E 00	2.84E 01
16	2.01E 01	2.58E 01	3.06E 01	3.35E 01	3.60E 01	2.42E 01
50	0.00E 00	0.00E 00	0.00E 00	2.13E 01	2.83E 01	2.47E 01
14	0.00E 00	0.00E 00	0.00E 00	2.69E 00	0.00E 00	0.00E 00

AVE	2.47E 01	2.57E 01	3.11E 01	2.71E 01	3.11E 01	2.42E 01
LE	47.6	47.6	23.8	23.8	23.8	23.8
COMP	OUTLET	7TH	6TH		5TH	

*2

BAFFLE SPACING (MM)=47.6 BAFFLE CUT (%) =18.4
B/S CLEARANCE (MM) ,=0.00 T/B CLEARANCE (MM) =0.00
FLOW RATE =51.0 TEMP (DEG.C) =25.8 VELOCITY =0.470
REYNOLDS NO. =0.4332E 04 SCHMIDT NO. =1500.

INDIVIDUAL TUBE COEFFICIENTS

TUBE						
69	7.35E 01	7.57E 01	8.25E 01	8.37E 01	6.74E 01	7.55E 01
73	8.16E 01	8.48E 01	6.13E 01	7.56E 01	8.45E 01	8.08E 01
44	6.71E 01	7.06E 01	6.05E 01	8.86E 01	6.30E 01	6.97E 01
34	7.20E 01	7.49E 01	6.97E 01	9.06E 01	7.53E 01	7.16E 01
79	7.30E 01	7.62E 01	5.82E 01	7.84E 01	8.36E 01	6.80E 01
29	6.62E 01	6.96E 01	0.00E 00	9.61E 01	6.61E 01	6.50E 01
78	7.26E 01	7.65E 01	5.71E 01	0.00E 00	8.00E 01	6.67E 01
63	7.87E 01	8.23E 01	6.36E 01	6.85E 01	6.85E 01	9.00E 01
36	6.22E 01	6.45E 01	5.35E 01	8.07E 01	6.30E 01	6.42E 01
55	0.00E 00	0.00E 00	0.00E 00	0.00E 00	0.00E 00	0.00E 00
9	6.16E 01	8.30E 01	6.05E 01	7.35E 01	7.00E 01	0.00E 00
28	6.21E 01	3.97E 01	6.08E 01	9.56E 01	6.14E 01	0.00E 00
20	6.11E 01	6.77E 01	7.89E 01	0.00E 00	5.83E 01	7.22E 01
62	6.14E 01	8.44E 01	7.11E 01	6.88E 01	7.19E 01	9.08E 01
64	5.71E 01	0.00E 00	6.80E 01	6.57E 01	4.71E 01	7.39E 01
10	0.00E 00	6.79E 01	8.25E 01	8.41E 01	5.77E 01	7.25E 01
4	6.32E 01	6.86E 01	8.05E 01	7.42E 01	0.00E 00	6.60E 01
16	7.11E 01	7.01E 01	6.05E 01	9.40E 01	5.97E 01	6.77E 01
50	0.00E 00	0.00E 00	6.28E 01	7.16E 01	5.85E 01	8.09E 01
14	0.00E 00	0.00E 00	0.00E 00	0.00E 00	0.00E 00	0.00E 00

AVE	6.38E 01	7.[illegible] 01	6.75E 01	8.11E 01	6.68E 01	[illegible] 01
LE	47.6	47.6	23.8	23.8	23.8	23.8
COMP	INLET	SECOND	THIRD		FOURTH	

*2

BAFFLE SPACING (MM)=47.6 BAFFLE CUT (%) =18.4
B/S CLEARANCE (MM) =0.00 T/B CLEARANCE (MM) =0.0
FLOW RATE =80.0 TEMP (DEG.C) =25.5 VELOCITY =0.7
REYNOLDS NO. =0.6750E 04 SCHMIDT NO. =1522.

INDIVIDUAL TUBE COEFFICIENTS

TUBE						
69	6.55E 01	0.00E 00	9.43E 01	8.41E 01	0.00E 00	0.00E
73	0.00E 00	0.00E 00	7.92E 01	9.92E 01	1.09E 02	1.07E
44	7.66E 01	0.00E 00	8.12E 01	1.19E 02	7.92E 01	9.28E
34	8.25E 01	0.00E 00	9.36E 01	1.21E 02	9.95E 01	1.00E
79	0.00E 00	0.00E 00	7.89E 01	1.08E 02	1.13E 02	9.41E
29	7.72E 01	0.00E 00	0.00E 00	1.28E 02	8.37E 01	8.26E
78	7.27E 01	0.00E 00	7.33E 01	1.00E 02	1.08E 02	8.94E
63	7.72E 01	0.00E 00	0.00E 00	9.26E 01	9.27E 01	1.23E
36	8.31E 01	0.00E 00	6.81E 01	1.20E 02	7.99E 01	8.60E
55	0.00E 00	0.00E 00	0.00E 00	0.00E 00	0.00E 00	0.00E

AVE	7.64E 01	[illegible]	8.12E 01	1.08E 02	9.57E 01	9.62E
LE	47.6	47.6	23.8	23.8	23.8	23.
COMP	INLET	SECOND	THIRD		FOURTH	

BAFFLE SPACING (MM)= 47.6 BAFFLE CUT (%) =18.4
B/S CLEARANCE (MM) =0.00 T/B CLEARANCE (MM) =0.00
FLOW RATE =44.0 TEMP (DEG.C) =26.0 VELOCITY =0.405
REYNOLDS NO. =0.3755E 04 SCHMIDT NO. =1485.

INDIVIDUAL TUBE COEFFICIENTS

TUBE						
69	[illegible]	[illegible]	7.49E 01	7.71E 01	6.25E 01	6.79E 01
73	5.64E 01	[illegible]	5.47E 01	7.02E 01	8.03E 01	7.53E 01
44	5.80E 01	[illegible]	[illegible]	7.05E 01	5.66E 01	6.35E 01
34	[illegible]	[illegible]	[illegible]	8.11E 01	6.94E 01	6.89E 01
79	[illegible]	[illegible]	[illegible]	7.23E 01	7.53E 01	6.30E 01
29	[illegible]	[illegible]	0.00E 00	8.62E 01	5.93E 01	6.00E 01
78	[illegible]	[illegible]	4.38E 01	0.00E 00	7.50E 01	6.15E 01
63	[illegible]	[illegible]	[illegible]	6.14E 01	0.00E 00	8.41E 01
36	[illegible]	[illegible]	[illegible]	7.98E 01	5.69E 01	6.00E 01
55	[illegible]	0.00E 00	0.00E 00	0.00E 00	0.00E 00	0.00E 00
9	[illegible]	[illegible]	0.00E 00	0.00E 00	0.00E 00	0.00E 00
28	[illegible]	0.00E 00	0.00E 00	0.00E 00	0.00E 00	0.00E 00
20	[illegible]	[illegible]	0.00E 00	0.00E 00	0.00E 00	0.00E 00
62	[illegible]	[illegible]	0.00E 00	0.00E 00	0.00E 00	0.00E 00
64	[illegible]	[illegible]	0.00E 00	0.00E 00	0.00E 00	0.00E 00
10	[illegible]	[illegible]	0.00E 00	0.00E 00	0.00E 00	0.00E 00
4	[illegible]	[illegible]	0.00E 00	0.00E 00	0.00E 00	0.00E 00
16	[illegible]	[illegible]	0.00E 00	0.00E 00	0.00E 00	0.00E 00
50	[illegible]	[illegible]	0.00E 00	0.00E 00	0.00E 00	0.00E 00
14	[illegible]	[illegible]	0.00E 00	0.00E 00	0.00E 00	0.00E 00

AVE	[illegible]	[illegible]	[illegible]	7.58E 01	6.69E 01	6.72E 01
LE	47.6	47.6	23.8	23.8	23.8	23.8
COMP	INLET	SECOND	THIRD		FOURTH	

BAFFLE SPACING (MM)=47.6 BAFFLE CUT (%) =18.4
B/S CLEARANCE (MM) =0.00 T/B CLEARANCE (MM) =0.00
FLOW RATE =51.0 TEMP (DEG.C) =24.0 VELOCITY =0.470
REYNOLDS NO. =0.4157E 04 SCHMIDT NO. =1640.

INDIVIDUAL TUBE COEFFICIENTS

TUBE						
69	5.69E 01	6.80E 01	6.73E 01	6.11E 01	8.43E 01	9.90E
73	0.00E 00	7.92E 01	5.94E 01	7.30E 01	8.38E 01	8.15E
44	5.67E 01	6.60E 01	6.07E 01	8.74E 01	6.15E 01	7.17E
34	5.86E 01	6.60E 01	6.68E 01	8.74E 01	7.47E 01	7.28E
79	5.27E 01	7.09E 01	5.89E 01	7.82E 01	8.39E 01	7.05E
29	5.66E 01	6.00E 01	0.00E 00	9.29E 01	6.29E 01	6.29E
78	5.38E 01	7.13E 01	5.36E 01	7.56E 01	8.25E 01	6.76E
63	5.50E 01	1.00E 02	0.00E 00	6.66E 01	6.60E 01	9.34E
36	5.94E 01	6.04E 01	5.30E 01	8.68E 01	5.37E 01	6.54E
55	3.97E 01	5.69E 01	6.20E 01	6.69E 01	6.66E 01	6.48E
9	5.77E 01	5.67E 01	7.28E 01	7.75E 01	0.00E 00	7.01E
28	5.01E 01	0.00E 00	5.41E 01	8.59E 01	5.52E 01	0.00E
20	4.95E 01	0.00E 00	6.27E 01	0.00E 00	5.49E 01	6.52E
62	4.85E 01	0.00E 00	5.85E 01	6.15E 01	6.66E 01	8.80E
64	4.53E 01	4.13E 01	5.74E 01	6.06E 01	4.02E 01	7.36E
10	3.85E 01	3.85E 01	7.22E 01	7.80E 01	5.04E 01	0.00E
4	5.18E 01	5.53E 01	7.32E 01	7.02E 01	0.00E 00	6.99E
16	5.81E 01	5.51E 01	4.97E 01	8.26E 01	4.99E 01	6.14E
50	4.12E 01	0.00E 00	6.53E 01	6.47E 01	5.38E 01	7.69E
14	3.59E 01	3.99E 01	4.97E 01	6.86E 01	5.42E 01	6.15E

AVE	[illegible]	[illegible]	6.65E 01	7.30E 01	6.36E 01	7.35E
LE	47.6	47.6	23.8	23.8	23.8	23.8
COMP	INLET	SECOND	THIRD		FOURTH	

2

BAFFLE SPACING (MM)=47.6 BAFFLE CUT (%) =18.4
B/S CLEARANCE (MM) =0.00 T/B CLEARANCE (MM) =0.00
FLOW RATE = 9.4 TEMP (DEG.C) =26.5 VELOCITY =0.087
REYNOLDS NO. =0.8112E 03 SCHMIDT NO. =1450.

INDIVIDUAL TUBE COEFFICIENTS

TUBE						
69	2.31E 01	2.73E 01	3.02E 01	2.47E 01	3.35E 01	3.57E 01
73	0.00E 00	3.02E 01	2.39E 01	2.80E 01	0.00E 00	3.07E 01
44	2.32E 01	2.51E 01	2.67E 01	3.12E 01	2.50E 01	2.50E 01
34	0.00E 00	0.00E 00	0.00E 00	0.00E 00	0.00E 00	0.00E 00
79	2.24E 01	2.73E 01	2.41E 01	2.86E 01	3.06E 01	2.60E 01
29	2.30E 01	2.49E 01	0.00E 00	3.19E 01	2.60E 01	2.43E 01
78	2.43E 01	2.76E 01	2.19E 01	0.00E 00	3.13E 01	2.52E 01
63	2.31E 01	0.00E 00	0.00E 00	2.65E 01	2.64E 01	3.12E 01
36	2.51E 01	2.31E 01	2.38E 01	3.12E 01	2.42E 01	2.47E 01
55	0.00E 00	0.00E 00	0.00E 00	0.00E 00	0.00E 00	0.00E 00
9	2.50E 01	2.52E 01	3.02E 01	3.08E 01	2.88E 01	2.99E 01
28	0.00E 00	0.00E 00	2.43E 01	3.34E 01	0.00E 00	0.00E 00
20	2.28E 01	2.29E 01	2.43E 01	1.08E 01	2.35E 01	2.69E 01
62	0.00E 00	0.00E 00	0.00E 00	0.00E 00	0.00E 00	0.00E 00
64	2.17E 01	0.00E 00	2.52E 01	2.08E 01	1.90E 01	2.70E 01
10	0.00E 00	2.39E 01	3.05E 01	3.02E 01	2.24E 01	0.00E 00
4	2.30E 01	2.39E 01	3.03E 01	2.71E 01	0.00E 00	2.80E 01
16	2.37E 01	2.41E 01	2.80E 01	3.14E 01	2.35E 01	2.54E 01
50	0.00E 00	0.00E 00	0.00E 00	1.93E 01	2.30E 01	2.00E 01
14	0.00E 00	0.00E 00	0.00E 00	0.00E 00	0.00E 00	0.00E 00

AVE	2.31E 01	2.41E 01	1.90E 01	2.00E 01	2.09E 01	2.77E 01
LE	47.6	47.3	23.8	23.8	23.8	23.8
COMP	INLET	SECOND	THIRD		FOURTH	

2

BAFFLE SPACING (MM)=47.6 BAFFLE CUT (%) =18.4
B/S CLEARANCE (MM) =0.00 T/B CLEARANCE (MM) =0.00
FLOW RATE =24.0 TEMP (DEG.C) =26.0 VELOCITY =0.221
REYNOLDS NO. =0.2048E 04 SCHMIDT NO =1485.

INDIVIDUAL TUBE COEFFICIENTS

TUBE						
69	4.55E 01	4.83E 01	5.50E 01	5.50E 01	4.51E 01	5.14E 01
73	4.09E 01	5.42E 01	4.04E 01	5.13E 01	5.92E 01	5.65E 01
44	3.96E 01	4.33E 01	4.07E 01	5.50E 01	4.21E 01	4.63E 01
34	0.00E 00	0.00E 00	0.00E 00	0.00E 00	4.86E 01	4.63E 01
79	3.77E 01	4.68E 01	3.70E 01	5.07E 01	5.31E 01	4.45E 01
29	4.03E 01	4.13E 01	0.00E 00	5.03E 01	4.21E 01	4.16E 01
78	3.73E 01	4.67E 01	0.00E 00	5.04E 01	5.43E 01	4.39E 01
63	0.00E 00	4.89E 01	3.97E 01	4.31E 01	4.57E 01	5.92E 01
36	4.19E 01	3.89E 01	3.95E 01	5.50E 01	4.10E 01	4.18E 01
55	0.00E 00	0.00E 00	0.00E 00	0.00E 00	0.00E 00	0.00E 00
9	3.79E 01	4.82E 01	4.27E 01	4.95E 01	4.49E 01	4.28E 01
28	0.00E 00	0.00E 00	4.27E 01	4.12E 01	3.85E 01	0.00E 00
20	3.44E 01	3.49E 01	4.04E 01	0.00E 00	3.55E 01	4.43E 01
62	0.00E 00	0.00E 00	0.00E 00	0.00E 00	0.00E 00	0.00E 00
64	3.28E 01	0.00E 00	3.77E 01	3.77E 01	2.69E 01	4.69E 01
10	0.00E 00	3.60E 01	4.69E 01	4.79E 01	3.23E 01	4.61E 01
4	3.55E 01	0.00E 00	4.61E 01	4.20E 01	0.00E 00	4.70E 01
16	3.71E 01	3.71E 01	3.40E 01	5.13E 01	3.58E 01	4.09E 01
50	0.00E 00	0.00E 00	3.58E 01	4.03E 01	3.20E 01	4.06E 01
14	4.42E 01	0.00E 00	5.31E 01	6.19E 01	4.19E 01	0.00E 00

AVE	3.66E 01	4.00E 01	4.17E 01	5.00E 01	4.20E 01	5.00E 01
LE	47.6	47.3	23.8	23.8	23.8	23.8
COMP	INLET	SECOND	THIRD		FOURTH	

2

BAFFLE SPACING (MM)=47.6 BAFFLE CUT (%) =18.4
B/S CLEARANCE (MM) =0.00 T/B CLEARANCE (MM) =0.00
FLOW RATE = 3.7 TEMP (DEG.C) =26.0 VELOCITY =0.034
REYNOLDS NO =0.3157E 03 SCHMIDT NO. =1495.

INDIVIDUAL TUBE COEFFICIENTS

TUBE						
69	1.37E 01	1.69E 01	1.69E 01	1.51E 01	2.14E 01	2.05E 01
73	0.00E 00	1.51E 01	1.40E 01	1.04E 01	1.61E 01	1.61E 01
44	1.39E 01	1.56E 01	1.59E 01	1.80E 01	1.61E 01	1.61E 01
34	0.00E 00	0.00E 00	0.00E 00	0.00E 00	0.00E 00	0.00E 00
79	1.32E 01	1.68E 01	1.40E 01	1.76E 01	1.87E 01	1.65E 01
29	1.34E 01	1.48E 01	0.00E 00	1.84E 01	1.53E 01	1.51E 01
78	1.46E 01	1.75E 01	1.37E 01	0.00E 00	1.87E 01	1.58E 01
63	1.37E 01	2.28E 01	0.00E 00	1.50E 01	1.55E 01	1.83E 01
36	1.45E 01	1.44E 01	1.48E 01	1.84E 01	1.51E 01	1.54E 01
55	0.00E 00	0.00E 00	0.00E 00	0.00E 00	0.00E 00	0.00E 00
9	1.46E 01	1.40E 01	1.81E 01	2.07E 01	1.65E 01	1.84E 01
28	0.00E 00	0.00E 00	1.54E 01	1.91E 01	0.00E 00	0.00E 00
20	1.36E 01	1.31E 01	1.61E 01	0.00E 00	1.40E 01	1.56E 01
62	0.00E 00	0.00E 00	0.00E 00	0.00E 00	0.00E 00	0.00E 00
64	1.32E 01	0.00E 00	1.55E 01	1.50E 01	1.14E 01	1.63E 01
10	0.00E 00	1.33E 01	1.74E 01	1.77E 01	1.20E 01	0.00E 00
4	1.35E 01	1.33E 01	1.73E 01	1.54E 01	0.00E 00	1.73E 01
16	1.30E 01	1.37E 01	1.42E 01	1.84E 01	1.37E 01	1.50E 01
50	0.00E 00	0.00E 00	0.00E 00	1.54E 01	1.29E 01	1.59E 01
14	0.00E 00	0.00E 00	0.00E 00	0.00E 00	0.00E 00	0.00E 00

AVE	1.22E 01	1.[illegible]	1.[illegible] 01	1.24E 01	1.56E 01	1.67E 01
LE	47.6	47.6	23.8	23.89	23.8	23.8
COMP	INLET	SECOND	THIRD		FOURTH	

2

BAFFLE SPACING (MM)=47.6 BAFFLE CUT (%) =18.4
B/S CLEARANCE (MM) =0.00 T/B CLEARANCE (MM) =0.0
FLOW RATE = 3.7 TEMP (DEG.C) =29.5 VELOCITY =0.0
REYNOLDS NO. =0.3122E 03 SCHMIDT NO =1522

INDIVIDUAL TUBE COEFFICIENTS

TUBE						
69	1.55E 01	1.67E 01	2.02E 01	1.[illegible] 01	1.61E 01	1.61
73	1.42E 01	1.90E 01	1.39E 01	1.[illegible] 01	2.03E 01	1.90
44	1.51E 01	1.62E 01	1.58E 01	1.73E 01	1.64E 01	1.67
34	1.44E 01	1.58E 01	1.59E 01	1.77E 01	1.70E 01	1.59
79	1.37E 01	1.75E 01	1.45E 01	1.98E 01	1.90E 01	1.67
29	1.42E 01	1.55E 01	0.00E 00	1.89E 01	1.55E 01	1.58
78	1.54E 01	1.79E 01	0.00E 00	0.00E 00	1.90E 01	5.81
63	1.45E 01	2.21E 01	1.55E 01	1.[illegible] 01	1.65E 01	1.90
36	1.53E 01	1.46E 01	1.43E 01	1.81E 01	1.53E 01	1.59
55	0.00E 00	0.00E 00	1.61E 01	1.58E 01	1.67E 01	1.77
9	1.42E 01	1.70E 01	1.50E 01	1.[illegible] 01	1.75E 01	2.12
28	1.48E 01	0.00E 00	1.[illegible] 01	1.94E 01	1.53E 01	0.00
20	1.30E 01	1.38E 01	1.64E 01	0.00E 00	1.36E 01	1.60
62	1.35E 01	1.[illegible] 01	1.58E 01	1.52E 01	1.65E 01	1.86
64	1.35E 01	0.00E 00	1.61E 01	1.55E 01	1.[illegible] 01	1.60
10	0.00E 00	1.31E 01	1.81E 01	1.78E 01	1.22[illegible] 01	0.00
4	1.43E 01	1.40E 01	1.94E 01	1.67E 01	0.00E 00	1.70
16	1.40E 01	1.38E 01	1.49E 01	1.05E 01	1.37E 01	1.58
50	0.00E 00	0.00E 00	1.49E 01	1.55E 01	1.22[illegible] 01	1.67
14	0.00E 00	0.00E 00	1.03E 01	1.04E 01	1.47[illegible] 01	1.01

AVE	1.44E 01	1.[illegible]	1.[illegible] 01	1.[illegible] 01	1.[illegible] 01	1.[illegible]
LE	47.6	47.6	23.8	23.8	23.8	23.
COMP	INLET	SECOND	THIRD		FOURTH	

BAFFLE SPACING (MM)=47.6 BAFFLE CUT (%) =18.4
T/B CLEARANCE (MM) =0.00 T/B CLEARANCE (MM) =0.00
FLOW RATE =30.0 TEMP (DEG.C) =25.5 VELOCITY =0.737
REYNOLDS NO. =.6750E 04 SCHMIDT NO. =1522. END COMP. REYNOLDS NO.=.6750E 04

INDIVIDUAL TUBE COEFFICIENTS

TUBE					
9	6.47 01	7.35E 01	7.55E 01	7.35E 01	6.63E 01	7.03E 01
73	6.09 01	6.09E 01	7.31E 01	8.15E 01	7.67E 01	7.95E 01
44	5.43E 01	7.13E 01	7.51E 01	8.15E 01	4.94E 01	5.99E 01
34	6.39E 01	7.09E 01	6.71E 01	8.19E 01	6.67E 01	6.95E 01
79	0.00E 00	7.45E 01	7.19E 01	8.28E 01	8.07E 01	6.95E 01
29	6.27E 01	6.71E 01	0.00E 00	8.24E 01	5.5?E 01	5.30E 01
78	0.00E 00	0.00E 00	6.83E 01	7.59E 01	7.15E 01	6.39E 01
58	6.53E 01	0.00E 00	0.00E 00	7.99E 01	6.55E 01	8.56E 01
36	6.41E 01	6.01E 01	6.19E 01	7.79E 01	5.02E 01	5.22E 01
55	6.70E 01	0.00E 00	7.35E 01	7.11E 01	5.95E 01	7.91E 01
57	5.78E 01	7.57E 01	7.27E 01	7.75E 01	6.75E 01	8.60E 01
28	5.42E 01	0.00E 00	5.91E 01	8.36E 01	5.7?E 01	0.00E 00
20	0.00E 00	6.45E 01	6.55E 01	0.00E 00	5.67E 01	6.35E 01
62	5.54E 01	7.87E 01	7.35E 01	6.95E 01	6.75E 01	8.24E 01
64	5.58E 01	0.00E 00	7.15E 01	7.47E 01	4.66E 01	6.79E 01
10	0.00E 00	7.01E 01	7.15E 01	6.51E 01	5.36E 01	0.00E 00
4	6.93E 01	6.71E 01	7.15E 01	6.59E 01	5.82E 01	6.39E 01
16	6.71E 01	6.99E 01	6.59E 01	7.51E 01	6.07E 01	5.78E 01
50	0.00E 00	0.00E 00	6.27E 01	6.87E 01	5.58E 01	6.91E 01
14	7.39E 01	6.63E 01	6.95E 01	8.56E 01	6.35E 01	6.55E 01
	6.49E 01	7.07E 01	6.94E 01	7.64E 01	6.15E 01	6.88E 01

BAFFLE SPACING (MM)=47.0 BAFFLE CUT (%) =18.4
T/B CLEARANCE (MM) =0.00 T/B CLEARANCE (MM) =0.00
FLOW RATE =44.0 TEMP (DEG.C) =25.7 VELOCITY =0.475
R YNOLDS NO. =.3729E 04 SCHMIDT NO. =1507.END COMP. REYNOLDS NO.=.3729E 04

INDIVIDUAL TUBE COEFFICIENTS

TUBE						
9	[illegible]	5.44E 01	5.75E 01	5.43E 01	4.94E 01	5.10E 01
72	[illegible]	5.79E 01	5.26E 01	5.94E 01	5.64E 01	5.47E 01
44	[illegible]	4.53E 01	4.78E 01	4.99E 01	3.37E 01	4.37E 01
34	[illegible]	4.67E 01	4.53E 01	5.26E 01	4.55E 01	4.67E 01
79	[illegible]	4.74E 01	4.86E 01	5.73E 01	5.3[illegible] 01	4.75E 01
29	[illegible]	4.51E 01	3.91E 01	5.29E 01	4.16E 01	[illegible]
78	4.49E 01	0.00E 00	4.61E 01	5.24E 01	4.79E 01	4.59E 01
63	[illegible]	0.00E 00	0.00E 00	4.97E 01	4.52E 01	5.83E 01
36	[illegible]	4.13E 01	4.04E 01	4.59E 01	3.69E 01	3.96E 01
55	[illegible]	0.00E 00	5.15E 01	4.78E 01	4.15E 01	5.62E 01
69	[illegible]	4.93E 01	5.32E 01	5.70E 01	5.13E 01	6.84E 01
28	[illegible]	0.00E 00	4.31E 01	5.70E 01	4.40E 01	0.00E 00
20	[illegible]	0.00E 00	4.64E 01	0.00E 00	3.96E 01	4.42E 01
62	[illegible]	0.00E 00	5.24E 01	4.86E 01	4.89E 01	5.89E 01
64	[illegible]	0.00E 00	5.32E 01	5.13E 01	3.50E 01	4.78E 01
10	[illegible]	0.00E 00	4.86E 01	4.48E 01	3.69E 01	4.18E 01
4	[illegible]	0.00E 00	4.83E 01	4.29E 01	3.85E 01	4.50E 01
16	[illegible]	0.00E 00	4.23E 01	4.91E 01	4.12E 01	3.88E 01
50	[illegible]	0.00E 00	0.00E 00	0.00E 00	5.49E 01	2.71E-01
14	5.33E 01	0.00E 00	5.05E 01	5.67E 01	4.31E 01	4.59E 01
	[illegible]	4.85E 01	4.82E 01	5.10E 01	4.42E 01	4.60E 01

FLOW RATE =51.0 TEMP (DEG.C) =26.0 VELOCITY =0.472
R YNOLDS NO. =.4352E 04 SCHMIDT NO. =1485.END COMP. REYNOLDS NO.=.4352E 04

INDIVIDUAL TUBE COEFFICIENTS

TUBE						
9	[illegible]	6.04E 01	6.07E 01	5.80E 01	5.72E 01	5.77E 01
72	[illegible]	6.3[illegible] 01	5.83E 01	6.57E 01	6.4[illegible] 01	6.59E 01
44	[illegible]	5.58E 01	6.01E 01	6.33E 01	4.13E 01	4.64E 01
34	[illegible]	5.43E 01	5.45E 01	6.36E 01	5.63E 01	5.54E 01
79	[illegible]	5.89E 01	5.86E 01	6.65E 01	6.62E 01	5.51E 01
29	[illegible]	5.10E 01	4.92E 01	6.42E 01	4.92E 01	4.48E 01
78	[illegible]	0.00E 00	5.57E 01	6.30E 01	5.98E 01	5.19E 01
63	[illegible]	0.00E 00	0.00E 00	6.24E 01	5.36E 01	6.95E 01
36	[illegible]	4.61E 01	4.81E 01	5.95E 01	4.31E 01	4.37E 01
55	[illegible]	0.00E 00	5.98E 01	5.66E 01	4.84E 01	6.59E 01
69	[illegible]	5.73E 01	6.01E 01	6.39E 01	5.83E 01	7.36E 01
28	[illegible]	0.00E 00	4.75E 01	6.62E 01	5.01E 01	4.78E 01
20	[illegible]	4.97E 01	5.45E 01	0.00E 00	4.93E 01	5.42E 01
62	[illegible]	5.58E 01	6.30E 01	5.74E 01	5.77E 01	6.95E 01
64	[illegible]	0.00E 00	6.10E 01	6.07E 01	4.89E 01	5.63E 01
10	[illegible]	5.23E 01	5.77E 01	5.28E 01	4.72E 01	5.33E 01
4	[illegible]	5.5[illegible] 01	5.77E 01	5.01E 01	4.95E 01	5.56E 01
16	[illegible]	5.25E 01	5.31E 01	5.95E 01	5.1[illegible] 01	4.81E 01
50	[illegible]	0.00E 00	5.31E 01	5.83E 01	5.77E 01	5.66E 01
14	[illegible]	5.04E 01	5.69E 01	6.80E 01	5.44E 01	5.69E 01
	[illegible]	5.40E 01	5.62E 01	[illegible]	5.32E 01	5.64E 01

BAFFLE SPACING (MM)=47.8 BAFFLE CUT (%) =16.4
S/T CLEARANCE (MM) =0.00 T/B CLEARANCE (MM) =0.00
FLOW RATE =15.5 TEMP (DEG.C) =26.5 VELOCITY =0.120
REYNOLDS NO.=.1596E 04 SCHMIDT NO. =1450.END COMP. REYNOLDS NO.=.1596E 04

INDIVIDUAL TUBE COEFFICIENTS

TUBE						
9	3.42 01	3.37E 01	3.58E 01	3.26E 01	3.13E 01	3.21E 01
23	2.97E 01	3.53E 01	3.21E 01	3.42E 01	3.62E 01	3.58E 01
44	3.06 01	3.01E 01	3.46E 01	3.62E 01	2.44E 01	2.85E 01
54	2.91 01	3.01E 01	3.17E 01	3.38E 01	3.17E 01	3.05E 01
79	3.10 01	3.05E 01	3.30E 01	3.83E 01	3.78E 01	3.21E 01
29	2.97 01	2.83E 01	0.00E 00	3.46E 01	2.81E 01	2.48E 01
78	3.13 01	0.00E 00	3.01E 01	3.62E 01	3.46E 01	3.01E 01
63	2.43 01	4.60E 01	0.00E 00	3.50E 01	3.01E 01	3.78E 01
36	3.34 01	2.93E 01	2.89E 01	3.58E 01	3.13E 01	3.05E 01
55	0.00E 00	0.00E 00	3.30E 01	3.13E 01	2.89E 01	3.53E 01
69	2.71E 01	3.42E 01	3.30E 01	3.50E 01	3.30E 01	4.18E 01
120	2.71E 01	0.00E 00	2.81E 01	3.62E 01	2.93E 01	0.00E 00
20	0.00E 01	3.03E 01	3.05E 01	0.00E 00	2.81E 01	3.46E 01
62	2.71E 01	3.56E 01	3.46E 01	3.17E 01	3.34E 01	4.03E 01
64	3.73 01	0.00E 00	3.58E 01	3.30E 01	2.36E 01	3.26E 01
10	0.00E 00	3.21E 01	3.36E 01	3.05E 01	2.85E 01	3.42E 01
4	3.39 01	3.21E 01	3.30E 01	2.97E 01	2.85E 01	3.30E 01
16	3.01 01	3.19E 01	3.21E 01	3.21E 01	3.21E 01	2.93E 01
50	3.07E 01	3.26E 01	0.00E 00	0.00E 00	0.00E 00	3.50E 01
14	3.13 01	3.24E 01	3.42E 01	3.87E 01	3.17E 01	3.34E 01
	3.39 01	3.23E 01	3.26E 01	3.40E 01	3.07E 01	3.31E 01

FLOW RATE =31.0 TEMP (DEG.C) =26.4 VELOCITY =0.246
REYNOLDS NO.=.2669E 04 SCHMIDT NO. =1457.END COMP. REYNOLDS NO.=.2669E 04

INDIVIDUAL TUBE COEFFICIENTS

TUBE						
9	4.15 01	4.60E 01	4.81E 01	4.49E 01	4.43E 01	4.65E 01
23	4.09 01	4.89E 01	4.46E 01	5.03E 01	4.94E 01	5.16E 01
44	4.22 01	4.12E 01	4.49E 01	4.71E 01	3.18E 01	3.79E 01
54	4.06 01	4.16E 01	4.20E 01	4.75E 01	4.33E 01	4.27E 01
79	0.00E 00	4.51E 01	4.46E 01	5.32E 01	4.97E 01	4.33E 01
29	4.04E 01	3.27E 01	0.00E 00	4.81E 01	3.79E 01	3.44E 01
78	3.90E 01	0.00E 00	4.14E 01	4.66E 01	4.59E 01	4.11E 01
63	3.59E 01	0.00E 00	0.00E 00	4.59E 01	4.01E 01	5.29E 01
36	4.12 01	3.34E 01	3.66E 01	4.49E 01	3.38E 01	3.47E 01
55	0.00E 00	0.00E 00	4.62E 01	4.33E 01	3.98E 01	5.00E 01
69	3.79E 01	4.57E 01	4.62E 01	4.97E 01	4.49E 01	5.92E 01
120	4.00E 01	0.00E 00	3.85E 01	5.19E 01	3.96E 01	0.00E 00
20	0.00E 01	4.06E 01	4.24E 01	0.00E 00	3.89E 01	4.59E 01
62	3.94E 01	4.76E 01	4.81E 01	4.46E 01	4.55E 01	5.60E 01
64	3.76 01	0.00E 00	4.75E 01	4.81E 01	3.09E 01	4.43E 01
10	0.00E 00	4.28E 01	4.55E 01	4.24E 01	3.89E 01	0.00E 00
4	4.49 01	4.25E 01	4.46E 01	4.11E 01	3.95E 01	4.43E 01
16	4.47 01	4.24E 01	4.24E 01	4.55E 01	4.33E 01	4.04E 01
50	0.00E 00	0.00E 00	4.27E 01	0.00E 00	0.00E 00	4.52E 01
14	4.54 01	4.11E 01	4.39E 01	5.35E 01	4.35E 01	4.65E 01

RUN NUMBER 2.

TUBE	a_1	b_1	η	a_2	b_2	η	a_3	b_3	η	a_4	b_4	η	a_5	b_5	η	a_6	b_6	η
69	0.67	0.54	7	[illegible]	[illegible]	8	0.92	0.52	9	0.74	0.55	9	0.99	0.51	7	0.64	0.55	7
72	0.41	0.51	4	[illegible]	[illegible]	7	0.65	0.54	9	0.89	0.54	9	0.61	0.59	8	0.59	0.59	9
44	0.44	0.50	4	[illegible]	[illegible]	9	0.69	0.51	9	0.59	0.60	9	0.80	0.52	9	0.61	0.57	9
34	0.71	0.50	6	0.58	[illegible]	5	0.67	0.55	6	0.49	0.62	6	0.64	0.57	7	0.50	0.60	7
79	0.72	0.52	6	[illegible]	[illegible]	8	0.62	0.54	8	0.64	0.58	9	0.64	0.58	9	0.62	0.57	9
54	0.61	0.57	4	[illegible]	[illegible]	0	0.66	0.43	1	0.49	0.63	9	0.64	0.55	9	0.55	0.57	9
75	0.57	0.51	4	[illegible]	[illegible]	8	0.81	0.61	7	0.61	0.56	8	0.74	0.56	9	0.01	1.06	9
62	0.66	0.51	6	1.09	0.46	7	0.72	0.52	4	0.56	0.57	9	0.59	0.57	8	0.52	0.62	9
24	0.81	0.51	9	[illegible]	[illegible]	9	0.79	0.50	9	0.53	0.61	9	0.69	0.54	9	0.62	0.56	9
11	0.00	0.00	1	[illegible]	[illegible]	1	0.33	0.52	2	0.62	0.56	2	0.77	0.54	2	0.99	0.50	2
9	0.63	0.54	7	[illegible]	[illegible]	7	[illegible]	[illegible]	6	[illegible]	[illegible]	6	0.60	0.53	5	0.95	0.53	5
13	0.75	0.52	4	0.00	0.00	1	0.71	0.52	6	0.62	0.60	6	0.81	0.51	4	0.00	0.00	0
22	0.62	0.56	7	0.47	0.53	6	0.62	0.56	6	0.00	0.00	1	0.63	0.54	6	0.72	0.54	6
82	0.65	0.54	4	0.51	0.60	3	0.71	0.54	3	0.62	0.56	0	0.70	0.55	3	0.58	0.60	3
64	0.65	0.53	7				0.77	0.52	6	0.69	0.59	6	0.61	0.51	6	0.61	0.57	6
10	0.00	0.00	1	0.63	0.53	7	0.72	0.52	6	0.64	0.58	6	0.56	0.54	6	0.46	0.60	2
4	0.58	0.55	7	0.53	0.58	6	0.60	0.54	6	0.59	0.57	6	0.00	0.00	0	0.87	0.52	6
16	0.44	0.60	7	0.51	0.57	7	0.79	0.53	6	0.58	0.60	6	0.67	0.53	6	0.69	0.54	6
30	0.00	0.00	1	0.00	0.00	0	0.79	0.55	4	0.51	0.58	6	0.60	0.54	6	0.50	0.60	6
			3	0.00	0.00	1	1.59	0.42	3	1.06	0.51	3	0.76	0.52	3	0.90	0.54	3

RUN NUMBER 4.

TUBE	a_1	b_1	n	a_2	b_2	n	a_3	b_3	n	a_4	b_4	n	a_5	b_5	n	a_6	b_6	n
4	0.79	0.54	6	[illegible]	[illegible]	[illegible]	[illegible]	[illegible]	[illegible]	[illegible]	[illegible]	[illegible]	0.42	0.56	6	0.47	0.58	6
19	0.00	0.00	0	0.74	0.43	3	0.40	0.17	1	0.69	0.47	6	0.61	0.53	5	0.47	0.57	5
20	0.62	0.53	6	0.97	0.39	6	1.00	0.73	6	0.97	0.41	6	0.29	0.62	5	0.31	0.63	6
42	0.69	0.53	6	0.17	0.32	6	4.00	0.00	6	1.10	0.43	6	0.81	0.50	6	0.89	0.49	6
64	0.00	0.00	0	0.47	0.47	4	1.09	0.27	5	0.59	0.50	2	0.53	0.56	6	0.47	0.58	6
89	0.62	0.56	6	0.61	0.39	6	0.83	0.40	6	0.57	0.47	6	0.64	0.50	6	0.73	0.53	6
4	0.00	0.00	0	0.00	0.00	2	0.64	0.33	4	0.34	0.66	2	0.00	0.00	0	0.33	0.61	6
15	0.89	0.47	6	0.81	0.33	4	1.00	0.35	6	1.04	0.36	5	0.68	0.53	6	0.53	0.59	6
35	0.43	0.33	6	0.80	0.36	6	1.08	0.37	6	0.62	0.47	6	0.27	0.62	5	0.27	0.65	4
14	0.61	0.55	6	0.90	0.34	6	0.00	0.45	5	2.34	0.31	2	0.62	0.51	6	0.47	0.58	6
29	0.00	0.00	0	0.00	0.00	1	0.74	0.31	3	0.37	0.59	4	0.31	0.61	5	0.30	0.61	5
73	0.92	0.56	5	0.00	0.00	1	0.73	0.51	4	0.81	0.49	5	0.33	0.61	5	0.43	0.58	5
44	1.04	0.42	4	0.35	0.43	3	0.89	0.24	4	2.32	0.33	5	0.59	0.54	5	0.45	0.58	5
61	0.00	0.00	0	0.00	0.00	0	0.85	0.17	4	1.54	0.39	5	0.52	0.56	5	0.76	0.50	4
79	0.00	0.00	0	0.00	0.00	0	0.00	0.00	1	1.82	0.34	5	0.77	0.46	4	0.70	0.53	3
10	0.79	0.50	5	0.22	0.52	4	1.61	0.31	3	0.00	0.00	1	0.62	0.52	5	0.44	0.57	5
28	0.78	0.51	5	0.92	0.32	4	1.18	0.35	4	0.99	0.41	4	0.00	0.00	0	0.54	0.53	5
80	0.78	0.52	5	0.87	0.30	4	1.02	0.38	4	1.34	0.39	5	0.55	0.52	5	0.44	0.56	5
34	0.00	0.00	1	0.29	0.50	3	2.36	0.33	3	1.35	0.42	5	0.57	0.55	4	0.54	0.54	5
55	0.83	0.50	4	0.00	0.00	1	0.00	0.00	0	2.05	0.33	5	0.68	0.50	5	0.84	0.50	5

RUN NUMBER 6

TUBE	a_1	b_1	η	a_2	b_2	η	a_3	b_3	η	a_4	b_4	η
73	0.33	0.55	9	0.41	0.54	9	0.48	0.53	9	0.45	0.53	9
79	0.30	0.59	9	0.40	0.57	9	0.39	0.55	9	0.41	0.[illegible]	9
9	0.40	0.56	7	0.48	0.53	9	0.45	0.54	9	0.48	0.[illegible]	9
78	0.00	0.00	0	0.39	0.56	2	0.37	0.55	2	0.55	0.[illegible]	9
69	0.49	0.51	9	0.38	0.58	9	0.56	0.52	9	0.42	0.[illegible]	8
10	0.44	0.54	9	0.37	0.[illegible]	9	0.41	0.54	9	0.48	0.[illegible]	9
29	0.39	0.54	8	0.52	0.52	3	0.40	0.56	9	0.45	0.56	8
62	0.35	0.56	8	0.43	0.56	9	0.[illegible]	0.51	9	0.46	0.[illegible]	9
44	0.50	0.52	9	0.54	0.51	9	0.61	0.50	8	0.53	0.[illegible]	8
4	0.43	0.53	9	0.43	0.53	9	0.[illegible]	0.50	9	0.[illegible]	0.[illegible]	9
34	0.00	0.00	1	0.55	0.51	8	0.49	0.53	9	0.51	0.[illegible]	9
20	0.44	0.55	8	0.47	0.53	6	0.46	0.53	7	0.61	0.[illegible]	9
55	0.00	0.00	1	0.39	0.55	9	0.96	0.44	8	0.45	0.[illegible]	9
14	0.90	0.44	4	0.37	0.57	3	1.05	0.40	4	0.80	0.[illegible]	1
28	0.43	0.55	6	0.63	0.50	6	0.38	0.57	6	0.42	0.[illegible]	6
16	0.55	0.51	9	0.37	0.56	9	0.61	0.50	9	0.43	0.[illegible]	6
50	0.49	0.51	9	2.70	0.22	8	4.07	0.16	9	0.56	0.[illegible]	9
63	0.51	0.52	9	0.49	0.54	9	0.49	0.53	9	0.50	0.[illegible]	9
64	0.44	0.54	9	1.01	0.44	4	1.44	0.39	3	3.29	0.[illegible]	8
36	0.47	0.51	9	0.38	0.54	9	0.47	0.51	8	0.42	0.[illegible]	6

RUN NUMBER 8

TUBE	a_1	b_1	η	a_2	b_2	η	a_3	b_3	η	a_4	b_4	η
20	0.20	0.60	8	0.34	0.55	2	0.48	0.52	8	0.31	0.56	8
14	0.00	0.00	0	0.41	0.52	8	0.25	0.54	8	0.26	0.58	8
20	0.38	0.58	8	0.31	0.52	8	0.23	0.59	8	0.31	0.55	8
73	0.00	0.00	0	0.18	0.63	6	0.32	0.53	5	0.42	0.54	7
69	0.37	0.59	5	0.20	0.62	8	0.26	0.58	5	0.23	0.59	5
10	0.27	0.63	8	0.37	0.53	8	0.35	0.55	8	0.46	0.50	8
29	0.32	0.60	8	0.14	0.66	8	0.13	0.67	8	0.30	0.54	7
62	0.00	0.00	1	0.00	0.00	0	0.43	0.53	5	0.39	0.52	8
44	0.00	0.00	0	0.00	1.18	2	0.06	0.77	6	0.02	0.93	3
63	0.36	0.58	8	0.19	0.61	5	0.02	0.47	8	0.30	0.55	8
79	1.13	0.45	5	0.37	0.54	5	0.13	0.69	4	0.44	0.53	5
78	0.59	0.55	7	0.25	0.60	8	0.24	0.60	8	0.99	0.38	8
34	0.00	0.00	0	0.34	0.54	8	0.24	0.60	8	0.26	0.59	8
9	0.00	0.00	0	0.36	0.53	8	0.23	0.59	4	0.23	0.59	8
55	0.31	0.62	8	0.26	0.58	8	0.40	0.53	6	0.31	0.55	8
16	0.25	0.63	8	0.39	0.50	8	0.30	0.56	8	0.34	0.55	8
50	0.39	0.57	9	0.00	0.00	0	0.37	0.58	8	0.26	0.58	8
36	0.37	0.59	8	0.36	0.51	4	0.23	0.59	8	0.36	0.54	8
64	0.44	0.56	7	0.32	0.54	6	0.29	0.54	7	0.43	0.50	6
[illegible]	[illegible]	[illegible]	[illegible]	[illegible]	[illegible]	[illegible]	[illegible]	[illegible]	[illegible]	0.44	0.50	7

RUN NUMBER 10.

Tube	a_1	b_1	η	a_2	b_2	η	a_3	b_3	η	a_4	b_4	η	a_5	b_5	η	a_6	b_6	η
20	0.38	0.55	10	0.00	1.12	10	0.81	0.40	10	0.29	0.53	10	0.26	0.55	10	0.15	0.65	10
75	0.35	0.59	8	0.29	0.56	9	0.45	0.49	10	0.49	0.49	10	0.00	0.00	0	0.59	0.51	10
79	0.64	0.51	6	0.64	0.49	5	0.23	0.63	3	0.35	0.53	10	0.61	0.47	10	0.76	0.48	10
9	0.00	0.00	0	0.26	0.56	9	0.00	0.00	1	0.81	0.41	9	0.33	0.52	9	0.26	0.57	9
55	0.47	0.54	10	0.19	0.61	9	0.36	0.51	10	0.49	0.47	10	0.37	0.50	10	0.16	0.63	9
4	0.37	0.55	9	0.37	0.53	7	0.21	0.57	9	0.31	0.53	10	0.20	0.58	10	0.00	0.00	0
60	0.49	0.53	10	0.18	0.63	8	0.03	0.86	3	0.49	0.49	9	0.46	0.49	10	11.92	0.15	2
10	0.36	0.56	9	0.30	0.56	9	0.52	0.46	9	0.40	0.49	9	0.23	0.56	9	0.12	0.67	9
47	0.04	0.82	2	0.00	0.00	1	0.00	0.00	1	0.00	0.00	1	0.00	0.00	1	0.00	0.00	1
57	0.43	0.53	10	0.00	0.00	1	0.20	0.58	10	0.18	0.60	10	0.26	0.53	10	0.19	0.57	10
23	0.48	0.52	9	0.48	0.50	10	0.39	0.51	9	0.23	0.57	10	0.32	0.52	9	0.15	0.66	10
3	0.43	0.36	6	0.20	0.53	10	0.00	0.00	1	0.29	0.60	8	0.00	0.00	1	0.17	0.66	9
73	0.00	0.00	1	0.00	0.48	10	0.32	0.52	10	0.33	0.53	10	0.57	0.48	10	0.46	0.53	10
34	0.44	0.54	9	0.00	1.29	2	0.29	0.53	9	0.33	0.51	10	0.20	0.57	10	0.20	0.61	10
14	0.00	0.00	1	0.40	0.51	10	0.52	0.46	10	0.37	0.49	10	0.24	0.55	10	0.13	0.65	10
38	0.40	0.55	9	0.14	0.62	9	0.21	0.56	9	0.35	0.52	9	0.22	0.58	10	0.26	0.58	10
42	0.00	0.34	1	0.00	0.00	1	0.32	0.52	10	0.37	0.51	10	0.34	0.52	10	0.20	0.61	10
16	0.37	0.55	10	0.20	0.58	10	0.50	0.47	10	0.41	0.49	9	0.25	0.56	10	0.24	0.60	9
39	0.37	0.56	10	0.17	0.60	10	1.61	0.36	5	0.00	0.00	0	0.18	0.58	10	0.00	0.00	1
53	0.48	0.54	9	0.29	0.58	3	0.33	0.52	8	0.00	0.00	0	0.29	0.54	9	0.16	0.62	9

References

1. ENERGY WORLD BULLETIN OF INST. OF E., The U.S.A. heat exchanger market, 68, 25 (1980).

2. T. H. CHILTON and A. P. COLBURN, Mass transfer coefficients, Ind. Engng. Chem. 26, 1183-1187 (1934).

3. N. V. MACKLEY, Local shell-side coefficients in shell-and-tube heat exchangers - The use of a mass transfer technique, Ph.D. Thesis, University of Aston in Birmingham, (1973).

4. J. N. PROWSE, Local heat transfer coefficients in baffled shell-and-tube heat exchanger-end compartment study, Ph.D. Thesis, University of Aston in Birmingham, (1977).

5. STANDARDS OF THE TUBULAR EXCHANGER MANUFACTURERS ASSOCIATION, Standards of tubular exchanger manufacturers association, 5th Ed. TEMA, New York, (1968).

6. R. Hilpert, Forschung a.d. Geb. d. Ingenieurwes, 4, 215 (1933).

7. J. ULSAMER, Forschung a. d. Geb. d. Ingenieurwes, 3, 94 (1932).

8. E. POLHAUSEN, Theoretical equation for heat transfer in the flow of a fluid parallel to plane surfaces, Zeitchr. f. angew Math. u. Mech. 1, 252 (1921).

9. O. L. PIERSON, Experimental investigation of the influence of tube arrangement on convective heat transfer and flow resistance in cross flow of gases over tube banks, Trans. ASME, (7), 563 (1937).

10. W. M. KAYS, A. L. LONDON and R. K. LO, Heat transfer and friction characteristics of gas flow normal to tube banks, Trans. ASME 76, 387 (1954).

11. T. V. SHEEHAN, R. T. SCHOMER and O. E. DWYER, Heat transfer for cross flow of water through a tube bank at Reynolds numbers up to a million, Paper No. 54-F-19, ASME meeting, New York, (1954).

12. W. H. McADAMS, Heat transmission, 3rd ed. McGraw-Hill, New York, 1954.

13. A. P. COLBURN, A method of correlating forced convection heat transfer data and a comparison with fluid friction, Trans. A.I.Chem.E. 29, 174 (1933).

14. E. N. SIEDER and G. E. TATE, Ind. Engng. Chem. 23, 1429 (1936).

15. ENGINEERING SCIENCE DATA UNIT, Convective heat transfer during crossflow of fluids over plain tube banks, Item No. 73031 (1973).

16. A. ZUKAUSKAS, Heat Transfer from tubes in crossflow, Advances in heat transfer, 8, 93 (1972).

17. A. ZUKAUSKAS, V. J. MAKAREVICIUS and A. SLANCIAUSKAS, Heat transfer in banks of tubes in crossflow of fluid, Mintis, Vilnius (1968) (In Russian).

18. O. P. BERGELIN, E. S. DAVIS and H. L. HULL, A study of three tube arrangements in unbaffled tubular heat exchangers, Trans. ASME 71, 369 (1949).

19. O. P. BERGELIN, G. A. BROWN, H. L. HULL and F. W. SULLIVAN, Heat transfer and fluid friction during viscous flow across banks of tubes III - A study of tube spacing and tube size, Trans. ASME, 72, 881-888 (1950).

20. O. P. BERGELIN, G. A. BROWN and S. C. DOBERSTEIN, Part IV - Heat transfer and fluid friction during flow across banks of tubes, Trans. ASME, 79, 953 (1952).

21. O. P. BERGELIN, A. P. COLBURN and H. L. HULL, Heat transfer and pressure drop during viscous flow across unbaffled tube banks, University of Deleware Engineering Experiment Station, Bulletin No. 2 (1950).

22. O. P. BERGELIN, G. A. BROWN and A. P. COLBURN, Part V, A study of a cylindrical baffled exchanger without internal leakage, Trans. ASME, 74, 841-850 (1950).

23. G. A. BROWN, Heat transfer and fluid friction during turbulent flow through a baffled cylindrical shell-and-tube heat exchanger, Ph.D. Thesis, University of Deleware (1956).

24. O. P. BERGELIN, K. J. BELL and M. D. LEIGHTON, Part VI - Heat transfer and fluid friction during flow across banks of tubes: the effect of internal leakages; Trans. ASME, 80, 53-60 (1958).

25. O. P. BERGELIN, K. J. BELL and M. D. LEIGHTON, Part VII Bypassing between tube bundle and shell, heat transfer Chicago, Chem. Engng. Progress Symp. Series, No.29, 55, 45-58 (1959).

26. J. D. JENKINS, N. V. MACKLEY and B. GAY, The influence of property number in forced convection heat and mass transfer correlations, Letters, Heat Mass Transfer J. 3, 105-110 (1976).

27. W. H. EMERSON, Shell-side heat transfer and pressure drop with turbulent flow in segmentally baffled shell-and-tube heat exchangers - A survey, National Engineering Laboratory, Report No. 45, East Kilbride, Glasgow (1962).

28. D. Q. KERN, Process heat transfer, McGraw-Hill, New York (1950).

29. D. DONAHUE, Heat transfer and pressure drop in heat exchnagers, Ind. Engng. Chem. 41, 2499 (1949).

30. T. TINKER, Shell-side Characteristics of shell-and-tube heat exchangers, Trans. ASME 80, 36-52 (1958).

31. T. TINKER, Shell-side characteristics of shell-side heat exchangers (Parts I and II), in general discussions on heat transfer pp89-116, The Institution of Mech. Eng., London, (1951).

32. B. E. SHORT, Heat transfer and pressure drop in heat exchangers, University of Texas Publication No. 4324 (1934).

33. E. HIENRICH and R. STUCKLE, Ver. deut., Mitt. Forech. Gebiete Ingenieurw, Heft 271 (1925). (In German).

34. R. A. BOWMAN, Investigation of heat transfer rates on the external surface of baffled tube banks, ASME paper No. 28, New York (1947).

35. H. S. GARDNER and I. GILLER, Shell-side coefficients of heat transfer in a baffled heat exchanger, Trans. ASME 69, 687 (1947).

36. BRITISH SHIPBUILDING RESEARCH ASSOCIATION, A Correlation of current data on heat transfer and pressure drop in segmentally baffled shell-and-tube heat exchangers, Report No. 148 (1955).

37. K. J. BELL, Final report of the co-operative research programme on shell-and-tube heat exchangers, University of Deleware Engineering Experimental Station, Bulletin No. 5 (1963).

38. J. W. PALEN and J. TABOREK, Solution of shell-side flow pressure drop and heat transfer by stream analysis method, Chem. Engng. Prog. Symp. Series 65 (92), 53 (1968).

39. R. O. PARKER and Y. I. MOK, Shell-side pressure in baffled heat exchangers, Brit. Chem. Eng. 13, 124 (1968).

40. A. DEVORE, Try this simplified method for rating baffled exchangers, Petrol. Refiner 40 (5) 221, (1961).

41. I. GRANT, Private Communication, (1978).

42. D. F. BOUCHER and C. E. LAPPEL, Pressure drop across tube banks, Chem. Engng. Prog. 4 (2), 117-134 (1948).

43. A. Y. GUNTER and K. SENNSTROM, A study of flow patterns in baffled heat exchangers, Papers NO. 47-A-103 ASME Meeting, Atlantic City, New Jersey (1947).

44. R. K. GUPTA and D. L. KATZ, Flow patterns for predicting shell-side heat transfer coefficients for baffled shell-and-tube exchangers, Ind. Engng. Chem. 49(6), 998-999 (1957).

45. T. W. AMBROSE and I. G. KUNDSEN, Local shell-side heat transfer coefficient in baffled tubular heat exchangers, AIChE J. 4(3), 332 (1958).

46. M. S. GURUSHANKARIAH, and I. G. KNUDSEN, Local shell-side heat transfer coefficients in the vicinity of segmental baffles in tubular heat exchangers, Chem. Engng. Prog. Symp. Series 55, (29) 29 (1959).

47. J. W. STACHIEWICZ and B. E. SHORT, Local shell-side heat transfer coefficients in a leak-proof heat exchanger, International developments in heat transfer, Colorado, 959 (1961).

48. T. A. WILLIAMS, A mass transfer study of local transfer coefficients on the shell-side of a cylindrical shell-and-tubeheat exchanger fitted with segmental baffles, Ph.D. Thesis, University of Manchester (1962).

49. B. GAY and T. A. WILLIAMS, Heat transfer on the shell-side of a cylindrical shell-and-tube heat exchanger fitted with segmental baffles - Part I, Trans. Instn. Chem. Enggs. 46, T95-100 (1968).

50. B. E. SHORT, Shell-and-tube heat exchangers - Effect of by-pass and clearance streams on the main stream temperature, Paper No. 60-HT-16 ASME/AIChE, Heat transfer conference, Buffalo (1960).

51. P. C. O. Roberts, Individual tube transfer coefficients in a segmentally baffled shell-and-tube exchanger, Ph.D. Thesis, University of Aston (1969).

52. B. GAY and P. C. O. ROBERTS, Heat transfer on the shell-side of a cylindrical shell-and-tube heat exchanger fitted with segmental baffles - Part II, Trans. Inst. Chem. Engrs. 48, T3-T6 (1970).

53. J. D. JENKINS, J. N. PROWSE and B. GAY, The effect of baffle-spacing on the shell-side heat transfer coefficient for segmentally baffled shell-and-tube heat exchnagers, RS145, aere Report No. R8361, AERE Harwell (1976).

54. K. J. Bell, Exchanger design based on the Deleware Research Programme, Petrol. Engr. J. 32 (11), C26 and C40a (1960).

55. R. V. MACBETH, The effect of shell-side inlet nozzles on shell-side single-phase pressure drop in shell-and-tube heat exchangers, AERE R1071, AEE Winfrith (Commercial-in-confidence), (1976).

56 A. M. SUTEY and G. KNUDSEN, Effect of dissolved oxygen of Redox method for measurement of mass transfer coefficients, Ind. Engng. Chem. Fundls. 6 (1), 132 (1967).

57. A. M. SUTEY and J. G. KNUDSEN, Mass transfer of the solid-liquid interface for climbing film flow in an annular duct, AIChE. J. 15, 719 (1969).

58. D. M. LUCAS and R. M. DAVIES, Evaluation of local and average convective heat transfer coefficients in a furnace using an electrolytic mass transfer model, J. Inst. Fuel, 31, 3137 (1975).

59. M. EISENBERG, C. W. TOBIAS and C. R. WILKE, Selected physical properties of ternary electrolytes employed in ionic mass transfer studies, J. Electro-chem. Soc., 103, 413 (1950).

60. D. M. LUCAS, Prediction of the performance of rapid heating furnaces using physical and mathematical modelling techniques, Ph.D. Thesis, University of Aston in Birmingham, (1971).

61. P. VOGTLANDER and C. BAKKER, An experimental study of mass transfer from a liquid flow to wires and gauzes, Chem. Engng. Sci. 18, 583 (1963).

62. A. WRAGG, Mass transfer between a falling liquid film and a plane vertical surface, Int. J. Heat Mass Transfer, 11, 1287 (1968).

63. T. K. ROSS and A. A. WRAGG, Electrochemical mass transfer studies in Annuli, Electrochim. Acta. 10, 1093 (1965).

64. R. DOBRY and R. K. FINN, Mass transfer to a cylinder at low Reynolds numbers, Ind. Engng. Chem. 48, 1540 (1956).

65. T. MIZUSHINA, H. VEDA and N. UMEMIYA, Effect of free-stream turbulence on mass transfer from a circular cylinder in crossflow, Int. J. Heat Mass Transfer 15, 769 (1972).

66. Z. P. Shulman et al, Mass transfer peculiarities of a disc rotating in a non-Newtonian fluid, Int. J. Heat Mass Transfer 16, 1339 (1973).

67. A. F. J. SMITH and A. A. WRAGG, An electrochemical study of mass transfer in free convection at vertical arrays of horizontal cylinders, J. Appl. Electrochem. 4, 219-228 (1974).

68. A. F. PRICE and A-F. M-A. FATTAH, Hydrodynamic characteristics of a plate heat exchanger channel, Trans. IChemE. 56, 217-228 (1978).

69. R. J. GOLDSTIEN and D. K. KREID, The laser doppler anemometer - Measurements in heat transfer, McGraw-Hill, Washington D.C. (1976).

70. C. R. WILKE, M. EISENBERG and C. W. TOBIAS, Correlation of limiting currents under free convection conditions, J. Electrochem. Soc. 106, 513 (1953).

71. S. WHITAKER, Forced convection heat transfer correlations for flow in pipes past flat plates, single cylinders, single spheres, and for flow in packed beds and tube bundles, AIChE. J. 18(2), 361 (1972).

72. M. JACOB, Heat transfer, Vol. 1, JOHN WILKINSONS, Ed. 10 (1967).

73. A. J. ARVIA and J. S. W. CARROZZA, Mass transfer in the electrolysis of copper sulphate in aqueous solution under limiting current and forced convection employing a cylindrical cell with rotating electrodes, Electrochim. Acta, 7, 65 (1962).

74. M. EISENBERG, C. W. TOBIAS and C. R. WILKE, Ionic mass transfer and concentration polarisation at rotating electrodes, J. Electrochem, Soc. 101, 306 (1951).

75. ROTAMETER MANUFACTURES CO., Calibration data for metric series rotameters, 330 Purley Way, Croydon, Surrey.

76. M. MAZAR, Transfer coefficients of tubes in crossflow in laminar flow regime, M.Sc. Thesis, University of Aston (1978).

77. B. G. VAN DER HEGGE ZIJNEN, Heat transfer from horizontal cylinders to a turbulent air flow, Appl. Sci. Res., A7, 205-222 (1958).

78. D. E. CONDAPPA, Measurement of low pressure drops, M.Sc. Thesis, University of Aston in Birmingham, (1978).

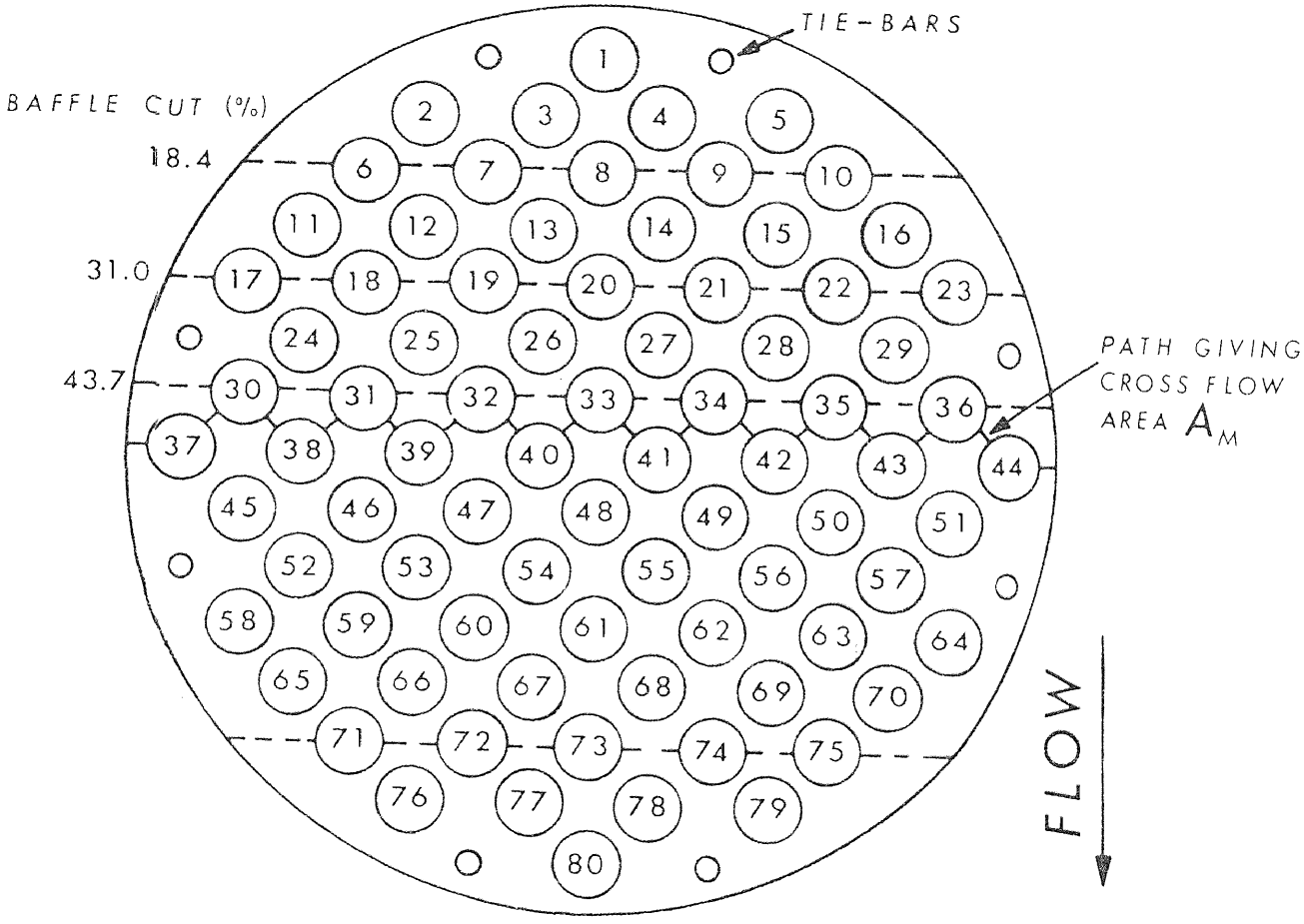

Tube Layout of Model Exchanger Bundle